NOTE TO USERS

MOLECULAR BASIS FOR ION CURRENT HETEROGENEITY IN NORMAL AND DISEASED HEARTS

by

Stephen Zicha

Department of Pharmacology and Therapeutics

Faculty of Medicine

McGill University, Montreal

A thesis submitted to the Faculty of Graduate Studies and Research

McGill University, Montreal, Canada

In partial fulfillment of the requirements for the degree of

Doctor of Philosophy

Your file Votre référence
ISBN: 0-494-12968-9
Our file Notre référence
ISBN: 0-494-12968-9

This thesis is dedicated to my parents who have always provided their unconditional support and love during the entire course of my graduate studies

ABSTRACT

Cardiac action potential characteristics are known to vary in different species, but also in the different regions of the heart within a given species and in cardiovascular disease. The heterologous expression of voltage-gated ion currents is believed to underlie these differences. The purpose of this thesis is to elucidate the molecular mechanisms which may underlie some of the observed current changes in different species, as well as regions and diseases of the heart.

Here, we describe the variable dependence on repolarizing K^+ currents in different species as being the result of the lack of I_{to} subunits in guinea pig heart with a greater expression of I_K subunits, while rabbits express all hypothesized I_{to} subunits, but express I_K subunits at low levels. Humans are found to lie in between these two species in terms of the expression of these voltage-gated K^+ channel subunits. The specialized function of certain regions of the heart, such as the ventricles and the SAN, have been attributed to the heterologous expression of I_{to} and the pacemaker current (I_f) respectively. Here were demonstrate that both Kv4.3 and KChIP2 gradients underlie an observed I_{to} transmural gradient and contribute to the dispersion of repolarization, while a greater expression of HCN2 and HCN4 subunits in the SAN compared to the right atrium account for the larger I_f current in this region. Cardiovascular diseases such as congestive heart failure (CHF) have been associated with ion channel remodelling. Here, we report the finding of changes in $Na_v1.5$, Kv4.3, HCN2 and HCN4 expression which may underlie some of the electrophysiological changes associated with this disease. Furthermore, we characterise a genetic polymorphism which is associated with another disease, atrial fibrillation.

The heterologous expression of voltage-gated ion channel subunits may account for many of the species-, region- and disease-specific differences which have been observed in the heart. Such heterogeneity contributes to the proper functioning of the heart under normal conditions, but may also contribute to the pathogenesis of cardiovascular disease.

FRENCH ABSTRACT

Les propriétés du potentiel d'action cardiaque varient selon l'espèce, mais aussi selon la région, dans une même espèce et selon les pathologies cardiovasculaires. L'expression hétérogène des courants dépendants du voltage contribue possiblement à cette variation. L'objectif de cette thèse est d'élucider les mécanismes moléculaires responsables des variations de courants observés dans différentes espèces ainsi que dans les différentes régions du tissu cardiaque et dans des pathologies cardiaques.

Ainsi, nous décrivons la différence observée au niveau des courants potassiques repolarisants de plusieurs espèces comme étant le résultat de l'absence des sous-unités portant le courant I_{to} dans le cochon d'Inde associée à l'expression plus importante des sous-unités portant le courant I_K. Au contraire, le lapin exprime toutes les sous-unités associées à I_{to} mais possède un niveau d'expression des sous-unités I_K plus faible. L'humain se situe entre ces deux espèces en terme d'expression de ces sous-unités potassiques. La spécialisation fonctionnelle de certaine région cardiaque telle que les ventricules ou le nœud SA a été associée à l'expression hétérogène des courants I_{to} et pacemaker (I_f), respectivement. Nous démontrons ici que le gradient d'expression des deux sous-unités Kv4.3 et KChIP2 est responsable de la dispersion de la repolarisation, alors que l'expression plus importante des sous-unités HCN2 et HCN4 dans le nœud SA comparé à l'oreillette droite explique la présence d'un courant I_f plus important dans cette région. Certaines maladies cardiovasculaires telles que la défaillance cardiaque ont été associées au remodelage des canaux ioniques. Dans cette thèse, nous rapportons des changements dans le niveau d'expression des sous-unités $Na_v1.5$, Kv4.3, HCN2 et HCN4 pouvant expliquer certaines modifications associées à cette maladie. De plus, nous caractérisons un polymorphisme génétique associé avec la fibrillation auriculaire.

Par conséquent, l'expression hétérogène des sous-unités de canaux ioniques dépendants du voltage peut expliquer les différences observées dans le tissu cardiaque selon les espèces, les régions et les pathologies. Une telle hétérogénéité contribue au bon fonctionnement du cœur dans des conditions normales, mais peut également contribuer à la pathogénicité des maladies cardiovasculaires.

ACKNOWLEDGEMENTS

I am forever indebted to Dr. Stanley Nattel, my supervisor, for first having patience and giving me a chance to realize my potential during my graduate studies. His extraordinary support, constant guidance and constructive criticisms have always been an inspiration for my work. His supervision has truly been second to none, and without it, this thesis and all my work would not be possible.

I am extremely grateful for the help Dr. Zhiguo Wang has provided me during my studies. His expertise in molecular biology, as well as his constant constructive and helpful suggestions, has always been sincerely appreciated.

I would like to thank my friends and colleagues at the Institut de cardiologie de Montreal, especially Marc Pourrier, Daniel Herrera, Gernot Schram and Joachim Ehrlich, who all helped create the best learning environment and made the research so much more enlightening and rewarding.

I would like to thank the Department of Pharmacology and Therapeutics for giving me the opportunity to pursue my graduate studies at McGill, and providing an excellent environment for learning within the department; and the Institut de cardiologie de Montreal for accepting me into its first class research facility which permitted me to realize these projects.

I am extremely appreciative of the excellent recommendations from Dr. Terrence Hebert and Dr. Zhiguo Wang which aided me during my application for studentship and fellowship funding.

Many thanks to the members of my graduate committee: Dr. Radan Čapek, Dr. Daya Varma, Dr. Céline Fiset, Dr. Terrence Hebert and Dr. Zhiguo Wang, whose comments, criticisms and suggestions I have benefited from.

I am forever grateful of the help the excellent technicians at the Institut de cardiologie de Montreal have provided, especially Evelyn Landry, Nathalie L'Heureux, Chantal Maltais and Chantal St-Cyr.

I would like to thank Dr. Bruce Allen, Dr. Terrence Hebert, Maya Mamarbachi and Louis Villeneuve for their selfless help and technical knowledge which has enabled me to complete these projects with varied technical backgrounds.

Marc Pourrier provided an enormous amount of help in translating the French abstract for which I am very grateful.

Lastly, many thanks go to the Fonds de recherche en santé de Québec for its financial support from 2003 to 2004.

PREFACE

Note on the format of this thesis:

In accordance with the Faculty of Graduate Studies and Research of McGill University, the candidate has the option of including as part of the thesis the text of original paper already published by learned journals, and original papers submitted or suitable for submission to learned journals. The exact wording relating to this option is as follows:

Candidates have the option of including, as part of the thesis, the text of one or more papers submitted or to be submitted for publication, or the clearly-duplicated text of one or more published papers. These texts must be bound as an integral part of the thesis.

If this option is chosen, connecting text that provide logical bridges between the different papers are mandatory. The thesis must be written in such a way that it is more than a mere collection of manuscripts; in other words, results of papers must be integrated.

The thesis must still conform to all other requirements of the "Guideline for Thesis Preparation". The thesis must include: a table of contents, and abstract in English and French, an introduction which clearly states the rational and objectives of the study, a review of the literature, a final conclusion and summary, and thorough bibliography or reference list.

Additional material must be provided where appropriate (e.g. appendices) and in sufficient detail to allow a clear and precise judgement to be made of the importance and originality of the research reported in the thesis.

In the case of manuscripts co-authored by the candidate and others, the candidate is required to make an explicit statement in the thesis as to who contributed to such work and to what extent. Supervisors must attest to the accuracy of such statement at the doctoral oral defense. Since the task of the examiners is made more difficult in these cases, it is in the candidate's interest to make perfectly clear the responsibilities of co-authored papers.

This thesis consists of the following papers and submitted papers co-authored by myself and others:

1. **Stephen Zicha**, Isaac Moss, Bruce Allen, Andras Varro, Julius Papp, Robert Dumaine, Charles Antzelevitch and Stanley Nattel. Molecular basis of species-specific expression of repolarizing potassium currents in the heart. *Am. J. Physiol. Heart Circ Physiol.* 2003; 285(4):H1641-1649.

2. **Stephen Zicha**, Victor A. Maltsev, Stanley Nattel, Hani N. Sabbah, Albertas I. Undrovinas. Post-transcriptional alterations in the expression of cardiac Na+ channel subunits in chronic heart failure. *J. Mol. Cell. Cardiol.* 2004; 37(1):91-100.

3. **Stephen Zicha**, Ling Xiao, Sara Stafford, Tae Joon Cha, Wei Han, Andras Varro and Stanley Nattel. Transmural expression of transient outward current subunits in normal and failing canine and human hearts. *J. Physiol* 2004; 561(3):735-748.

4. **Stephen Zicha**, María Fernández-Velasco, Giuseppe Lonardo, Nathalie L'Heureux and Stanley Nattel. Sinus node dysfunction and pacemaker current subunit remodeling in canine heart failure model. Submitted to *Cardiovasc. Res.* 2004.

5. Joachim R. Ehrlich*, **Stephen Zicha***, Pierre Coutu, Terence E. Hébert and Stanley Nattel. The atrial fibrillation-associated minK38G/S polymorphism modulates slow delayed-rectifier current function. Submitted to *Cardiovasc. Res.* 2004.

STATEMENT OF AUTHORSHIP

The following are statements regarding the contributions of co-authors and myself to the papers included in this thesis.

Paper 1. I performed all the total RNA and protein isolations from all species studied. I additionally performed all the competitive RT-PCRs and immunoblotting experiments, and analyzed all of the data and wrote the manuscript. Isaac Moss helped in the initial RT-PCR analysis of Kv subunit expression. Bruce Allen provided insightful technical knowledge regarding immunoblotting techniques. Andras Varro provided the normal human tissue samples which made this study complete. Robert Dumaine and Charles Antzelevitch provided an anti-KvLQT1 antibody which was used for initial experiments. Stanley Nattel provided close supervision, generated the initial idea, and helped produce the final version of the manuscript.

Paper 2. The paper is the result of a collaboration organized between Albertas Undrovinas and Stanley Nattel. I performed all the molecular biology techniques, including competitive RT-PCR and immunoblotting, as well as the respective analysis. I also wrote parts of the manuscript dealing with these aspects. Victor Maltsev and Hani Sabbah performed the electrophysiological experiments and provided the appropriate figures. Stanley Nattel provided supervision and suggested the collaboration to me, and was integral in the revision of the final manuscript. Albertas Undrovinas coordinated the collaboration and wrote the manuscript, especially those sections dealing with electrophysiological observations.

Paper 3. The idea came up after discussions between Sara Stafford, Stanley Nattel and myself. I performed all the Kv4.3 mRNA work, all the immunoblotting experiments, additional KChIP2 mRNA work, analysis and manuscript writing. Ling Xiao provided electrophysiological data and Sara Stafford performed initial KChIP2 mRNA analysis. Tae Joon Cha provided the canine model of CHF, while Wei Han previously designed the KChIP2 primers and mimics for competitive RT-PCR analysis. Andras Varro gratefully provided the normal human tissue samples. Stanley

Nattel provided supervision and coordinated all facets of the project, as well as correcting the final version of the manuscript.

Paper 4. This project was based on previous work (and lack thereof) in the literature concerning CHF and SAN function. I designed and completed all the *in vivo* experiments, as well as all the molecular work regarding HCN mRNA and protein analysis and the manuscript writing. Maria Fernandez-Velasco did initial work on testing the specificity of HCN primers for PCR, while Giuseppe Lonardo helped in the optimization of competitive RT-PCR reaction conditions. Nathalie L'Heureux helped with the surgeries required for the creation of the canine CHF model. Stanley Nattel helped come up with the initial idea, and corrected the final version of the manuscript.

Paper 5. This project was suggested by Stanley Nattel due to the lack of information regarding the genetic predisposition to atrial fibrillation, as well as providing me with a chance to become acquainted with patch-clamp techniques. Joachim Ehrlich and I both created the point mutation required for the single nucleotide polymorphism. Joachim Ehrlich performed initial patch-clamp experiments and immunohistochemical studies and wrote the initial version of the manuscript. I did the majority of the patch-clamp experiments and analysis, and immunohistochemical work and analysis. Terrence Hebert provided helpful guidance and suggestions for experiments. Stanley Nattel revised the final version of the manuscript and provided supervision throughout the project.

LIST OF ABBREVIATIONS

Cardiac Anatomy

SAN	Sino-atrial node
AVN	Atrio-ventricular node
L(R)V	Left or Right Ventricle
EPI	Ventricular epicardium
MID	Ventricular mid-myocardium
ENDO	Ventricular endocardium
L(R)A	Left or Right Atrium

Electrophysiological properties

AP	Action potential
APD	Action potential duration
V_{max}	Maximal upstroke velocity
I_{Na}	Inward Na^+ current
I_{Ca}	Inward Ca^{2+} current
$I_{Ca, L}$	L-type Ca^{2+} current
$I_{Ca, T}$	T-type Ca^{2+} current
I_f	Pacemaker, funny, hyperpolarization-activated inward current
I_A	Outward A-type K^+ current
I_{to}	Transient outward K^+ current
$I_{to, fast}$	Fast inactivating transient outward current
$I_{to, slow}$	Slow inactivating transient outward current
I_K	Delayed rectifier K^+ currents
I_{Kr}	Rapidly-activating delayed rectifier K^+ current
I_{Ks}	Slowly-activating delayed rectifier K^+ current
I_{Kur}	Ultra-rapid delayed rectifier K^+ current
I_{K1}	Inward rectifier K^+ current
I_{KACh}	Acetylcholine-induced inward rectifier K^+ current
I_{KATP}	ATP-induced inward rectifier K^+ current
I_{NCX}	Na^+-Ca^{2+} exchanger current

I-V relation	Current-voltage relationship
$V_{1/2}$	Half-maximal voltage for activation or inactivation
pA	Picoampere
pF	Picofarad
τ	Tau time constant

Signal transduction and modulators of cardiac activity

AC	Adenylate cyclase
ACh	Acetylcholine
Ang-II	Angiotensin-II
ACE	Angiotensin converting enzyme
cAMP	Cyclic adenosine 3, 5-monophosphate
DAG	Diacylglycerol
G_{α}	α-subunit of G-protein
$G_{\beta\gamma}$	β- and γ- subunits of G-protein
$G_{\alpha s}$	Stimulatory G-protein α-subunit
$G_{\alpha i}$	Inhibitory PTX-sensitive G-protein α-subunit
$G_{\alpha q}$	PTX-insensitive G-protein α-subunit
IP_3	Inositol 1, 4, 5-triphosphate
PIP_2	Phosphatidylinositol 4, 5-bisphosphate
PKA	Protein kinase A
PKC	Protein kinase C
PLC	Phospholipase C
PTX	Pertusis toxin
4-AP	4-aminopyridine
DTX	Dendrotoxin
ISO	Isoproterenol
STX	Saxitoxin
TEA	Tetraethylammonium
TTX	Tetrodotoxin

Molecular technical aspects

EB	Ethidium bromide
GSP(F,R)	Gene specific primer, forward or reverse
PCR	Polymerase chain reaction
RT	Reverse transcription
CHO	Chinese hamster ovary cell line
COS7	Green monkey kidney cell line

Pathophysiological aspects

CHF	Congestive heart failure
AF	Atrial fibrillation
EADs	Early afterdepolarizations
DADs	Delayed afterdepolarization
TdP	Torsades de pointes
LQT	Long QT syndrome

LIST OF FIGURES AND TABLES

CHAPTER 5

Paper 4

CHAPER 6

Paper 5

TABLE OF CONTENTS

CHAPTER 1: INTRODUCTION

1. Cardiac electrophysiology

The contraction of heart muscle is what pumps blood throughout the entire body. The rhythmical contraction of cardiac myocytes is the result of alterations in transmembrane potential by means of depolarization and repolarization. These changes are easily seen at the cellular level by means of the cardiac action potential (AP). In normal tissue, each cardiac cycle is composed of a wave of excitation originating in the sinoatrial node (SAN). This wave propagates through the atrium to the atrioventricular node (AVN) and then on to the ventricles via the His-Purkinje system. The excitation of the ventricles results in the forceful pumping action of the heart. Each of these regions is unique in terms of different cell types and cell density, and therefore AP morphology is distinct in each region as well (Figure 1) (Feng *et al.*, 1998;Li *et al.*, 2001;Wang *et al.*, 1998c). The distinct cardiac AP morphologies in different regions ensures the proper coordination of cardiac excitation.

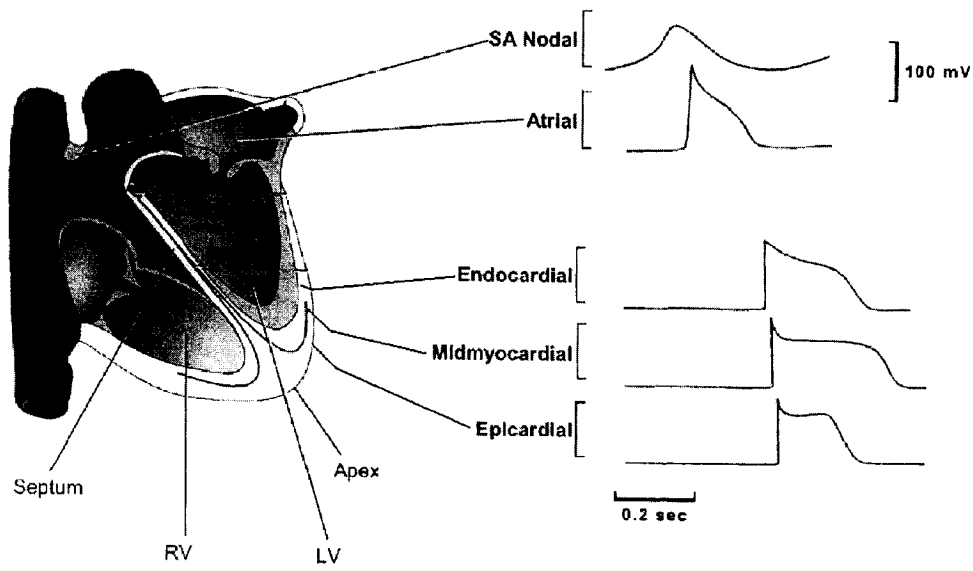

Figure 1. Schematic representation of the different regions in the heart (left), along with representative APs (right). SA, sino-atrial; AV, atrio-ventricular. Modified from Nerbonne, 2000 (Nerbonne, 2000).

1.1 The cardiac action potential

The cardiac AP is not as fast as those in other excitable tissue such as neurons, lasting hundreds of milliseconds compared to a few milliseconds. The normal resting potential of a cardiac myocyte is approximately -80mV. An influx of positively charged ions results in membrane depolarization, while an efflux results in membrane re-polarization. A typical cardiac AP consists of 5 distinct phases (Figure 2).

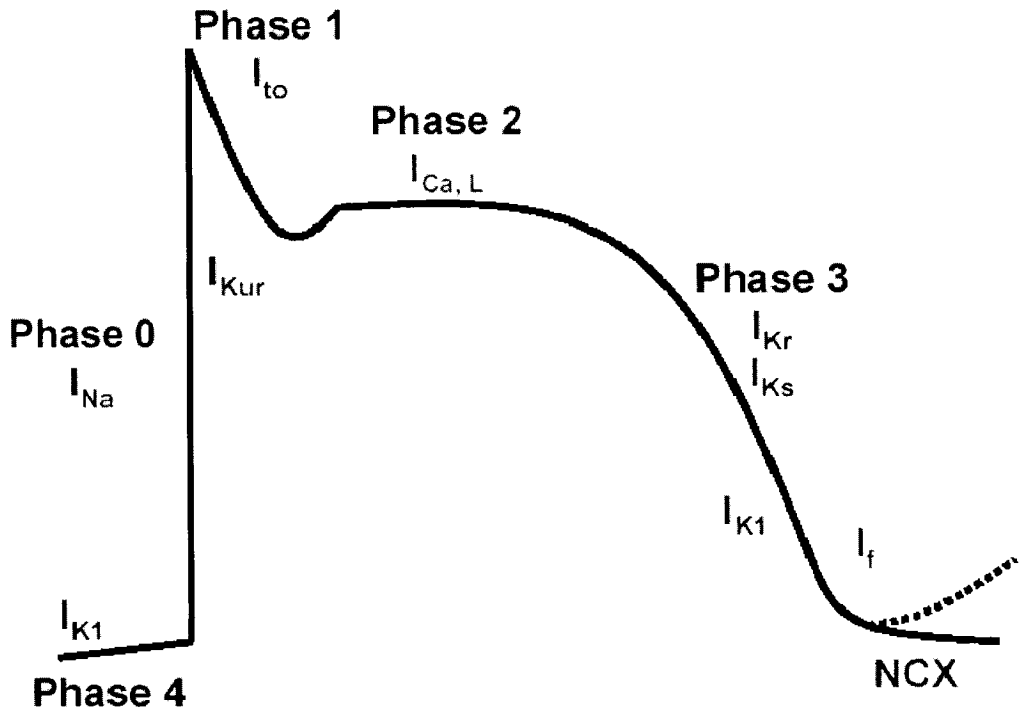

Figure 2. Cardiac action potential. Inward currents are shown in red, outward currents are in blue.

Each phase is characterized by the activation of different voltage-gated ion channels which are able to "shape" the action potential. Most of these currents will be discussed in further detail in later sections. Phase 0 consists of a rapid depolarization from the resting membrane potential of approximately −80 mV to +40 mV and is

caused by the influx of a large number of sodium (Na^+) ions through cardiac Na^+ channels, creating the Na^+ current (I_{Na}). Phase 0 depolarization results in the activation of various outward potassium (K^+) currents during Phase 1, such as the transient outward current (I_{to}) and the ultra-rapid delayed rectifier (I_{Kur}), which are sensitive to the depolarizing voltage changes. This early rapid repolarization phase is followed by the activation of Phase 2 currents. These constitute a fairly-balanced inward and outward flow resulting in a phase of relatively constant transmembrane potential, creating the so-called "plateau" which is typical of cardiac APs. During this phase, inward currents such as the L-type calcium current (I_{CaL}) and the late component of the sodium current ($I_{Na,L}$) balance outward currents such as I_{Kur} and the rapidly activating and slowly activating components of the delayed rectifier current, I_{Kr} and I_{Ks}. Ca^{2+} influx during the plateau phase is essential for electromechanical coupling, as Ca^{2+} ions trigger movement of the contractile filaments causing cardiac contraction. Phase 3 is the final rapid repolarization phase of the AP and is dominated by outward K^+ currents such as I_{Kr} and I_{Ks}. After repolarization is complete, maintenance of the resting membrane potential during Phase 4 is controlled by the inward rectifier current (I_{K1}). In regions with pacemaker activity, such as the SAN, the hyperpolarization-activated current I_f is able to depolarize cells during phase 4, reaching the threshold for firing and producing pacemaker activity. In addition to the currents mentioned above, other membrane currents such as I_{KATP}, I_{CaCl}, and the Na^+-Ca^{2+} exchanger current (NCX) play a role in determining AP morphology.

1.2 Cardiac AP regional heterogeneity

While every region of the heart is associated with a different AP morphology, the SAN, the atrial and ventricular AP are especially unique (see Figure 1). The ventricle can further be separated into three different layers based on AP morphology: the epicardium, the midmyocardium and the endocardium (Antzelevitch *et al.*, 1991;Sicouri *et al.*, 1994;Sicouri & Antzelevitch, 1991;Sicouri & Antzelevitch, 1995). The first noticeable characteristic of an epicardial or midmyocardial AP is the pronounced "spike and dome" shape in Phase 1 (Antzelevitch *et al.*, 1991;Litovsky & Antzelevitch, 1988). This has been attributed to a greater amount of I_{to} in these regions compared to the endocardium. Furthermore, the midmyocardial region displays a significantly longer AP duration (APD) at 90% (APD_{90}) repolarization compared to the epi- or endo-cardium. This has been attributed to a small amount of I_{Ks} and a larger $I_{Na,L}$ in this region (Liu & Antzelevitch, 1995;Zygmunt *et al.*, 2001).

Atrial myocytes have a much shorter APD compared to ventricular cells and are characterized by a slower Phase 3 repolarization compared to ventricular cells. They also have a less negative maximum diastolic potential, between -70 mV and -80 mV, compared to ventricular myocytes (-85mV) (Davis & Temte, 1969;Kus & Sasyniuk, 1975;Li *et al.*, 2001;Litovsky & Antzelevitch, 1989;Wang *et al.*, 1990;Yamashita *et al.*, 1995;Yue *et al.*, 1997). Both of these characteristics are most likely due to a smaller I_{K1} current in this region (Giles & Imaizumi, 1988;Wang *et al.*, 1998c).

The main distinguishing features of a SAN AP are its much more positive maximum diastolic potential of -50 mV and its Phase 4 depolarization (Bleeker *et al.*,

1980). These features allow the SAN to maintain its pacemaker dominance over other regions of the heart, a phenomenon termed overdrive suppression. SAN APs also have a much slower Phase 0 depolarization which is not carried by I_{Na} like in other regions, but rather by I_f and $I_{Ca,L}$ (DiFrancesco, 1993;Irisawa *et al.*, 1993;Zhang *et al.*, 2000). The more positive maximum diastolic potential is believed to be the result of a reduced I_{K1} expression (Guo *et al.*, 1997). The examples above briefly demonstrate how the heterogeneous expression of voltage-gated ion channels can have a profound effect on the shape and function of an AP in a given region of the heart.

1.3 Control of cardiac function

The heart is under the influence of the autonomic nervous system's sympathetic and parasympathetic branches. These two signalling pathways are able to elicit responses from the myocardium by affecting the functioning of many of the ionic currents which underlie the cardiac action potential. Normally, the two components have opposite effects: sympathetic nervous system increases heart rate and the force of contraction, while the parasympathetic system reduces these parameters. Sympathetic signalling is mediated by α and β subtypes of adrenergic receptors; while parasympathetic signalling is mediated by muscarinic cholinergic receptors. A schematic of this signalling is found in Figure 3. Adrenergic receptors are activated by adrenaline and noradrenaline, while muscarinic receptors are activated by acetylcholine. The one common feature among these two systems is that the receptors mediating cardiac control are all G-protein coupled receptors; however they differ in the types of secondary messenger/effectors they elicit after activation. β-adrenergic receptors are usually coupled to a $G\alpha_s$ protein which activates adenylate

cyclase (AC). In turn, adenylate cyclase catalyzes the conversion of ATP to cAMP which activates Protein Kinase A (PKA). Ultimately, the activated PKA is able to phosphorylate and activate its targets. α-adrenergic receptors have a similar signalling cascade; however they are coupled to a $G\alpha_q$ protein which activates phospholipase C (PLC). PLC is able to cleave inositol phospholipids into two secondary messengers, diacyglycerol (DAG) and inositol 1, 4, 5-trisphosphate (IP_3). IP_3 is able to increase intracellular Ca^{2+} levels by mediating the release of Ca^{2+} from the sarcoplasmic reticulum, while DAG and the elevated Ca^{+} activate Protein Kinase C (PKC). PKC acts much like PKA in phosphorylating ion channels, however the effects normally vary. Muscarinic receptors are coupled to $G\alpha_i$ proteins which act negatively on the same PKA signalling cascade as β-adrenergic receptors. $G\alpha_i$ proteins inhibit the activation of AC, and therefore would blunt its activation by β-adrenergic signalling. Other cardiac mediators such as angiotensin-II and endothelin also activate $G\alpha_q$ receptor subtypes and therefore elicit similar responses as α-adrenergic signalling.

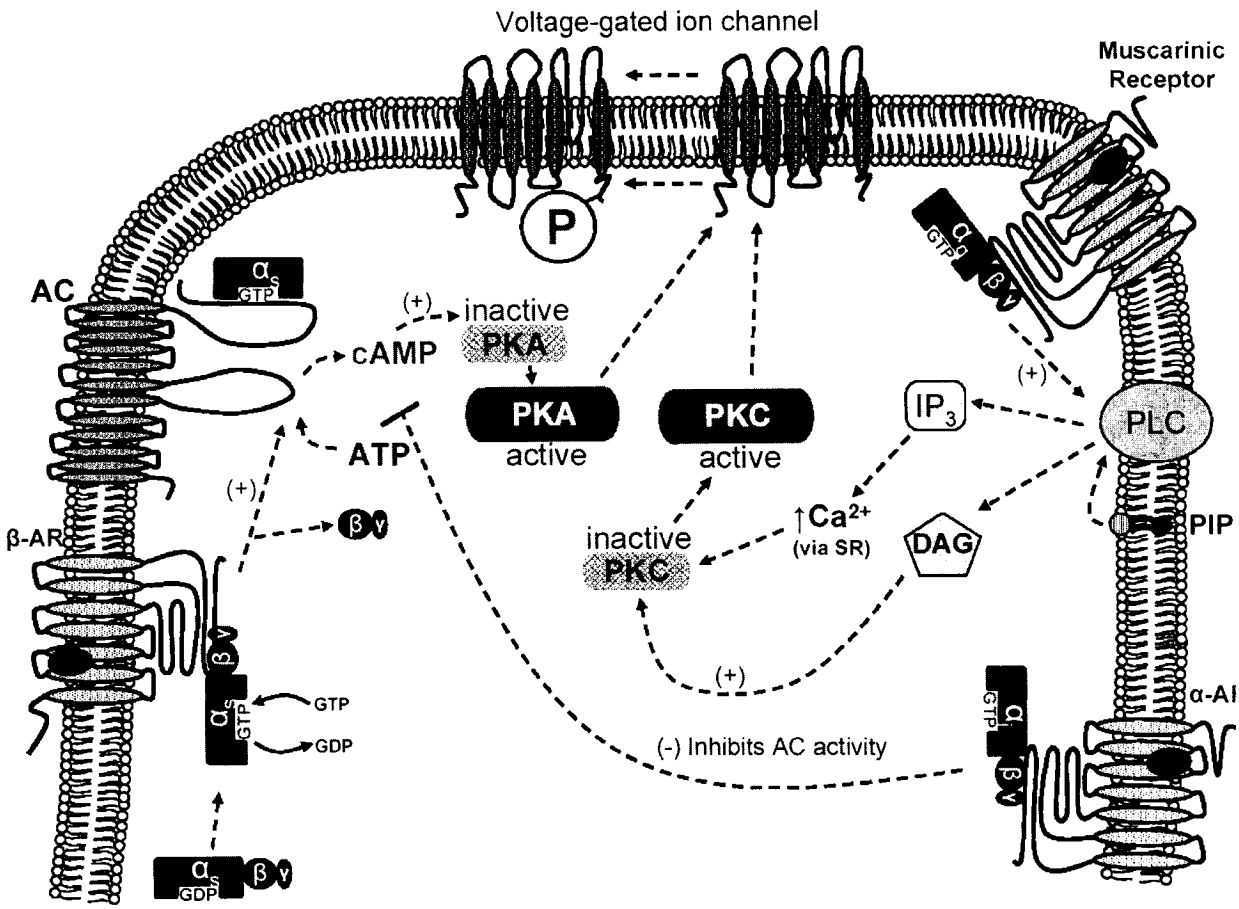

Figure 3. Schematic of G-protein coupled receptor mediated signalling pathways relevant to autonomic control of the heart. α-AR: α-adrenergic receptor; β-AR: β-adrenergic receptor; GDP: guanosine di-phosphate; GTP: guanosine tri-phosphate; ATP: adenosine tri-phosphate; cAMP: cyclic adenosine monophosphate; PKA: protein kinase A; PKC: protein kinase C; PLC: phospholipase C; IP_3: inositol 1, 4, 5-triphosphate; DAG: diacylglycerol; PIP_2: phospholipids.

2. Ionic currents underlying the AP

As it was mentioned above, many different ionic currents play a role in determining AP morphology. These currents can be divided into those which depolarize the myocardium due to an inward flux of positively charged ions, such as Na^+ currents; and those which repolarize the myocardium due to an outward movement of positive charged ions, such as K^+ currents. The study of such ion

currents was aided by the discovery of the patch-clamp technique and single cell isolation in the 1970's (Neher & Sakmann, 1976;Powell & Twist, 1976). By combining these two techniques, specific ion currents from single cardiac myocytes could be studied and characterized for the first time which has been paramount for the identification of novel pharmacological treatments of cardiovascular disease.

2.1 Depolarizing currents

Those currents which carry positive ions into a cell are depolarizing and render the transmural membrane potential more positive to -80 mV. The most common depolarizing currents found in the heart carry Na^+ or Ca^{2+} ions.

2.1.1 Sodium current (I_{Na})

The sodium current is responsible for the fast Phase 0 upstroke in the cardiac AP and is therefore important for rapid impulse conduction, especially in regions such as the atrium and the ventricles. The first cardiac electrophysiological studies were focused on Na^+ currents, most notably the studies of Hodgkin and Huxley who elucidated the fundamental properties of Na^+ channel function and fuelled modern channel theories (Hodgkin & Huxley, 1952). The basic properties of biphasic voltage-gated Na^+ channel function are activation and inactivation. Activation refers to the state of the channel when it is "open", while inactivation occurs when the channel closes during maintained depolarization. Two types of sodium current can be found in the heart and are divided based on their type of inactivation. The most commonly studied Na^+ current is the fast-inactivating I_{Na} which is responsible for cellular

depolarization. The slow-inactivating I_{Na} plays a greater role during the Phase 2 plateau and is important when considering the mechanisms of cardiac arrhythmias.

2.1.1.1 Fast I_{Na} electrophysiology

Before Hodgkin and Huxley derived their Na^+ channel theories, Weidmann demonstrated that Na^+ ions were responsible for the flow of positive inward charges during the initial spike of the AP (Weidmann, 1951). Still, the study of I_{Na} was hampered because of a lack of suitable control over changes in membrane potential in multicellular tissue preparations (Beeler & McGuigan, 1978;Fozzard & Beeler, Jr., 1975). Fast I_{Na} is a very large current which activates quickly, giving rise to depolarizations of 100–500 V/sec and a conduction velocity of 0.5-1.5 m/sec (Fozzard & Hiraoka, 1973). The first studies on I_{Na} were forced to use drastic, non-physiological conditions such as low extracellular Na^+ concentrations to reduce the size of the current and low temperatures to slow the kinetics of activation (Colatsky & Tsien, 1979). It wasn't until single cell isolation techniques were perfected that the proper characterization of fast I_{Na} could be made (Benndorf *et al.*, 1985;Bodewei *et al.*, 1982;Brown *et al.*, 1981;Bustamante & McDonald, 1983;Lee *et al.*, 1979). Fast I_{Na} current tracings are characterized by a sigmoidal shape during their activation and multi-exponential decay in both ventricular (Bodewei *et al.*, 1982;Brown *et al.*, 1981) and atrial (Bustamante & McDonald, 1983) cardiomyocytes. Fast I_{Na} is activated at a threshold of -70 to -60 mV, and a peak inward current at -30 mV in human atrial myocytes (Sakakibara *et al.*, 1992). The current-voltage relationships of activation have a half-activation potential of -38.9 ±0.9 mV and a slope factor of 6.5±0.1 mV. In addition, the half-inactivation potential is at -95.8±0.9 mV with a slope factor of

5.3±0.1 mV. Fast I_{Na} inactivates very quickly compared to its "late" counterpart, but slower than neuronal isoforms which are able to inactivate within 10 ms. The time course of I_{Na} inactivation is bi-exponential and voltage-dependent. Time constants for I_{Na} inactivation are 2 ms and 70 ms, with the slow component contributing 1-15% of total inactivation (Hanck & Sheets, 1992;Makielski *et al.*, 1987;Schneider *et al.*, 1994). Recovery from inactivation is voltage-dependent as well and is also fitted bi-exponentially with time constants of 16±10 ms and 53±33 ms (Schneider *et al.*, 1994). These properties are fairly well conserved across different regions and species such as humans (Schneider *et al.*, 1994), rats (Brown *et al.*, 1981), cats (Follmer *et al.*, 1987), and guinea pigs (Mitsuiye & Noma, 1992), which is testament to the importance of I_{Na} in the proper conduction of APs. More recently, the heterogeneous expression of I_{Na} throughout the heart has been characterized, with a larger I_{Na} in the guinea pig atrium compared to the ventricle (Li *et al.*, 2002b).

Cardiac Na^+ currents are easily differentiated from their neuronal counterparts by being tetrodotoxin (TTX) and saxitoxin (STX) insensitive. While neuronal Na^+ currents are easily blocked by nanomolar concentrations of TTX, the cardiac variants require micromolar concentrations (Brown *et al.*, 1981;Rogart, 1981;Rogart, 1986). Cardiac Na^+ channels are also more sensitive to cadmium and zinc (Frelin *et al.*, 1986) as well as the local anaesthetic lidocaine (Hanck *et al.*, 1994;Wright *et al.*, 1997).

2.1.1.2 Late I_{Na} electrophysiology

Unlike the fast I_{Na} which inactivates very quickly, late I_{Na} inactivates quite slowly. The nature of late I_{Na} is debatable, it is believed to actually be a different

gating mode of the same Na^+ channel described above. Supporting the hypothesis that late and fast I_{Na} are carried by the same channel, it was found that there was no difference between the conductance, voltage-dependence and TTX sensitivity in Na^+ channels which were active at the beginning of depolarization and those which remained open until the early repolarization phase around the plateau (Kiyosue & Arita, 1989;Liu *et al.*, 1992). It was believed that Na^+ channel gating is comprised of many different modes (Patlak & Ortiz, 1985). In opposition to this hypothesis, some experiments found late I_{Na} to have a different voltage-dependence of activation and sensitivity to TTX, so therefore two distinct channels must exist (Saint *et al.*, 1992). However, current theory suggests that late I_{Na} is carried by the same channels as the fast gating form.

Normally fast I_{Na} becomes quiescent during the plateau of the action potential and eventually recovers from this inactivation during the hyperpolarized diastolic period between AP stimuli. However, if the depolarization is prolonged or sustained, Na^+ channels may enter more stable, non-conducting conformational states which require more time during hyperpolarization to recover (Veldkamp *et al.*, 2000). The recovery time constant for late I_{Na} is greater than 1 second and is induced by depolarizations of ~60 sec. which is much longer than normal (Rudy, 1978). Late I_{Na} was first identified in Purkinje fibre experiments where low concentrations (10^{-7} M) of TTX were able to shorten phase 2 of the AP without affecting the V_{max} (an indicator of fast I_{Na} function) (Coraboeuf *et al.*, 1979). It was postulated that a second Na^+ current might exist which lacked inactivation. The importance of this observation was extended and in fact late I_{Na} may play a larger role than previously believed for the maintenance of the AP plateau (Wasserstrom & Salata, 1988;Zygmunt *et al.*,

2001), especially in the mid-myocardial layer of the ventricle. The ventricular transmural heterogeneity in late I_{Na} density may play a role in the dispersion of myocardial repolarization which is especially relevant when considering the development of cardiac arrhythmias (Antzelevitch, 2000;Marban, 1999;Sakmann *et al.*, 2000;Tomaselli & Marban, 1999;Zygmunt *et al.*, 2001).

Late I_{Na} has been described in ventricular myocytes of rabbits (Grant & Starmer, 1987), chick embryos (Liu *et al.*, 1992), guinea pigs (Sakmann *et al.*, 2000), dogs (Zygmunt *et al.*, 2001) and humans (Maltsev *et al.*, 1998). Its characteristics are also consistent throughout the different species with a threshold of activation at -80 mV and peak activation at -55 to -40 mV. Unlike fast I_{Na}, late I_{Na} can be blocked by 5 μM TTX (Eskinder *et al.*, 1993). Lidocaine also has a greater effect on late I_{Na} at lower concentrations than what are required to block fast I_{Na} (Wasserstrom & Salata, 1988).

2.1.1.3 Molecular determinants of I_{Na}

2.1.1.3.1 Sodium channel subunit topology and phylogeny

As mentioned above, although fast and slow I_{Na} are two separate electrophysiological entities, they are hypothesized to be the product of a single type of ion channel α-subunit. Na^+ channels were the first voltage-gated ion channels to be cloned and sequenced (Noda *et al.*, 1984). Using a radio-labelled TTX molecule, a large 220-250 kDa protein was identified as the major α-subunit underlying Na^+ channels in the electric eel (Agnew *et al.*, 1980). Subsequent experiments using similar techniques also found this subunit in chicken heart and in rat brain (Lombet & Lazdunski, 1984;Noda *et al.*, 1986). Today, cardiac Na^+ channels are known to be

composed of a single pore forming α-subunit and varying numbers of auxiliary β-subunits.

The nomenclature for Na^+ channel subunits has not been as structured as that of K^+ channel subunits until recently. Most voltage-gated K^+ channel subunits are classified according to the Kv annotation system: where "K" represents the ion which the subunit permeates and "v" indicates that this is regulated by voltage. Goldin et al. have proposed a new nomenclature for Na^+ channel subunits where the name of a channel is based on a similar $Na_vX.Y$ system. "X" represents the number of the gene subfamily and "Y" indicates the channel isoform. The isoform numbers have been arbitrarily assigned in the order in which they were discovered. Any splice variants of an isoform are indicated by a lower case letter after the numbers. There is only one subfamily identified to date ($Na_v1.Y$) with 9 different isoforms (Y=1 through 9) which are greater than 50% homologous in the transmembrane and extracellular domains. Figure 4 represents the phylogenic relationship of the different voltage-gated Na^+ channel isoforms based on the alignment of all amino acid sequences.

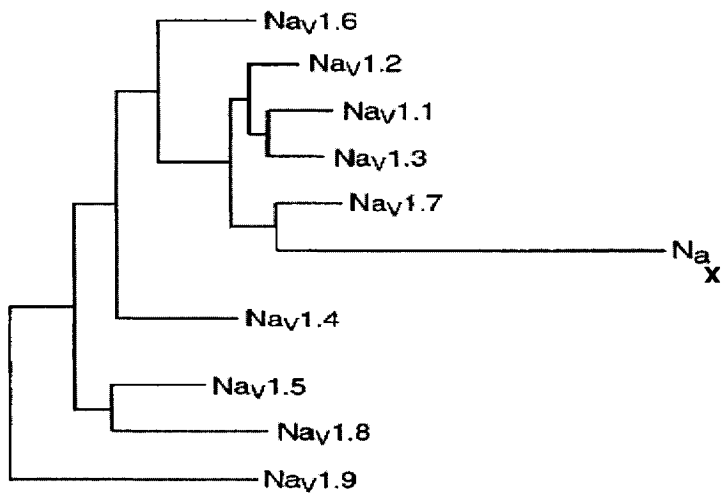

Figure 4. Phylogenic relationship of voltage-gated sodium channels in the rat (modified from (Catterall *et al.*, 2003)).

In addition to the nine α-subunit isoforms, there are four known β-subunits (β1 to β4) which are capable of modifying Na^+ channel gating and kinetics. Na_x is a newly found Na^+ channel-like protein in mice, rats and humans; however, it is not functionally expressed in heterologous cell lines. The full list of voltage-gated Na^+ channel subunits is shown in Table 1.

Table 1 Sodium channel α-subunits

Subtype	Former Name	Gene Symbol	Splice Variants	Tissue Location
$Na_v1.1$	rat I HBSCI GPBI SCN1A	SCN1A	$Na_v1.1a$	CNS PNS
$Na_v1.2$	Rat II HBSCII HBA	SCN2A	$Na_v1.2a$	CNS
$Na_v1.3$	rat III	SCN3A	$Na_v1.3a$ $Na_v1.3b$	CNS
$Na_v1.4$	SkM1 μ1	SCN4A		Skeletal muscle
$Na_v1.5$	SkM2 H1	SCN5A		Uninnervated skeletal muscle Heart
$Na_v1.6$	NaCh6 PN4 Scn8a CerIII	SCN8A	$Na_v1.6a$	CNS PNS
$Na_v1.7$	NaS hNE-Na PN1	SCN9A		PNS Schwann Cells
$Na_v1.8$	SNS PN3 NaNG	SCN10A		DRG
$Na_v1.9$	NaN SNS2 PN5 NaT SCN12A	SCN11A	$Na_v1.9a$	PNS
Na_vX	$Na_v2.1$ Na-G SCL11 $Na_v2.3$	SCN7A SCN6A		Heart, uterus, skeletal muscle, astrocytes, DRG

Adapted from Goldin et al., 2000

2.1.1.4 Cardiac sodium channel α-subunits

The composition of functional neuronal Na^+ channels is well defined, but the same cannot be said for the cardiac type. In the brain one α-subunit and two β-subunits form a functional channel. In the heart, one α-subunit is enough to form a functional channel (Catterall, 2000). The main cardiac isoform, $Na_v1.5$, has a molecular structure much like the other Na^+ channel α-subunit isoforms as shown in Figure 5.

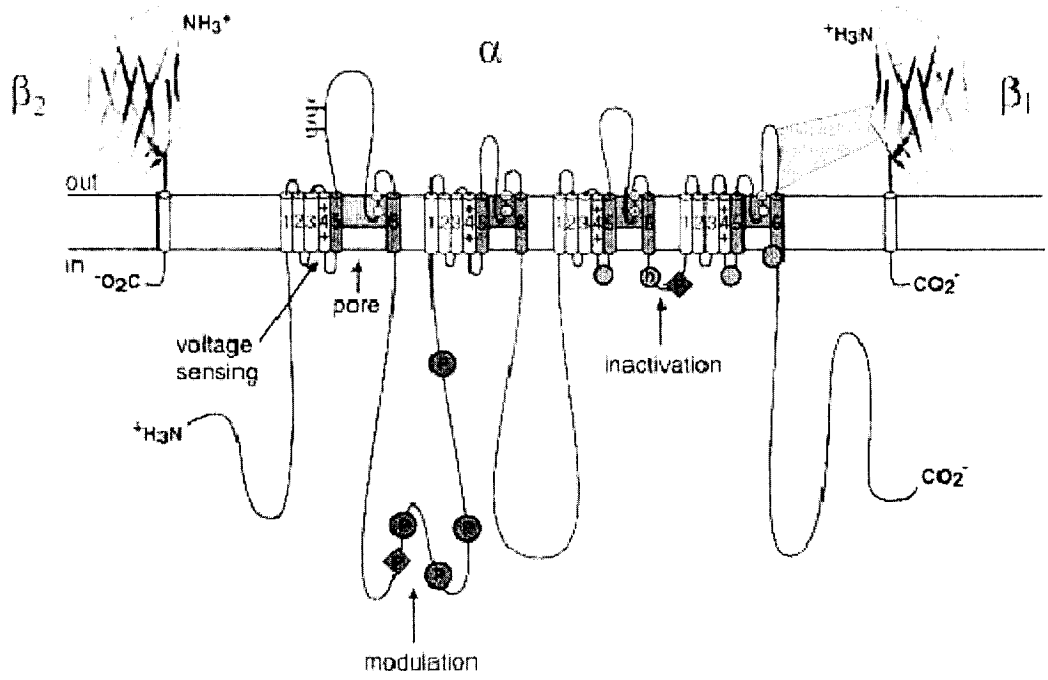

Figure 5. Topology of a voltage-gated Na^+ channel α-subunit (modified from (Catterall *et al.*, 2003)).

A typical Na^+ channel α-subunit has four structurally similar domains denoted as DI-DIV. Each domain contains six transmembrane spanning α-helices termed S1 to S6. This structure is very analogous to having 4 individual K^+ channel α-subunits connected by cytoplasmic linkers. The S4 segment in each domain contains a large number of positively charged amino acids which serve as a voltage sensor to regulate

channel activation and inactivation (Kontis *et al.*, 1997;Kontis & Goldin, 1997;Mitrovic *et al.*, 1998). The channel pore is formed by the P-loop region in between segments S5 and S6 (indicated in Figure 5 as "pore"). The sequence here is highly conserved among all species and tissue-specific isoforms. The heterologous nature of each P-loop in the different domains acts as a selectivity filter to permit Na^+ ions, and not others, to pass through. By mutating a lysine residue in the DIII P-loop (K1418), the critical selectivity for Na^+ is altered (Heinemann *et al.*, 1992;Perez-Garcia *et al.*, 1997). Regions in the DI P-loop also mediate divalent cation (Cd^{2+} and Zn^{2+}) binding and isoform-specific toxin (TTX and STX) affinity (Backx *et al.*, 1992;Satin *et al.*, 1992). Mapping studies of the pore have revealed that the relative position of each P-loop is asymmetrical and therefore have the possibility of individually defining ion permeation and drug binding (Chiamvimonvat *et al.*, 1996;Perez-Garcia *et al.*, 1996).

While the principal cardiac α-subunit subtype is believed to be $Na_v1.5$, other subtypes are expressed in the heart as well. The presence of $Na_v1.5$ and $Na_v1.1$ has been detected in rat, rabbit and mouse hearts (Baruscotti *et al.*, 1997;Dhar *et al.*, 2001;Petrecca *et al.*, 1997;Rogart *et al.*, 1989). $Na_v1.5$, or rH1 as it was termed, was first cloned in the rat heart (Rogart *et al.*, 1989), and then in the human heart (Gellens *et al.*, 1992). In both cases, this subtype was detected in the atria and ventricles, but not in the brain or skeletal muscle. When the hH1 (human $Na_v1.5$) subtype was expressed in *Xenopus* oocytes, a current with rapid activation and inactivation kinetics similar to native I_{Na} and resistant to TTX was detected. Further confirmation of $Na_v1.5$ being the predominant α-subtype came when cardiac diseases such as Long-QT Syndrome (LQTS), Brugada syndrome, conduction block and AV-block

were associated with mutations found in this Na^+ channel (Bezzina *et al.*, 1999;Chen *et al.*, 1998;Lupoglazoff *et al.*, 2001;Tan *et al.*, 2001;Wang *et al.*, 1995b).

Expression of $Na_v1.5$ is heterogeneous throughout the heart. mRNA expression, detected by Northern blot analysis in the sheep, is greater in the left atrium, right atrium and left ventricle compared to the right ventricle and Purkinje fibres. The expression within the left ventricle is variable as well, with a higher expression in the endocardium than the epicardium. The protein levels, as detected by Western blot, are higher in the left atrium and ventricle compared to the right (Fahmi *et al.*, 2001). Immunocytochemical experiments have shown the cellular distribution of $Na_v1.5$ is around the t-tubular system and the intercalated disks of ventricular myocytes, which is believed to allow the channels to be involved in the fast conduction of excitation impulses (Cohen, 1996;Maier *et al.*, 2004). These functional sodium channels are believed to aggregate in caveolin-rich membrane rafts which allow the channels to be coupled to regulatory adrenergic signalling (Yarbrough *et al.*, 2002).

As mentioned previously, $Na_v1.1$ is also detected in the rat heart (Schaller *et al.*, 1992), and two isoforms exist. Together, these represent a TTX-sensitive component in the heart. The relative expression of isoform $Na_v1.1a$ compared to $Na_v1.1$ is changed post-myocardial infarction such that it more resembles the fetal phenotype (Huang *et al.*, 2001). Two studies have examined the cellular organization of Na^+ channel subunits. The first identified $Na_v1.1$, $Na_v1.5$, $\beta1$ and $\beta2$ expression along the z-lines in adult rat and mouse cardiac myocytes (Dhar *et al.*, 2001). The second also demonstrated the expression of $Na_v1.5$ at the intercalated disks, whereas the neuronal subtypes $Na_v1.1$, 1.3 and 1.6 are located at the transverse tubules (Maier

et al., 2002;Maier *et al.*, 2004). Even though cardiac I_{Na} is not TTX sensitive, as one would expect if these channels did indeed contribute functionally to cardiac depolarization, small currents elicited from these channels can be elicited when scorpion β toxin is used to activate them. Low concentrations of TTX which are not supposed to affect $Na_v1.5$, do affect ventricular function, therefore it is believed that these neuronal forms may play a functional role, most probably in the coupling of electrical excitation to contraction (Maier *et al.*, 2002).

The two members of the atypical Na_x subtype, $Na_v2.1$ and $Na_v2.3$ are also expressed in the human heart and a mouse atrial tumour cell line (Felipe *et al.*, 1994;George, Jr. *et al.*, 1992;Shimizu *et al.*, 1991). These channels are considered "atypical" because some major features which are critical for normal Na^+ channel function are altered in these channels. Firstly, the S4 region of these channels lack some positive charges, therefore channel gating would be expected to be changed (Stuhmer *et al.*, 1989;Yang & Horn, 1995). Secondly, the sequence of the linker region between DIII and DIV is poorly conserved: an IFM motif is replaced with an IFI motif (Patton *et al.*, 1992;West *et al.*, 1992). These amino acids are critical for the fast inactivation of Na^+ channels. The effects of these differences are only hypothetical; no electrophysiological experiments have been conducted on these channels because there have been difficulties expressing them in a heterologous expression system (Akopian *et al.*, 1997;Felipe *et al.*, 1994).

2.1.1.5 Cardiac sodium channel β-subunits

Sodium channel β-subunits are not able to form ion-conducting channels by themselves, but rather modify the gating, kinetics and membrane localization of the

pore forming α-subunits. They may also be involved in interactions with cell adhesion molecules, cellular migration and aggregation (Isom, 2001). As mentioned above, four β subunit subtypes have been identified in the heart (Isom *et al.*, 1992;Isom *et al.*, 1995;Makita *et al.*, 1994;Morgan *et al.*, 2000). Furthermore, a splice variant of β1, termed β1A, has also been identified in the heart (Malhotra *et al.*, 2000). All are single transmembrane domain proteins with large extracellular domains and smaller cytosolic C-terminus (see Figure 5) (Stevens *et al.*, 2001). These auxiliary subunits assemble with the pore-forming α-subunits to form the final hetero-oligomeric complex and alter the gating, kinetics and amplitude of the expressed Na^+ current (Dhar *et al.*, 2001;Gordon *et al.*, 1988;Malhotra *et al.*, 2000;Wollner *et al.*, 1988).

Like most Na^+ channel proteins studied, the β1 subunit was originally identified in the rat brain (Isom *et al.*, 1992), but then was subsequently found in the human, mouse and rabbit brain (Belcher & Howe, 1996;Grosson *et al.*, 1996;McClatchey *et al.*, 1993). Its expression in the heart was only identified later (Makita *et al.*, 1994;Qu *et al.*, 1995), but there is still controversy over whether or not it contributes physiologically to cardiac I_{Na}. The original descriptions reported either no change in phenotype (Makita *et al.*, 1994), or an increase in current amplitude when co-expressed with $Na_v1.5$ in *Xenopus* oocytes (Qu *et al.*, 1995). It has also been reported that the co-expression of β1 with $Na_v1.5$ affects the resulting current in the same manner as neuronal Na^+ channel subtypes (Nuss *et al.*, 1995). Current hypotheses see the relevance of the β1 subunit changing developmentally, where it plays a greater role in mature cells, and has little function in immature cells. Mature cells are characterized by a slightly faster activation and inactivation which has been

attributed to the presence of the β1 subunit (Kupershmidt *et al.*, 1998). This is supported by four observations: firstly, when the mouse atrial tumour cell line (AT-1) is exposed to β1 antisense oligonucleotides, the resulting Na^+ current displayed a more immature phenotype compared to untreated cells (Kupershmidt *et al.*, 1998). This included a slower activation and inactivation, as well as a negative shift in the voltage dependence of inactivation. Secondly, a congenital Long QT mutation (LQT3) in $Na_v1.5$ results in an aspartate to glycine mutation at position 1790 and interferes with the proper co-association of α and β subunits as seen by electrophysiological changes (An *et al.*, 1998). Thirdly, the co-expression of β1 with $Na_v1.5$ reduces the resulting current's sensitivity to lidocaine, allowing it to recover faster from block (Bonhaus *et al.*, 1996;Makielski *et al.*, 1996). Lastly, β1 subunits, and not β2 subunits have been co-localized in the endoplasmic reticulum in HEK 293B cells, which facilitates this channel complex to be trafficked to the cell membrane (Zimmer *et al.*, 2002). There are some lines of evidence which would seem to contradict these observations, most notably the fact that β1 subunits are preferentially localized at the t-tubules in mouse cardiomyocytes, whereas $Na_v1.5$ is predominantly found at the intercalated disks (Maier *et al.*, 2002;Maier *et al.*, 2004).

The β1A splice variant of the β1 isoform contains an extra sequence derived from the retention of an intron in the genomic sequence and was first identified in the adrenal gland (Malhotra *et al.*, 2000). Like the β1 subunit, it appears that β1A may play a developmental role. While β1 is expressed in mature cell types, the opposite is true for β1A where is it detected during embryonic development. β1A has been found at the protein level in the heart, skeletal muscle and the adrenal gland, but not in the adult brain or spinal cord, with the expression the greatest in the heart and dorsal root

ganglia. No studies have looked at the effects of the heterologous expression this variant with $Na_v1.5$, however it has been expressed with $Na_v1.2$. This results in an increase in current density as well as subtle effects on current activation and inactivation (Qin *et al.*, 2003).

The $\beta 2$ subunit has also been cloned from the brain and then later identified in the heart as well (Eubanks *et al.*, 1997;Isom *et al.*, 1995). Little is known on the role of this subunit in the heart. Some reports have suggested it does not have any functional role (Dhar *et al.*, 2001), but it has been found to co-localize with $Na_v1.1$, $Na_v1.5$ and $\beta 1$. Furthermore, its sub-cellular localization seems to be around the intercalated disks, which is the same for $Na_v1.5$ (Maier *et al.*, 2004), as opposed to $\beta 1$ which is located at the t-tubules.

The $\beta 3$ subunit was first identified in the rat and human brain (Morgan *et al.*, 2000). It shares the most homology with the $\beta 1$ subunit, however it does not have the same homogenous distribution throughout the heart. Its mRNA and protein are primarily expressed in the ventricles, moderately in the Purkinje fibres, and least in the atria (Fahmi *et al.*, 2001). When co-expressed with $Na_v1.5$ in *Xenopus* oocytes, an increase in current density is observed which is similar to results with the co-expression of the $\beta 1$ subunit. However, an additional depolarizing shift in the steady-state inactivation with no difference in activation is also observed with the $\beta 3$ and not the $\beta 1$ subunit (Fahmi *et al.*, 2001). Both $\beta 1$ and $\beta 3$ auxiliary subunits affect the recovery from inactivation at -90 mV, however $\beta 1$ produces more of an effect.

A new $\beta 4$ subunit has recently been cloned from the rat brain and shares 35% homology with $\beta 2$ and only 20% with $\beta 1$ and $\beta 3$ (Yu *et al.*, 2003). Unlike the other β-subunits, when $\beta 4$ is co-expressed with either $Na_v1.2$ or $Na_v1.4$ in tsA-201 cells,

currents have a negative shift in the voltage-dependence of activation (Yu *et al.*, 2003). This effect was predominant over the effects of other β-subunits when both were expressed along with α-subunits. The β4 subunit has been identified in mouse ventricle and its localization is similar to that of β2 at the intercalated disks (Maier *et al.*, 2004). The functional importance of β4 is not completely understood at this point, however it has been suggested that it may contribute to the beneficial redundancy multiple β-subunits might offer in the event of the genetic or acquired loss of one of these members (Chen *et al.*, 2004).

While voltage-gated Na^+ channels were the first of this type of ion conducting channels to be discovered, many of the latest discoveries have come thanks to a better understanding of K^+ and Ca^{2+} channels. The exact molecular composition of cardiac I_{Na} is not yet known, but it is likely to be very diverse, especially when considering the different gating modes of Na^+ currents. The many possible permutations of different α-and β-subunits which are expressed in heart can contribute to the heterogeneity of cardiac Na^+ channel expression.

2.1.1.6 Physiological control of cardiac I_{Na}

The effects of autonomic control of cardiac I_{Na} are not completely clear. In terms of β-adrenergic signalling, I_{Na} has been found to be reduced in response to PKA activation (Ono *et al.*, 1993;Schubert *et al.*, 1989), but also increased by kinase stimulation (Gintant & Liu, 1992;Matsuda *et al.*, 1992). The reason for these discrepancies appears to lie within the individual methods used to record I_{Na}. By holding a cell at more positive potentials, there is an increased risk for misinterpreting the results due to a possible negative shift in the voltage dependence of inactivation.

In agreement with the later results, most studies have found an increase in I_{Na} with PKA stimulation in rat ventricular myocytes (Lu *et al.*, 1999) and in oocytes expressing human and rat clones of Na^+ channels (Frohnwieser *et al.*, 1997;Schreibmayer *et al.*, 1994). Normally one would expect the activation of PKA to increase channel activity by phosphorylating key residues on the channel complex, however it is unclear whether or not this happens for Na^+ channels. In agreement with this hypothesis, an increase in I_{Na} density and a negative shift in the voltage dependence of activation and inactivation were attributed partly to channel phosphorylation (Zhou *et al.*, 2000). At the same time, it has been proposed that PKA leads to an increase in the physical number of channels at the membrane (Lu *et al.*, 1999;Zhou *et al.*, 2000).

α-adrenergic signalling has also been implicated in modulating I_{Na} via PKC phosphorylation of a serine residue in the Na^+ channel III-IV linker region (Qu *et al.*, 1996). This phosphorylation results in altered channel conductance as well as altered channel gating (Benz *et al.*, 1992;Moorman *et al.*, 1989;Qu *et al.*, 1994;Watson & Gold, 1997). The actions of PKC and PKA are not constant amongst all the different Na^+ channel subtypes: for some, changes are readily noted by PKC or PKA activation, whereas in others no changes are seen (Frohnwieser *et al.*, 1997;Gershon *et al.*, 1992;Murphy *et al.*, 1996;Murray *et al.*, 1997;Schreibmayer *et al.*, 1994).

2.1.2 Hyperpolarization-activated current (I_f)

The hyperpolarization-activated current, also known as the pacemaker current or the "funny" current was first described in the 1970's (Noma & Irisawa, 1976a;Noma & Irisawa, 1976b;Tsien & Carpenter, 1978). It is responsible for the

maintenance of normal rhythmic activity in the heart and is also important for the sympathetic responsiveness of the myocardium (Bouman & Jongsma, 1986;DiFrancesco, 1995;Hauswirth *et al.*, 1968). It was believed a time-dependent current must exist in the SAN for its pacemaker activity; however the exact nature of this current was not known. It was hypothesized that the current could be either an activating Na^+ or a deactivating K^+ conducting channel. Evidence first citied in patch-clamp experiments indicated that it was in fact a K^+ carrying channel (Noble & Tsien, 1968;Peper & Trautwein, 1969;Vassalle, 1966), however it was not a deactivating channel. I_f was identified an inward K^+ current which was activated by hyperpolarization negative to the resting membrane potential of SAN cells of ~-50 mV (DiFrancesco, 1981;DiFrancesco & Ojeda, 1980). This hallmark feature enables I_f to generate diastolic depolarizations leading to spontaneous activity.

2.1.2.1 I_f electrophysiology

I_f was termed "funny" because of many unusual electrophysiological features. As mentioned above, it is activated at hyperpolarized membrane potentials with a threshold of -40/-50 mV in the SAN and a maximal activation at -100 mV (Cerbai *et al.*, 1999). The kinetics of I_f activation and deactivation are also very voltage-dependent: more negative potentials cause faster activation rate constants, while more positive voltages lead to faster deactivation. The fully activated pacemaker current has a reversal potential near -10/-20 mV, meaning it is permeable to both K^+ and Na^+ ions (DiFrancesco, 1993). However, the selectivity is four-fold higher for K^+ compared to Na^+ (Ho *et al.*, 1994;Wollmuth & Hille, 1992). I_f is sensitive to Cs^+ (Isenberg, 1976), but insensitive to Ba^{2+} (Yanagihara & Irisawa, 1980). These

properties may help in the identification of the exact molecular basis for I_f in normal cardiac tissue.

The SAN is heavily innervated by both sympathetic and parasympathetic nervous systems and its effects are partially mediated via I_f. Adrenaline, the main sympathetic neurotransmitter, causes a reversible increase in I_f density and increases the rate of activation (Brown *et al.*, 1979). This effect is extremely pertinent when considering the effects of increased sympathetic tone in cardiovascular diseases such as congestive heart failure (CHF) where heart rate is significantly increased and contributes to the pathogenesis of the disease. Adrenaline causes an increase in intracellular cyclic-adenosine-monophosphate (cAMP) levels via β-adrenergic receptors which are able to directly affect I_f channels (DiFrancesco, 1993). The binding of cAMP to the open state of I_f channels causes a positive shift of 11 to 14 mV in the activation curve and is phosphorylation independent.

2.1.2.2 Molecular determinants of I_f

Despite the fact that studies on I_f electrophysiology have taken place for several decades, the molecular determinants of I_f were not elucidated until recently (Santoro *et al.*, 1997). Pacemaker currents are believed to be carried by members of the hyperpolarization-activated cyclic nucleotide-gated (HCN) family of membrane proteins. These include members HCN1 (Moroni *et al.*, 2001), HCN2 (Vaccari *et al.*, 1999), and HCN4 (Ishii *et al.*, 1999) in the heart. These subunits have the typical voltage-gated K^+ channel topology which contain six-transmembrane spanning domains and arrange in tetramers to form active channels (see Figure 3 in the section on topology of K^+ channels). The first HCN family member was cloned from the

mouse brain using a yeast two-hybrid technique to find proteins which interacted with the SH3 binding domain of a neural N-Src protein (Santoro *et al.*, 1997). Later, other family members were identified based on homology with this first channel. Another defining feature of HCN subunits is their cyclic nucleotide-binding domain located on the carboxy-terminus (Wainger *et al.*, 2001) which allows the channels to bind cyclic nucleotides such as cAMP and cGMP and is necessary for HCN channels' response to adrenergic signalling. Each of the HCN subunits found in the heart differ in their rates of activation and deactivation. HCN1 is known to have the fastest kinetics of activation, while HCN4 has the slowest and HCN2 is in between (Altomare *et al.*, 2001). The half-maximal voltage of mean activation ($V_{1/2}$) for HCN1 is reported to be -73 mV, -92 mV for HCN2, and -81 mV for HCN4 (Chen *et al.*, 2001;Ishii *et al.*, 1999;Ludwig *et al.*, 1998;Moroni *et al.*, 2000;Ulens & Tytgat, 2001). The binding of cAMP to HCN subunits results in a positive shift in the activation curve, however not all family members are affected equally. A maximum shift of 2-6.7 mV has been found for HCN1, 12-15 mV for HCN2, and 15.2-23 mV for HCN4 (Ishii *et al.*, 1999;Ludwig *et al.*, 1998;Moroni *et al.*, 2000;Moroni *et al.*, 2001;Santoro *et al.*, 1997;Santoro *et al.*, 1998).

The expression of HCN subunits varies across species. Early studies in humans found that no HCN1 was expressed (Ludwig *et al.*, 1999), however it is readily expressed in rabbit and mouse SAN (Moosmang *et al.*, 2001;Moroni *et al.*, 2001;Shi *et al.*, 1999). In addition, HCN4 is the predominant subunit expressed in rabbit and mouse SAN (Moosmang *et al.*, 2001;Shi *et al.*, 1999); while rabbit SAN contains more HCN4 than the atrium (Ishii *et al.*, 1999), consistent with its function as a pacemaker.

The kinetic characterization of each subunit is especially relevant when considering that none are able to recapitulate native I_f individually. For example, cAMP induces an 11-14 mV positive shift in the activation curve of native I_f (Accili *et al.*, 1997), which is not found for any of the individual HCN subunits. Recently, HCN subunit heteromerization has been detected between HCN1/HCN2 (Ulens & Tytgat, 2001) and HCN1/HCN4 (Altomare *et al.*, 2003) subunits. Additionally, the auxiliary β-subunit MiRP1 (see section on I_{Kr}) has been found to interact with all members of the HCN family expressed in the heart (Decher *et al.*, 2003;Qu *et al.*, 2004;Yu *et al.*, 2001), resulting in faster activation kinetics as well as expression changes. These findings complicate the study of the relationship between subunit expression and the native pacemaker current.

2.1.2.3 Physiological control of I_f

Consistent with its role as a pacemaking current, I_f is modulated by adrenergic stimulation. Since the SAN is heavily innervated and I_f is highly expressed in this region, its modulation confirms the importance of I_f for the maintenance of cardiac rhythm. HCN subunits contain a cyclic nucleotide binding domain in the C-terminus, and therefore I_f gating is regulated by cyclic nucleotides like cAMP. After β-adrenergic stimulation, cAMP levels increase after a $G\alpha_s$ subunit induces adenylate cyclase to catalyze its conversion from ATP. cAMP does not directly activate channels, but rather shifts the activation curve to more positive potentials so that activity is increased. Normally this binding domain inhibits channel gating, but when cAMP is bound a conformational change occurs so that channel gating is unimpeded (Wainger *et al.*, 2001). Increased I_f may underlie ectopic tachycardias, particularly in

situations of increased adrenergic drive. β-adrenergic blockade antagonizes adrenergically-induced I_f augmentation and can thereby suppress ectopic tachycardias.

2.2 Repolarizing currents

The fast influx of positively charged Na^+ ions during Phase 0 causes the membrane potential to become more positive and triggers the activation of a whole set of other voltage-sensitive ion channels. These currents will help shape the cardiac action potential on its way back to a resting membrane potential usually around -80 mV. One of the defining characteristics of a cardiac action potential is its delayed repolarization, which is in contrast to action potentials from the nervous system which repolarize very quickly. The delayed repolarization allows the cardiac myocardium to couple the wave of excitation to contraction.

2.2.1 Potassium currents

Voltage-gated K^+ currents are probably the most important group of ion channels in the heart in terms of regulating cardiac function. They are the most diverse group of ion channels in the heart and each has unique pharmacological, time- and voltage-dependent properties. Together, they help regulate the amplitude of the action potential, the heart rate by setting the resting membrane potential, and determine the duration of the action potential and by extension its refractoriness (Barry & Nerbonne, 1996;Nerbonne, 2000;Roden & Kupershmidt, 1999;Snyders, 1999). They also help mediate the sympathetic and parasympathetic control of the heart and are the targets of Class III anti-arrhythmic drugs. The transient outward current, I_{to}, and the delayed rectifier currents, I_K, are two of the main repolarizing K^+

currents in the heart. Others include the ultra-rapid delayed rectifier current, I_{Kur}, the inward rectifiers (I_{K1}), and the acetylcholine-sensitive and ATP-sensitive rectifying currents, I_{KACh} and I_{KATP}.

2.2.1.1 Topology and phylogeny of voltage-gated K^+ channels

The first K^+ channel subunit was cloned from the *Drosophila* fruit fly (Papazian *et al.*, 1987), and now there are over 200 genes that have been discovered which encode K^+ channel subunits. Although their structures differ, the one constant amongst all these genes is that they contain an amino acid sequence within the pore region which is able to select for K^+ ions (Hartmann *et al.*, 1991;Yellen *et al.*, 1991). Currently, there are three different types of K^+ channels: 1) voltage-gated K^+ channels with the characteristic six-transmembrane spanning domains; 2) four-transmembrane domain channels with two pore regions (4-TM); and 3) the inward rectifier K^+ channels which only have two transmembrane domains and a single pore. All of the K^+ channels discussed in this thesis are of the first voltage-gated type.

Typically, the α-subunits are given a name based on the "Kv" system (which the newer Na^+ channel nomenclature was based upon). The "K" refers to the chemical symbol of the ion which these channels normally conduct, while the small case "v" refers to the fact that these channels are activated by voltage. Table 2 lists the names and genes of the channel subunits which shall be discussed here.

Table 2: Nomenclature of Voltage-gated K^+ channel subunits

Channel Type	Gene	Nomenclature	Modulators	Location
Shaker (Kv channels)	KCNA1	Kv1.1	α-DTX, HgTX1	Neurons, Heart
	KCNA2	Kv1.2	CTX, α-DTX	Brain, Heart
	KCNA3	Kv1.3	AgTX2, α-DTX	Lymphocytes
	KCNA4	Kv1.4	UK78282	Brain, Heart
	KCNA5	Kv1.5	4AP, clofilum	Brain, Heart
	KCNA6	Kv1.6	α-DTX	Brain
	KCNA7	Kv1.7	4AP, capsaicin	Heart
Shab (Kv channels)	KCNB1	Kv2.1-2	Hanatoxin, TEA	Brain, Heart, Kidney, Retina
Shaw (Kv channels)	KCNC1	Kv3.1	4AP, TEA	Brain, Muscle
	KCNC2	Kv3.2	4AP, TEA	Brain
	KCNC3	Kv3.3	4AP, TEA	Brain, Liver
	KCNC4	Kv3.4	4AP, TEA	Brain, Muscle
Shal (Kv channels)	KCND1	Kv4.1	4AP	Brain, Heart
	KCND2	Kv4.2	4AP, PaTX	Brain, Heart
	KCND3	Kv4.3	4AP, PaTX	Heart, Brain
Ether-a-go-go (EAG)	KCNH1	ERG	E4031, dofetilide	Brain
	KCNH2	hERG		Brain, Heart
	KCNH3	BEC1		Brain
	KCNH4	BEC2		Brain
KvLQT1	KCNQ1	KvLQT1	Chromanol-293B	Heart, Kidney
	KCNQ2	KvLQT2		Brain, Neuron
	KCNQ3	KvLQT3	TEA, L735,821	Brain, Neuron
	KCNQ4	KvLQT4	TEA, linopirdine	Hair cell
	KCNQ5	KvLQT5	linopirdine	Brain, Muscle
β-subunits	KCNAB1	Kvβ1		Brain (1.1), Heart (1.2)
	KCNAB2	Kvβ2		
	KCNAB3	KvB3		Brain, Heart
	KCNE1	minK		Brain
	KCNE2	MiRP1		Heart, Kidney
	KCNE3	MiRP2		Heart
	KCNIP2	KChIP2		Muscle
				Heart

All the α-subunits listed in Table 2 share the same characteristic six-transmembrane domain topology (Figure 6) where the six domains are annotated S1-S6 and the pore is located between the S5 and S6 domains (P-loop). These individual subunits are believed to arrange in tetramers with four pore loop containing α-subunits (MacKinnon, 1995;MacKinnon & Doyle, 1997). The P-loop regions contain the signature G(Y/F)G motif for K^+-ion selectivity. The outer region of the pore is composed of portions from the P-loop as well as adjacent regions of the S5 and S6 domains and this serves as a binding site for many toxins or pharmacological agents (Goldstein & Miller, 1993;MacKinnon *et al.*, 1988;MacKinnon & Yellen, 1990;Pascual *et al.*, 1995;Yellen *et al.*, 1991). The inner pore region which consists of residues from the S5 and S6 domains contains binding sites for some of the common tools used to differentiate voltage-gated K^+ channel subunits such as 4-AP and tetraethylammonium (TEA).

The S4 domain contains 5-7 strategically placed positively charged amino acids which are believed to be responsible for voltage sensing properties of these channels. Some residues in the S2 region are believed to play a role as well (Seoh *et al.*, 1996). Biophysical studies have demonstrated that membrane depolarizations trigger the outward movement of the S4 region which leads to other conformational changes which open the channel pore.

The intracellular N-terminus of the voltage-gated K^+ channel also plays an important role in ion conduction. After the channels are activated, most go into a stable, non-conducting state known as the inactivated state. This is normally accomplished by the "ball and chain"-like N-terminus moving to block to open cytoplasmic side of the pore. This N-type inactivation is usually very fast (Hoshi *et*

al., 1990;Isacoff *et al.*, 1991). Aside from N-type inactivation, there also exist C- and P- types, however these are slower and involve more components of the outer pore and specific residues within the pore as well (De Biasi *et al.*, 1993;Liu *et al.*, 1996;Yellen *et al.*, 1994).

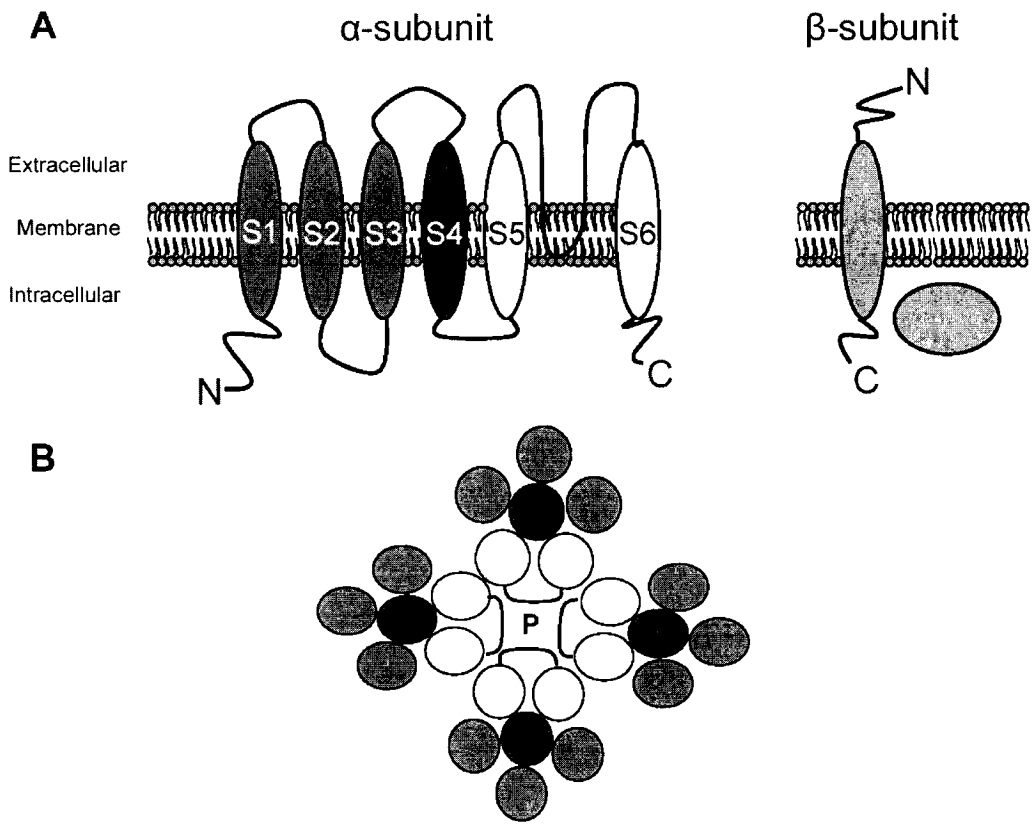

Figure 6. A. Topology of a typical voltage-gated K^+ channel subunit with six-transmembrane spanning domains. B. Arrangement of four subunits in pore forming tetramer.

The β-subunits as listed in Table 2 usually associate with the pore-forming α-subunit and alter its kinetics, cell surface expression and trafficking. These subunits can be either single transmembrane domain proteins or intracellular proteins which interact with the main channels, possibly as chaperones. The possibility of having different possible β-subunits associate with channel complexes adds to heterogeneity

of the various K^+ channels and can ultimately contribute to the diversity of action potential morphologies.

2.2.2 Transient outward current (I_{to})

I_{to} is responsible for the brief repolarization in Phase 1 of the cardiac action potential, right after the fast depolarization caused by I_{Na} and before the plateau phase. The "spike and dome" morphology typical of a ventricular epicardial action potential is believed to be the result of the rapid activation and inactivation of this outward current, followed by the activation of Ca^{2+} during the plateau (Boyett, 1981a;Boyett, 1981b;Giles & Imaizumi, 1988). The current is termed "transient" because of its fast activation and then inactivation after membrane depolarization, and "outward" because of the efflux of positively charged K^+ ions. An I_{to}-like current was first identified in neurons and was called the A-type current (I_A) (Hagiwara *et al.*, 1961). A cardiac counterpart was first discovered in Purkinje fibre cells (Dudel *et al.*, 1967). However, the study was complicated by the later finding of two transient outward-like currents (Coraboeuf & Carmeliet, 1982;Kenyon & Gibbons, 1979a;Kenyon & Gibbons, 1979b). These two currents were termed I_{to1} and I_{to2} respectively. There were questions, however, on the exact nature of the ions which were carried by these channels, and the initial lack of suitable techniques to quantitatively asses the currents did not help (Kenyon & Gibbons, 1979a;Kenyon & Gibbons, 1979b;Siegelbaum & Tsien, 1980;Zygmunt & Gibbons, 1991;Zygmunt & Gibbons, 1992). Today, it is understood that there are two repolarizing transient outward currents: I_{to1} is the most common one which is 4-aminopyridine (4-AP) sensitive and Ca^{2+}-independent, while what was previously termed I_{to2} is now known as a 4-AP resistant Ca^{2+}-activated

chloride current. The complicated story continues and now I_{to} can be divided according to its inactivation kinetics into $I_{to,fast}$ and $I_{to,slow}$ (Brahmajothi *et al.*, 1999;Xu *et al.*, 1999a).

2.2.2.1 I_{to} electrophysiology

One defining characteristic of I_{to} is its time-dependent fast activation and inactivation. The amount of time required to reach the maximal current is in the order of milliseconds to tens of milliseconds (Yue *et al.*, 1996). As stated above, I_{to} can be divided into a fast-inactivating component which has time constants for inactivation in the order of tens of milliseconds, and a slow-inactivating component whose constant is in the order of hundreds of milliseconds. Furthermore, the inactivation can be fitted by mono-exponential and bi-exponential functions (Campbell *et al.*, 1993b;Li *et al.*, 1998b;Nabauer *et al.*, 1996).

Both components are believed to have a similar linear current-voltage relationship. The threshold for activation is in the range of -40 to +10 mV and the $V_{1/2}$ ranges from -12 to +22 mV (Nabauer *et al.*, 1993). The voltage-dependent steady-state inactivation occurs between -70 and -10 mV, while the $V_{1/2}$ for inactivation is between -50 and -15 mV (Nabauer *et al.*, 1993;Shibata *et al.*, 1989;Yue *et al.*, 1996). There is some discrepancy on the single channel conductance of I_{to}, depending on the study it is believed to range from 4 to 20 pS (Campbell *et al.*, 1993b;Nakayama & Irisawa, 1985). This may be due to the fact that the two components of I_{to} were not identified in earlier studies.

After inactivation, a slight delay occurs before a channel is capable of being activated again. This phenomenon is termed the recovery from inactivation and is

voltage dependent. When a more positive holding potential is used, the recovery slows (Han *et al.*, 2000;Li *et al.*, 2000a). Furthermore, I_{to} with slow recovery kinetics shows very strong frequency dependence where the current amplitude decreases as the time between stimulations decreases (the frequency increases). This is especially evident in the rabbit atrium and ventricle (Giles & Imaizumi, 1988), dog ventricular endocardium and Purkinje fibres (Tseng & Hoffman, 1989), and sheep Purkinje fibres (Boyett, 1981a;Boyett, 1981b).

2.2.2.2 Species and regional differences in I_{to}

As mentioned in the previous section, there are some discrepancies concerning some of the electrophysiological attributes of I_{to}. This is partly due to the use of different species for exploring these properties. I_{to} has been studied in cat ventricles (Furukawa *et al.*, 1990), dog ventricles (Litovsky & Antzelevitch, 1988;Tseng & Hoffman, 1989) and atrium (Yue *et al.*, 1996), ferret ventricles (Campbell *et al.*, 1993b;Campbell *et al.*, 1993a), human ventricles (Amos *et al.*, 1996;Kaab *et al.*, 1998;Konarzewska *et al.*, 1995;Nabauer *et al.*, 1996;Wettwer *et al.*, 1993;Wettwer *et al.*, 1994) and atrium (Escande *et al.*, 1987;Fermini *et al.*, 1992;Shibata *et al.*, 1989), mouse ventricle and atrium (Xu *et al.*, 1999b;Xu *et al.*, 1999a); and rat ventricle (Apkon & Nerbonne, 1991;Himmel *et al.*, 1999;Wickenden *et al.*, 1999c;Wickenden *et al.*, 1999a) and atria (Boyle & Nerbonne, 1991;Boyle & Nerbonne, 1992). One interesting fact is that I_{to} has not been recorded from guinea pig myocytes and these cells are therefore believed to lack this current which seems to be ubiquitous in other closely related species (Sanguinetti & Jurkiewicz, 1990;Sanguinetti & Jurkiewicz, 1991). An I_{to}-like current is found in this species

when extracellular Ca^{2+} is removed, but it does not have all the properties of a characteristic I_{to} (Inoue & Imanaga, 1993), and is most likely some type of chloride current.

Even amongst the species where I_{to} has been found, it has varying properties. Rabbit I_{to} typically has slow reactivation kinetics which is very characteristic for this species (Fermini *et al.*, 1992;Wang *et al.*, 1999). The density of I_{to} in rabbits, as well as rats and human, is much larger in the atrium than the ventricle (Boyle & Nerbonne, 1992;Giles & Imaizumi, 1988;Varro *et al.*, 1993), but the opposite it true for mice (Xu *et al.*, 1999b). Differences can be found even within a species. Rat atrial myocytes have a slower inactivation and recovery from inactivation component which is not seen in ventricular myocytes (Apkon & Nerbonne, 1991;Boyle & Nerbonne, 1992). Larger mammals such as dogs and humans have a distinct I_{to} transmural gradient across the ventricular wall. Epicardial I_{to} has a much larger peak current density and faster recovery kinetics compared to endocardial myocytes in the left ventricle (Kaab *et al.*, 1998;Li *et al.*, 1998a;Liu *et al.*, 1993;Nabauer *et al.*, 1996). This gradient is also seen in the ferret (Brahmajothi *et al.*, 1999). Right ventricular I_{to} consistently has a much greater density than left ventricular in dog and humans as well (Di Diego *et al.*, 1996;Volders *et al.*, 1999a). These regional differences play a large role in determining the different action potential morphologies in the epicardium and endocardium and leads to a more synchronous repolarization throughout the ventricles (Antzelevitch *et al.*, 1991;Baker *et al.*, 2000;Burgess, 1979). In addition, the heterogeneity may contribute to the dispersion of the action potential in a disease setting which can lead to arrhythmogenic events as will be shown in latter sections.

2.2.2.3 Molecular determinants of I_{to}: α-subunits

Identifying the exact molecular basis for I_{to} has proven to be a great challenge. Due to the diversity in the nature of I_{to} depending on the region or species, various clones have been hypothesized to under this current. Conversely, the differing properties of I_{to} currents in different species can be a consequence of which α-subunits they might express. Currently, it has been proposed that I_{to} is not encoded by a single specific α-subunit, but possibly by multiple α-subunits depending on the region and species, and β-subunits play a large role in modifying biophysical properties (McKinnon, 1999). The fast and slow components of I_{to} are believed to have their own distinct molecular makeup. Currently, Kv1.4, Kv3.4, Kv4.2 and Kv4.3 are believed to be the major determinants of I_{to} since all express I_{to}-like currents when heterologously expressed. They all share similar biophysical properties, including kinetics, ion selectivity, conductance and voltage-dependence, with native I_{to}. In addition, they have similar pharmacological profiles in terms of being 4-AP sensitive and are all detectable in cardiac myocytes. In most cases, antisense or gene knockout of these subunits leads to a loss of I_{to} current.

Fast-inactivating I_{to} is believed to be encoded by Kv4.2 and Kv4.3 subunits. Antisense oligonucleotides directed against Kv4.2 significantly decreased I_{to} currents in rats and rabbits (Bou-Abboud & Nerbonne, 1999;Fiset *et al.*, 1997;Wang *et al.*, 1999), while Kv4.2 transgenic mice had altered I_{to} properties (Barry *et al.*, 1998;Guo *et al.*, 2000;Wickenden *et al.*, 1999b). Therefore Kv4.2 is believed to underlie $I_{to, fast}$ in most rodents such as mouse, rat, rabbit and ferret. Further evidence comes from examining the expression of these subunits in the different regions which demonstrate unique I_{to} properties. Rat left ventricles show a transmural I_{to} gradient (Dixon &

McKinnon, 1994;Wickenden *et al.*, 1999a), however Kv1.4 and Kv4.3 mRNA expression remains constant throughout the ventricle. Only Kv4.2 expression varies across the ventricular wall where it is greatest in the epicardium and lowest in the endocardium (Dixon & McKinnon, 1994). On the other hand, Kv4.3 is believed to form $I_{to,\ fast}$ channels in larger mammals such as dogs and humans (Dixon *et al.*, 1996).

Kv1.4 shows slower inactivation kinetics and is believed to underlie $I_{to,\ slow}$ in most species (Beck *et al.*, 1998). Similar to experiments for Kv4.2, antisense directed against Kv1.4 reduced I_{to} in rabbit atrial myocytes (Wang *et al.*, 1999), and gene knockout resulted is a loss of $I_{to,\ slow}$ in mice (Guo *et al.*, 2000;London *et al.*, 1998). The different I_{to} currents have also been well characterized in the ferret, and all three subunits seem to underlie the regional differences of $I_{to,\ fast}$ and $I_{to,\ slow}$ in this species (Brahmajothi *et al.*, 1999). Still, all of these individual α-subunits are unable to completely recapitulate native I_{to} properties and knockout/antisense experiments are still not conclusive. The treatment of rabbit atrial myocytes with Kv1.4 antisense oligonucleotides resulted in only a partial reduction of I_{to}, while larger decreases were seen when Kv4.2 and Kv4.3 antisense were used (Wang *et al.*, 1999). Such difficulty in recapitulating native I_{to} makes a stronger case for the importance of accessory β-subunits in the channel complex.

2.2.2.4 Molecular determinants of I_{to}: β-subunits

There have been many different β-subunits which have been found to associate with I_{to} subunits in the heart and increase the functional diversity of this K^+ current in the heart. The first group of auxiliary subunits identified were the Kvβ types which were cloned from the bovine brain after they were found to associate

with the neuronal DTX receptor (Scott *et al.*, 1994). Homology searches later identified three members of this family: Kvβ1 and Kvβ2 from the rat brain (Rettig *et al.*, 1994), and Kvβ3 from the ferret (Morales *et al.*, 1995) and human heart (England *et al.*, 1995;Majumder *et al.*, 1995). Kvβ1 and β2 were found to increase Kv4.3 current density and Kv4.3 protein expression (Yang *et al.*, 2001), and increase the rate of inactivation of Kv1.4 (Rettig *et al.*, 1994). Similarly, Kvβ2 and β3 also increase the rate of inactivation of human and ferret Kv1.4 currents (Majumder *et al.*, 1995;Morales *et al.*, 1995).

While the Kvβ subunits contain transmembrane domains, KChAP is believed to modulate Kv channels via cytoplasmic interactions (Wible *et al.*, 1998). KChAP is actually related to a family of transcription factor binding proteins and has been co-immunoprecipitated along with Kv4.3 from rat hearts (Kuryshev *et al.*, 2000). When Kv4.3 is co-expressed with KChAP, the resulting currents have increased amplitude compared to Kv4.3 alone while the current's kinetics and gating are unaltered (Kuryshev *et al.*, 2000;Wible *et al.*, 1998). Due to the fact that KChAP is a cytoplasmic protein and does not change any kinetic parameters of the channels it associates with, it is believed to be a chaperone which helps direct channel complexes to the cell surface. The one major question concerning KChAP is that physiological interactions have not been demonstrated, possibly diminishing its contribution *in vivo* since it is not known whether the interactions observed are simply a artefact of *in vitro* manipulations. Other cytoplasmic proteins have also been shown to interact with I_{to} subunits. The Ca^{2+}-binding protein frequenin is also expressed in the heart and increases I_{to} density, slows Kv4.2 inactivation and accelerates its recovery from inactivation in a Ca^{2+}-dependent manner (Nakamura *et al.*, 2001). Filamin is also a

cytoplasmic protein which interacts with Kv4.2 and the cellular cytoskeleton. It is believed to play more of a scaffolding function in regulating Kv4.2 currents (Petrecca *et al.*, 2000).

In terms of I_{to} auxiliary subunits, most attention is now given to the KChIP family of proteins. These Kv Channel Interacting Proteins interact with the cytoplasmic N-terminus of Kv4 α-subunits and are related to a family of Ca^{2+}-binding proteins. When co-expressed with Kv4 subunits, they have multiple effects including increasing current density, slowing current inactivation, accelerating the recovery from inactivation, and shifting the voltage-dependence of inactivation (An *et al.*, 2000;Decher *et al.*, 2001). The three KChIP family members were first identified by using the N-terminus of Kv4.3 as bait in a yeast two-hybrid screen, however only KChIP2 is readily expressed in the heart (Patel *et al.*, 2002;Rosati *et al.*, 2001). KChIP2 has been found to be expressed in rat and mouse (Ohya *et al.*, 2001), dog (Rosati *et al.*, 2001), and human hearts (Ohya *et al.*, 2001;Rosati *et al.*, 2001). When KChIP2 is co-expressed with rat or human Kv4.2 or Kv4.3, the resulting currents resemble native I_{to} from rat (An *et al.*, 2000;Bou-Abboud & Nerbonne, 1999;Wickenden *et al.*, 1999c) and human epicardium (Decher *et al.*, 2001). However, there still remains some controversy over how much of a functional role KChIP2 might play, especially in determining the observed ventricular I_{to} transmural gradient (Li *et al.*, 1998a;Liu *et al.*, 1993;Nabauer *et al.*, 1996). It was originally thought that since Kv4.3 expression was believed to be constant throughout the ventricle, varying KChIP2 expression might underlie this gradient (Rosati *et al.*, 2001). Contradicting observations related to KChIP2 protein expression has put this hypothesis to question (Deschenes *et al.*, 2002;Rosati *et al.*, 2003). Still, the

importance of KChIP2 in the recapitulation of native I_{to} has been proven by examining KChIP2 knockout mice (Kuo *et al.*, 2001). While these KChIP2-/- mice had no structural abnormalities or arrhythmias, they lacked I_{to} currents and had prolonged action potential duration. When stimulated by programmed electrical pulses, a non-sustained polymorphic ventricular tachycardia was seen in most of these knockout mice, but not in any wild type mice. Therefore it has been postulated that the genetic loss of I_{to} can confer susceptibility to ventricular tachyarrhythmias which often degenerates into sudden death (Sanguinetti, 2002).

2.2.2.5 Physiological control of I_{to}

Like most ionic currents in the heart, I_{to} is also under the control of physiological regulators; however the exact adrenergic effects are unclear (Nakayama & Fozzard, 1988). Chronic treatment with β-adrenergic receptor antagonists is believed to result in the downregulation of I_{to} and increase the APD (Workman *et al.*, 2003). However, forskolin and 8-bromo-cAMP are able to increase I_{to} amplitude, reduce the amplitude of the fast inactivation time constant and increase the amplitude of the slow inactivation time constant (without altering the time constants themselves) (Nakayama *et al.*, 1989). This would suggest that PKA is somehow involved in this process; however the activation of PKA by forskolin or isoproterenol in feline ventricular myocytes did not affect I_{to}.

The acute application of α-adrenergic receptor agonists also causes the reduction of I_{to} in adult rat ventricular myocytes (Apkon & Nerbonne, 1988;Fedida & Bouchard, 1992;Tohse *et al.*, 1990) and rabbit atrial and ventricular myocytes (Braun *et al.*, 1990;Fedida *et al.*, 1989;Fedida *et al.*, 1990;Fedida *et al.*, 1991). On the other

hand, results in the dog vary: some observations noted no changes in canine epicardial myocytes (Robinson *et al.*, 2000), while others saw inhibition of I_{to} in epicardial and Purkinje cells with α-adrenergic agonists (Nakayama & Fozzard, 1988;Robinson *et al.*, 2000;Wang *et al.*, 2001). The inhibition of I_{to} current by α-adrenergic mediators appears to involve the PKC branch of intracellular signalling. PKC activators such as phenylephrine and methoxamine are able to recapitulate the inhibitory effects on I_{to}. Furthermore, PKC activation causes the downregulation of I_{to} in canine epicardial myocytes (Wang *et al.*, 2001). These observations are also unclear in light of the finding that the phorbol ester PMA is able to increase I_{to} density in the presence of α-adrenergic agonists which reduce I_{to}, implying PKC and IP_3 are not involved in its regulation (Braun *et al.*, 1990). It is still possible that α-adrenergic agonists affect I_{to} via a PKC-independent pathway (Parker *et al.*, 1999). α-adrenergic agonists seem to reduce I_{to} by reducing α-subunit expression. Specifically, Kv4.2 protein is reduced while Kv1.4 is increased (Guo *et al.*, 1998). When Kv4.2 and Kv4.3 α-subunits are expressed in heterologous cells, PMA is able to reduce the expressed current (Nakamura *et al.*, 1997), while Kv1.4 is reduced only after the current initially increases in density (Murray *et al.*, 1994). Increases in adrenergic stimulation are often seen in many types of cardiovascular disease (see section regarding congestive heart failure). Therefore, the modulation of I_{to} by α-adrenergic signalling via the PKC pathway is believed to contribute to the pathogenesis of many diseases. In fact, PKC-inhibitors are able to reverse the disease induced I_{to} reduction in hypertrophied rat myocytes (Shimoni & Severson, 1995) and in rats with diabetes (Shimoni *et al.*, 1998;Wang *et al.*, 1995a). Overall, the modulation of I_{to} by

adrenergic signalling appears to be quite complex and conclusions on its precise role are difficult to discern.

I_{to} can be modulated by other types of transmitters as well. These include modulators such as angiotensin-II which is able to reduce I_{to} current amplitude although it has no effects on Kv4.3 or Kv1.4 expression in the dog (Yu *et al.*, 2000). The Ca^{2+}/calmodulin-dependent protein kinase II (CaMKII) is able to modulate the inactivation of I_{to} in atrial myocytes. The inactivation was accelerated when treated with a CaMKII inhibitor, KN-92. This would indicate that CaMKII has the ability to slow I_{to} inactivation (Tessier *et al.*, 1999). Thyroid hormone (T3) is able to increase current density, most likely by increasing the expression of α-subunits such as Kv4.2 and Kv4.3 (Shimoni *et al.*, 1997). The fatty acid metabolites palmitoylcarnitine and palmitoyl-coenzyme A (palmitoyl-CoA) which are elevated during pathophysiological conditions have been found to decrease I_{to} current density as well (Xu & Rozanski, 1998).

2.2.3 The delayed rectifier currents

The delayed rectifier currents (I_K) are responsible for the final repolarization of the cardiomyocyte membrane. Because of this property, they can have a large influence on the time it takes a cardiomyocyte to repolarize, the action potential duration (APD). The delayed rectifier was originally identified in sheep Purkinje fibres where it was characterized as a slowly activating, non-inactivating outward current with a delayed onset from the activation of I_{Na} (Noble & Tsien, 1969). This current activated much after the onset of the action potential during the plateau phase and was originally termed I_x. Although in this initial report it was observed that the

current could be fitted by the sum of two exponentials, I_{x1} and I_{x2} respectively, later experiments disregarded this as being a recording artefact and it was then believed the current was conducted by one population of channels (Bennett *et al.*, 1985). This has proved to be an incorrect interpretation and with the help of single cell isolation techniques, two components of I_K were discovered again in guinea pig myocytes. The rapidly activating component I_{Kr} and the slowly activating component I_{Ks} can be distinguished based on differential pharmacological, time- and voltage-dependence profiles (Sanguinetti & Jurkiewicz, 1990;Sanguinetti & Jurkiewicz, 1991). Presently, I_{Kr} and I_{Ks} have been distinguished in many different species and regions: rabbit atrioventricular node and SAN (Howarth *et al.*, 1996;Ono & Ito, 1995;Shibasaki, 1987), guinea pig SAN (Anumonwo *et al.*, 1992a); atrial myocytes from guinea pig (Sanguinetti & Jurkiewicz, 1991), dog (Gintant, 1996;Yue *et al.*, 1996), and human (Wang *et al.*, 1994); ventricular myocytes from rabbit (Salata *et al.*, 1996), guinea pig (Sanguinetti & Jurkiewicz, 1990), cat (Follmer & Colatsky, 1990), dog (Gintant, 1996;Liu & Antzelevitch, 1995), and human (Li *et al.*, 1996).

2.2.3.1 Rapidly activating delayed rectifier current (I_{Kr}) electrophysiology

The rapidly-activating component plays a larger role during the early parts of Phase 3 repolarization, right after the plateau phase as the cell membrane becomes more negative to 0 mV. In specialized regions such as the SAN where the action potential morphology is quite different, I_{Kr} still plays a large role in myocardial repolarization (Ono & Ito, 1995). As explained by its name, I_{Kr} activates more rapidly than I_{Ks}. One of its defining features is its non-linear I-V relationship. This is due to

inward rectification which occurs around 0 to +10 mV. This phenomenon of inward rectification can also be demonstrated by the faster inactivation of I_{Kr} rather than activation at voltages positive to 0 mV (Shibasaki, 1987). It has a more negative activation threshold around -40 to -30 mV (Sanguinetti & Jurkiewicz, 1990).The $V_{1/2}$ for I_{Kr} is approximately -20mV, while it has a slope factor of 7.5 mV. Native I_{Kr} has a single channel conductance of 10-13 pS (Balser *et al.*, 1990). The time constant of activation varies depending on the species: from 40 msec in guinea pig atria to 600 msec in dog ventricle at 0 mV, however both are significantly faster than I_{Ks} (Tseng, 2001). Deactivation is also species-dependent ranging from a very fast 30 msec in guinea pig atria (Sanguinetti & Jurkiewicz, 1991), to a slow 250 msec in rabbit ventricles at -60 mV (Clay *et al.*, 1995). It is worthwhile to mention that guinea pig I_{Kr} tends to always have faster activation and deactivation kinetics, while dogs, rabbits and cats are slow and humans lie somewhere in between these two extremes. I_{Kr} also shows the property of inactivation, which limits the outward current during the plateau phase, but then as the cell repolarizes past 0 mV, I_{Kr} is able to rapidly recover from this inactivation and progressively contributes more to the final phase 3 repolarization. Reducing the extracellular K^+ concentration $[K^+]_o$ results in a decrease in the driving force for the current which has been attributed to a shift in the voltage-dependence of inactivation without changing the voltage dependence of activation (Sanguinetti & Jurkiewicz, 1992;Shibasaki, 1987;Wang *et al.*, 1996). This property is especially important when considering drug effects on I_{Kr}, especially during hypokalemia (low blood K^+ levels) where further blocking I_{Kr} while its driving force is low can lead to a drug induced Long-QT syndrome.

The rapidly activating delayed rectifier has garnered much attention recently with the realization that it is a large pharmacological target, be it intentional or not. Many anti-arrhythmic agents target this current intentionally, while other types of medication are also capable of blocking it, often producing an undesirable pro-arrhythmogenic state. Methanesulfonanilides, which are Class III anti-arrhythmics, are selective I_{Kr} blocking agents. These include E-4031, dofetilide, almokalant and D-sotalol (Mounsey & DiMarco, 2000). In terms of electrophysiological tools to separate delayed rectifier currents, dofetilide and E-4031 are most often used. As it was alluded to previously, other types of anti-arrhythmic agents are able to affect I_{Kr} in addition to their intended primary effect. Quinidine, a Class 1A Na^+ channel blocker, is able to affect I_{Kr} (Balser *et al.*, 1991;Roden *et al.*, 1988), as are Class 1B mexiletine and Class IC flecainide (Follmer & Colatsky, 1990;Mitcheson & Hancox, 1997). Much attention has been given to the I_{Kr}-blocking properties of drugs because it notoriously produces a reverse frequency-dependent prolongation of the action potential duration where there is less drug effect at higher heart rates (Heath & Terrar, 1996;Sanguinetti & Jurkiewicz, 1992). This makes such drugs undesirable and limits their therapeutic value since they would not be able to terminate fast tachyarrhythmias and can actually produce early afterdepolarizations (EADs) at slower heart rates which can also trigger arrhythmia. Similar evidence for the importance of I_{Kr} is found in genetic mutations affecting I_{Kr} channel subunits. These so called Long QT mutations (LQT) cause the prolongation of the QTc interval and predispose affected individuals to potentially lethal ventricular arrhythmias.

2.2.3.2 Molecular determinants of I_{Kr}

The human ether-a-go-go gene, HERG, is the sole α-subunit which is believed to carry I_{Kr} current. It was initially discovered in Drosophila fruit flies which had an X-linked mutation which caused them to shake in the presence of ether (Warmke *et al.*, 1991). This shaking was likened to "go-go" dancing and therefore the gene locus was termed *eag*. Later, homologous genes were identified in human hippocampus and mouse cDNA libraries and it was found to be readily expressed in the heart as well (Warmke & Ganetzky, 1994). HERG is only 10-15% homologous with the first *Shaker*-like Kv channel α-subunits which were discovered previously (Butler *et al.*, 1989), however it still shares the same typical six-transmembrane α-helices which are able to form functional channels (Zhong & Wu, 1991;Zhong & Wu, 1993). Some differences are found in the S4 domain and pore region which have a slightly modified version of the signature K^+ selectivity sequence (Doyle *et al.*, 1998;Heginbotham *et al.*, 1994).

HERG channels produce a current with pharmacological and kinetic properties similar to native I_{Kr} when expressed in heterologous cell systems, however they are not identical. The expressed cloned channels share similar voltage dependence for activation and rectification, sensitivity to methanesulfonanilides and single channel conductance (Hancox *et al.*, 1998;Kiehn *et al.*, 1996;Sanguinetti *et al.*, 1995;Spector *et al.*, 1996a;Trudeau *et al.*, 1995;Zhou *et al.*, 1998;Zou *et al.*, 1997). The cloning and heterologous expression of HERG has permitted the investigation into the mechanisms of I_{Kr} inward rectification. As mentioned previously, the rectification is due to a faster inactivation than activation (Shibasaki, 1987). Mutation analysis has revealed that when residues within the pore loop region are altered, this inactivation mechanism is disrupted (Smith *et al.*, 1996). This suggests the

inactivation requires some sort of a conformational change in the outer pore region. This type of inactivation is seen in *Shaker*-related channels where it is known as C-type inactivation (Hoshi *et al.*, 1990;Lopez-Barneo *et al.*, 1993;Panyi *et al.*, 1995). When the N-terminal region of HERG is truncated, no effect is seen on the current inactivation. This would indicate that HERG does not have the same N-type inactivation which is typical for true *Shaker* channels (Schonherr & Heinemann, 1996;Spector *et al.*, 1996b). However, if amino acids 2-354 or 2-373 are deleted from the N-terminus, a 10 fold acceleration of deactivation is observed, indicating that the HERG N-terminal is important for deactivation (Schonherr & Heinemann, 1996;Spector *et al.*, 1996b;Wang *et al.*, 1998a). Other mutations in the S4-S5 linker region, as well as the S6 region closest to the C-terminal, impact voltage dependence as well as activation and deactivation kinetics (Holmgren *et al.*, 1998;Lees-Miller *et al.*, 2000;Sanguinetti & Xu, 1999).

Despite this investigation into its biophysical properties, HERG alone does not seem to completely recapitulate native cardiac I_{Kr} currents (Sanguinetti *et al.*, 1995). Alternative splicing variants were first discovered in 1997, and these variants had activation and deactivation kinetic properties more like native I_{Kr} (Lees-Miller *et al.*, 1997;London *et al.*, 1997). Furthermore, these splice variants are able to assemble with wild-type HERG and form heteromultimeric channel complexes (London *et al.*, 1997). It was hypothesized that the varying properties of the heteromultimers could underlie region- and species-specific differences in I_{Kr} gating kinetics (Barajas-Martinez *et al.*, 2000); however only the wild-type full length HERG protein is detectable in rat, mouse and human hearts, therefore it is unlikely that these splice variants contribute to native I_{Kr} currents (Pond *et al.*, 2000). Still, inherited Long-QT

syndrome mutations have been found in the HERG gene, supporting its principal role in determining I_{Kr} currents (Curran *et al.*, 1995), but native channels must include some other factor aside from the α-subunit alone.

More insight into the exact molecular composition of I_{Kr} channels came with the discovery of β-subunits which were believed to interact with HERG. The family of KCNE genes, KCNE1-4 (Abbott *et al.*, 1999), seem to interact with different K^+ channel α-subunits. The product of the KCNE1 gene, minK, was the first to be characterized. *In vitro* experiments using a minK antisense oligonucleotide showed a reduction of HERG current (Yang *et al.*, 1995). Mice which contained a knockout of the minK KCNE1 gene demonstrated a clear reduction in I_{Kr} current amplitude and a change in current kinetics (Kupershmidt *et al.*, 1999). These electrophysiological observations were supported by the co-immunoprecipitation of stable minK/HERG complexes *in vitro* (McDonald *et al.*, 1997). Later, other members of the KCNE family, the minK-related proteins, or MiRPs, have also been found to interact with HERG. The co-expression of MiRP1 (KCNE2) with HERG results in a current which has similar properties to native I_{Kr}, including an accelerated deactivation and a more positive voltage dependence of activation compared to HERG alone (Abbott *et al.*, 1999). These findings were supported by the discovery of an inherited Long-QT mutation in the KCNE2 gene (LQT6) (Abbott *et al.*, 1999;Sesti *et al.*, 2000;Splawski *et al.*, 2000). Although these findings seem promising in terms of elucidating the molecular basis of I_{Kr} channels, there are still some discrepancies between the current expressed by HERG/MiRP1 channels and native I_{Kr} (Weerapura *et al.*, 2002). Furthermore, proof of the *in vivo* association between MiRP1 and HERG by co-immunoprecipitation is still missing. More recently, descriptions of novel

KvLQT1/HERG α-subunit interactions has also raised the possibility that such associations could contribute to native I_{Kr} currents (Ehrlich *et al.*, 2004). It is likely that I_{Kr} channels are composed of α- and β- subunits, however other factors such as the presence of other α-subunits can play a role in determining native I_{Kr} properties.

The region-specific expression of HERG subunits can account for some of the distinct region-specific action potential morphologies. Variability in action potential duration across the ventricular wall can be attributable to differences in I_{Kr} and I_{Ks} density (Li *et al.*, 2001;Liu & Antzelevitch, 1995). The epicardium has I_{Kr} currents with a greater macroscopic density than other layers of the ventricle; however the current shares similar single channel conductance and open probability, which would imply that the increased current is simply due to the presence of more channels rather than a composition difference (Furukawa *et al.*, 1992). Supporting this hypothesis, epicardial myocytes have a greater HERG mRNA and protein expression compared to endocardial layers in the ferret (Brahmajothi *et al.*, 1996). There are also differences between the two atria, with the left atrium containing a larger I_{Kr} current compared to the right atrium (Li *et al.*, 2001). The differences in HERG protein expression parallel these electrophysiological observations and may contribute to shorter action potential durations in the left atrium. Guinea pigs are known to have small I_{Kr} and I_{Ks} currents in endocardial myocytes, compared to epicardial or mid-myocardial regions (Bryant *et al.*, 1998). This is quite different in the dog where it has been shown that smaller I_{Ks} in the mid-myocardium is responsible for longer APD in that region compared to the epi- or endo- cardium (Liu & Antzelevitch, 1995). There are no differences in I_{Kr} kinetics or density in these cells.

2.2.3.3 Physiological control of I_{Kr}

Given its importance in determining action potential repolarization, one would expect HERG to be heavily regulated by the autonomic nervous system. The β-adrenergic system appears to have the greatest influence on I_{Kr} properties. Initial studies on I_{Kr} demonstrated that the current was insensitive to β-adrenergic stimulation (Roden *et al.*, 1996;Sanguinetti & Jurkiewicz, 1991). However, the molecular cloning of HERG allowed the realization that it contained four putative PKA phosphorylation sites. Of these four serine residues, only S238 is located in the N-terminus, while S890, S895, and S1137 are all found on the C-terminus (Thomas *et al.*, 1999). The PKA mediated phosphorylation of these sites results in a 19-40% reduction of HERG current, which is not solely due to a reduction in amplitude, but also caused by a positive shift in the activation curve by 12-14 mV (Thomas *et al.*, 1999). HERG channels also contain a putative nucleotide binding domain which can bind cAMP directly, giving HERG two possible ways to be modulated by the β-adrenergic system (Cui *et al.*, 2000). The direct binding of cAMP results in positive shift in the voltage-dependence of activation, again diminishing HERG current. In fact, the direct effect of cAMP is accentuated when HERG is co-expressed with MiRP1 (Cui *et al.*, 2001). There is some evidence implying a different signaling pathway of the β-adrenergic in the modulation of I_{Kr} as well. I_{Kr} is increased in guinea pig ventricular myocytes which have been given isoprenaline, a β-adrenergic agonist. However, this effect could only be attenuated when bisindolymaleimide I or staurosporine, two PKC inhibitors, were administered (Heath & Terrar, 2000). This would imply some cross-talking between two G-protein coupled receptor signaling

pathways. Because of these two differing actions of β-adrenergic stimulation, it is still not entirely understood how I_{Kr} is modulated *in vivo*.

2.2.3.4 Slowly activating delayed rectifier current (I_{Ks}) electrophysiology

I_{Ks} is active during the final Phase 3 repolarization of the cardiac action potential, however its precise role has been questioned due to its slow kinetics and more positive activation voltage. Instead, I_{Ks} is thought to play a larger role in regions where the action potential duration is relatively longer such as in the ventricular mid-myocardial region (Liu & Antzelevitch, 1995). It is believed that I_{Ks} may play a greater role when the functioning of other repolarizing currents is altered. For example, when heart rate is increased such as in congestive heart failure, increased I_{Ks} contributes to rate dependent AP abbreviation (Jurkiewicz & Sanguinetti, 1993). Also, when APD is prolonged due to excessive I_{Kr} blockade, I_{Ks} can counteract this effect and help complete the final repolarization (Varro *et al.*, 2000). I_{Ks} plays a large role in guinea pig myocytes and even contributes to the slow diastolic depolarization in the SAN (Anumonwo *et al.*, 1992b;Lu *et al.*, 2001), while rabbits seem to have very little I_{Ks} and therefore I_{Kr} must help modulate pacemaker activity in this species (Lu *et al.*, 2001;Ono & Ito, 1995;Shibasaki, 1987).

The defining feature of I_{Ks} as compared to I_{Kr} is its slow activation kinetics. In fact, the time course of I_{Ks} activation is so slow that it may not even achieve steady state during a 10 sec stimulation (Freeman & Kass, 1993a). In terms of deactivation kinetics, I_{Ks} is also slightly slower than I_{Kr}: the τ values are in the range of a hundred msec to seconds at -40 mV (Varro *et al.*, 2000). I_{Ks} activates at more positive

potentials than I_{Kr}, around -20 mV, which indicates its importance during the later part of Phase 3 repolarization (Sanguinetti & Jurkiewicz, 1990). The I-V curve for I_{Ks} is a linear relationship and has a $V_{1/2}$ of +24 mV and a slope factor of 15.7 mV (Sanguinetti & Jurkiewicz, 1990). The single channel conductance of I_{Ks} is smaller than the rapidly activating component, around 3-5 pS (Balser *et al.*, 1990;Veldkamp *et al.*, 1993). Another differing feature between the two components of I_K is that the slow-activating current does not inactivate, and as it was mentioned previously, takes a long time to reach steady state current.

Initially it was difficult to separate I_{Ks} from I_{Kr} because there were few pharmacological tools which selectively blocked the former. Currently there are several selective blockers of I_{Ks}, albeit not as many as have been found to interact with I_{Kr}. These include chromanol 293B (Busch *et al.*, 1996), a benzodiazepine L-735,821 (Jurkiewicz *et al.*, 1996), a diuretic indapamide (Turgeon *et al.*, 1994), and the anti-arrhythmic HMR 1556 (Thomas *et al.*, 2003). Other anti-arrhythmic agents such as amiodarone also block I_{Ks}, but have similar effects on other currents including I_{Kr} (Balser *et al.*, 1991). I_{Ks} is also sensitive to divalent cations: an elevated intracellular Ca^{2+} concentration increases I_{Ks} amplitude, while an elevated Mg^{2+} concentration has the opposite effect (Nitta *et al.*, 1994). In light of the problems associated with blocking I_{Kr}, it was believed that I_{Ks} might be a more suitable anti-arrhythmic target. Chromanol 293B is reported to prolong the action potential duration in a more favourable frequency-dependent manner in human and guinea pig ventricular myocytes (Bosch *et al.*, 1998). Such an observation would indicate that a I_{Ks} blocker could be useful in treating tachyarrhythmias, while still being safe at slower heart rates, unlike I_{Kr} blockers (Hondeghem & Snyders, 1990). However, there

are observations that even I_{Ks} blockers are able to increase the APD in a reverse frequency-dependent manner, similar to I_{Kr} (Lu *et al.*, 2001). More recently, it was found that the I_{Ks} blocker HMR 1556 did not show reverse frequency dependence when β-adrenergic control of the heart was intact. However, when β-blocking agents were given simultaneously, the reverse use dependence property was observed. This would suggest that the favourable effects of HMR 1556 blockade on refractoriness might be due the increase sympathetic tone associated with tachycardia which increases I_{Ks} as well (see section below on control of I_{Ks}), rather than an intrinsic APD prolongation (Nakashima *et al.*, 2004). These observations would indicate that I_{Ks}-blocking therapy is likely to be a more favourable anti-arrhythmic strategy.

2.2.3.5 Molecular determinants of I_{Ks}

Originally, it was believed that a single transmembrane domain subunit was capable of carrying I_{Ks} currents. This protein, minimal potassium (K^+) channel subunit minK, is the product of the KCNE1 gene, the founding member of this accessory subunit family. The gene was first cloned in 1988 from the kidney and encoded a small 129 amino acid protein (Takumi *et al.*, 1988). Later, it was also found in neonatal rat (Folander *et al.*, 1990), guinea pig (Zhang *et al.*, 1994) and mouse heart libraries (Honore *et al.*, 1991), as well as human lymphocyte library (Attali *et al.*, 1992). Evidence for this subunit underlying I_{Ks} currents came from the heterologous expression of minK in oocytes which produced currents much like the native current. Even though this protein was unlike any other K^+ channel subunit found to date, mutations in this small protein altered the properties of the expressed current, which suggested that it was capable of forming an ion conducting pore

(Goldstein & Miller, 1991;Takumi *et al.*, 1988). It was even suggested that a minimum of 14 of these subunits were required to form functional channels (Tzounopoulos *et al.*, 1995). There was one major problem with these findings. No matter how much minK cDNA was transfected in mammalian cell lines, no current was ever recorded. Only later was it postulated that there might be some other endogenous factor which is expressed in oocytes, but not mammalian cells, which could associate with minK to form functional channels (Lesage *et al.*, 1992). It should also be noted that even very small amounts of injected minK cRNA were capable of saturating the expressed current, even though larger amounts of cRNA showed substantial membrane expression in order to express a current (Blumenthal & Kaczmarek, 1994;Freeman & Kass, 1993b). Taken together, it was still believed that a typical six-transmembrane domain α-subunit might be found to underlie the current, and such a protein was probably expressed endogenously in oocytes (Mitcheson & Sanguinetti, 1999).

It wasn't until eight years after the original finding of minK that the true pore forming α-subunit, KvLQT1 was discovered. The product of the KCNQ1 gene was discovered by a positional cloning approach (Barhanin *et al.*, 1996;Sanguinetti *et al.*, 1996). KvLQT1 is a typical voltage-gated K^+ channel α-subunit with six transmembrane spanning α-helices, a pore loop with the conserved K^+ selectivity sequence and a molecular size of 676 amino acids. KvLQT1 alone produces a current which is unlike any other native current in cardiac myocytes, it activated too quickly to be considered for the slowly-activating delayed rectifier, and therefore it was believed it must co-assemble with some other protein. Coincidentally, minK and KvLQT1 had very similar tissue distribution in the heart and kidney (Barhanin *et al.*,

1996), and minK was already postulated to form I_{Ks} currents, so it was a natural candidate to test for association with KvLQT1. When both these subunits were expressed in a mammalian cell line, a current exhibiting very similar properties to native I_{Ks}, including the slow activation at more positive potentials, was seen for the first time (Barhanin *et al.*, 1996;Sanguinetti *et al.*, 1996). This current also had a much greater density than the expression of KvLQT1 alone. Mutations in both genes, KCNQ1 and KCNE1, are able to cause Long-QT syndromes (LQT1 and LQT5 respectively) (Splawski *et al.*, 2000). The stoichiometry of functional KvLQT1/minK channels is still under much debate. It is certain that four α-subunits are required to for the pore complex, like a typical tetrameric K^+ channel. However, it was initially believed that only a single minK subunit was necessary to stabilize this conformation (Mitcheson & Sanguinetti, 1999). Further mutation studies have revealed that minK actually interacts with the pore region of a single KvLQT1 subunit (Tapper & George, Jr., 2001), raising the possibility that four minK subunits might also be required. Other studies where various minK/KvLQT1 fusion proteins were created demonstrated that either having two minK, or four minK subunits elicited currents with similar properties and much like native I_{Ks} (Wang *et al.*, 1998b). Lastly, studies using charybdotoxin as a pharmacological tool supported the notion that only two minK subunits were necessary for a functional channel complex (Chen *et al.*, 2003a).

Other proteins besides minK have also been found to associate with KvLQT1 and modify its properties. MiRP1 and its relative MiRP2 have been reported to interact with KvLQT1 (Bianchi *et al.*, 1999;Schroeder *et al.*, 2000). In fact, such members of the KCNE family have proven to be quite promiscuous, being able to interact with and modify the function of various α-subunits. These include KvLQT1

and HERG as seen in this section on delayed rectifier currents, but also Kv4.2 channels (Zhang *et al.*, 2001), KvLQT1, KCNQ3 (another member of the KvLQT1 family), and Kv3.4 (Abbott *et al.*, 2001;Bianchi *et al.*, 1999;Schroeder *et al.*, 2000). The main question concerning these interactions remains is how relevant are they in a normal, *in vivo* physiological situation. There is no question that they raise the possibility of contributing to the region- and species-specific diversity in ion channel expression.

In terms of regional differences in I_{Ks} expression, it has already been mentioned that in the dog left ventricle, a smaller I_{Ks} current contributes to the longer mid-myocardial action potential duration while I_{Kr} remains constant (Liu & Antzelevitch, 1995). Right ventricles show similar current profiles, however the overall I_{Ks} density is larger compared to the left ventricle (Volders *et al.*, 1999a). The molecular basis of the smaller mid-myocardial I_{Ks} current is quite interesting. Using RNAse protection assays, it was found that the mRNA expression levels of KvLQT1 and minK were constant across the ventricular wall (Pereon *et al.*, 2000). However, a novel dominant negative isoform of KvLQT1 was identified with an N-terminus truncation which, when co-expressed with wild type KvLQT1, reduced KvLQT1 current to only 25% of the normal peak current density (Demolombe *et al.*, 1998;Jiang *et al.*, 1997). This KvLQT1 isoform 2 was shown to have a greater expression in the mid-myocardial region and could therefore account for the reduced I_{Ks} in this region. It is possible therefore that I_{Ks} expression may be regulated by a novel dominant negative type mechanism which has not been detected for any other channel types (Pereon *et al.*, 2000).

2.2.3.6 Physiological control of I_{Ks}

Unlike I_{Kr}, the effect of sympathetic stimulation on I_{Ks} is well documented. β-adrenergic stimulation is known to increase I_{Ks} current density 3-5 fold (Bennett *et al.*, 1986;Tsien *et al.*, 1972). β-adrenoceptor agonists are able to achieve this augmentation by shifting the voltage dependence of activation to more negative values so channels open sooner during the action potential, as well as increasing the maximum peak conductance and accelerating the activation of I_{Ks} (Giles *et al.*, 1989;Han *et al.*, 2001b). This effect helps ensure the APD is not excessively prolonged when β-adrenergic stimulation also causes the increase in I_{Ca} current density (Han *et al.*, 2001b). β-adrenoceptors are able to modulate KvLQT1/minK channel complexes via the typical cAMP/PKA cascade. KvLQT1 can form a complex with yotiao which acts as an A-kinase anchoring protein to recuit PKA and directly phosphorylate the channel (Marx *et al.*, 2002). Because I_{Ks} stimulation by β-adrenergic activation is important to offset I_{Ca} augmentation and prevent excessive APD prolongation, in situations in which I_{Ks} is reduced, such as congenital long QT syndrome types 1 and 5 (Priori & Napolitano, 2004) and possibly acquired channelopathy due to cardiac remodeling (Li *et al.*, 2002a), β-adrenergic stimulation can lead to EADs and potentially-malignant ventricular tachyarrhythmias.

The effects of α-adrenergic stimulation are not as consistent as those reported for the β-adrenergic system. Increasing PKC activity using α-adrenergic receptor agonists has been shown to increase (Bennett *et al.*, 1986;Tsien *et al.*, 1972;Walsh *et al.*, 1991;Walsh & Kass, 1988) and decrease (Lee & Rosen, 1994;Satoh & Hashimoto, 1988) I_{Ks}. These differences may be due to species-specific differences in the modulation of I_{Ks} by α-adrenergic receptors. Increased PKC activity leads to the

increase of I_{Ks} in guinea pigs, but a reduction in rats and mice (Varnum *et al.*, 1993). Interestingly, mutating an asparagine residue at position 102 in the guinea pig minK sequence changes its response to PKC activation so that it becomes more like that of rats and mice (Varnum *et al.*, 1993). KvLQT1 does have a putative PKC phosphorylation site (Kathofer *et al.*, 2003), suggesting that it is likely regulated by this kinase. More recently, the lesser expressed β_3-adrenoceptor has been implicated in increasing I_{Ks} current via the PKC pathway (Kathofer *et al.*, 2003), further complicating the interpretation of the role of PKC in I_{Ks} modulation.

3. Cardiovascular disease

Of all the different possible causes of mortality seen in the world today, cardiovascular disease remains the most prevalent in our society. It affects over 60 million Americans, while causing death in over one million each year (American Heart Association, Heart Disease and Stroke Statistics, Update 2003). This outstanding number accounts for 39.4 % of all deaths in the United States alone, equalling 1 death every 33 seconds. This has placed an enormous burden on the health care system with expenses arising from hospital costs for the treatment of cardiovascular disease patients totalling ~$350 billion annually. Obviously there is a need for a greater awareness of the risk factors which can lead to cardiovascular disease, but also better treatments for such maladies. Of particular interest are cardiovascular diseases which involve the cardiac ion channels mentioned in later sections. These include congestive heart failure (CHF) and atrial fibrillation (AF).

3.1 Congestive heart failure (CHF)

3.1.1 Epidemiology and characteristics of CHF

CHF accounts for almost 5 million of all cardiovascular disease cases and is actually a common endpoint for many other diseases such as hypertension and coronary artery disease. A diagnosis of CHF is not a favourable one since 75-80% of people with the disease under the age of 65 will die within 8 years of diagnosis. Even more alarming is the fact that in affected persons, sudden cardiac death occurs at 6-9 times the rate of the general population, and strains the medical system with $24 billion in expenses.

CHF is the amalgamation of many different pathophysiological mechanisms. These include structural abnormalities such as myocardial fibrosis, necrosis, apoptosis and hypertrophy; left ventricular ionic remodeling, dilatation and wall thinning; as well as functional abnormalities like mitral valve regurgitation, intermittent ischemia and induced ventricular or atrial arrhythmias (Jessup & Brozena, 2003). Many different signalling pathways are also implicated in the mechanism underlying CHF, including the renin-angiotensin system, vasodilators like nitrous oxide and bradykinin, cytokines and natriuretic peptides. The sympathetic nervous system, especially β-adrenergic signalling, also plays a large role in the pathogenesis of CHF where sympathetic tone is drastically increased. Other factors such as genetics (such as sex), age, and other background cardiovascular diseases all play a role in the mechanisms of heart failure. Of particular interest is the role of myocardial ionic remodeling in CHF.

3.1.2 Electrical remodelling in CHF

The most common observation in CHF patients is a significant prolongation of the APD (Beuklemann *et al.*, 1993). This repolarization deficiency is believed to underlie the high incidence of sudden cardiac death due to ventricular arrhythmias in CHF (Cohn JN *et al.*, 1986). Ventricular arrhythmias can occur by a variety of mechanisms such as reentry, early afterdepolarizations (EADs), delayed afterdepolarizations (DADs), or abnormal automaticity. When considering CHF, the most common mechanisms for arrhythmia are by triggered EADs and DADs.

EADs are caused by depolarizing activity before the full repolarization of an AP. A prolonged APD can lead to an imbalance in the plateau ionic currents, either a decrease in the net outward current or an excessive increase in inward currents. Therefore EADs occur during phase 2 or early phase 3 of the AP and tend to originate in the midmyocardial M cells or Purkinje fibers (Nattel & Quantz, 1988;Sicouri & Antzelevitch, 1995). Decreased plateau outward currents such as I_{to} and I_K (see below) allow inward currents such as $I_{Ca,\,L}$ (Nattel & Quantz, 1988; DeFerrari GM *et al.*, 1995;January & Riddle, 1989;Luo & Rudy, 1994a) and $I_{Na,\,late}$ or I_{NCX} (Luo & Rudy 1994b) to trigger an EAD. If one of these depolarizations reaches threshold, it can trigger a new premature AP which can perpetuate (Cranefield PF, 1977).

DAD triggered activity can also occur due to a prolonged APD and takes place soon after final phase 3 repolarization, occuring most often in the ventricles, Purkinje fibers and atria. They are caused by cellular Ca^{2+} overload which triggers a secondary release of Ca^{2+} from the sarcoplasmic reticulum after AP repolarization (Fabiato & Fabiato, 1975;Pogwizd & Bers, 2004). The spontaneous release of Ca^{2+} enhances activity of the NCX, which exchanges one Ca^{2+} ion for three Na^+ ions,

resulting in a net inward flow of positive charges. I_{CaL} plays a significant role in determining cellular Ca^{2+} influx, and by extension, Ca^{2+} overload contributing to DAD formation as well. The sympathetic nervous system is often activated in diseased CHF myocardium and leads to increased I_{CaL} which in turn can contribute to Ca^{2+} overloading (Wit & Cranefield, 1976;Belardinelli & Isenberg, 1983;Malfatto G *et al.*, 1988).

Aside from its predisposition to triggered arrhythmias, CHF is also associated with SAN dysfunction. Reduced sinus node automaticity has been noted in a rabbit model of heart failure (Opthof T *et al.*, 2000). This has been attributed to an increase in the intrinsic cycle length of SAN cells in heart failure which is due to a decreased diastolic depolarization rate (Verkerk AO *et al.*, 2003). This dysfunction has tremendous implications on cardiac function since a decreased automaticity may lead to a bradycardic state which further predisposes the myocardium to EAD triggered arrhythmias (Faggiano P *et al.*, 2001).

3.1.3 Ion current remodeling in CHF

Ionic remodelling occurs when dynamic changes in ion channel behaviour occur as a result of altered gene expression which can change channel synthesis and function (Allessie, 1998). CHF is associated the remodelling of many ion channels, including I_{Na}, I_{to}, I_f, I_{Kr} and I_{Ks} which generally lead to a prolongation of the APD. Experimental results regarding I_{Na} in congestive heart failure are actually few, but there are many more in regards to other predictors of CHF such as hypertrophy. Initially in a rat hypertrophy model, no changes in the fast or late components were observed (Gulch *et al.*, 1979). However, more recent studies have detected changes in

Na^+ channel properties in hypertrophied myocardium from rats with 3 to 4 week old anterior myocardial infarction (Huang *et al.*, 2001). It was observed that the late component of I_{Na} was increased and played a greater role in prolonging APD. In actual canine CHF models, it was found that there is an increase in a persistent steady-state component of I_{Na} in ventricular myocytes, which most likely corresponds to the late component (Undrovinas *et al.*, 1999).

The changes in K^+ currents associated with CHF have been well documented. I_{to} is consistently found to be downregulated in humans with CHF as well as animal models of CHF, while no changes are seen in its kinetic or voltage dependent properties (Bailly *et al.*, 1997;Beuckelmann *et al.*, 1993;Cerbai *et al.*, 2000;Kaab *et al.*, 1996;Kaab *et al.*, 1998;Kaprielian *et al.*, 1999;Lee *et al.*, 1997;Li *et al.*, 2000a;Nabauer *et al.*, 1996;Rozanski *et al.*, 1997;Tsuji *et al.*, 2000;Yokoshiki *et al.*, 1997).

The delayed rectifier currents are also affected by CHF. A canine rapid ventricular pacing model of CHF showed a clear reduction of I_{Ks}, while I_{Kr} remained unaffected (Li *et al.*, 2000a;Li *et al.*, 2002a). In contrast, both components were downregulated in a rabbit tachycardia-induced heart failure model (Tsuji *et al.*, 2000), and in a dog model of biventricular hypertrophy which was induced by AV block (Volders *et al.*, 1999b). Additionally, neither delayed rectifier current was affected by CHF when looking at Purkinje fibres cells from dogs (Han *et al.*, 2001a).

Although SAN dysfunction has been documented in CHF, there has only been one study which has examined the effects of CHF on ionic current remodelling. It was found that CHF causes a significant downregulation of I_f and I_{Ks}. Since I_{Ks} does not play a role in automaticity, the changes in I_f are believed to underlie the reduction

of the intrinsic cycle length, while I_{Ks} changes can contribute to the development of EADs.

3.1.4 Effects of CHF on ion channel subunit expression

Ion channel subunit remodelling has been found to underlie many of the observed electrophysiological changes associated with CHF. In terms of alteration in I_{Na}, many studies have found no change was seen in the expression of the cardiac specific isoform $Na_v1.5$, but one recent study has identified a 30-50% reduction of this subunit in the left ventricle (Borlak & Thum, 2003). Additionally, it has been found that the expression of a neuronal isoform $Na_v1.1$ was increased. Therefore the expressed I_{Na} had properties which reverted to an intermediate between an adult and a fetal phenotype. The only other proposed mechanism underlying such a change in I_{Na} phenotype in heart failure has been a deficient glycosylation of the Na^+ channel as evidenced by studies in a genetically engineered mouse lacking the muscle LIM protein (Ufret-Vincenty *et al.*, 2001). These alterations could predispose the myocardium to EAD triggered arrhythmias.

A downregulation in Kv4.2 and Kv4.3 mRNA and protein expression have been cited as being the cause for the reduction of I_{to} in CHF, and contributes to APD prolongation (Gidh-Jain *et al.*, 1996;Kaab *et al.*, 1998;Rozanski *et al.*, 1998;Takimoto *et al.*, 1997;Borlak & Thum, 2003). However, the expression of Kv1.4 which is believed to underlie the slowly inactivating $I_{to,\,slow}$ is increased in a rat infarct model and in renovascular hypertensive rats (Gidh-Jain *et al.*, 1996;Kaab *et al.*, 1998;Kaprielian *et al.*, 1999;Takimoto *et al.*, 1997). Many mechanisms have been proposed for the downregulation of I_{to} in CHF. These include the alteration of

neurohumoral and paracrine factors, as well as regulatory subunits, the cytoskeleton and cell metabolism (Oudit *et al.*, 2001). Evidence for the contribution of neurohumoral factors comes from experiments using angiotensin converting enzyme (ACE) inhibitors and the angiotensin receptor antagonist losartan. These pharmacological interventions were able to reverse changes in APD and I_{to} density in the hypertensive rat model (Cerbai *et al.*, 2000;Yokoshiki *et al.*, 1997), as well as returning Kv4.2 and Kv4.3 mRNA levels to normal in the renovascular hypertensive rat model (Takimoto *et al.*, 1997).

There are obviously a wide range of possible changes in the delayed rectifier currents which are associated with CHF. An increase in KvLQT1 mRNA has been noted in human left and right ventricles, while HERG was increased in right ventricles only (Borlak & Thum, 2003). These observations would tend to contradict the paradigm that outward currents should be reduced in order to see a prolongation of APD. It likely that more research is needed in order to examine the changes incurred at the protein level for I_K channel subunits such as HERG, KvLQT1, minK and MiRP1. Furthermore, the specific molecular mechanisms which underlie the downregulation of I_f in the SAN have not been elucidated. Only the expression of HCN4 has been examined in CHF at the mRNA level in the ventricles where it was found to be increased. No studies have examined the effect of CHF on HCN subunit expression in the SAN where I_f is most predominant. This may be partly due to the fact that its molecular determinants have only recently been identified, as well as the difficulties in isolating the relatively small SAN region. It is likely that species- and regional specificity also play a large role in determining the type of remodelling observed in CHF.

3.2 Atrial fibrillation

3.2.1 Epidemiology and characteristics of AF

Atrial fibrillation (AF) is the most common sustained clinical arrhythmia in the population today with prevalence in approximately 2 million people in the United States alone. Unlike ventricular fibrillation, AF is not lethal: it can persist for a long time and ultimately lead to other cardiovascular complications such as thromboembolisms. The total mention mortality due to AF is about 9,000 people annually. Another point of consideration is that the incidence of AF increases with age such that 70% of people diagnosed with AF are between the ages of 65 and 85 (Benjamin *et al.*, 1994). This statistic becomes alarming when it is considered that most of the "baby boomer" population is, or will be, reaching this age range in the years to come. Therefore the costs associated with treating AF should be expected to rise from the more than $2 billion/year which are expended presently. A major problem with AF is that there is no completely effective therapy which is available to treat the disease. Current therapy can be divided into rhythm or rate control (Khairy & Nattel, 2002). Rhythm control usually involves the use of anti-arrhythmic drugs which attempt to maintain the normal sinus rhythm of a patient and therefore their natural electrical functions as well. Rate control serves to maintain ventricular rate so as to ensure a proper heart pumping action, but allowing AF to continue. Pharmacological interventions include the use of β-blockers and Ca^{2+} channel antagonists. These treatments often include anti-coagulant therapy so as to prevent the thromboembolisms associated with AF. Other non-pharmacological treatments include catheter ablation and implantable cardioverter defibrillators to maintain rhythm or rate control. Risk factors for the development of AF include age, male sex,

heart failure, smoking, diabetes, hypertension, left ventricular hypertrophy and myocardial infarction (Benjamin *et al.*, 1994).

While some cases of AF can be asymptomatic, those patients who do experience symptoms usually complain of heart palpitations, chest pain, dizziness and fatigue (Kerr *et al.*, 1998). One of the large concerns with AF is the increased risk of stroke (Wolf *et al.*, 1991). This occurs because of blood pooling in the atria, especially the left atrial appendage, which are unable to contract properly. AF is characterized by rapid atrial rate (>400 beats per minute) and uncoordinated activity as seen on ECG recordings. As opposed to CHF, AF is usually associated with a shortening of the atrial action potential duration and by extension, its refractory period as well (Yue *et al.*, 1997).

3.2.2 Ion current remodelling in AF

AF is a persistent arrhythmia and is associated with ion channel remodelling such that it can maintain itself, or in other words "AF begets AF" (Wijffels *et al.*, 1995). AF is generally thought to be caused by multiple re-entrant circuits which propagate in different circular paths leading to discordant activity. For this mechanism to be viable, the pathlength of the re-entrant circuit must be equal or larger than the size of its wavelength (Allessie *et al.*, 1977). The wavelength is the distance travelled by an electrical impulse in a single refractory period, and is the product of conduction velocity and the refractory period (Nattel, 2002). This "leading circle" hypothesis indicates that re-entry establishes itself in a pathway the size of its wavelength (Allessie *et al.*, 1977), therefore the number of re-entrant circuits possible depends on the size of the atria available and the wavelength.

Recent research has indicated that AF may be initiated by other mechanisms as well: Ectopic foci have been found to be able to initiate AF, especially when arising from the pulmonary vein region in the left atrium (Haissaguerre *et al.*, 1998;Mandapati *et al.*, 2000). Additionally, single re-entrant circuits have also been found to cause AF in CHF models of disease (Derakhchan *et al.*, 2001). The fact that Na^+ channel blockers are able to terminate AF in some cases by slowing conduction velocity, contradicting the leading circle theory, supports the notion that other AF mechanisms are possible (Allessie *et al.*, 1977). One constant factor with all mechanisms is that AF does initiate ion channel remodelling to ensure its self-propagation. This remodelling leads to the shortening of the APD which shortens the refractory period, allowing a leading wave of excitation to persist (Yue *et al.*, 1997). I_{to} is usually found to be downregulated in AF (Li *et al.*, 2000a;Yue *et al.*, 1997), while no change is seen in the delayed rectifiers I_{Kr} and I_{Ks} which is usually seen in CHF (Yue *et al.*, 1997). These changes, along with a significant decrease in the Ca^{2+} current (Yue *et al.*, 1997), allow the delayed rectifiers to repolarize cardiomyocytes more quickly, and therefore shorten APD. These effects leading to faster repolarization are supported by findings that a genetic mutation in KvLQT1, the α-subunit of I_{Ks}, leads to a gain of function for this current (Chen *et al.*, 2003b). Although familial AF cases have been noted, no other genetic mechanisms for AF have been elucidated. These ionic changes may provide novel targets for anti-arrhythmic therapy seeking to restore the normal electrical activity of the heart.

6. Questions raised from this overview

The fact that cardiovascular disease remains the primary cause of mortality in our society should emphasize the importance of cardiovascular research in order to better understand basis and mechanisms for such diseases. Much work is needed to completely understand the changes which are associated with such diseases, especially in identifying potential pharmacological targets for their treatment. Molecular biology techniques have come into mainstream use in recent years and have permitted the elucidation of mechanisms underlying past electrophysiological observations. These include techniques such as competitive RT-PCR and Real-time PCR for the quantification of mRNA levels, as well as Western blotting and immunostaining for protein characterization.

At the same time, many potential pharmacological agents are tested in animal models before arriving at Phase I clinical testing. However, the precise correlation between humans and such animal models in terms of their cardiac ion current profiles is lacking. Understanding such similarities or differences can help gain insight into the proper functioning of human cardiovascular activity, as well as ensuring that proper animal models are used when testing novel pharmacological treatments.

The changes induced by or which underlie cardiovascular diseases, such as CHF and familial AF, are still not completely understood. The effects of CHF on regions such as the SAN have not been examined to date, and are very important given this region's importance in maintaining proper sinus rhythm in the heart. Part of this lack of information is due to the difficulty in identifying and isolating the SAN in many species. Additionally, the effects of CHF on other regions such as the ventricle have not been completely addressed, especially in terms of the effects on I_{to}.

This has been due to some recent controversies concerning the exact molecular composition of this ion channel in human and canine ventricles. Lastly, while genetic predispositions to AF have been noted, precise mechanisms and determinants are few.

The elucidation of the molecular basis for these heterogeneities in ion current expression, be it a consequence of region, species or disease, can help contribute to our own knowledge of cardiac functioning in normal and disease situations, and may provide insight for the identification of novel pharmacological targets. Therefore, answering the following specific questions is essential:

1) How does the expression of voltage-gated K^+ channels vary amongst different species, especially in guinea pig and rabbits which rely on different K^+ currents for repolarization?
2) What is the molecular composition of human I_K currents, and how does this compare to other species?
3) How does CHF affect the expression of I_{Na} subunits in the ventricle given reports of delays in action potential conduction?
4) What is the exact molecular basis for the I_{to} transmural gradient in humans and dogs?
5) How does CHF affect the expression of the I_{to} β-subunit KChIP2?
6) How does CHF affect the function of the SAN?
7) What is the expression profile of I_f HCN subunits in the SAN compared to the right atrium, and how is this affected by CHF?
8) Are there any other molecular determinants of familial AF? If so, how can these affect ionic currents and action potential morphology?

7. Approaches to address these questions

In order to provide answers to the questions listed above, the following procedures and techniques will be employed:

1) Total RNA and membrane protein will be isolated from human, rabbit and guinea pig ventricles in order to asses the mRNA and protein expression profiles of I_{to} and I_K subunits. Competitive RT-PCR must be used for mRNA quantification in order to obtain an absolute concentration of each subunit mRNA, thus allowing a comparison between species and between channel subunits.
2) Similarly, protein and mRNA will extracted from a canine model of CHF and the expression profiles of $Na_v1.5$ and Na^+ channel β-subunits will be determined.
3) Kv4.3 and KChIP2 mRNA and protein expression will be examined in human and canine epicardium and endocardium to elucidate the possible molecular determinants of the I_{to} transmural gradient
4) A canine model of CHF will be employed to determine the effects of this disease on I_{to} subunit expression across the ventricular wall, and to gain further insight into the determinants of I_{to} expression.
5) This same canine CHF model will be used to determine the effect of disease on SAN function, and to assess the expression profiles of HCN subunits in the right atrium and SAN in control and CHF dogs.
6) A recently reported minK single nucleotide polymorphism will be characterized to determine how it can lead to a greater propensity to AF.

CHAPTER 2: MOLECULAR BASIS FOR SPECIES-SPECIFIC DIFFERENCES IN REPOLARIZING K^+ CURRENT EXPRESSION

Certain species, especially rabbits and guinea pigs, rely on different K^+ currents for repolarization. In the case of the guinea pig, electrophysiology studies show a large I_K current is found, but no true I_{to} has ever been recorded from this species. The opposite is almost true in the rabbit, which relies heavily on I_{to} for repolarization, but has very small I_K currents (Lu *et al.*, 2001). In fact, typical I_{Kr}-blocking drugs have been found to increase the propensity of rabbits to ventricular tachyarrhythmias such as Torsades de pointes, indicating the lack of I_{Kr} in this species for repolarization (Carlsson *et al.*, 1990). Both of these currents are detectable in the human ventricle; however the exact composition of the channels which carry these currents is unknown. However, it is known that genetic deficiencies in I_{Kr} and I_{Ks} subunits, such as in inherited Long QT syndromes, predispose the heart to potentially lethal tachyarrhymias. A similar effect is seen with I_{Kr}-blockers as well. Elucidating the molecular basis for species-specific heterogeneity in expression profiles can help our own understanding of the molecular determinants of action potential repolarization. Additionally, determining how the expression of voltage-gated K^+ channel subunits varies among species could also potentially help in the determination of which small-animal models would be appropriate for pre-clinical drug testing. Of course, a model which best recapitulates all the currents found in man would be the most desirable.

In order to directly compare expression profiles between species, the absolute quantification of subunit mRNA must be made, a relative comparison would be insufficient. For this reason, competitive RT-PCR was used to determine mRNA concentrations. Furthermore, careful consideration for the conservation of epitopes must be made between the different species, otherwise comparative immunoblotting procedures would no be valid.

ABSTRACT

There are important species-specific differences in K^+-current profiles and arrhythmia susceptibility, but inter-species comparisons of K^+-channel subunit expression are lacking. We quantified ventricular K^+-channel subunit mRNA and protein in rabbits, guinea-pigs and humans. Kv1.4, Kv4.2 and Kv4.3 mRNA was present in rabbits but undetectable in guinea-pigs. MinK mRNA concentration in guinea-pigs was ~3-fold values in humans and 20-fold vs. rabbits. MinK protein expression in guinea-pig was >2-fold human and 6-fold rabbit. KvLQT1 mRNA concentration was greatest in man, and protein expression in humans was ~2-fold and ~7-fold values in rabbits and guinea-pigs respectively. ERG1 mRNA was more concentrated in man, but ERG1 protein expression could not be compared across species because of epitope sequence differences. We conclude that important inter-species differences in cardiac K^+-channel subunit expression exist and may contribute to: 1) lack of I_{to} in guinea pig (α-subunit transcription absent in guinea-pig heart); 2) small slow delayed-rectifier current and Torsades de Pointes susceptibility in rabbit (low-level minK expression); 3) large I_{Ks} in guinea-pig (strong minK expression).

Keywords: arrhythmia; ion channels; electrophysiology; species

INTRODUCTION

Electrophysiological studies have demonstrated differences in the K^+-current profiles responsible for cardiac action potential repolarization among different species, including the guinea-pig, rabbit and human. The transient outward current K^+-current (I_{to}) plays an important role in rabbit (9, 21) and human (7) cardiac action potential (AP) repolarization, and is believed to be absent in the guinea-pig (21). On the other hand, the delayed-rectifier current (I_K) is very prominent in the guinea-pig (13, 16, 21) and smaller in the rabbit (9, 13, 16, 21) and man (13, 22). These ionic current profiles are associated with distinct action potential properties in each species (21). There are species-dependent particularities in sensitivity to class III drug-induced early afterdepolarizations (EADs) and long-QT syndromes (LQTSs), with rabbits being particularly susceptible to EAD and LQTS induction by blockers of the rapid delayed-rectifier current (I_K) (5, 15).

The molecular basis of species-specific repolarizing K^+-current profiles has not been established. The pore-forming α-subunits of rapid (I_{Kr}) and slow (I_{Ks}) components of I_K are formed by subunits encoded by the ether-a-go-go related gene (*ERG*) and *KvLQT1* gene respectively (2, 19, 20). MinK is an essential β-subunit for I_{Ks} formation (2, 19). It has been suggested that minK-related peptide-1 (MiRP1) is essential for the formation of I_{Kr} (1), but the precise role of MiRP1 in I_{Kr} has been questioned (26). The transient outward K^+-current I_{to} is formed by Kv1.4, 4.2 and 4.3 subunits in rabbits and by Kv4.3 subunits in man (6, 23). The present study was designed to assess: 1. Whether the absence of I_{to} in the guinea-pig heart can be attributed to lack of cardiac expression of the relevant subunits; 2. Whether I_K-encoding subunit expression differences between rabbit and guinea-pig are consistent

with their current and EAD-sensitivity profiles; and 3. How I_K-subunit expression in human hearts compares to rabbit and guinea-pig.

MATERIALS AND METHODS

RNA Purification

New Zealand White rabbits (1.8-2.2 kg) or Dunkin-Hartley guinea-pigs (500 g) were euthanized by cervical dislocation. The left ventricular free wall was separated and frozen in liquid nitrogen. The left ventricular free wall from the basal region of undiseased human tissues were obtained from five general organ donor patients(3 females, 2 males) under procedures approved by the Ethical Review Board of the Medical Center of the University of Szeged. These tissues were stored in cardioplegic solution (NaCl 110 mM, KCl 16 mM, $MgCl_2$ 16 mM, $CaCl_2$ 1.2 mM and $NaHCO_3$ 5 mM) and kept at 4°C for approximately 6-8 hours before freezing in liquid nitrogen. Total RNA was isolated from 0.5-1.0 g samples using Trizol reagent (Invitrogen) followed by chloroform extraction and isopropanol precipitation. Genomic DNA was eliminated by incubating in DNase I (0.1 U/μl, 37°C) for 30 min followed by acid phenol-chloroform extraction. RNA was quantified by spectrophotometric absorbency at 260 nm, purity confirmed by A_{260}/A_{280} ratio and integrity evaluated by ethidium-bromide staining on a denaturing agarose gel. RNA samples were stored at -80°C in RNAsecure Resuspension Solution (Ambion).

PCR Primers

Degenerate primers for initial RT-PCR were designed based on published cDNA sequences for Kv1.4, Kv4.2, Kv4.3, KvLQT1, ERG1, minK and MiRP1. Highly-

conserved and specific sequences were selected and primer-pair specificity was confirmed by comparison with the GenBank database using BLAST. Alpha-actin was used as a positive control for reverse transcription (RT)- polymerase chain-reaction (PCR). In preliminary studies, MiRP1 signals were extremely weak and further quantification was not performed. Competitive RT-PCR was used to obtain the absolute mRNA concentrations essential for inter-species comparison. Species-specific Gene Specific Primers (GSPs) for competitive RT-PCR were based on previously-published sequences or, when a sequence was not available, the DNA product of PCR with degenerate primers was sequenced for nested primer design (Table 1). Chimeric primer pairs for RNA-mimic synthesis were constructed with a human cardiac α-actin sequence flanked by GSPs. An 8-nucleotide sequence, GGCCGCGG, corresponding to the 3' end of the T7-promoter, was conjugated to the 5'-end of each forward chimeric primer.

Synthesis of RNA Mimic

First-strand cDNA synthesized by reverse-transcription with ventricular mRNA samples was used as a template for subsequent PCR amplification steps with chimeric primer pairs. The resulting cDNA mimic contains a 460-bp α-actin sequence flanked at the 5'-end by the sense GSP sequence and an 8-bp T7-promoter sequence and at the 3'-end by the antisense GSP sequence. Products were gel-purified with the QIAquick Gel Extraction Kit (Qiagen Inc.). The RNA mimic (internal standard) was created by *in vitro* transcription (mMESSAGE MACHINE, Ambion). The product was incubated with RNase-free DNase I (30 min, 37°C) to eliminate cDNA contamination, followed by phenol/chloroform extraction and isopropanol

precipitation. Mimic size and concentration were determined by migration on a denaturing RNA gel alongside pre-determined RNA concentrations to create a standard curve.

Competitive RT-PCR

RNA mimic samples of serial 10-fold dilutions were added to reaction mixtures containing 1-μg total RNA. RNA was denatured at 65°C (15 min). RT was conducted in a 20-μl reaction mixture containing reaction buffer (10 mmol/l Tris-HCl, pH 8.3, 50-mmol/l KCl), 2.5 mmol/l $MgCl_2$, 1 mmol/l dNTPs (Roche), 3.2 μg random primers $p(dN)_6$ (Roche), 5 mmol/l DTT, 50 U RNase inhibitor (Promega), and 200 U M-MLV reverse-transcriptase (Gibco-BRL). First-strand cDNAs were synthesized at 42°C (1 h) and remaining enzymes heat-deactivated (99°C, 5 min).

First-strand cDNA from the RT-step was used as a template in 25-μl reaction mixtures including 10-mmol/l Tris-HCl (pH 8.3), 50-mmol/l KCl, 1.5-mmol/l $MgCl_2$, 1-mmol/l dNTPs, 0.5-μmol/l GSPs, 0.625-mmol/l DMSO and 2.5 U of Taq Polymerase (Gibco BRL). Reactions were hot-started at 93°C for 3 min of denaturing, followed by 30 amplification cycles (93°C, 30 sec [denaturing]; 55-58°C, 30 sec [annealing]; 72°C, 30 sec [extension]). A final 72°C extension step was performed for 5 min. RT-negative controls were obtained to exclude genomic contamination for all RT-PCR reactions.

PCR products were visualized under UV light with ethidium bromide staining in 1.5% agarose gels. Images were captured by a Nighthawk camera, and band density determined with Quantity One software. A DNA Mass Marker (100 ng) was used to determine the size and quantity of DNA bands, and to create a standard curves in

each experiment for absolute quantification. Plots of LN([target]/[mimic]) vs. LN([mimic]) were fit by linear regression to determine the absolute concentration of target mRNA as previously described (23, 25, 28).

Western Blot Studies

Membrane protein was extracted with 5-mmol/l Tris-HCl (pH7.4), 2-mmol/l EDTA, 5-μg/ml leupeptin, 10-μg/ml benzamidine, and 5-μg/ml soybean trypsin inhibitor, followed by tissue homogenization. All procedures were performed at 4°C. Membrane proteins were fractionated on either 8% (ERG1, KvLQT1) or 12% (minK) SDS-polyacrylamide gels and transferred electrophoretically to Immobilon-P polyvinylidene fluoride membranes (Millipore) in 25-mmol/l Tris-base, 192-mmol/l glycine and 5%-methanol at 0.09 mA for 18 h (ERG1, KvLQT1) or 65 V for 20 min (minK). Membranes were blocked in 5% non-fat dry milk (Bio-Rad) in TTBS (Tris-HCl 50 mmol/l, NaCl 500 mmol/l; pH 7.5, 0.05% Tween-20) for 2 h (room temperature), then incubated with primary antibody (1:200 dilution) in 5% non-fat dry milk in TTBS for 18 h at 4°C (minK) or 1 h at room temperature (KvLQT1, ERG1). The ERG1 antibodies for human and guinea-pig were purchased from Alomone, while the KvLQT1, minK, and ERG1 (for rabbit) antibodies were from Santa Cruz Biotechnology. The epitopes for the KvLQT1 and minK antibodies were shared across species. Membranes were washed three times in TTBS, reblocked in 5% non-fat dry milk in TTBS (10 min) and then incubated with horseradish peroxidase-conjugated goat anti-rabbit IgG secondary antibody (1:5000, for Alomone ERG1) or donkey-anti-goat IgG secondary antibody (1:10,000, for Santa Cruz antibodies) in 5% non-fat dry milk in TTBS (40 min). They were subsequently

washed three times in TTBS and once in TBS. Signals were obtained with Western Lightning Chemiluminescence Reagent Plus (PerkinElmer Life Sciences). Band densities were determined with a laser-scanner (PDI 420oe) and Quantity One software (PDI). Protein loading was controlled by probing all Western blots with anti-GAPDH antibody (RDI) and normalizing ion-channel protein band intensity to that of GAPDH.

Data Analysis

All data are expressed as mean ± SEM. Each determination was performed on an individual heart: *n* values represent the number of hearts studied. Western blot band intensities are expressed quantitatively as arbitrary OD units, which correspond to laser-densitometric K^+-channel subunit membrane protein band intensity following background subtraction, divided by GAPDH signal intensity for the same sample. Statistical comparisons were performed with ANOVA and Student's *t*-test with Bonferroni's correction. A two-tailed $P < 0.05$ was taken to indicate statistical significance.

RESULTS

I_{to}-encoding Subunit mRNA Expression

Figure 1 shows RT-PCR signals for Kv1.4, 4.2 and 4.3 in the rabbit heart (lanes 3, 5 and 7). In contrast, no mRNA encoding these subunits could be identified in the guinea-pig heart (lanes 4, 6 and 8). Lanes 1 and 2 demonstrate the presence of α-actin in both rabbit and guinea-pig mRNA samples, indicating their intactness. Lane

9 shows the presence of two bands corresponding to Kv4.3 mRNA in guinea-pig brain, representing the previously-identified long and short splice variants. Thus, the absence of Kv4.3 in the guinea-pig heart is due to a lack of transcription rather than absence in the guinea-pig genome.

Results of Competitive RT-PCR

Figure 2 shows examples of gels obtained from human (A), rabbit (B), and guinea-pig (C) KvLQT1 competitive RT-PCR reactions. In all cases, lane 0 contains 100 ng of DNA Mass Ladder to create the standard curve for each gel. Lanes 1 through 6 were obtained with serial dilutions of the RNA mimic along with 1 μg total RNA. The upper bands represent the internal standard PCR product, while the lower bands are the target KvLQT1 bands co-amplified with the mimics in the same reaction tube. As the mimic concentration decreases from left to right, the target band gets stronger, demonstrating the competition between mimic and target. For each experiment, the sample KvLQT1 mRNA concentration was calculated based on the target and mimic band intensities at all dilutions as described in Methods. Figure 2*D* shows the mean data for each dilution in each species. The average absolute amounts of KvLQT1 mRNA in human, rabbit and guinea-pig hearts were 15.5 ± 2.7, 8.6 ± 3.3 and 5.3 ± 1.4 attomol/μg total RNA respectively.

Figures 3*A-C* show representative gels from minK competitive RT-PCRs. Particularly small mimic concentrations had to be used for rabbit hearts because of the weak minK expression and the point of equivalence was well to the right of the gel, corresponding to low mRNA concentrations. Mean data for all minK competitive RT-PCRs are shown in Figure 3*D*. They confirm that for any mimic

concentration, the highest target/mimic band intensities were observed in guinea-pig hearts and the lowest in rabbit hearts, with human hearts being intermediate. Mean calculated mRNA concentrations were 34.1 ± 12.5, 1.5 ± 0.3 and 12.7 ± 3.6 attomol/μg total RNA for guinea-pig, rabbit and human hearts respectively.

Examples of ERG1 competitive RT-PCR gels are shown in Figures 4*A-C*. Mean data are provided in Figure 4*D*. The target/mimic ratios are largest in human, followed by rabbit and then guinea-pig. Mean calculated ERG1 concentrations averaged 18.1 ± 4.0, 20.2 ± 7.1 and 92.8 ± 19.4 attomol/μg total RNA for guinea-pig, rabbit and human respectively.

Figure 5 shows comparisons between mRNA concentrations of various subunits among species. There was an ~2-fold difference in mean KvLQT1 mRNA concentrations between human and rabbit hearts (Fig. 5*A*) and rabbit heart concentrations were slightly higher than in guinea-pigs. There were major differences among species in the expression of minK mRNA (Fig. 5*B*). MinK expression was about 3-fold stronger in guinea-pig hearts, but weaker in rabbit hearts than human hearts. ERG1 mRNA was significantly more strongly expressed in human hearts than in the other species (Fig. 5*C*). Since KvLQT1 and minK co-assemble to form I_{Ks} (2, 19), the ratio of the concentrations of these subunits may be important in determining subunit assembly and channel formation. Figure 5*D* shows mean minK/KvLQT1 mRNA concentration ratios based on calculations for both subunits in each heart. The ratio was highest in the guinea-pig hearts, lower in humans and lower still in the rabbit.

Western Blot Studies

Figure 6A shows representative KvLQT1 protein bands detected at the expected molecular weight (~75 kDa, with the band in guinea-pigs having a slightly smaller molecular weight). The KvLQT1 signal was suppressed by pre-incubation with antigenic peptide (Fig. 6*A*, last three lanes). Corresponding GAPDH signals to which KvLQT1 bands were normalized are shown in Figure 6*B*. Figure 6*C* shows that humans had a significantly greater amount of KvLQT1 protein (3.1 ± 0.5 arbitrary OD units) as compared to both guinea-pigs (0.4 ± 0.2) and rabbits (1.5 ± 0.4, $n = 5$/group, $P < 0.05$).

Figure 7*A* shows a typical minK Western blot. Signals were detected in all species at ~27 kDa. An additional, very faint band was detected at 24 kDa in guinea-pigs. Pre-incubation with antigenic peptide suppressed the minK signal (+ control antigen, Fig. 7*A*, last three lanes). MinK band intensity was clearly strongest in guinea-pig hearts (0.6 ± 0.1 arbitrary OD units), weaker in human (0.3 ± 0.04) and the weakest in rabbit (0.08 ± 0.01, $n = 5$ for each group, $P < 0.05$, Fig. 7*C*).

ERG1 Western blots had to be performed with three different antibodies because of species-related amino-acid sequence differences in the epitopes against which commercially-available antibodies had been raised (Fig. 8). An antibody raised against a rat epitope (Alomone, APC-016) detected ERG1 in guinea-pig samples as a single band at ~145 kDa (Fig. 8*A*), and gave no signal in human samples. An antibody raised against human ERG1 (HERG1, Alomone, APC-062) identified a band at 165 kDa in human protein samples (Fig. 8*B*), but could not detect a clear signal from guinea-pig samples (first two lanes). Both of these antibodies were raised in rabbits, and gave a multitude of non-specific signals upon probing rabbit samples,

rendering them useless for detecting ERG1 in the rabbit. In order to detect ERG1 in rabbits, an antibody raised in goats against a different human ERG1 epitope (Santa Cruz) was used and detected a single 165 kDa band in rabbit samples (Fig. 8*C*). As expected, a band was detected with human samples as well. Since three different antibodies had to be used to detect properly ERG1 in humans, rabbits and guinea-pigs, and since the epitope sequences varied, meaningful band intensity comparisons could not be made.

DISCUSSION

In the present study, we examined the expression of K^+-channel subunits underlying time-dependent repolarizing currents in various species. We noted clear species-dependent differences in subunit expression that parallel and shed potential light on the mechanisms of differences in K^+-current profiles.

Species-specific Time-dependent K^+-currents and Molecular Basis

Time-dependent K^+-currents play an important role in governing cardiac repolarization, thereby determining the occurrence of a broad range of arrhythmias and mediating a wide variety of antiarrhythmic and pro-arrhythmic drug actions (11, 17, 18). Animal models have been essential for an appreciation of the determinants of repolarization of action potentials and of the mechanisms underlying cardiac arrhythmias. One limitation in using animal models to understand the determinants of repolarization and arrhythmias in man has been a lack of information about how the relative distributions of ion channel subunits in different species compare with each other and with the ion-channel subunit distribution in man.

There are well-recognized differences in I_K between rabbit and guinea-pig hearts (9, 13, 16, 21). Guinea-pig I_{Ks} is much larger and shows slower kinetics than in the rabbit (16). Our observation that minK is much more strongly-expressed in the guinea-pig than the rabbit at both the mRNA (Fig. 5) and protein (Fig. 7) levels provides a possible molecular basis for the differences. In the absence of minK, KvLQT1 is known to form small, rapidly-activating currents, whereas co-expression of KvLQT1 and minK carries robust currents with the typical properties of I_{Ks} (2, 19). Therefore, the relative lack of minK in rabbits is a plausible explanation for their small and more rapidly-activating I_{Ks}.

It has been difficult to record I_K in human cardiac myocytes (3, 7, 13, 22). This has led to the suggestion that I_K may be quantitatively less important in human hearts than in other species. Our data suggest strong I_K-subunit expression in the human heart, with evidence for stronger KvLQT1 and ERG1 expression in man than in rabbits or guinea-pigs and minK expression that is intermediate between guinea-pigs and rabbits. These results suggest that I_K is likely of the same order of importance in human hearts as in other species, and that the difficulties reported in recording I_K in human hearts may be related to the sensitivity of I_K to cell isolation (27) and the fact that human tissue preparations are never available for cell isolation under the conditions achievable for animal models, rather than to lesser importance of I_K in the human heart.

It is well known that guinea-pig cardiac I_K density is particularly large (13, 16, 21). Our findings suggest that strong expression of I_{Ks} subunits (Fig. 7), particularly minK, accounts at least in part for the large guinea-pig I_K. The rabbit is known have small I_K (9, 13, 16, 21) and to be particularly prone to class III drug-induced EADs

and Torsades de Pointes (5, 15). There is evidence that I_{Ks} acts as a safety mechanism against excessive action potential duration prolongation with I_{Kr}-inhibition, and that, in circumstances in which I_{Ks} is reduced, I_{Kr} inhibition produces enhanced repolarization delays and a greater risk of EADs (4, 10, 29). Thus, the relatively low level of minK expression in the rabbit heart, resulting in small I_{Ks}, may provide the molecular basis for the sensitivity of the rabbit to I_{Kr} blocking drug-induced repolarization abnormalities and related arrhythmias. The rabbit may thus provide a natural model analogous to human long QT syndromes associated with relative minK deficiency; however further pharmacological and electrophysiological studies are needed to evaluate this notion.

The rabbit and guinea-pig have long been recognized to be at opposite ends of the repolarizing current and action potential profile spectrum, with the rabbit showing large I_{to} and small I_K (9, 13, 16, 21) and the guinea-pig showing large I_K and little or no I_{to} (13, 16, 21). In fact, there has been some controversy about the presence or absence of I_{to} in the guinea-pig. Although many investigators have reported a lack of I_{to} in guinea-pig hearts, sensitivity of guinea-pig action potential repolarization to 4-aminopyridine and the recording of rapidly-inactivating depolarization-induced outward currents has led to some doubt about the possible expression of I_{to} in the guinea-pig heart (8, 12, 14, 24). Our results show that the transcripts corresponding to I_{to} K^+-channel α-subunits, Kv1.4, 4.2 and 4.3, are lacking in guinea-pig hearts, and provide molecular confirmation for the conclusions of recent experimental studies indicating that no transient outward K^+-current is present in the guinea-pig heart (8). We did not compare I_{to} subunit distribution in rabbit vs. man, because this has been

the object of a previous detailed publication (23), which showed that rabbit cardiac I_{to} reflects the presence of Kv1.4, 4.2 and 4.3, whereas Kv4.3 is predominant in man.

Potential Limitations

It is apparent that differences in repolarization properties between species may be due to species-specific differences in the expression of voltage-gated K^+ channel subunits. However, it is also well known that these channels are modulated by a variety of signalling mechanisms and regulatory factors, so that differences in such modulation between species could also contribute to the observed electrophysiological differences. The much smaller minK expression in rabbits compared to guinea pigs is an appealing explanation for the smaller rabbit I_{Ks} density, but we cannot exclude a contribution from other factors such as regulatory differences and the role of other (presently unidentified) subunits that might contribute to I_{Ks}.

A particular advantage of competitive RT-PCR is that it provides absolute quantification of transcript concentration, allowing for comparisons in the expression of each K^+-channel subunit across different species as well as comparisons between the expression of different subunits within a species. Quantitative analysis of Western blots provides important complementary information, allowing for relative quantification of protein expression across species when the antigenic epitope is identical in different species. A limitation of Western blot analyses is that, because of potential antibody affinity differences, meaningful quantitative comparisons are not possible for the expression of different subunits within the same species or for expression of the same subunit with epitope sequence differences across species. Our

mRNA analysis provides precise information about the relative expression of the various I_K subunits in different species, as well as about the relative expression of transcripts encoding different molecular species with one another. MinK and KvLQT1 epitopes are the same among the species we studied, allowing quantitative comparisons for their protein expression across species. However, the relative protein expression of minK versus KvLQT1 cannot be compared and we therefore cannot comment on the relative protein within each species. Because of epitope differences, we were not able to compare quantitatively ERG1 protein expression across species.

Only normal human tissue was used for this study. Because of the rarity of such samples, we were not able to control for the sex of the samples, but the number of male and female subjects from whom tissues were obtained was about equal. The guinea pig and rabbit samples were similarly mixed for consistency.

CONCLUSIONS

There are quantitative differences in cardiac K^+-channel subunit expression among guinea-pigs, rabbits and man which shed light on the molecular basis of species-specific repolarization properties and arrhythmia susceptibility. The present observations provide potentially useful insights into the relationships between repolarizing currents and the expression of underlying K^+-channel subunits in commonly used experimental animals compared to those in man. These findings are important for the understanding of the molecular control of repolarization and for the interpretation of electrophysiological studies in various animal models.

ACKNOWLEDGEMENTS

The authors thank Evelyn Landry for technical assistance and France Thériault for secretarial help with the manuscript, and Dr. Miklos Opincariu of the Department of Cardiac Surgery, University of Szeged, for help and tissue procurement. Funding was provided by the Canadian Institutes of Health Research, the Quebec Heart and Stroke Foundation, and the Hungarian National Research Foundation (OTKA-T32558).

REFERENCES

1. **Abbott GW, Sesti F, Splawski I, Buck ME, Lehmann MH, Timothy KW, Keating MT, and Goldstein SA.** MiRP1 forms IKr potassium channels with HERG and is associated with cardiac arrhythmia. *Cell* 97: 175-187, 1999.

2. **Barhanin J, Lesage F, Guillemare E, Fink M, Lazdunski M, and Romey G.** K(V)LQT1 and lsK (minK) proteins associate to form the I(Ks) cardiac potassium current. *Nature* 384: 78-80, 1996.

3. **Beuckelmann DJ, Nabauer M, and Erdmann E.** Alterations of K+ currents in isolated human ventricular myocytes from patients with terminal heart failure. *Circ Res* 73: 379-385, 1993.

4. **Biliczki P, Virag L, Iost N, Papp JG, and Varro A.** Interaction of different potassium channels in cardiac repolarization in dog ventricular preparations: role of repolarization reserve. *Br J Pharmacol* 137: 361-368, 2002.

5. **Carlsson L, Almgren O, and Duker G.** QTU-prolongation and torsades de pointes induced by putative class III antiarrhythmic agents in the rabbit: etiology and interventions. *J Cardiovasc Pharmacol* 16: 276-285, 1990.

6. **Dixon JE, Shi W, Wang HS, McDonald C, Yu H, Wymore RS, Cohen IS, and McKinnon D.** Role of the Kv4.3 K+ channel in ventricular muscle. A molecular correlate for the transient outward current. *Circ Res* 79: 659-668, 1996.

7. **Escande D and Coraboeuf E.** Two types of transient outward currents in adult human atrial cells. *Am J Physiol* 252: H142-H148, 1987.

8. **Findlay I.** Is there an A-type K+ current in guinea-pig ventricular myocytes? *Am J Physiol Heart Circ Physiol* 10:[epub ahead of print], 2002.

9. **Giles WR, and Van Ginneken AC.** A transient outward current in isolated cells from the crista terminalis of rabbit heart. *J Physiol* 368: 243-264, 1985.

10. **Han W, Chartier D, Li D, and Nattel S.** Ionic remodeling of cardiac Purkinje cells by congestive heart failure. *Circulation* 104: 2095-2100, 2001.

11. **Haverkamp W, Breithardt G, Camm AJ, Janse MJ, Rosen MR, Antzelevitch C, Escande D, Franz M, Malik M, Moss A, and Shah R.** The potential for QT prolongation and pro-arrhythmia by non-anti-arrhythmic drugs: clinical and regulatory implications. Report on a Policy Conference of the European Society of Cardiology. *Cardiovasc Res* 47: 219-233, 2000.

12. **Inoue M, and Imanaga I.** Masking of A-type K+ channel in guinea-pig cardiac cells by extracellular Ca2+. *Am J Physiol* 264: C1434-C1438, 1993.

13. **Lathrop DA, Nanasi PP, Schwartz A, and Varro A.** Ionic basis for OPC-8212-induced increase in action potential duration in isolated rabbit, guinea-pig and human ventricular myocytes. *Eur J Pharmacol* 24: 127-137, 1993.

14. **Li GR, Yang B, Sun H, and Baumgarten CM.** Existence of a transient outward K(+) current in guinea-pig cardiac myocytes. *Am J Physiol Heart Circ Physiol* 279: H130-H138, 2000.

15. **Lu HR, Marien R, Saels A, and De Clerck F.** Species plays an important role in drug-induced prolongation of action potential duration and early afterdepolarizations in isolated Purkinje fibers. *J Cardiovasc Electrophysiol* 12: 93-102, 2001.

16. **Lu Z, Kamiya K, Opthof T, Yasui K, and Kodama I.** Density and kinetics of I(Kr) and I(Ks) in guinea-pig and rabbit ventricular myocytes explain different efficacy of I(Ks) blockade at high heart rate in guinea-pig and rabbit: implications for arrhythmogenesis in humans. *Circulation* 104: 951-956, 2001.

17. **Nattel S.** The molecular and ionic specificity of antiarrhythmic drug actions. *J Cardiovasc Electrophysiol* 10: 272-282, 1999.

18. **Roden DM, Balser JR, George AL Jr, and Anderson ME.** Cardiac ion channels. *Annu Rev Physiol* 64: 431-475, 2002.

19. **Sanguinetti MC, Curran ME, Zou A, Shen J, Spector PS, Atkinson DL, and Keating MT.** Coassembly of K(V)LQT1 and minK (IsK) proteins to form cardiac I(Ks) potassium channel. *Nature* 384: 80-83, 1996.

20. **Sanguinetti MC, Jiang C, Curran ME, and Keating MT.** A mechanistic link between an inherited and an acquired cardiac arrhythmia: HERG encodes the IKr potassium channel. *Cell* 21: 299-307, 1995.

21. **Varro A, Lathrop DA, Hester SB, Nanasi PP, and Papp JG.** Ionic currents and action potentials in rabbit, rat, and guinea-pig ventricular myocytes. *Basic Res Cardiol* 88: 93-102, 1993.

22. **Virag L, Iost N, Opincariu M, Szolnoky J, Szecsi J, Bogats G, Szenohradszky P, Varro A, and Papp JG.** The slow component of the delayed rectifier potassium current in undiseased human ventricular myocytes. *Cardiovasc Res* 49: 790-797, 2001.

23. **Wang Z, Feng J, Shi H, Pond A, Nerbonne JM, and Nattel S.** Potential molecular basis of different physiological properties of the transient outward K^+ current in rabbit and human atrial myocytes. *Circ Res* 84: 551-561, 1999.

24. **Wang Z, Fermini B, and Nattel S.** Repolarization differences between guinea-pig atrial endocardium and epicardium - evidence for a role of I_{to}. *Am J Physiol Heart Circ Physiol* 260: H1501-H1506, 1991.

25. **Wang Z, Yue L, White M, Pelletier G, and Nattel S.** Differential distribution of inward rectifier potassium channel transcripts in human atrium versus ventricle. *Circulation* 98: 2422-2428, 1998.

26. **Weerapura M, Nattel S, Chartier D, Caballero R, and Hebert TE.** A comparison of currents carried by HERG, with and without coexpression of MiRP1, and the native rapid delayed rectifier current. Is MiRP1 the missing link? *J Physiol* 540: 15-27, 2002.

27. **Yue L, Feng J, Li GR, and Nattel S.** Transient outward and delayed rectifier currents in canine atrium: properties and role of isolation methods. *Am J Physiol Heart Circ Physiol* 270: H2157-H2168, 1996.

28. **Yue L, Melnyk P, Gaspo R, Wang Z, and Nattel S.** Molecular mechanisms underlying ionic remodeling in a dog model of atrial fibrillation. *Circ Res* 84: 776-784, 1999.

29. **Zeng J, Laurita KR, Rosenbaum DS, and Rudy Y.** Two components of the delayed rectifier K+ current in ventricular myocytes of the guinea-pig type. Theoretical formulation and their role in repolarization. *Circ Res* 77: 140-152, 1995.

Table 1. *Primers for RT-PCR*

Current	Clone	Primer Pair	Position, bp	Size, bp	Tm, °C
I_{to}	Kv1.4	F: AACAGTCACATGCCTTATG	3-390	388	55
		R: TAGTAAAACCTTCCCTCCTC			
	Kv4.2	F: CTTCACTATCCCCGCCAT	1377-1756	378	55
		R: GTTTCCACCACATTCGCG			
	Kv4.3	F: GAAGAGGAGCACATGGGC	1381-1832	452	55
		R: GTGATCTGGGATGTTTTGC			
I_{Ks}	HKvLQT1	F: CCACCATTAAGGTCATTCG	1114-1461	348	54.9
		R: CCTTGTCTTCTACTCGGTTCA			
	RKvLQT1	F: GCCGCAGCAAGTATGTCG	86-402	317	57.6
		R: CCTTCTCAGCAGGTACACGA			
	GPKvLQT1	F: GTTTGCCACATCAGCCATCA	66-362	297	56.6
		R: GGGACCTTGTCGCCGTAA			
	HminK	F: ACGCCCTTTCTGACCAAGC	28-255	228	55
		R: ATCGGACTCGATGTAGACG			
	RminK	F: CCGTGATGCCCTTTCTGACC	23-285	263	58.4
		R: GTACGCCCTGTCTTTCTCCTG			
	GpminK	F: GGGGACAGTTCAACCCAGTA	54-330	277	55
		R: TTCAATGACGCAACACGAT			
I_{Kr}	HERG1	F: TCGCCGTCCACTACTTCAA	1466-1846	381	57.3
		R:AGAGCGCCGTCACATACTT			
	RERG1	F: TACGGAGTGGGAAGGTGGATT	2577-2890	314	62.3
		R: TCTCGCAGTCTTCGGTCAGG			
	GPERG1	F: TGGCTCATCCTACTGCTGG	13-232	220	55.1
		R: GGCTGACCACTTCCTCGTT			

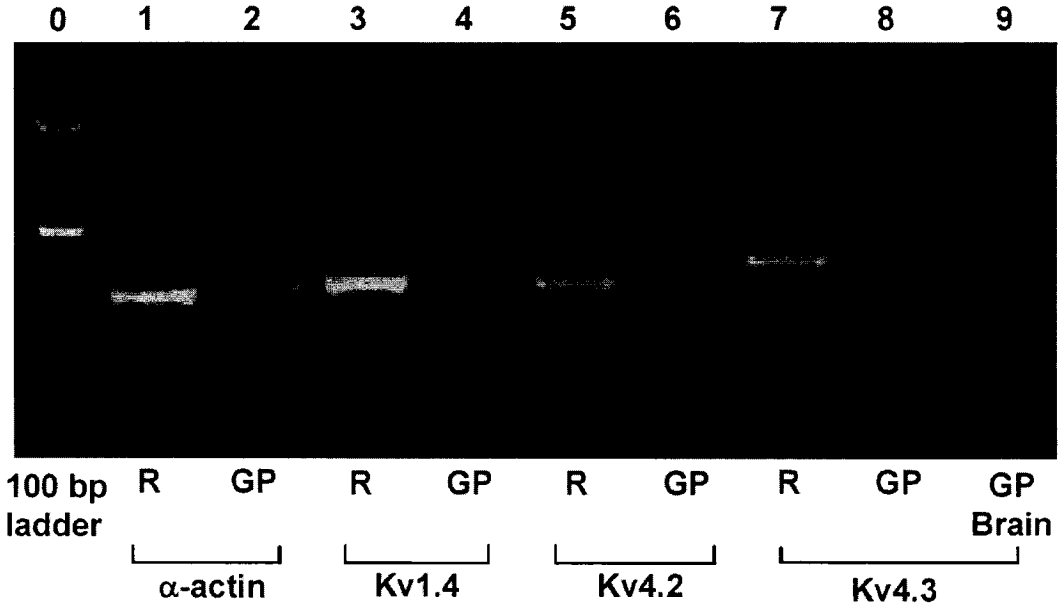

Figure 1 RT-PCR products for α-actin (positive control), Kv1.4, 4.2 and 4.3 in rabbit (R) and guinea-pig (GP) heart and GP brain.

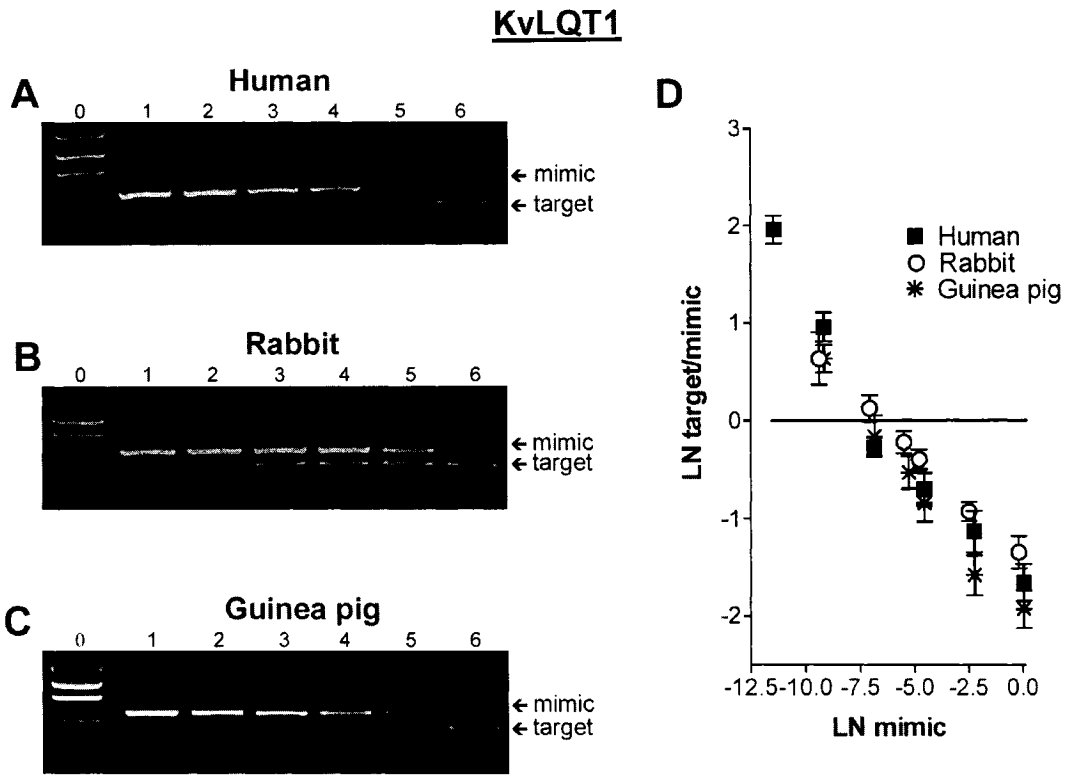

Figure 2 Competitive RT-PCR analysis of KvLQT1 mRNA expression. Representative gels are shown in A-C, mean data are in D. **A.** Results for a human heart. Lanes 1-6: initial reaction tube contained 106 ng, 10.6 ng, 1.1 ng, 106 pg, 10.6 pg and 1.1 pg of mimic RNA respectively. **B.** Results obtained in a rabbit heart with 84.9 ng, 8.5 ng, 850 ng, 425 pg, 85 pg and 8.5 pg mimic (lanes 1-6 respectively). **C.** Results in a guinea-pig heart with 106 ng, 10.6 ng, 1.1 ng, 532 pg, 106 pg and 10.6 pg respectively in lanes 1-6. **D.** Mean ± SEM data ($n = 5$ hearts/determination.

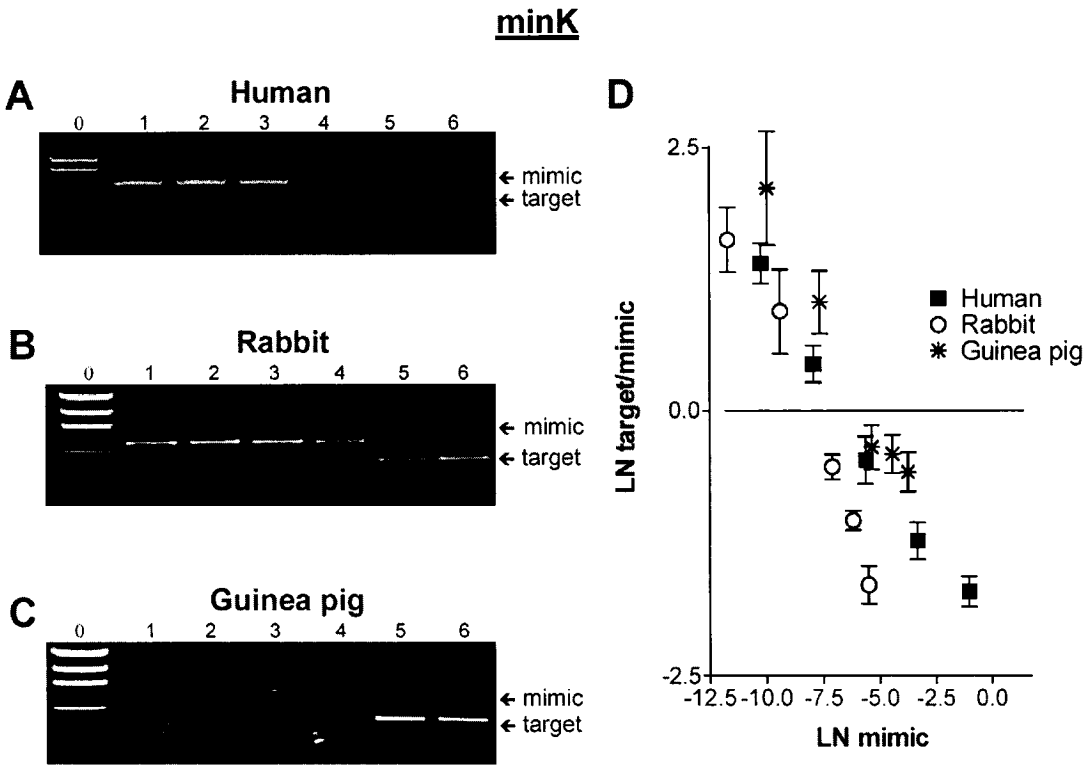

Figure 3 MinK competitive RT-PCR. **A.** Results for a human heart. Initial reaction tubes contained 359 ng, 35.9 ng, 3.6 ng, 359 pg, 35.9 pg and 3.6 pg of mimic RNA in lanes 1-6 respectively. **B.** Results obtained in a rabbit heart with 830 pg, 415 pg, 207 pg, 83 pg, 8.3 pg and 0.83 pg mimic (lanes 1-6). **C.** Results in a guinea-pig heart with 4.8 ng, 2.4 ng, 1.2 ng, 475 pg, 47.5 pg and 4.8 pg in lanes 1-6. **D.** Mean ± SEM data (n = 5 hearts/determination).

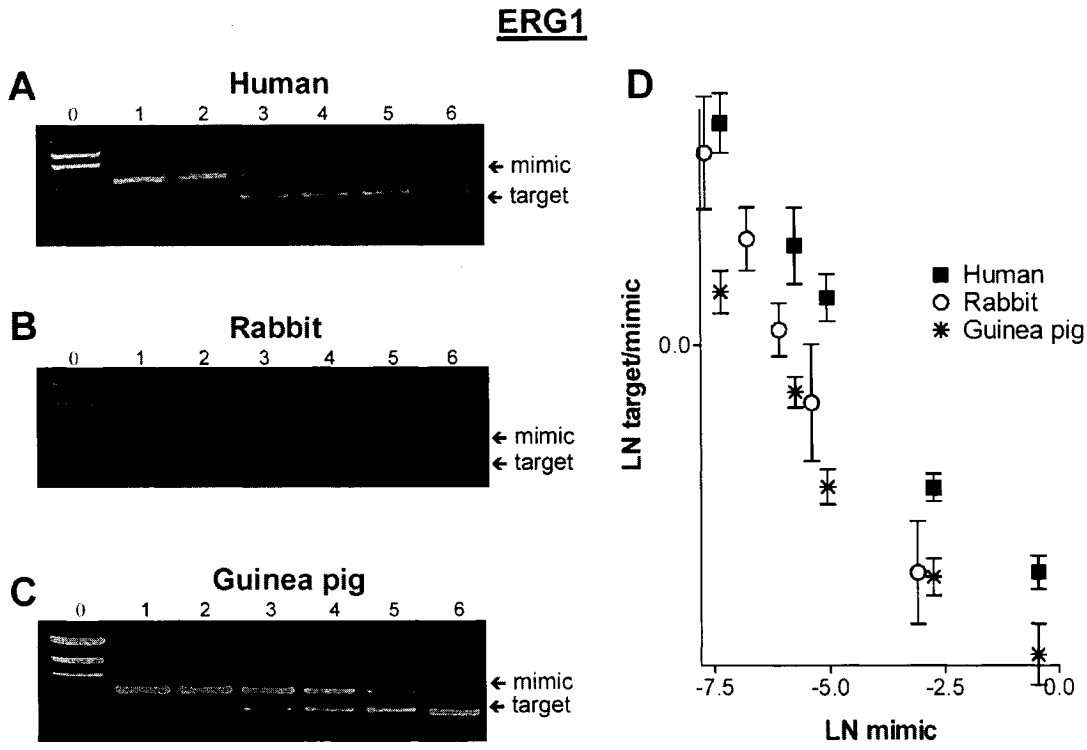

Figure 4 ERG1 competitive RT-PCR. **A-C.** Representative gels. Mimic dilutions for both human and guinea-pig samples were: 64 ng, 6.4 ng, 640 pg, 320 pg, 64 pg and 6.4 pg. For the rabbit, mimic concentrations in the initial reaction tubes were: 4.5 ng, 453 pg, 227 pg, 113 pg, 45.3 pg and 4.5 pg. **D.** Mean ± SEM data (n = 5 hearts/determination).

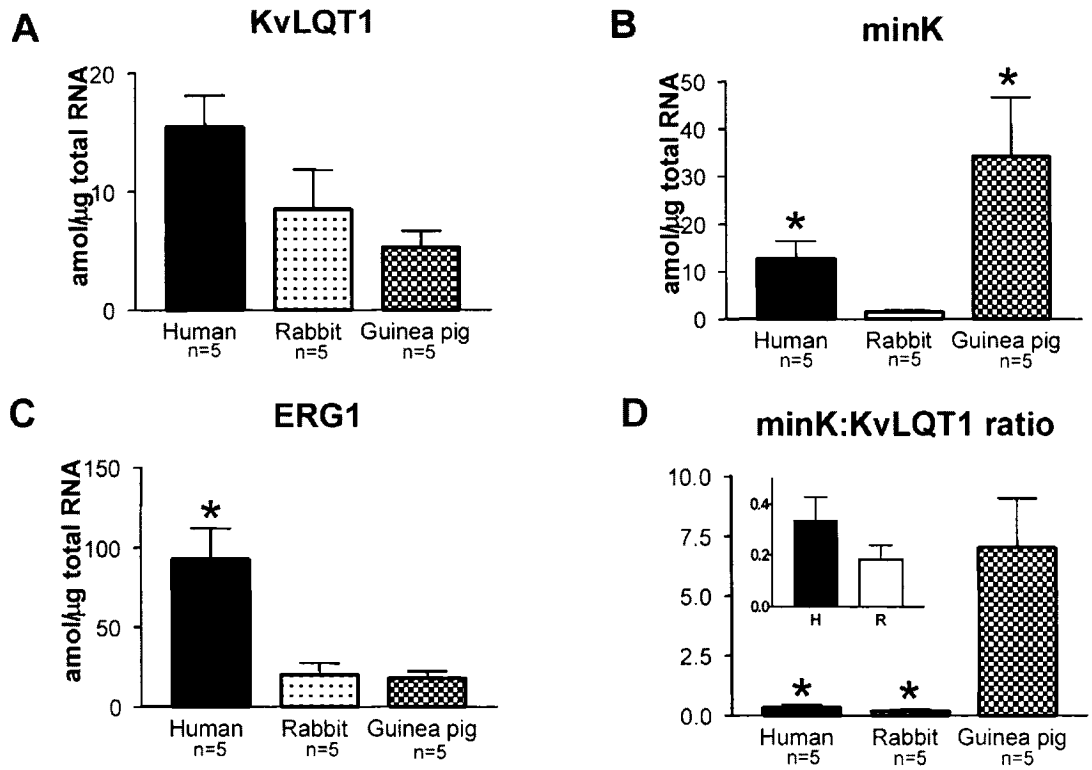

Figure 5 Mean (± SEM) mRNA concentrations for KvLQT1 (**A**), minK (**B**) and ERG1 (**C**). $*P < 0.05$ vs. rabbit. **D**. Mean (± SEM) KvLQT1/minK concentration ratio. $*P < 0.05$ vs. guinea-pig. Inset: Human (H) and rabbit (R) values on larger scale.

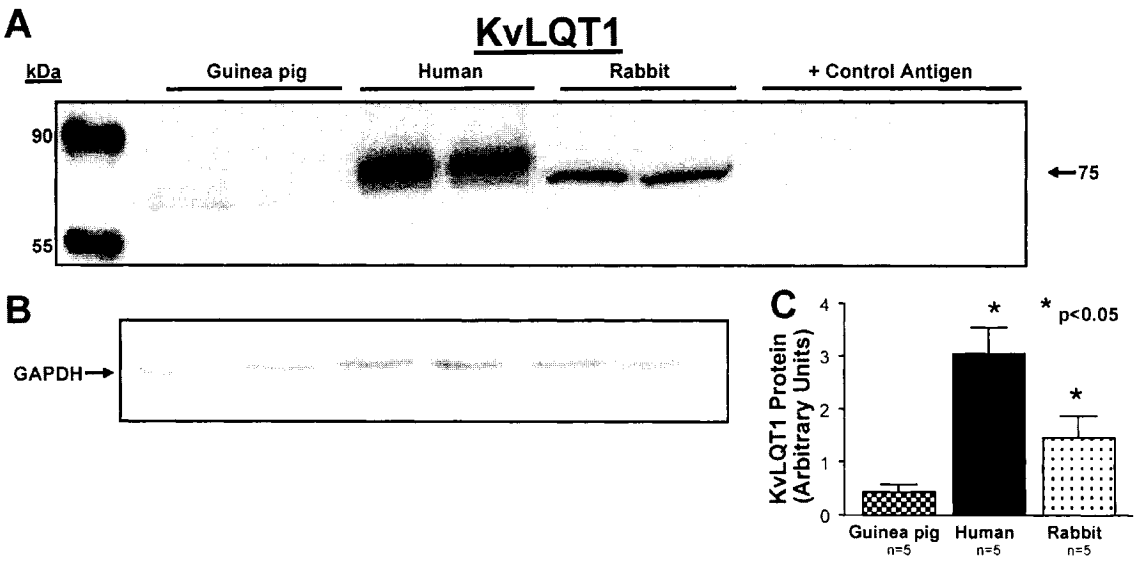

Figure 6 Examples of Western blots for KvLQT1 α-subunits. **A.** Example of membrane probed for KvLQT1 protein, with two lanes representing samples from two separate hearts for each species. A single band is detected at ~75 kDa in all species. + Control antigen represents examples with one sample per species blotted with primary antibody pre-incubated with the peptide against which it was raised. **B.** GAPDH bands for the same lanes in the same gel as corresponding samples in A. **C.** KvLQT1 protein concentrations (mean ± SEM, $n = 5$ per species). $^*P < 0.05$ vs. guinea-pig, $n = 5$.

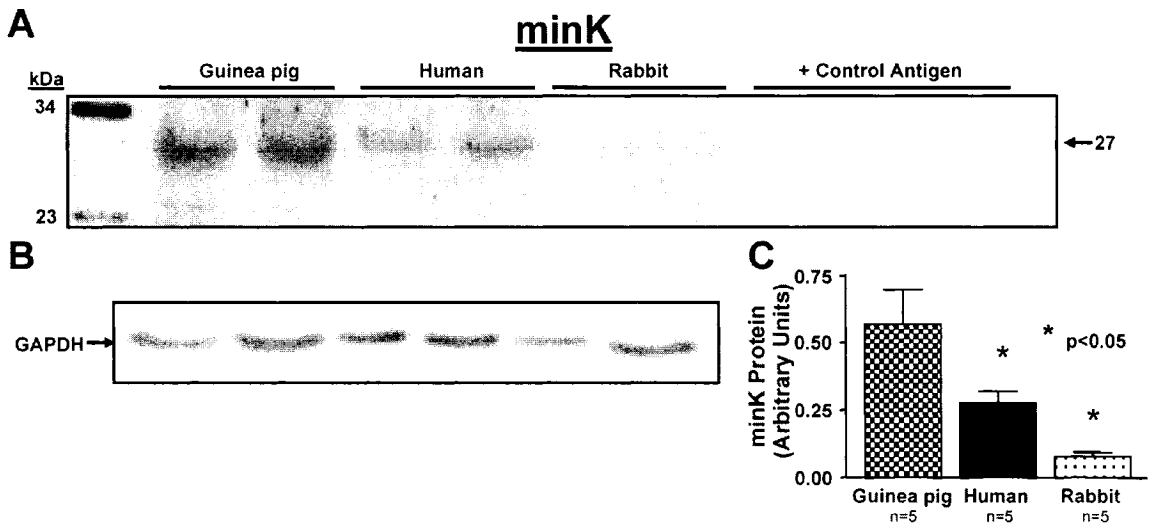

Figure 7 Examples of Western blots for minK protein (**A**). Left: a band is detected at ~27 kDa in all species, with separate lanes run with samples from two hearts per species. Right: results for one sample per species probed with antibody pre-incubated with antigenic peptide. All western blot results were normalized to the amount of GAPDH detected in a given sample (**B**). The mean amounts of minK protein are shown in (**C**) (mean ± SEM, $n = 5$ for each group, $^*P < 0.05$ vs. guinea-pig).

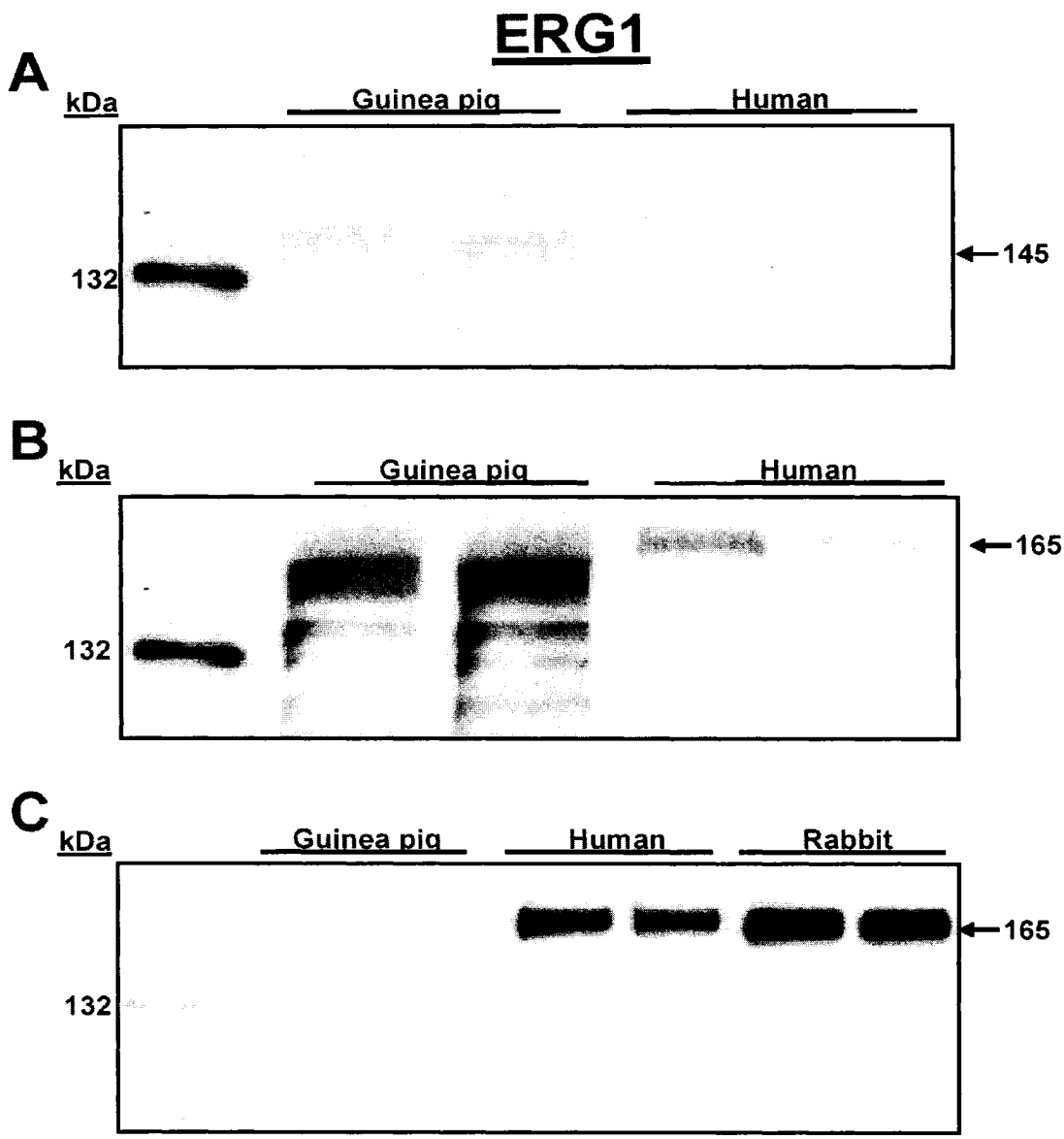

Figure 8 Examples of blots of cardiac membrane proteins probed with different antibodies for ERG1. Two lanes with separate heart samples were run for each species were run on each gel. **A.** Clear ERG1 protein expression detected in guinea-pig but not in human tissue with the use of an antibody to rat ERG1 raised in rabbits. **B.** Probing with an antibody to human ERG1 protein raised in rabbit detected a single band at ~165 kDa in human cardiac tissue and multiple lower molecular weight bands in guinea-pig. Because the antibodies used for the experiments illustrated in panels A and B were raised in rabbits, blotting of rabbit membrane proteins yielded many non-specific bends. **C.** Western blot obtained with an antibody raised in goats against a different human ERG1 epitope from that shown in **B**. A single band is detected in human and rabbit tissue at ~165 kDa. No bands are present in guinea pig blots.

CHAPTER 3: MOLECULAR CHARACTERIZATION OF CHANGES IN SODIUM CURRENT INDUCED BY CONGESTIVE HEART FAILURE

Cardiac Na^+ currents are important for the propagation of impulses originating in the SAN and conducting over the entire myocardium. As the primary determinant of the Phase 0 upstroke in the cardiac action potential, I_{Na} is extremely influential on the conduction velocity throughout much of the heart. Any defect in I_{Na} can alter the coordinated activity of myocardial excitation by slowing conduction velocity. Similar results can be obtained by blocking I_{Na} using selective channel blockers such as flecainide, encainide and quinidine. Therefore, these Class I drugs are generally considered pro-arrhythmic rather than anti-arrhythmic (1989). Cardiovascular diseases such as CHF and dilated cardiomyopathy are also associated with conduction slowing (Sanders *et al.*, 2003), and a reduced I_{Na} has been noted in a canine model of CHF (Maltsev *et al.*, 2002). In this paper, we sought to determine the molecular basis for this heterogeneous downregulation of I_{Na} in the ventricular mid-myocardium.

ABSTRACT

Clinical and experimental evidence has been recently accumulated about the importance of alterations of Na^+ channel function and slow myocardial conduction for arrhythmias in infarcted and failing hearts (HF). The present study evaluated the molecular mechanisms of local alterations in the expression of NaCh subunits which underlie Na^+ current density decrease in HF. HF was induced in 5 dogs by sequential coronary microembolization and developed approximately 3 months after the last embolization (left ventricle, LV, ejection fraction = 27±7%). 5 normal dogs served as a control group. Ventricular cardiomyocytes (VCs) were isolated enzymatically from LV mid-myocardium and I_{Na} was measured by whole-cell patch-clamp. The mRNA encoding the cardiac specific sodium channel (NaCh) α-subunit $Na_v1.5$, and one of its auxiliary subunits β1 (NaChβ1), was analyzed by competitive RT-PCR. Protein levels of $Na_v1.5$, NaChβ1 and NaChβ2 were evaluated by Western blotting. The maximum density of I_{Na}/C_m was decreased in HF (n=5) compared to control hearts (32.3±2.6 vs. 50.8±6.5 pA/pF, mean±SEM, n=5, $P<0.05$). The steady-state inactivation and activation of I_{Na} remained unchanged in HF compared to control hearts. The levels of mRNA encoding $Na_v1.5$, and NaChβ1 were unaltered in failing hearts. However, $Na_v1.5$ protein expression was reduced about 30% in HF, while NaChβ1 and NaChβ2 protein were unchanged in dogs with HF. We conclude that experimental chronic HF in dogs results in post-transcriptional changes in cardiac NaCh α-subunit expression.

Key Words: heart failure, sodium channel, β-subunits, patch clamp, RT-PCR, Western blot

INTRODUCTION

Sudden cardiac death, due largely to ventricular tachyarrhythmias, remains a major public health care problem and accounts for nearly 40% of all deaths in patients with heart failure (HF). Local or regional electrical instabilities are considered a major risk factor in sudden cardiac deaths. [1] In addition to arrhythmias, another important potential consequence of slow trans-myocardial conduction is poor hemodynamic performance of the failing heart. In fact, patients with HF frequently manifest intra-ventricular conduction delays, which can be treated by cardiac resynchronization therapy. [2] Since the primary function of Na^+ channels (NaChs) is to provide the electrical charge for cardiac impulse propagation, NaCh alterations may represent destabilizing influence within diseased myocardium. Previous studies did not reveal changes in sodium current density (I_{Na}) in dogs with pacing-induced HF [3] or in levels of mRNA encoding cardiac NaCh in patients with terminal HF.[4] Recent discovery of transmural regional differences in NaCh expression [5, 6] that have not been addressed in the previous studies [3, 4] raises the question about the importance of local alterations of NaChs in HF. Indeed, down-regulation of NaChs has been found in canine chronic atrial fibrillation [7] and chronic heart failure [8] models and in myocytes from the epicardial border zone of infarcted hearts. [9] Recent studies have indicated that alterations of NaChs may contribute to the genesis of cardiac arrhythmias [10], including those in HF. Changes in I_{Na} can slow myocardial conduction and cause sustained, isolated conduction defects [11] and reentrant arrhythmias.[12]

The present study evaluated the molecular mechanism of local alterations of expression of NaCh subunits in chronic HF. The cardiac NaCh is comprised of the main pore forming α-subunit ($Na_v1.5$) as well as auxiliary β1 (NaChβ1), and β2

subunits (NaChβ2) [13], which are transmembrane proteins that modulate α-subunit function. The auxiliary β-subunits have been implicated in regulation of $Na_v1.5$ kinetics associated with the LQT3 mutation[14], aggravation of NaCh dysfunction in Brugada syndrome[15], modification of block of NaCh by fatty acids [16] and lidocaine[17], and modulation trafficking of $Na_v1.5$ [18]. Recently β3 and β4 subunits were discovered in brain.[19-21] The discovery increases the complexity of NaCh and raises further questions about the role of β subunits in heart.

To avoid known difficulties (interacting diseases, drug therapies, problems in sample procurement, etc) in human studies, a reproducible canine chronic HF model that mimics coronary artery disease and infarction was employed in the study. This HF model manifests extensive and sustained depression of ventricular function, marked ventricular ectopy, and sudden death in ~13% of animals.[22, 23] Multiple diffuse infarctions were produced by sequential coronary embolizations with microspheres. Chronic HF developed approximately 3 months after the last embolization. To avoid potential misinterpretations due to transmural regional differences in NaCh subunits expression [5], voltage-clamp studies, competitive RT-PCR, and Western blots were performed using LV mid-myocardial slices and enzymatically-isolated cardiomyocytes (VCs) from these slices.

MATERIALS AND METHODS

Canine Chronic Heart Failure Model

The dog model of chronic HF was previously described in detail [22]. Healthy mongrel dogs, weighing between 24 and 31 kg, underwent multiple sequential

coronary microembolizations, to produce HF. Embolizations were performed 1 to 3 weeks apart and were discontinued when LV ejection fraction, determined angiographically, was ≤35%. At the time of harvesting the heart (~3 months after the last microembolization) LV ejection fraction was 27±7%. LV tissue specimens were obtained from 5 normal dogs and 5 HF dogs. This study is in compliance of the Recommendation from the Declaration of Helsinki and the Guiding Principles in the Care and Use of Animals requirements, and has been approved by the Henry Ford Health System Institutional Animal Care and Use Committee.

Design of the Study

The study population represents a sub-study of a larger trial. [8] To test our hypothesis, 5 dogs with chronic HF were randomly selected for patch-clamp experiments and heart tissue samples were frozen for further molecular biology analysis.

Cardiomyocyte Isolation

VCs were enzymatically isolated from slices of the apical third of the LV mid-myocardium as previously described. [24] The yield of viable, Ca^{2+}-tolerant, rod-shape VCs isolated from both normal and failed hearts varied from 20% to 80%.

Patch-Clamp Measurements

I_{Na} was recorded by whole cell patch clamp technique as previously reported.[25] The pipette solution contained (in mM): CsCl 133, NaCl 5, ethylene glycol-bis (beta-aminoethyl ether) N,N,N',N'-tetraacetic acid (EGTA) 10, MgATP 5,

tetraethylammonium 20, HEPES 5 (pH 7.3 with CsOH). The patch pipette tip resistance was 0.5-0.8 MΩ. Whole cell currents were measured at room temperatures of 22°-24°C in symmetric Na^+ (5/5 mM, inside/outside) conditions, with the bath solution containing (in mM): NaCl 5, CsCl 133, $MgCl_2$ 2, $CaCl_2$ 1.8, nifedipine 0.002, HEPES 5 (pH 7.3 with CsOH). To minimize spontaneous steady-state availability and activation shifts[25], the current measurements were performed approximately 20-25 min after the membrane rupture. The peak of I_{Na} ranged from 2 nA to 10 nA. The cell capacitance was measured by means of voltage ramp of 20 mV and 2 ms duration applied from –80 mV. The quality of the voltage clamp was controlled in each cardiomyocyte by estimating deviation (V_{dev}) from voltage command as previously described.[25] Satisfactory voltage control was assumed if V_{dev}<2 mV, and only those cells which met this criterion were included in the study.

RNA Isolation

Sections of mid-myocardial tissue were removed from the dogs and frozen immediately in liquid nitrogen. Total RNA was isolated using Trizol reagent (Invitrogen) followed by chloroform extraction and isopropanol precipitation. Genomic DNA was eliminated by incubating in DNase I (0.1U/μL, 37°C) for 30 minutes followed by acid phenol-chloroform extraction. RNA was quantified by spectrophotometric absorbency at 260 nm, purity confirmed by A_{260}/A_{280} ratio and integrity evaluated by ethidium-bromide staining on a denaturing agarose gel. RNA samples were stored at -80°C in RNAsecure Resuspension Solution (Ambion).

Primers

Primers specific for canine $Na_V1.5$ and $Na\beta1$ genes (Gene specific primers, GSPs) were designed based on previously published sequences (GenBank accession number AF017428). Chimeric primer pairs for the synthesis of the RNA mimic were constructed with a sequence homologous to rabbit cardiac α-actin flanked on both 5' and 3' sides by the GSPs. An 8-nucleotide sequence, GGCCGCGG, corresponding to the 3' end of the T7 promoter was conjugated to the 5' end of each forward chimeric primer.

Synthesis of RNA mimic

Reverse transcription was used to synthesize first-strand cDNA from rabbit ventricular total RNA sample. This cDNA was used as a template for the subsequent PCR steps. First, a PCR reaction was performed with the chimeric mimic primers. The product from this PCR consists of a 460-bp rabbit α-actin sequence, flanked at each end by either the dog $Na_V1.5$ or $Na\beta1$ gene-specific sequence. In addition, there is an 8-bp sequence corresponding to the 3' end of the T7 promoter at the 5' end of the PCR product. A second PCR is performed with the T7 promoter as the sense primer, as well as the anti-sense GSP (either $Na_V1.5$ or $Na\beta1$). The DNA product from this PCR contains the full T7 promoter and was gel-purified using the QIAquick Gel Extraction Kit (Qiagen Inc.). This DNA template was used for the subsequent *in vitro transcription* reactions using the T7 mMESSAGE MACHINE kit (Ambion Inc.) to create the RNA mimic. Any potential DNA contamination was removed after the reaction with RNase-free DNase I (30mis. at 37°C), followed by a phenol/chloroform

extraction and isopropanol precipitation. The final RNA mimic contains the GSPs flanking a 460-bp rabbit α-actin sequence. The correct size was verified on a denaturing RNA gel. Pre-determined concentrations of RNA were run alongside the mimics in order to create a standard curve with which the concentration of the mimic was determined.

Reverse Transcription

Reaction mixtures containing serial 10-fold dilutions of the RNA mimic along with 1μg of total RNA sample were prepared and denatured at 65°C for 15 minutes. Reverse transcription was conducted in a 20-μL reaction containing 10 mM Tris-HCl, pH 8.3, 50 mM KCl, 2.5 mM $MgCl_2$, 1 mM dNTPs (Roche), 3.2 μg random primers $p(dN)_6$ (Roche), 5 mM DTT, 50 U RNase inhibitor (Promega), and 200 U M-MLV RT (Gibco RBL). The first strand synthesis was conducted at 42°C for 1 hour and then the enzymes were deactivated at 99°C for 5 minutes.

PCR

The reverse transcription products were used as a template for the subsequent PCR amplification. 25-μL reaction mixtures were prepared containing 10 mM Tris-HCl (pH 8.3), 50 mM KCl, 1.5 mM $MgCl_2$, 1 mM dNTPs, 0.5 μM of each gene specific primer, 0.625 mM DMSO and 2.5 U of *Taq* Polymerase (Gibco BRL). The reactions were hot-started at 93°C for 3 minutes of denaturing before the *Taq* polymerase was added. The reactions were then cycled 30 times; with each cycle consisting of 30 seconds of denaturing at 93°C, 30 seconds of annealing at 55°C, and

30 seconds of elongation at 72°C, and finishing with a final elongation step of 5 minutes at 72°C.

Quantification of PCR Products

PCR products were visualized under UV light with ethidium bromide staining on a 1.5% agarose gel. The images were captured using a "Nighthawk" camera under UV light, and the band density was determined using Quantity One software (PDI). A low DNA mass ladder (Invitrogen) was used to determine the size of both the target and mimic bands, and to create a standard curve for each gel from which the band density could be quantified. The band density was converted to an absolute quantity using the standard curve and molecular weight correction for each band. The natural logarithm (LN) of the ratio of target over the mimic concentration should be linearly related to the logarithm of initial amount of mimic. Therefore, the x-intercept (LN target/mimic = 0) is the point where the mimic concentration and the target concentration are equal (ratio of target/mimic = 1). The LN of the target/mimic ratio was plotted against the LN of the mimic, and a linear regression gave the calculated x-intercept for each sample. The absolute amount of gene-specific mRNA was calculated from the x-intercept of each data set.

Western Blot Studies

Total protein was isolated from normal and CHF dog left ventricle samples that had previously been frozen. 1 g of tissue was homogenized in RIPA buffer (1% NP40, 0.5% sodium deoxycholate, 0.1% SDS, 1xPBS) and a protease inhibitor cocktail (10 mM -β-mercaptoethanol, 10 μg/mL PMSF, 5 μg/mL aprotinin, 0.1

mg/mL benzamidine, 1 μg/mL pepstatin A, 1 μg/mL leupeptin, 100 mM sodium orthovanadate). All protease inhibitors were obtained from Sigma Chemicals and all procedures were performed on ice. The proteins were fractionated on 8% SDS-polyacrylamide gels and then transferred electrophoretically to Immobilon-P polyvinylidene fluoride membranes in 25 mM Tris-base, 192 mM glycine and 5% methanol. The membranes were blocked in 5% non-fat dry milk (NFDM, BioRad) in TTBS (Tris-HCl 50 mM, NaCl 500 mM; pH 7.5, 0.05% Tween-20) for 2 hours at room temperature and then probed with primary antibody at a dilution of 1:200 for 4 hours at room temperature in 5% NFMD TTBS. The anti-pan Na_v antibody was obtained from Alomone Labs (ASC-003) while the Naβ1, and Naβ2 antibody was a kind gift from Dr. Isom, and was the same as previously reported [13]. The membranes were subsequently washed three times in TTBS and then re-blocked in 5% NFDM in TTBS for 10 minutes and incubated along with a HRP-conjugated goat anti-rabbit secondary antibody (Jackson Immuno Labs) for 40 minutes in 5% NFDM in TTBS at a dilution of 1:10,000. The membranes were washed three more times in TTBS before antibody detection was performed using the Western Lightning Chemiluminescence Reagent Plus (PerkinElmer Life Sciences). The films were scanned with a PDI 420oe laser densitometer and the density of the bands was calculated using Quantity One software (PDI).

Experimental Protocols and Data Analysis

Data were acquired and analyzed using pClamp 8 software (Axon Instruments Inc.). The experimental protocols and data analysis were similar to those we previously reported. [25] The steady-state availability parameters ($V_{½A}$, the midpoint

and k_A, the slope of the relationship) were measured by a standard double-pulse protocol with the 2 s-duration pre-pulse (V_p) ranging from -140 mV to -40 mV. I_{Na} at each prepulse voltage was normalized to maximum I_{Na} measured at a prepulse voltage of -140 mV and fitted to a Boltzmann function $A(V_p)$:

$$A(V_p)= 1/(1+\exp((V_p-V_{½A})/k_A)) \qquad (1)$$

The steady-state activation parameters were determined from the I_{Na}-voltage relationships by fitting data points of the normalized current with the function:

$$I_{Na}(V_t)/ C_m = G_{max}* (V_r-V_t)/(1+\exp((V_{½G}-V_t)/k_G)) \qquad (2)$$

Where G_{max} is a normalized maximum Na^+ conductance, V_r is a reversal potential, $V_{½G}$, and k_G are the midpoint and the slope of the respective Boltzmann function underlying steady-state NaCh activation. The data points for I_{Na}/ C_m were fitted by Clampfit 8 software using an optional "Custom function" with four independent parameters corresponding to G_{max}, V_r, $V_{½G}$, and k_G. The peak current (I_{Na})-voltage relationship was determined in each cell with a series of depolarizing pulses of 50 ms duration applied to different testing voltages (V_t) at a rate of 0.5 Hz from a holding potential of -150 mV. I_{Na} density was determined from these I_{Na}-voltage relations as the maximum peak I_{Na} (V_t= -30 mV) normalized to membrane electric capacitance, C_m, measured by a voltage ramp pulse with a slope (dV/dt) of -10 V/s from -80 mV to -100 mV. The C_m values were calculated according to $C_m = (I_{ramp}-I_{ss})/(dV/dt)$, where I_{ss} is steady-state level of membrane current at -100 mV and I_{ramp} is membrane current at the end of the ramp pulse.

Chemicals

All other chemicals not mentioned above were purchased from Sigma Chemical Co (St. Louis, MO).

Statistics

If not specifically stated, all measurements are reported as mean±SEM with "n" representing number of hearts. Comparison between mean values was performed with unpaired Student's t-test with Bonferroni's correction. A two-tailed probability <0.05 was taken to indicate statistical significance.

RESULTS

I_{Na} density is significantly decreased in chronic HF

The whole-cell Na^+ currents were compared using VCs isolated from hearts of two groups of animals of similar age and weight: 1) a group of 5 normal dogs and 2) a group of 5 dogs with a reduced LV ejection fraction and HF. The currents were normalized to cell membrane capacitance, which on average was significantly higher in VC isolated from failing hearts (FVC) compared to those isolated from normal hearts (NVC), 200±12 pF (n=30) vs. 138±10 pF (n=22), respectively. I_{Na} density in FVC was decreased compared to NVC over a wide range of membrane potentials. Figures 1A and B show raw traces of I_{Na} recordings at different membrane potentials in NVC and FVC, accordingly. Figure C represents superimposed current voltage plots obtained in these cardiomyocytes. Summarized data on maximum I_{Na} density measured at Vm=-30mV are shown in Figure 1D. It can be seen from the figure that

the maximum density of I_{Na} is significantly lower in failing hearts than in normal hearts (32.3±2.6 vs. 50.8±6.5 pA/pF, mean±SEM, $P<0.05$, Fig. 1D). The current was completely blocked by 25-μM tetrodotoxin, a specific blocker of NaCh (not shown). The currents reversed at around 0 mV (see Fig 1C), as expected for the symmetrical Na^+ concentration conditions used in our experiments.

I_{Na} density changes were not related to steady state activation and availability

We measured steady-state activation and availability in each set of experiments to rule out the possibility that the observed changes in I_{Na} density to alterations of these parameters. We found that voltage dependency of both steady-state activation (see Table 1) and availability remained almost unchanged throughout the study (Fig 2). These data are summarized in Table 1. Accordingly, both NVC and FVC exhibited identical I_{Na} activation thresholds, over a range from -60 mV to -55 mV. For both cell types, the currents reached a maximum peak density at voltages ranging between -30 mV and -25 mV, similar to findings of others in normal canine cardiomyocytes under similar conditions.[9]

Competitive RT-PCR of NaCh subunits

Competitive RT-PCR was used to determine the absolute concentration of mRNA encoding both the $Na_V1.5$ and NaChβ1 subunits, which are hypothesized to comprise NaChs. Figure 3 shows examples of $Na_V1.5$ competitive RT-PCR using total RNA isolated from normal heart (NH, Fig. 3A) and HF (Fig. 3B) mid-

myocardial slices. In both cases, lane 0 contains 100 ng of DNA Mass Ladder used to create a standard curve for each gel. Lanes 1 through 5 were obtained with serial dilutions of the RNA mimic along with 1 μg total RNA. The upper bands represent the internal standard PCR product, while the lower bands are the target $Na_V1.5$ bands co-amplified with the mimics in the same reaction tube. As the mimic concentration decreases from left to right, the target band gets stronger, demonstrating the competition between mimic and target. For each experiment, the sample $Na_V1.5$ mRNA concentration was calculated based on the target and mimic band intensities at the following dilutions: 7 ng, 700 pg, 70 pg, 7 pg and 0.7 pg. Figure 3C shows the means for each dilution of mimic used for the quantitative analysis. Figure 3D shows the average absolute concentration of mRNA. The concentrations of $Na_V1.5$ mRNA in normal and HF samples were 389±99 and 396±109 attomol/μg total RNA respectively (n=4/group, P=NS).

A similar analysis was performed for the auxiliary β1 subunit. Figures 4A and 4B show representative gels from NaChβ1 competitive RT-PCR experiments for normal and failing hearts, respectively. Total RNA from mid-myocardial regions of normal and CHF dogs along with the following dilutions of mimic were used: 537 pg, 53.7 pg, 5.4 pg, 537 fg and 53.7 fg. The means for each dilution used for the quantification are shown in Fig 4C, while the bar chart in Figure 4D shows the average absolute amount of mRNA encoding the NaChβ1 subunit: 72±23 attomol/μg total RNA for normal dogs and 74±20 attomol/μg total RNA for CHF dogs.

Western Blot Studies

Western blots were used to determine the expression levels of $Na_V1.5$, as well as NaChβ1 and NaChβ2 proteins in the mid-myocardial region of normal and HF dogs. Figure 5A shows results from a Western blot probed with an anti-pan Na_V antibody. A single band at ~220 kDa was detected. Specificity of the band was confirmed by pre-incubation of the antibody with a control antigen against which the antibody was raised. The elimination of the band (last two lanes) by this pre-incubation demonstrates that the band is indeed specific. The band densities were used to determine the level of expression. Normal dogs were found to have an average band density of 13.4±1.9 OD units, compared to an average density of 10.5±1.9 OD units in HF dogs (Figure 5B). This difference in band density was statistically significant (n=5 per group, $p<0.05$). Figure 5C shows results from Western blots probed with an anti-NaChβ1 antibody. Two bands were detected, one at 43 kDa that corresponds to the anticipated fully glycosylated protein, and a smaller faint band at 36 kDa, that corresponds to an incompletely glycosylated product. Figure 5D shows that the relative amount of protein corresponding to the 43kDa band was unchanged in failing hearts (4.8±0.8 normal hearts vs. 3.7±1.0 HF, $p>0.05$, n=5/group). Fig. 5E shows results of Western blots probed with an anti-NaChβ2 antibody. A single specific band at 35kDa was detected in both normal and failing dog samples. Summarized data are shown in Fig 5F. There was no difference in the amount of NaChβ2 protein in failing hearts compared to normal hearts (4.8±0.1 NH vs. 4.1±0.4 HF arbitrary OD Units, n=5/group, p=NS).

DISCUSSION

We have demonstrated that NaCh function and protein expression are downregulated in a canine model of ischemic cardiomyopathy. Expression of mRNAs encoding $Na_v1.5$, and the NaChβ1 auxiliary subunit remained unchanged in failing hearts. The protein levels for both the β1 and the β2 subunits were unchanged. Our results suggest a post-transcriptional mechanism for $Na_v1.5$ subunit expression changes in failing hearts.

Molecular studies support electrophysiological observations of decreased I_{Na} in heart failure

Peak I_{Na} density was significantly reduced in the mid-myocardial region of dogs with chronic heart failure. We searched for a molecular mechanism, which could underlie these changes. Using competitive RT-PCR, we found that there was no difference in the absolute amount of mRNA encoding $Na_V1.5$ and NaChβ1 subunits. Western blotting for the $Na_v1.5$, NaChβ1 and NaChβ2 subunits revealed that there is a significant difference in the amount of $Na_V1.5$ protein. This would suggest that the changes seen at the physiological level are due to post-transcriptional modifications in the processing of $Na_V1.5$.

Possible clinical relevance

The I_{Na} downregulation found in the present study may provide a new candidate mechanism potentially contributing to the development of ventricular arrhythmias in HF related to coronary artery disease. Na^+ and K^+ current [4] changes

can both contribute to arrhythmogenesis in HF. Indeed, together with geometric non-uniformities (structural alterations) within the healed infarction tissue (including fibrosis or myocardial scarring) and decreased cell-to-cell coupling in HF [26], the decline of functional NaCh density reported in the present study can contribute to the incidence of unidirectional block, slowed impulse propagation, and re-entrant arrthythmias arising in the failing heart. It has recently been shown that similar changes in I_{Na} can slow myocardial conduction and cause sustained, isolated conduction defects. [11]

Second, this mechanism can contribute to the pro-arrhythmic effect of Class I antiarrhythmic drugs, [27] as further blockade of down-regulated NaCh can make impulse propagation even worse. Class I antiarrhythmics agents have not been studied in heart failure trials, but were associated with increased mortality in studies of patients at high risk for ventricular arrhythmia, including patients with left ventricular dysfunction.[28-30] Because this increase in mortality is thought to be due to pro-arrhythmic properties of the drugs, further trials in heart failure patients are unlikely to occur.[30]

Possible mechanisms of I_{Na} post-transcriptional downregulation

The abundance of NaCh in the surface membrane is dependent on the balance between NaCh protein insertion into the membrane and its internalization. Recent studies highlighted the importance of the signal transduction in modulation of cell surface NaCh expression through the PKA, G protein, PKC and calpain pathways . ([18, 31, 32] for review see[33]) Activation of PKA or G protein stimulatory subunits *via* β-adrenoreceptors increases abundance of NaCh by promoting insertion of channels

into the membranes of cardiomyocytes [18, 31, 32]. Insertion of NaCh by this mechanism may be weakened in failing hearts because of down-regulated β-adrenoreceptors. [34, 35] On the other hand, activation of Ca^{2+}-dependent PKC and calpain by augmented $[Ca^{2+}]_i$ reduces surface expression of NaCh by accelerated NaCh internalization in adrenal cromaffin cells [36, 37]. Defective Ca^{2+} handling resulting in elevation of diastolic $[Ca^{2+}]_i$ and delayed Ca^{2+} uptake by the SR, [38, 39], together with increased activity of Ca^{2+}-dependent PKC in HF, [40, 41] may also accelerate NaCh internalization, resulting in the reduced I_{Na} density reported here. Thus, these Ca^{2+}-mediated intracellular signaling pathways may be important for post-trancriptional abnormalities of NaCh processing in HF. In support to this idea we have recently demonstrated that buffering of $[Ca^{2+}]_i$ by 24-hour exposure of cardiomyocytes from failing dog hearts to cell permeable BAPTA-AM (20 mM) may partially restore NaCh density.[8] Cytoskeleton damage documented in HF [42] may also contribute to reduced I_{Na}.[25, 43] Analysis of the contribution of these mechanisms to NaCh regulation in HF awaits further studies.

Study limitations

To avoid contamination by cells from different myocardial locations, we studied changes in NaChs expression in LV mid-myocardium from the apex region. Accordingly, the difference between our results and the previous finding of unchanged I_{Na} density in total LV of dogs with pacing-induced HF [44] can be explained by the HF model (pacing vs. multiple infarctions), as well as potentially by local variations in NaCh density. A more detailed understanding of differences in NaCh expression changes across the ventricular wall [5] awaits further exploration.

The antibody used to determine $Na_V1.5$ protein expression was not specific for this subunit, but rather detects the presence of all Na_V isoforms. An unexpected role for the brain-type NaCh in heart has been recently discovered.[45] This study showed that $Na_v1.1$, $Na_v1.3$, $Na_v1.5$ and $Na_v1.6$ are differentially located within the VC of mice and that the major cardiac isoform, α-subunit $Na_v1.5$, is present in the intercalated disks.[45] The highly TTX-sensitive brain isoforms, $Na_v1.1$, $Na_v1.3$, and $Na_v1.6$, are located in the transverse tubules and can generate a very small current detectable only after activation with β-scorpion toxin.[45] However, it has been shown previously that $Na_V1.5$ is the predominant isoform responsible for I_{Na}, so the results presented here most likely reflect the expression of this principal subunit. Unfortunately, no control peptide was available for negative control studies using the NaChβ1 and NaChβ2 antibodies. Also contamination from the nerves could interfere with PCR and Western blot studies and mask changes in β subunits expression. Still, the data shown here were in accordance with other previously published results using the same antibody.[13]

In conclusion, experimental chronic HF results in down-regulation of I_{Na} in LV *via* post-transcriptional mechanisms.

ACKNOWLEDGMENTS

The authors thank Dr. Lori Isom for kindly providing anti-NaChβ antibodies and critical reading of the manuscript. The study was supported in part by grants from the National Heart, Lung and Blood Institute HL-53819, HL074328-01 (A.I. Undrovinas) and HL-49090 (H.N. Sabbah), by a grant in-aid 0350472Z from the American Heart Association (A.I. Undrovinas), and by a Canadian Institutes of Health Research Award (S. Nattel).

REFERENCES

1. **Spooner PM, Albert C, Benjamin EJ, et al.** Sudden cardiac death, genes, and arrhythmogenesis : consideration of new population and mechanistic approaches from a national heart, lung, and blood institute workshop, part I. Circulation 2001; 103: 2361-2364.

2. **Breithardt OA, Stellbrink C, Franke A, et al.** Acute effects of cardiac resynchronization therapy on left ventricular Doppler indices in patients with congestive heart failure. Am Heart J 2002; 143: 34-44.

3. **Kaab S, Nuss HB, Chiamvimonvat N, et al.** Ionic mechanism of action potential prolongation in ventricular myocytes from dogs with pacing-induced heart failure. Circulation Research 1996; 78: 262-273.

4. **Kaab S, Dixon J, Duc J, et al.** Molecular basis of transient outward potassium current downregulation in human heart failure: a decrease in Kv4.3 mRNA correlates with a reduction in current density. Circulation 1998; 98: 1383-1393.

5. **Sakmann BF, Spindler AJ, Bryant SM, et al.** Distribution of a persistent sodium current across the ventricular wall in guinea pigs. Circ Res 2000; 87: 910-914.

6. **Zygmunt AC, Eddlestone GT, Thomas GP, et al.** Larger late sodium conductance in M cells contributes to electrical heterogeneity in canine ventricle. Am J Physiol Heart Circ Physiol 2001; 281: H689-697.

7. **Yue L, Melnyk P, Gaspo R, et al.** Molecular mechanisms underlying ionic remodeling in a dog model of atrial fibrillation. Circ Res 1999; 84: 776-784.

8. **Maltsev VA, Sabbah HN and Undrovinas AI.** Down-regulation of sodium current in chronic heart failure: effects of long-term therapy with carvedilol. Cell Molec Life Sci 2002; 59: 1561-1568.

9. **Pu J and Boyden PA.** Alterations of Na+ currents in myocytes from epicardial border zone of the infarcted heart. A possible ionic mechanism for reduced excitability and postrepolarization refractoriness. Circulation Research 1997; 81: 110-119.

10. **Ufret-Vincenty CA, Baro DJ, Lederer WJ, et al.** Role of sodium channel deglycosylation in the genesis of cardiac arrhythmias in heart failure. J Biol Chem 2001; 276: 28197-28203.

11. **Tan HL, Bink-Boelkens MT, Bezzina CR, et al.** A sodium-channel mutation causes isolated cardiac conduction disease. Nature 2001; 409: 1043-1047.

12. **Pinto JM and Boyden PA.** Electrical remodeling in ischemia and infarction. Cardiovasc Res 1999; 42: 284-297.

13. **Malhotra JD, Chen C, Rivolta I, et al.** Characterization of sodium channel α- and β- subunits in rat and mouse cardiac myocytes. Circulation 2001; 103: 1303-1310.

14. **An RH, Wang XL, Kerem B, et al.** Novel LQT-3 mutation affects Na+ channel activity through interactions between alpha- and beta1-subunits. Circulation Research 1998; 83: 141-146.

15. **Makita N, Shirai N, Wandg DW, et al.** Cardiac Na+ channel dysfunction in Brugada syndrome is aggravated by β1 - subunit. Circulation 2000; 101: 54-60.

16. **Xiao YF, Wright SN, Wang GK, et al.** Coexpression with β1-subunit miodifies the kinetics and fatty acid block of $hH1_{\alpha}$ Na^{+} channels. Am J Physiol 2000; 279: H35-H46.

17. **Makielski JC, Limberis J, Fan Z, et al.** Intrinsic lidocaine affinity for Na channels expressed in Xenopus oocytes depends on α (hH1 vs. rSkM1) and β1 subunits. Cardiovasc Res 1999; 42: 503-509.

18. **Zhou J, Yui J, Hu NN, et al.** Activation of proteinkinase A modulates trafficking of the human cardiac sodium channel in Xenopus oocytes. Circ Res 2000; 87: 33-38.

19. **Qu Y, Curtis R, Lawson D, et al.** Differential modulation of sodium channel gating and persistent sodium currents by the beta1, beta2, and beta3 subunits. Mol Cell Neurosci 2001; 18: 570-580.

20. **Yu FH, Westenbroek RE, Silos-Santiago I, et al.** Sodium Channel {beta}4, a New Disulfide-Linked Auxiliary Subunit with Similarity to {beta}2. J Neurosci 2003; 23: 7577-7585.

21. **Morgan K, Stevens EB, Shah B, et al.** beta 3: an additional auxiliary subunit of the voltage-sensitive sodium channel that modulates channel gating with distinct kinetics. Proc Natl Acad Sci U S A 2000; 97: 2308-2313.

22. **Sabbah HN, Stein PD, Kono T, et al.** A canine model of chronic heart failure produced by multiple sequential coronary microembolizations. American Journal of Physiology 1991; 260: H1379-1384.

23. **Sabbah HN, Goldberg AD, Schoels W, et al.** Spontaneous and inducible ventricular arrhythmias in a canine model of chronic heart failure: relation to

haemodynamics and sympathoadrenergic activation. European Heart Journal 1992; 13: 1562-1572.

24. **Maltsev VA, Sabbah HN, Higgins RSD, et al.** Novel, ultraslow inactivating sodium current in human ventricular cardiomyocytes. Circulation 1998; 98: 2545-2552.

25. **Maltsev VA and Undrovinas AI.** Cytoskeleton modulates coupling between availability and activation of cardiac sodium channel. American Journal of Physiology 1997; 273 (Heart Circ. Physiol. 42): H1832-H1840.

26. **De Mello WC.** Cell coupling and impulse propagation in the failing heart. J Cardiovasc Electrophysiol 1999; 10: 1409-1420.

27. **Echt DS, Liebson PR, Mitchell LB, et al.** Mortality and morbidity in patients receiving encainide, flecainide, or placebo. The Cardiac Arrhythmia Suppression Trial. New England Journal of Medicine 1991; 324: 781-788.

28. **Epstein AE, Hallstrom AP, Rogers WJ, et al.** Mortality following ventricular arrhythmia suppression by encainide, flecainide, and moricizine after myocardial infarction. The original design concept of the Cardiac Arrhythmia Suppression Trial (CAST). Jama 1993; 270: 2451-2455.

29. **Connolly SJ.** Meta-analysis of antiarrhythmic drug trials. Am J Cardiol 1999; 84: 90R-93R.

30. **Ball TA, Kerns JW and Nashelsky J.** Do antiarrhythmics prevent sudden death in patients with heart failure? J Fam Pract 2003; 52: 719-721.

31. **Yarbrough TL, Lu T, Lee HC, et al.** Localization of cardiac sodium channels in caveolin-rich membrane domains: regulation of sodium current amplitude. Circ Res 2002; 90: 443-449.

32. **Lu T, Lee HC, Kabat JA, et al.** Modulation of rat cardiac sodium channel by the stimulatory G protein alpha subunit. J Physiol 1999; 518: 371-384.

33. **Kobayashi H, Shiraishi S, Yanagita T, et al.** Regulation of voltage-dependent sodium channel expression in adrenal chromaffin cells: involvement of multiple calcium signaling pathways. Ann N Y Acad Sci 2002; 971: 127-134.

34. **Vatner DE, Vatner SF, Fujii AM, et al.** Loss of high affinity cardiac beta adrenergic receptors in dogs with heart failure. J Clin Invest 1985; 76: 2259-2264.

35. **Gengo PJ, Sabbah HN, Steffen RP, et al.** Myocardial beta adrenoceptor and voltage sensitive calcium channel changes in a canine model of chronic heart failure. Journal of Molecular & Cellular Cardiology 1992; 24: 1361-1369.

36. **Yanagita T, Wada A, Yamamoto R, et al.** Protein kinase C-mediated down-regulation of voltage-dependent sodium channels in adrenal chromaffin cells. J Neurochem 1996; 66: 1249-1253.

37. **Shiraishi S, Shibuya I, Uezono Y, et al.** Heterogeneous increases of cytoplasmic calcium: distinct effects on down-regulation of cell surface sodium channels and sodium channel subunit mRNA levels. Br J Pharmacol 2001; 132: 1455-1466.

38. **Beuckelmann DJ and Erdmann E.** Ca(2+)-currents and intracellular [Ca2+]i-transients in single ventricular myocytes isolated from terminally failing human myocardium. Basic Res Cardiol 1992; 87: 235-243.

39. **Maltsev VA, Sabbah HN, Tanimura M, et al.** Relationship between action potential, contraction-relaxation pattern, and intracellular Ca^{2+} transient in cardiomyocytes of dogs with chronic heart failure. Cellular and Molecular Life Sciences 1998; 54: 597-605.

40. **Bowling N, Walsh RA, Song G, et al.** Increased protein kinase C activity and expression of Ca^{2+}-sensitive isoforms in the failing human heart. Circulation 1999; 99: 384-391.

41. **Wang J, Liu X, Arneja AS, et al.** Alterations in protein kinase A and protein kinase C levels in heart failure due to genetic cardiomyopathy. Can J Cardiol 1999; 15: 683-690.

42. **Hein S, Kostin S, Heling A, et al.** The role of the cytoskeleton in heart failure. Cardiovasc Res 2000; 45: 273-278.

43. **Undrovinas AI, Shander GS and Makielski JC.** Cytoskeleton modulates gating of voltage-dependent sodium channel in heart. American Journal of Physiology 1995; 269: H203-214.

44. **Nuss HB, Johns DC, Kaab S, et al.** Reversal of potassium channel deficiency in cells from failing hearts by adenoviral gene transfer: a prototype for gene therapy for disorders of cardiac excitability and contractility. Gene Therapy 1996; 3: 900-912.

45. **Maier SK, Westenbroek RE, Schenkman KA, et al.** An unexpected role for brain-type sodium channels in coupling of cell surface depolarization to contraction in the heart. Proc Natl Acad Sci U S A 2002; 99: 4073-4078.

Preparation	$V_{1/2A}$,mV	k_A,Mv	$V_{1/2G}$,Mv	k_G,mV
Normal heart	-80.6±2.1	5.0±0.1	-36.4±2.1	6.1±0.1
Failing heart	-80.6±0.9	5.2±0.1	-36.5±0.9	6.4±0.1

Table 1 Parameters of steady-state availability ($V_{1/2A}$ and k_A) and activation ($V_{1/2G}$ and k_G) for Na^+ current remained unchanged in all preparation of cardiomyocytes used in the study. Parameters were obtained from Na^+ current recordings using protocols and fitting function described in Methods (Equations 1 and 2). Data for were obtained from 5 normal (25 cardiomyocytes) and 5 failing hearts (30 cardiomyocytes), respectively.

FIGURES

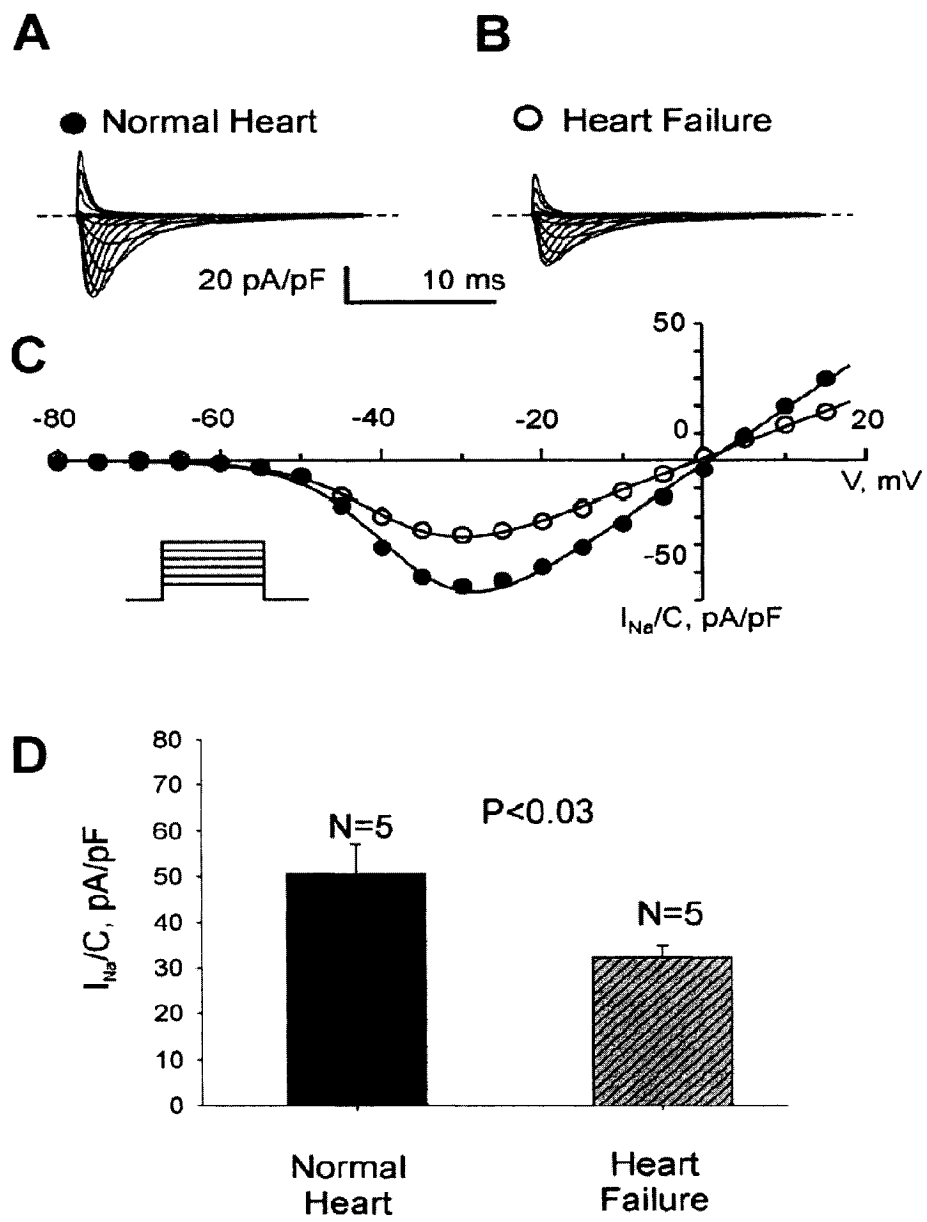

Figure 1 Sodium current, I_{Na}, in ventricular cardiomyocytes of dogs with chronic HF is downregulated. Representative examples of whole-cell I_{Na} current traces recorded at different membrane potentials in cardiomyocytes from normal (A) and failing (B) heart. Amplitude and time calibration is the same for both experiments. C, current-voltage relationship for peak Na^+ current density in normal (closed circles) and failing myocardium (open circles), respectively. The solid lines show theoretical curves fitted to data points in accordance with Equation 2 (see methods). Inset shows a schematic representation of the voltage clamp protocol. D, Average data for maximum I_{Na} density (I_{Na}/C) measured in 5 normal and 5 failing canine hearts (22 and 30 cardiomyocytes, respectively). Shown are mean±SEM for n, number of hearts used in the study.

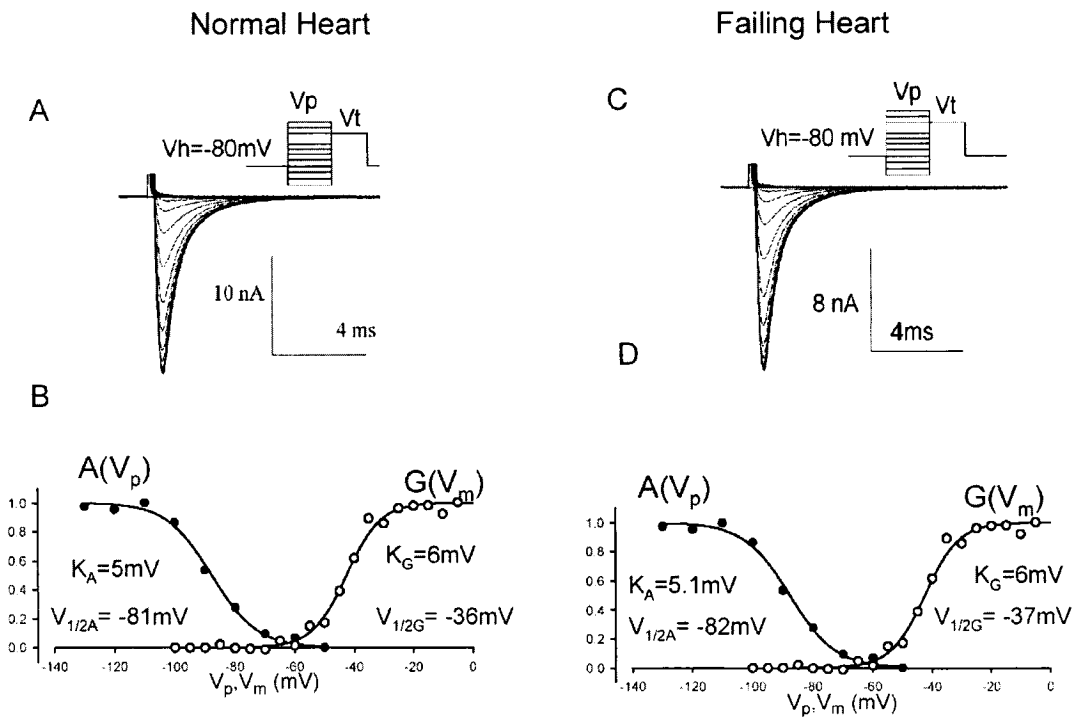

Figure 2 Voltage dependency of the steady-state activation and inactivation remains unchanged in failing hearts. A,B left panels - raw current traces recorded in normal (A) and failing (B) hearts in response to a voltage-clamp protocol (shown in insets) to evaluate steady-state inactivation, respectively. A,B right panels- steady-state inactivation (closed circles) plot vs. membrane potential obtained from experiment shown in left panels in normal and failing cardiomyocytes, respectively. Solid lines ($A(V_p)$) represent theoretical fit to a Bolzmann function (Equation 1, Methods). Steady-state activation (open circles) was obtained from the current-voltage relationship and was fit to the theoretical model (G(Vm)) with four independent parameters (Equation 2, Methods). Note, that mid-potential and slope (shown at in plot) for steady-state inactivation were similar in cardiomyocytes of normal (A) and failing (B) hearts, respectively. Summarized data is presented in Table 1.

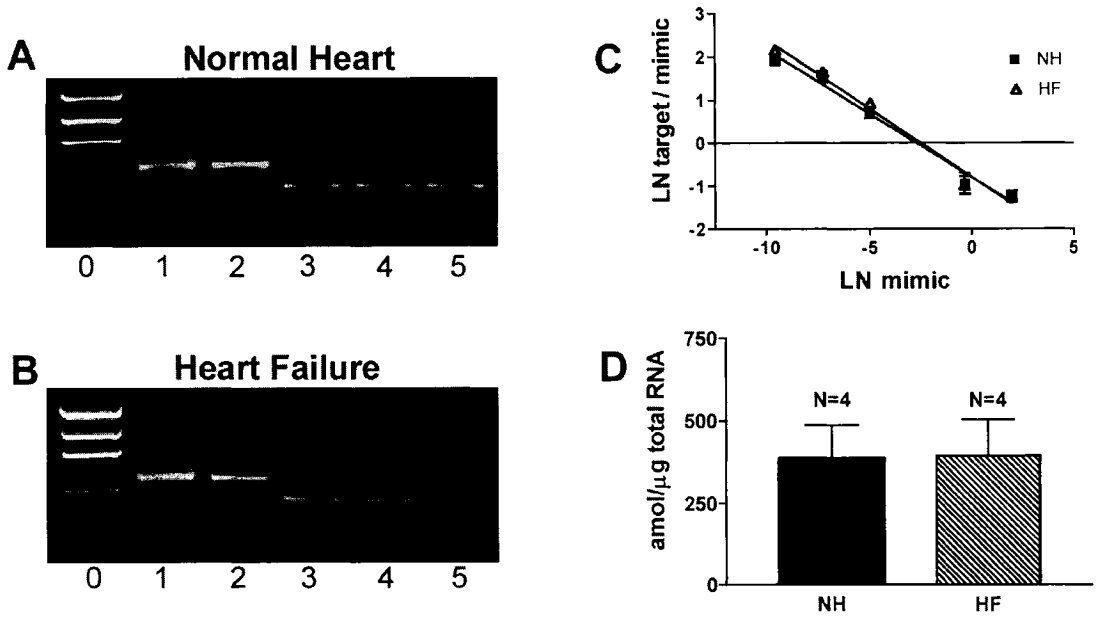

Figure 3 Quantification of mRNA encoding $Na_V1.5$ in normal and failing dog hearts by competitive RT-PCR. **A,** Shown is a representative gel of $Na_V1.5$ competitive RT-PCR using total RNA isolated from mid-myocardial slices of normal dog heart. Lane 0 contains 100ng of Low DNA Mass Ladder used to make standard curve for each gel. Dilutions of mimic in lanes 1 through 5 are 7 ng, 700 pg, 70 pg, 7 pg and 0.7 pg. **B,** A sample of a $Na_V1.5$ competitive RT-PCR result using heart failure total RNA from mid-myocardial sections. Dilutions are the same as in A. **C,** abundance of $Na_v1.5$ was determined from a linear regression to the logarithmic ratio of optical density of amplified target DNA/mimic DNA versus logarithm of mimic concentration plot. Point of equivalence found, as regression line intercept with zero line, indicates the absolute target mRNA concentration. D, Histogram comparing the absolute concentrations of $Na_V1.5$ mRNA evaluated by the graphic method shown in C in normal and heart failure mid-myocardium. There was no significant difference in the amount of $Na_V1.5$ mRNA between normal and heart failure groups.

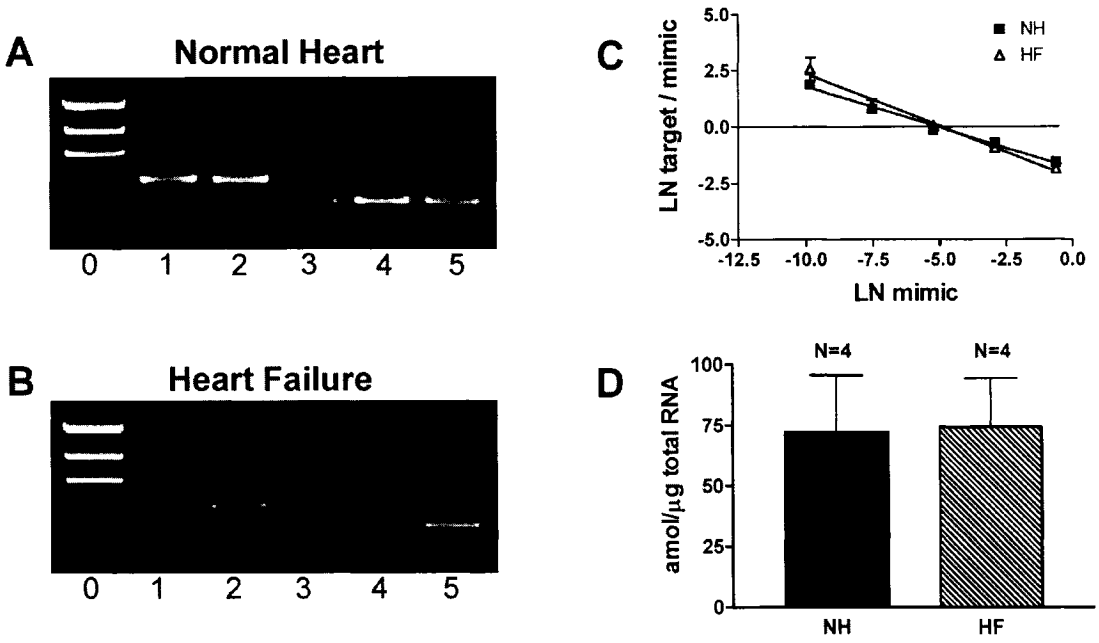

Figure 4 Results of competitive RT-PCR for sodium channel β1 subunit (NaChβ1). **A,** An example of NaChβ1 competitive RT-PCR using total RNA from normal dog mid-myocardium. Lanes 1 through 5 contain 537 pg, 53.7 pg, 5.4 pg, 537 fg and 53.7 fg of mimic. **B,** shows an example of NaChβ1 competitive RT-PCR using heart failure total RNA samples. The dilutions used are the same as in A. **C**, abundance of mRNA encoding NaChβ1 was determined from a linear regression to the logarithmic ratio of optical density of amplified target DNA/mimic DNA versus logarithm of mimic concentration plot. Point of equivalence found, as regression line intercept with dashed zero line, indicate the absolute target mRNA concentration.**D,** Histogram comparing absolute amounts of NaChβ1 mRNA in normal and heart failure canine mid-myocardium. Normal dogs had 72.2±23.3 attomol/µg total RNA compared to 74.3±19.9 attomol/µg total RNA for heart failure dogs. This difference was not significantly different (n=5 for both groups, $p>0.05$).

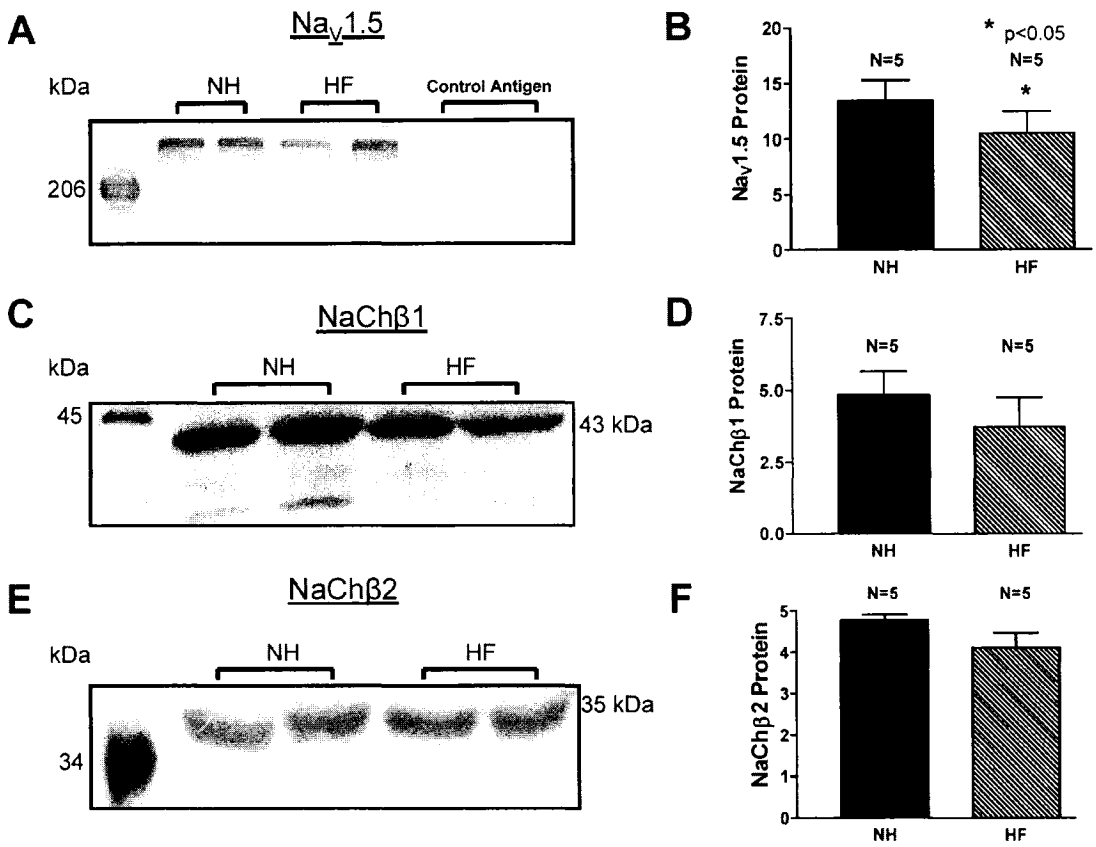

Figure 5 Western blot analysis of cardiac Na^+ channel $Na_V1.5$ subunit and its auxiliary subunits in normal and failing hearts. **A,** Result of Western blot using membrane protein fractions probed with anti-pan Na_V antibody. An anticipated single band corresponding to $Na_V1.5$ at 220 kDa is detected. The band disappears when primary antibody is pre-incubated with control antigen (last two lanes), indicating specificity of the band. **B,** Bar chart comparing the mean band intensities of $Na_V1.5$ protein between N and HF dog mid-myocardial samples. HF dogs had a significantly lesser amount of $Na_V1.5$ protein as compared to N dogs: 10.5±1.9 vs. 13.4±1.9 arbitrary OD units respectively (n=5 for both groups, $p<0.05$). **C,** Example of a membrane probed with anti-NaChβ1 antibody. The 43Da band that corresponds to fully glycosylated NaChβ1 protein was idenetified in both N and HF hearts. The faint 36 kDa band may represent an incompletely glycosylated protein, and was not quantified. **D,** Bar chart comparing densities of NaChβ1 protein bands. No significant difference was found in the density of the 43kDa band in HF (3.7±1.0) compared with N hearts (4.8±0.8, $p>0.05$, n=5/group). E, Shows an example of a Western blot probed with an NaChβ2 antibody. A single band was detected at 35kDa. F, Mean data comparing the density of NaChβ2 in NH dogs and dogs with HF. No significant difference was detected (4.8±0.1 NH vs. 4.1±0.4 HF arbitrary OD Units, n=5/group, $p>0.05$).

CHAPTER 4: MOLECULAR BASIS FOR THE I_{TO} TRANSMURAL GRADIENT AND DOWNREGULATION IN CONGESTIVE HEART FAILURE

The transient outward current is responsible for the brief repolarization seen during Phase 1 of the cardiac action potential. Electrophysiological studies have demonstrated that an I_{to} ventricular transmural gradient exists such that its current density is largest in the epicardium and smallest in the endocardium. Under normal conditions, this gradient contributes to the transmural dispersion of repolarization in the ventricle, and whose features can be observed in the T wave portion of a surface ECG (Antzelevitch & Fish, 2001). Alterations in this transmural gradient can predispose the ventricular myocardium to lethal ventricular arrhythmias. Despite the importance of I_{to} in the repolarization of human and canine myocardium, data regarding its exact molecular determinants in the ventricle are lacking. Kv1.4 and Kv4.3 α-subunits are both readily expressed in the ventricles of these species, however Kv1.4 expression is known to be constant (Rosati *et al.*, 2001). Kv4.3 expression is also believed to be homogenous; however CHF is known to cause a downregulation of this subunit which is thought to ultimately be responsible for the reduction of I_{to} (Kaab *et al.*, 1998). Recently, an accessory β-subunit KChIP2 was discovered to associate with Kv4.3 and increase its current density and other kinetic parameters (An *et al.*, 2000). Its mRNA expression pattern matched that of the transmural I_{to} gradient; therefore, it was prematurely concluded that KChIP2 expression determined this gradient (Rosati *et al.*, 2001). However, there have been conflicting reports concerning KChIP2 protein expression: some have found a similar protein gradient, while others have found none indicating that KChIP2 could not determine the I_{to} gradient (Deschenes *et al.*, 2002;Rosati *et al.*, 2003). Our study sought to clarify these discrepancies and to demonstrate how K^+ channel subunit expression varies depending on the region in the heart. Furthermore, no studies have examined the effect of CHF on the transmural expression of I_{to} subunits; therefore, this study represents the first time such observations are made. By elucidating the effects of CHF on Kv4.3 and KChIP2 expression, we hope to further our knowledge on the precise determinants of I_{to} expression in the ventricle.

ABSTRACT

The transient outward current (I_{to}), an important contributor to transmural electrophysiological heterogeneity, is significantly remodeled in congestive heart failure (CHF). The molecular bases of transmural I_{to} gradients and CHF-dependent ionic remodeling are incompletely understood. To elucidate these issues, we studied mRNA and protein expression of Kv4.3 and KChIP2, the principal alpha and beta subunits believed to form I_{to}, in epicardial and endocardial tissues and in isolated cardiomyocytes from control dogs and dogs with CHF induced by 240-bpm ventricular tachypacing. CHF decreased I_{to} density in both epicardium and endocardium (by 73% and 55% at +60 mV respectively), without a significant change in relative current density (endocardium/epicardium 0.11 control, 0.17 CHF). There were transmural gradients in mRNA expression of both Kv4.3 (endocardium/epicardium ratio 0.3 under control conditions) and KChIP2 (endocardium/epicardium ratio 0.2 control), which remained in the presence of CHF (Kv4.3 endocardium/epicardium ratio, 0.4; KChIP2 0.4). There were qualitatively-similar protein expression gradients in human and canine cardiac tissues and isolated canine cardiomyocytes; however, the KChIP2 gradient was only detectable with a highly-selective monoclonal antibody and closely approximated the I_{to}-density gradient. Kv4.3 mRNA expression was reduced by CHF, but KChIP2 mRNA was not significantly changed. CHF decreased Kv4.3 protein expression in canine cardiac tissues and cardiomyocytes, as well as in terminally-failing human-heart tissue samples, but KChIP2 protein was not downregulated in any of the corresponding sample sets. We conclude that both Kv4.3 and KChIP2 may contribute to epicardial-endocardial gradients in I_{to}, and that I_{to} downregulation in human and canine CHF appears due primarily to changes in Kv4.3.

INTRODUCTION

The Ca^{2+}-independent voltage-gated transient outward potassium current (I_{to}) plays an important role in cardiac action potential repolarization and is implicated in the pathogenesis of congestive heart failure (Oudit *et al.* 2001). Normal ventricles display a transmural I_{to} gradient, with an I_{to} density much larger in the epicardium than the endocardium (Litovsky & Antzelevitch, 1988; Furukawa *et al.* 1990; Antzelevitch *et al.*1991; Fedida & Giles, 1991; Wettwer *et al.* 1994; Näbauer *et al.* 1996). Local alterations in I_{to} density are believed to underlie significant aspects of cardiac pathophysiology and arrhythmogenesis in conditions like CHF (Kääb *et al.* 1996; Oudit *et al.* 2001; Li *et al.* 2002), myocardial ischemia and infarction (Lue & Boyden 1992; Lukas & Antzelevitch, 1993; Rozanski *et al.* 1998; Kaprielian *et al.* 2002), and Brugada syndrome (Yan & Antzelevitch, 1999; DiDiego *et al.* 2002).

Human and canine ventricular I_{to} is believed to be carried primarily by channels composed of Kv4.3 α-subunits (Dixon *et al.* 1996) and KChIP2 β-subunits (An *et al.* 2000; Decher *et al.* 2001; Kuo *et al.* 2001; Patel *et al.* 2002). KChIP2 co-expression increases current density, slows inactivation and accelerates recovery from inactivation of I_{to} resulting from Kv4 subunit expression in heterologous systems (An *et al.* 2000; Decher *et al.* 2001; Deschênes & Tomaselli, 2002; Patel *et al.* 2002). Targeted deletion of KChIP2 in mice causes loss of I_{to} and a susceptibility to ventricular arrhythmias (Kuo *et al.* 2001).

The molecular basis of transmural I_{to} gradients has been controversial. In rats (Dixon & McKinnon, 1994) and ferrets (Brahmajothi *et al.* 1999), transmural gradients in Kv4.2 and Kv4.3 appear to be key contributors. In ferrets, dogs and man, there are striking transmural gradients in KChIP2 mRNA, leading to the notion that

KChIP2 contributes to transmural heterogeneity in these species (Rosati *et al.* 2001; Rosati *et al.* 2003, Patel *et al.* 2002), but this notion has been contested based on electrophysiological observations and an apparent lack of a transmural gradient in KChIP2 protein expression (Deschênes *et al.* 2002). Downregulation of Kv4.3 mRNA has been observed in cardiac tissues from humans with CHF, and has been considered to be a primary mechanism of I_{to} suppression in this condition (Kääb *et al.* 1998). However, we are not aware of studies of the potential contribution of KChIP2 to I_{to} changes in CHF, which could be substantial in view of the importance of KChIP2 in I_{to} expression.

The present study was designed to assess the expression of KChIP2 and Kv4.3 subunits in epicardial and endocardial tissues of normal dogs and dogs with pacing-induced CHF. We quantified mRNA copy number with competitive reverse transcription (RT)- polymerase chain reaction (PCR) and confirmed some observations with real-time PCR, and analyzed protein expression by Western blot. To exclude contamination of results by a contribution from the non-cardiac cell population in cardiac tissue, we performed analyses in isolated cardiomyocytes as well as whole cardiac tissues. Finally, to verify potential the potential relevance of our findings to man we evaluated Kv4.3 and KChIP2 protein expression in normal and failing human hearts.

MATERIALS AND METHODS

Canine CHF model

CHF was induced in dogs by ventricular tachypacing as previously reported (Cha *et al.* 2004). Briefly, custom-modified pacemakers (Medtronic) were implanted

in the necks of adult mongrel dogs and attached to pacing leads inserted in the right ventricular apex under fluoroscopy. After 24 hours for recovery, pacing was initiated at 240 bpm and maintained for 2 weeks. After hemodynamic confirmation of the presence of CHF under morphine (2 mg/kg s.c.)/ α-chloralose (100 mg/kg i.v.) anesthesia (Table 1), the dogs were euthanized with an overdose of α-chloralose. The hearts were removed and the ventricles isolated. Epicardial and endocardial tissues were obtained by cutting 1-mm thick slices from the epicardial and endocardial surfaces respectively. Any free-running Purkinje fibres were removed prior to isolation of the endocardial layer. Unpaced dogs served as controls and tissue was obtained in a similar fashion. All animal handling procedures adhered to the guidelines of the Canadian Council on Animal Care and were approved by the Montreal Heart Institute Animal Research Ethics Committee.

Canine cardiomyocyte isolation

Hearts were excised through a left lateral thoracotomy and immersed in oxygenated Tyrode solution at room temperature. The anterior left ventricular free wall (~30 × 50 mm) was dissected and the artery perfusing it was cannulated. Cell isolation was performed as previously described, by perfusion with a solution containing collagenase (120U/mL, Worthington, type II) (Li *et al.* 2002). When the tissue was well-digested, cells were taken from the subepicardial and subendocardial layers (~1 mm thick). Cells were dispersed by gentle trituration with a Pasteur pipette, and were kept in a high-K^+ storage solution (see *solutions*) at 4°C. Some cells were washed and stored in Krebs solution and then spun at 500 x g (4°C) to

remove any contaminants. Cells were then resuspended in 5-mM Tris-HCl (pH 7.4), 2-mM EDTA, 5-μg/ml leupeptin, 10-μg/ml benzamidine, and 5-μg/ml soybean trypsin inhibitor for membrane protein isolation. Other cells were placed in storage solution and used for patch clamp measurements on the same day, in order to confirm the relative I_{to} properties of tissues used for biochemical determinations.

Human tissue samples

The undiseased human hearts were obtained from general organ donors whose hearts were explanted to obtain pulmonary and aortic valves for transplant surgery. The human donor heart experiments complied with the Helsinki Declaration of the World Medical Association and approwed by the Albert Szent-Gyorgyi Medical University Ethical Review Board (No. 51-57/1997OEj). Diseased human tissue was obtained from terminally failing human hearts explanted at the time of cardiac transplantation. Human hearts were stored in cold cardioplegic solution for <6 hours before small epicardial and endocardial left ventricular free wall samples were prepared in a fashion similar to that for dogs and then fast-frozen in liquid nitrogen.

Solutions

The standard Tyrode solution contained (in mM) NaCl 136, KCl 5.4, $MgCl_2$ 1, $CaCl_2$ 1, NaH_2PO_4 0.33, HEPES 5 and dextrose 10 (pH 7.35 with NaOH). The high-K^+ storage solution contained (in mM) KCl 20, KH_2PO_4 10, dextrose 10, mannitol 40, L-glutamic acid 70, β-OH-butyric acid 10, taurine 20, EGTA 10 and 0.1% BSA (pH

7.3 with KOH). The standard pipette solution contained (in mM) K-aspartate 110, KCl 20, $MgCl_2$ 1, MgATP 5, GTP 0.1, HEPES 10, Na-phosphocreatine 5, EGTA 5, with pH adjusted to 7.3 with KOH. For I_{to} recording, atropine (1 μM) and $CdCl_2$ (200 μM) were added to external solutions to eliminate muscarinic K^+ currents and to block Ca^{2+} currents. Na^+ current contamination was avoided by using a holding potential (HP) of –50 mV.

Electrophysiological data acquisition

The whole-cell patch-clamp technique was applied for ionic current recording from canine cardiomyocytes at 36°C. Small cells were selected to optimize spatial voltage control. The compensated series resistance and capacitive time constant (τ_c) averaged 2.3±0.1 MΩ and 294±10 μs. Leakage compensation was not used. Cell capacitance averaged: 139.9±13.7 pF in control epicardial cells (n = 7) and 137.2±13.9 pF in CHF epicardial cells (n = 7), 103.2±11.7 pF in control endocardial cells (n = 8) and 124.3±7.9 pF in CHF endocardial cells (n = 8). Currents are expressed in terms of density. Nonlinear least-square curve-fitting algorithms were used for curve fitting.

Western blot studies

Membrane protein was extracted from tissue samples with 5-mM Tris-HCl (pH 7.4), 2-mM EDTA, 5-μg/ml leupeptin, 10-μg/ml benzamidine, and 5-μg/ml soybean trypsin inhibitor, followed by tissue homogenization. The homogenized mixture was centrifuged for 15 mins at 500 x g to eliminate cellular components and

then the supernantant was centrifuged at 45,000 x g for 30 mins to isolate the membrane fractions. All procedures were performed at 4°C. Membrane proteins were fractionated on either 8% (Kv4.3, caldesmon and Na^+-K^+ ATPase) or 10% (KChIP2) SDS-polyacrylamide gels and transferred electrophoretically to Immobilon-P polyvinylidene fluoride membranes (Millipore) in 25-mM Tris-base, 192-mM glycine and 5%-methanol at 0.09 mA for 18 h (Kv4.3) or 65 V for 35 min (KChIP2). Membranes were blocked in 5% non-fat dry milk (Bio-Rad) in TTBS (Tris-HCl 50 mM, NaCl 500 mM; pH 7.5, 0.05% Tween-20) for 2 hrs (room temperature) and then incubated with primary antibody (1:250 dilution) in 5% non-fat dry milk in TTBS for 4 hrs at room temperature. Kv4.3 antibody was purchased from Alomone Labs; a KChIP2 polyclonal antibody was purchased from Santa Cruz Biotechnology, a second polyclonal antibody was a kind gift from Dr. Gordon Tomaselli, and a KChIP2 monoclonal antibody was a kind gift from Dr. James Trimmer at the University of California, Davis. The monoclonal KChIP2 antibody recognizes an epitope located in the highly conserved core region of the protein which is similar for most KChIP2 isoforms. The caldesmon and Na^+-K^+ ATPase antibodies used for protein sample validation were purchased from Research Diagnostics Inc. Membranes were washed three times in TTBS, reblocked in 5% non-fat dry milk in TTBS (15 min) and then incubated with horseradish peroxidase-conjugated goat anti-rabbit IgG secondary antibody (1:5000, for Alomone antibodies) or donkey-anti-goat IgG secondary antibody (1:10,000, for Santa Cruz antibodies) in 5% non-fat dry milk in TTBS (40 min). They were subsequently washed 3 times in TTBS and once in TBS (same as TTBS but without Tween-20). Signals were obtained with Western Lightning Chemiluminescence Reagent Plus (PerkinElmer

Life Sciences). Band densities were determined with a laser-scanning densitometer (PDI 420oe) and Quantity One software (PDI). Protein loading was controlled by probing all Western blots with anti-GAPDH antibody (Research Diagnostics Incorporated) and normalizing ion-channel protein band intensity to that of GAPDH. Blots with antibody pre-incubated with the antigenic peptide were performed for Kv4.3 and the commercially available KChIP2 antibody. There was no antigenic peptide sample available for the monoclonal KChIP2 antibody provided to us by Dr. Trimmer.

Cell culture

Chinese hamster ovary (CHO) cells were grown in culture at 37°C with 5% CO_2 in F12 medium supplemented with 10% FBS, 0.5% glutamine and 1% penicillin/streptomycin. Cells were transfected with 1 μg of either Kv4.3 or KChIP2 cDNA subcloned in a pcDNA3.1 vector using lipofectamine (Invitrogen). Cells were allowed to grow for 24 hrs and then membrane proteins were isolated using the protocol described above.

RNA purification

Total RNA was isolated from 0.5-1.0 g samples using Trizol reagent (Invitrogen) followed by chloroform extraction and isopropanol precipitation. Genomic DNA was eliminated by incubating in DNase I (0.1 U/μl, 37°C) for 30 min followed by acid phenol-chloroform extraction. RNA was quantified by spectrophotometric absorbency at 260 nm, purity confirmed by A_{260}/A_{280} ratio and integrity evaluated by

ethidium-bromide staining on a denaturing agarose gel. RNA samples were stored at -80°C in RNAsecure Resuspension Solution (Ambion).

PCR primers

Gene specific primers (GSPs) for competitive RT-PCR were designed based on published cDNA sequences for canine Kv4.3 and KChIP2 (Table 2). Chimeric primer pairs for RNA-mimic synthesis were constructed with a rabbit cardiac α-actin sequence flanked by the same GSPs. An 8-nucleotide sequence, GGCCGCGG, corresponding to the 3' end of the T7-promoter, was conjugated to the 5'-end of each forward chimeric primer.

Synthesis of RNA mimic

First-strand cDNA (synthesized by reverse-transcription with canine ventricular mRNA samples) was used as a template for subsequent PCR amplification steps with chimeric primer pairs. The resulting cDNA mimic contains a 460-bp α-actin sequence flanked at the 5'-end by the sense GSP sequence and an 8-bp T7-promoter sequence at the 3'-end flanking the antisense GSP sequence. Products were gel-purified with the QIAquick Gel Extraction Kit (Qiagen Inc.). The RNA mimic (internal standard) was created by *in vitro* transcription (mMESSAGE MACHINE, Ambion). The product was incubated with RNase-free DNase I (30 min, 37°C) to eliminate cDNA contamination, followed by phenol/chloroform extraction and isopropanol precipitation. Mimic size and concentration were determined by migration on a denaturing RNA gel alongside markers of known molecular weight and pre-determined RNA concentrations to create a standard curve. Before

conducting experiments, the mimic was checked to make sure it amplified at the same rate as the expected target band. Samples of mimic and target PCR reactions were taken at various PCR cycles to verify the intensity of both bands increased at the same rate (see Online supplement, Figure 1).

Competitive RT-PCR

RNA mimic samples were added with serial 10-fold dilutions to reaction mixtures containing 1-μg total RNA. RNA was denatured at 65°C (15 min). RT was conducted in a 20-μl reaction mixture containing reaction buffer (10 mM Tris-HCl, pH 8.3, 50-mM KCl), 2.5 mM $MgCl_2$, 1 mM dNTPs (Roche), 3.2 μg random primers $p(dN)_6$ (Roche), 5 mM DTT, 50 U RNase inhibitor (Promega), and 200 U M-MLV reverse-transcriptase (Gibco-BRL). First-strand cDNAs were synthesized at 42°C (1 hr) and remaining enzymes heat-deactivated (99°C, 5 min).

First-strand cDNA from the RT-step was used as a template in 25-μl reaction mixtures including 10-mM Tris-HCl (pH 8.3), 50-mM KCl, 1.5-mM $MgCl_2$, 1-mM dNTPs, 0.5-μM GSPs, 0.625-mM DMSO and 2.5 U of Taq Polymerase (Gibco BRL). Reactions were hot-started at 93°C for 3 min of denaturing, followed by 30 amplification cycles (93°C, 30 sec [denaturing]; 55-58°C, 30 sec [annealing]; 72°C, 30 sec [extension]). A final 72°C extension step was performed for 5 min. RT-negative controls were obtained to exclude genomic contamination for all RT-PCR reactions.

PCR products were visualized under UV light with ethidium bromide staining in 1.5% agarose gels. Images were captured with a Nighthawk camera, and band intensity determined with Quantity One software. A DNA Mass Marker (100 ng)

was used to determine the size and quantity of DNA bands, and to create a standard curves in each experiment for absolute quantification. Plots of ln([target]/[mimic]) vs. ln([mimic]) were fit by linear regression to determine the absolute concentration of target mRNA as previously described (Zicha *et al.* 2003).

Real-time PCR

In order to confirm the competitive RT-PCR results obtained for Kv4.3, real-time PCR was applied. Two-step real time PCR was conducted with the Perkin-Elmer Gene Amp 5700 sequence detection system. Primers used for the detection of Kv4.3 and GAPDH are shown in Table 2. Real-time PCR was run in the presence of a double-stranded DNA binding dye (SYBR green, Applied Biosystems). Since this dye binds to any double-stranded DNA, PCR products were run on a 1.5% agarose gel with ethidium bromide staining to ensure that only one product was detected. A single peak in the dissociation plot also confirmed the specificity of the products. GAPDH was used as an internal standard, and all Kv4.3 results were normalized to GAPDH data obtained from the same samples at the same time. A standard curve with 100, 10, 1 and 0.1 ng of control epicardial total RNA was run in duplicate for each experiment.

Data analysis

All data are expressed as mean ± S.E.M. Each biochemical determination was performed on an individual heart: unless otherwise specified, *n* values represent the number of hearts studied. Western blot band intensities are expressed quantitatively as arbitrary OD units, which correspond to laser-densitometric K^+-channel subunit

membrane protein band intensity following background subtraction, divided by GAPDH signal intensity for the same sample. Real-time PCR results are similarly expressed in arbitrary units, corresponding to the intensity of SYBR green captured by the Gene Amp 5700 as normalized to GAPDH. Statistical comparisons were performed with ANOVA and Student's *t*-test with Bonferroni's correction. A two-tailed $P < 0.05$ was taken to indicate statistical significance.

RESULTS

I_{to} properties in canine hearts

Typical I_{to} was recorded in cells obtained from control and CHF dogs, as illustrated in Fig. 1*A* (epicardial recordings) and 1*B* (endocardial). Currents were considerably smaller in endocardium and were reduced by CHF. The characteristic transmural I_{to} gradient was observed in control hearts, with a mean epicardial current density of 41±5 pA/pF (n = 7 cells), compared to 4.4±0.6 pA/pF in endocardium (Fig. 1*C*, n = 8 cells, $P < 0.001$). CHF reduced I_{to} by 72% in the epicardium, to 11±2 pA/pF (n = 7 cells, $P < 0.005$); and by 55% in the endocardium, to 2.0±0.9 pA/pF (n = 8 cells, $P < 0.05$). There were no significant differences in the fast and slow phase I_{to} inactivation time constants as a function of transmural layer or the presence of CHF (Fig. 1*D*). These results indicate that the tissue and cell samples that we used to evaluate local I_{to} subunit expression show the expected differences in currents and are therefore valid samples for examination of the molecular correlates of epicardial/endocardial and CHF-related differences.

Expression of I_{to} subunit mRNA

Figure 2*A* shows examples of gels obtained from competitive RT-PCR reactions for Kv4.3 mRNA with representative control epicardial and endocardial samples. Figure 2*B* shows examples obtained with tissues from CHF dogs. In all cases, lane 0 contains 100 ng of DNA Mass Ladder to create the standard curve for each gel. Lanes 1 through 6 were obtained with serial dilutions of the RNA mimic along with 1 μg total RNA. The upper bands represent the internal standard PCR product, while the lower bands are the target Kv4.3 bands co-amplified with the mimics in the same reaction tube. The molecular masses of target and mimic bands are indicated. As the mimic concentration decreases from left to right, the relative intensity of the target band to that of the mimic gets stronger, demonstrating the competition between mimic and target. The mimic quantities for Kv4.3 were 3.7 ng, 367 pg, 36.7 pg, 3.7 pg, 367 fg and 36.7 fg. Figure 2*C* compares the average absolute amounts of Kv4.3 mRNA in all samples. A transmural gradient was found for Kv4.3 mRNA, with the endocardial/epicardial concentration ratio averaging 0.3 in control and 0.4 in CHF.

Because transmural Kv4.3 gradients have not previously been reported in the dog, we used real-time PCR to confirm the Kv4.3 mRNA differences we observed with competitive RT-PCR. The amplification plot for Kv4.3 is shown in Fig. 3*A*. All calculations for the relative quantity of Kv4.3 mRNA were obtained with values obtained from the logarithmic phase of DNA amplification (indicated by L.P. in the Fig.). The mean results in Fig. 3*B* show a significant transmural Kv4.3 mRNA gradient under control conditions and CHF-induced downregulation, qualitatively similar to the competitive RT-PCR findings.

Figures 4*A* and *B* show representative gels from KChIP2 competitive RT-PCRs. The last lane in each gel shows an example of an RT-negative control, to detect any genomic DNA contamination in the total RNA samples. The mimic dilutions used for KChIP2 competitive RT-PCR were 3.1 ng, 310 pg, 31 pg, 3.1 pg and 310 fg. Mean data in Fig. 4*C* show a transmural gradient in KChIP2 mRNA, with an endocardial/epicardial concentration ratio of 0.2 in control tissue and 0.4 in CHF. However, KChIP2 mRNA was not downregulated by CHF- if anything; there was a trend towards an increase.

Canine Kv4.3 Western blot studies

Figure 5*A* shows a representative Western blot probed with anti-Kv4.3 antibody. A single band is detected at the expected molecular weight (~75 kDa). The Kv4.3 signal was suppressed by pre-incubation with antigenic peptide (last two lanes), confirming the specificity of the band. Corresponding GAPDH signals are shown in the lower panel of Fig. 5A. Figure 5*B* shows mean data for Kv4.3 membrane protein, which indicate a significant transmural gradient, with endocardial/epicardial expression ratios of 0.5 in control and 0.4 in CHF hearts. Kv4.3 protein was also significantly decreased in CHF, with a value in epicardium averaging 50% of control and in endocardium 40% of control. To exclude contamination by non-cardiomyocyte elements, Western blots were repeated using membrane protein fractions from isolated canine cardiomyocytes obtained from control dogs. Figure 5*C* shows an example of such a Western blot probed for Kv4.3. The last two lanes show that the 75-kDa-bands disappeared when antibody pre-incubated with control antigen was used. The transmural gradient in Kv4.3 protein expression in isolated myocytes

was similar to that seen in whole tissue (Fig. 5D), with an endocardial/epicardial expression ratio of 0.5. The specificity of the anti-Kv4.3 antibody was verified by immunoblotting proteins isolated from CHO cells transfected with Kv4.3. Lane 1 in Fig. 5*E* shows that two bands are detected by the Kv4.3 antibody. Pre-incubation with control antigen (Lane 2) eliminated the band at ~75 kDa. The Kv4.3 protein was also probed with the monoclonal KChIP2 antibody used for KChIP2 Western blots, and no signal was detected in the range of 75 kDa (Lane 3).

Characterization of KChIP2 antibodies

In preliminary studies, we were unable to detect a transmural gradient in KChIP2 protein expression with the use of a polyclonal antibody (Zicha *et al.* 2003). Because of conflicting results in the recent literature regarding transmural protein gradients in KChIP2 (Deschênes *et al.* 2002; Rosati *et al.* 2003), we decided to verify the specificity of various antibodies before performing definitive experiments. Membrane proteins were isolated from CHO cells transfected with KChIP2 and were probed with various polyclonal and monoclonal KChIP2 antibodies (Fig. 6*A*). When protein was probed with the monoclonal KChIP2 antibody (lane 1, Fig. 6*A*), a single band at the expected size of ~30 kDa was detected. When the same protein sample was probed with a commercially-available polyclonal KChIP2 antibody, multiple bands were detected (lane 2). With the use of this antibody, we obtained equal endocardial (1.9±0.3 OD units) and epicardial (2.1±0.3 OD units) intensities for the band closest in molecular weight to that expected (n = 5 hearts, matched endocardial and epicardial samples from each). A similar result was obtained when probing the membrane with a polyclonal anti-KChIP2 antibody similar to the one used by

Deschênes *et al.* (2002) (lane 3). When the protein sample was probed with the Kv4.3 antibody, a single non-specific band at ~140 kDa was detected, confirming that the Kv4.3 antibody does not detect KChIP2. Similar to the results obtained with KChIP2-transfected CHO cells, preliminary studies with the commercially available polyclonal KChIP2 antibody to probe protein isolated from canine epicardium showed a large number of bands (Fig. 6*B*), whereas the monoclonal antibody detected a distinct band at the expected molecular weight (Fig. 6*C*). Therefore, further KChIP2 protein expression studies were performed with the monoclonal KChIP2 antibody.

Canine KChIP2 Western blot studies

Figure 7A shows a typical KChIP2 Western blot, with a distinct signal detected at ~30 kDa. A clear transmural expression gradient was observed for KChIP2 protein, with much stronger bands in epicardial than endocardial tissues (Fig. 7*A*) when probed with the monoclonal antibody. This finding is confirmed by the mean data in Fig. 7*B*, with endocardial/epicardial protein ratios of 0.14 and 0.16 in control and CHF samples respectively. Unlike Kv4.3 protein, KChIP2 expression was not changed in CHF, with mean values in control and CHF being very similar for a given transmural layer (Fig. 7*B*). The transmural gradient in KChIP2 protein expression was also observed for Western blots performed on membrane proteins from isolated cardiomyocytes (Fig. 7*C*). Mean results for isolated cardiomyocyte proteins (Fig. 7*D*) showed an endocardial/epicardial expression ratio of 0.13, of the same order as obtained in whole cardiac tissues.

Western blot studies on human cardiac tissues

Membrane protein samples were isolated from 5 normal human hearts and 5 patients with NYHA Class III-IV CHF. Figure 8*A* shows an example of a Kv4.3 Western blot on human heart samples. A clear band at ~75 kDa was observed in all human samples and disappeared when antibody was pre-incubated along with the blocking peptide (last 2 lanes). The mean data in Fig. 8*B* show that there was a significant transmural gradient in Kv4.3 protein in the human heart (endocardial/epicardial ratios of 0.6 and 0.4 in control and CHF respectively). Furthermore, Kv4.3 expression was significantly reduced by CHF. Probing human cardiac membrane proteins with the monoclonal KChIP2 antibody (Fig. 8C) revealed strong bands at the expected molecular mass of ~30 kDa, as well as weaker bands at a smaller mass (~27 kDa). Mean data showed a strong transmural gradient (endocardial/epicardial ration 0.3 and 0.2 in control and CHF respectively), but no significant change with CHF.

DISCUSSION

In this study, we assessed the expression of the K^+-channel subunits Kv4.3 and KChIP2 in the epicardium and endocardium of normal and failing hearts. We found that both subunits show a transmural gradient, with endocardial expression being less than epicardial, suggesting a significant role in the transmural gradient of I_{to}. However, only Kv4.3 was downregulated by CHF, suggesting that changes in this α-subunit are the primary factor in CHF-induced I_{to} suppression.

Comparison with previous studies of transmural cardiac I_{to} subunit expression

Dixon and McKinnon were the first to show a transmural expression gradient for an I_{to} channel subunit, when they demonstrated that Kv4.2 mRNA expression across the rat left ventricular wall, but not that of Kv1.4, parallel the I_{to} density gradient (Dixon & McKinnon, 1994). Subsequently, Brahmajothi *et al.* (1999) showed that Kv4.2 and 4.3 mRNA and protein are more strongly expressed in ferret epicardium than endocardium, whereas Kv1.4 mRNA is expressed symmetrically and Kv1.4 protein appears more concentrated in the endocardium. Rosati *et al.* (2001) subsequently showed that KChIP2 mRNA expression follows a steep gradient across the myocardium, paralleling the gradient in current, but that Kv4.3 mRNA expression showed no gradient. Deschênes *et al.* (2002) revisited this issue, providing functional and protein expression data indicating that KChIP2 expression does not vary across the ventricular wall and that the biophysical properties of canine I_{to} do not reflect the variations one would expect if varying contributions of KChIP2 were involved. Recently, Rosati *et al.* (2003) used a monoclonal antibody to evaluate the protein expression of KChIP2 across the ventricular wall and confirmed a strong epicardial/endocardial gradient.

Unlike Rosati *et al.* (2001; 2003), we did observe a clear difference in epicardial versus endocardial Kv4.3 expression. Because of the discrepancy, we used four different approaches to confirm the finding: mRNA measurement by competitive RT-PCR, mRNA measurement by real time RT-PCR, protein measurements on protein extracts from whole cardiac tissues and protein measurements on extracts from isolated canine cardiomyocytes. Furthermore, we observed similar Kv4.3

protein gradients in human cardiac tissue samples. Like Rosati, we observed strong transmural gradients in KChIP2 protein expression. Our findings suggest that the discrepancies between different studies of transmural KChIP2 protein expression (Deschênes *et al.* 2002; Rosati *et al.* 2003) may be due to differences in the antibodies used, with the polyclonal antibody having insufficient specificity for KChIP2.

Relation to previous studies of I_{to} subunit alterations in CHF

Relatively little published information is available about I_{to} subunit changes in CHF. Kääb *et al.* (1998) showed that Kv4.3 mRNA is reduced in cardiac tissue samples from CHF patients, and Borlak & Thum (2003) similarly found Kv4.3 mRNA to be reduced in explanted hearts of patients with end-stage CHF. Neither Kv4.3 protein expression nor KChIP2 mRNA or protein was evaluated. We are not aware of other studies that have examined I_{to} ion channel expression in CHF.

Novel elements and potential significance

Our study is the first of which we are aware that examines expression changes in Kv4.3 protein, as well as KChIP2 mRNA and protein, in CHF. The results suggest that in both our well-defined canine model and in human CHF, changes in Kv4.3 and not KChIP2 expression participate in I_{to} downregulation. With respect to the molecular basis for the well-known transmural I_{to} gradient, the present paper presents a number of novel elements. Our study is the first of which we are aware that shows a transmural gradient in Kv4.3 expression across the canine left ventricle. We were surprised by our results in the dog, and therefore repeated them in a number of complementary ways, obtaining consistent results with all methods. Our observations

regarding KChIP2 suggest that previously discrepant results may be due to differences in the antibodies used for Western blotting, with the highly-specific monoclonal antibody consistently showing stronger KChIP2 expression in epicardium than endocardium for both canine and human samples.

The functional significance of the various differences in subunit expression that we noted is an interesting question. KChIP2 and Kv4.3 appear to associate with 1:1 stoichiometry to create functional channels containing four molecules of each subunit (Kim *et al.* 2004). KChIP2 co-expression greatly increases membrane trafficking of Kv4 subunits and current density resulting from their expression in heterologous systems (An *et al.* 2000; Decher *et al.* 2001; Patel *et al.* 2002; Shibata *et al.* 2003). KChIP2 deletion strongly suppresses I_{to} in genetically engineered mice (Kuo *et al.* 2001). However, the effect of varying expression levels of Kv4.3 and KChIP2, as noted for endocardial/epicardial and CHF-related differences in the present study, is harder to predict. Because of the strong effect of KChIP2 in determining Kv4.3 membrane trafficking, the transmural gradients in KChIP2 expression alone might be sufficient to create the physiological gradient in I_{to}. This notion is consistent with the close agreement between the endocardial/epicardial protein gradients for KChIP2 protein and I_{to} density ratios. Nevertheless, the epicardial-endocardial gradients that we observed in Kv4.3 expression may also play a role. Data suggesting an important contribution of α-subunit expression gradients to regional I_{to} expression have been presented previously for rat (Dixon & McKinnon, 1994; Wickenden *et al.* 1999), ferret (Brahmajothi *et al.* 1999) and mouse (Guo *et al.* 1999; Guo *et al.* 2002) hearts. Evidence supporting a role for Kv4.3 expression differences in determining variations in I_{to} is provided by our CHF data, since in CHF Kv4.3 was downregulated without a

change in KChIP2, and Kv4.3 downregulation paralleled the CHF-induced decrease in I_{to} density. In addition to the levels of Kv4.3 and KChIP2 expression, the properties of I_{to} across the ventricular wall may be affected by differential regulation and by potential interactions with a variety of other membrane proteins (Deschênes & Tomaselli, 2002; Deschênes *et al.*, 2002).

Physiologically, the transmural gradient in I_{to} plays an important role in establishing repolarization gradients that are crucial for a variety of electrocardiographic phenomena and arrhythmia mechanisms (Antzelevitch *et al.* 1991; Antzelevitch & Fish, 2001). In addition, changes in I_{to} are likely important in the pathophysiology of a variety of cardiac disease entities involving ion-channel remodeling, ventricular tachyarrhythmias and impaired cardiac contractility (Antzelevitch & Fish, 2001; Oudit et al, 2001). Thus, understanding the molecular basis of I_{to} expression differences is potentially of great significance.

Potential limitations

We were able to study Kv4.3 and KChIP2 expression in isolated canine cardiomyocytes as well as dog atrial tissues, whereas for humans we were only able to work with whole tissue samples. However, the similarity between human and canine results, and the fact that results in canine tissues were consistent for mRNA across two methods and for protein expression in tissues and cells diminishes concerns about contamination of human cardiac samples by non-cardiac elements.

An additional lower molecular weight band was seen around 55 kDa when probing blots for Kv4.3 protein. The exact nature of this band is not completely known since it is much lower than the reported molecular weight of Kv4.3 (75 kDa).

The band did not completely disappear during the control antigen negative control experiments. It is possibly a proteolytic fragment of Kv4.3, or may even be a lower molecular weight isoform. More experiments are likely needed to properly characterize this band, however this was not within the scope of this study.

We are unsure why we observed gradients in Kv4.3 expression from epicardium to endocardium and Rosati *et al.* (2001, 2003) did not. They quantified Kv4.3 expression in whole tissue with RNase protection assay, whereas we used competitive RT-PCR and real-time PCR, as well as Western blot on whole tissues and isolated cardiomyocytes. The differences may be related to different methodologies or to subtle differences in tissue sampling sites. Both competitive RT-PCR and Real-time PCR also indirectly measure mRNA amounts since cDNA is used for end point calculations. However, these measurements were made during the logarithmic phase of cDNA amplification and can therefore be considered reflective of the amount of mRNA in a given sample. Discrepancies may also be related to differences in the types of dogs used. Both studies were performed with tissues from mongrel dogs, for which the race and genetic background are unknown and could be highly variable.

ACKNOWLEDGMENTS

The authors thank James Trimmer for providing us with the monoclonal antibody, Evelyn Landry for technical assistance and France Thériault for secretarial help with the manuscript. Funding was provided by the Canadian Institutes of Health Research, the Quebec Heart and Stroke Foundation (SN), and the Mathematics of Information Technology and Complex Systems (MITACS) Network of Centers of Excellence. SZ was supported by a graduate studentship from the "Fonds de la recherche en santé de Québec (FRSQ)".

REFERENCES

An WF, Bowlby MR, Betty M, Cao J, Ling HP, Mendozza G, Hinson JW, Mattsson KI, Strassle BW, Trimmer JS & Rhodes KJ (2000). Modulation of A-type potassium channels by a family of calcium sensors. *Nature* **403**, 553-556.

Antzelevitch C & Fish J (2001). Electrical heterogeneity within the ventricular wall. *Basic Res Cardiol* **96**, 517-527.

Antzelevitch C, Sicouri S, Litovsky SH, Lukas A, Krishnan SC, DiDiego JM, Gintant GA & Liu DW (1991). Heterogeneity within the ventricular wall: electrophysiology and pharmacology of epicardial, endocardial, and M-cells. *Circ Res* **69**, 1427-1449.

Borlak J & Thum T (2003). Hallmarks of ion channel gene expression in end-stage heart failure. *FASEB J* **17**, 1592-1608.

Brahmajothi MV, Campbell DL, Rasmusson RL, Morales MJ, Trimmer JS, Nerbonne JM & Strauss HC (1999). Distinct transient outward potassium current (Ito) phenotypes and distribution of fast-inactivating potassium channel alpha subunits in ferret left ventricular myocytes. *J Gen Physiol* **113**, 581-600.

Cha TJ, Ehrlich JR, Zhang L, Shi YF, Tardif JC, Leung TK & Nattel S (2004). Dissociation between ionic remodeling and ability to sustain atrial fibrillation during recovery from experimental congestive heart failure. *Circulation* **109**, 412-418.

Decher N, Uyguner O, Scherer CR, Karaman B, Yüksel-Apak M, Busch AE, Steinmeyer K & Wollnik B (2001). hKChIP2 is a functional modifier of hKv4.3 potassium channels: cloning and expression of a short hKChIP2 splice variant. *Cardiovasc Res* **52**, 255-264.

Deschênes I, DiSilvestre D, Juang GJ, Wu RC, An WF & Tomaselli GF (2002). Regulation of Kv4.3 current by KChIP2 splice variants. A component of native cardiac I_{to}? *Circulation* **106**, 423-429.

Deschênes I & Tomaselli GF (2002). Modulation of Kv4.3 current by accessory subunits. *FEBS Letters* **528**, 183-188.

DiDiego JM, Cordeiro JM, Goodrow RJ, Fish JM, Zygmunt AC, Perez GJ, Scornik FS & Antzelevitch C (2002). Ionic and cellular basis for the predominance of the Brugada syndrome phenotype in males. *Circulation* **106**, 2004-2011.

Dixon JE & McKinnon D (1994). Quantitative analysis of potassium channel mRNA expression in atrial and ventricular muscle of rats. *Circ Res.* **75**, 252-260.

Dixon JE, Shi W, Wang HS, McDonald C, Yu H, Wymore RS, Cohen IS & McKinnon D (1996). Role of Kv4.3 K^+ channel in ventricular muscle. A molecular correlate for the transient outward current. *Circ Res* **79**, 659-668.

Fedida D & Giles WR (1991). Regional variations in action potentials and transient outward current in myocytes isolated from rabbit left ventricle. *J Physiol* **442**, 191-209.

Furukawa T, Myerburg RJ, Furukawa N, Bassett & Kimura S (1990). Differences in transient outward currents of feline endocardial and epicardial myocytes. *Circ Res* **67**, 1287-1291.

Guo W, Li H, Aimond F, Johns DC, Rhodes KJ, Trimmer JS & Nerbonne JM (2002). Role of heteromultimers in the generation of myocardial transient outward K^+ currents. *Circ Res* **90**, 586-593.

Guo W, Xu H, London B & Nerbonne JM (1999). Molecular basis of transient outward K^+ current diversity in mouse ventricular myocytes. *J Physiol* **521**, 587-599.

Kääb S, Dixon J, Duc J, Ashen D, Näbauer M, Beuckelmann DJ, Steinbeck G, McKinnon D & Tomaselli GF (1998). Molecular basis of transient outward potassium current downregulation in human heart failure. A decrease in Kv4.3 mRNA correlates with a reduction in current density. *Circulation* **98**, 1383-1393.

Kääb S, Nuss HB, Chiamvimonvat N, O'Rourke B, Pak PH, Kass DA, Marban E & Tomaselli GF (1996). Ionic mechanism of action potential prolongation in ventricular myocytes from dogs with pacing-induced heart failure. *Circ Res* **78**, 262-273.

Kaprielian R, Sah R, Nguyen T, Wickenden AD & Backx PH (2002). Myocardial infarction in rat eliminates regional heterogeneity of AP profiles, I(to) K(+) currents, and [Ca(2+)](i) transients. *Am J Physiol Heart Circ Physiol* **283**, H1157-H1168.

Kim LA, Furst J, Butler MH, Xu S, Grigorieff N & Goldstein SA (2004). I_{to} channels are octomeric complexes with four subunits of each Kv4.2 and K+ channel-interacting protein 2. *J Biol Chem* **279**, 5549-5554.

Kuo HC, Cheng CF, Clark RB, Lin JJC, Lin JLC, Hoshijima M, Nguyen-Tran VTB, Gu Y, Ikeda Y, Chu PH, Ross J, Giles WR & Chien KR (2001). A defect in the Kv channel-interacting protein 2 (KChIP2) gene leads to a complete loss of I_{to} and confers susceptibility to ventricular tachycardia. *Cell* **107**, 801-813.

Li GR, Lau CP, Ducharme A, Tardif JC & Nattel S (2002). Transmural action potential and ionic current remodeling in ventricles of failing canine hearts. *Am J Physiol Heart Circ Physiol* **283**, H1031-H1041.

Litovsky SH & Antzelevitch C (1988). Transient outward current prominent in canine ventricular epicardium but not endocardium. *Circ Res* **62**, 116-126.

Lue WM & Boyden PA (1992). Abnormal electrical properties of myocytes from chronically infarcted canine heart. Alterations in Vmax and the transient outward current. *Circulation* **85**, 1175-1188.

Lukas A & Antzelevitch C (1993). Differences in the electrophysiological response of canine ventricular epicardium and endocardium to ischemia. Role of the transient outward current. *Circulation* **88**, 2903-2915.

Näbauer M, Beuckelmann DJ, Überfuhr P & Steinbeck G (1996). Regional differences in current density and rate-dependent properties of the transient outward current in subepicardial and subendocardial myocytes of human left ventricle. *Circulation* **93**, 168-177.

Oudit GY, Kassiri Z, Sah R, Ramirez RJ, Zobel C & Backx PH (2001). The molecular physiology of the cardiac transient outward potassium current (I(to)) in normal and diseased myocardium. *J Mol Cell Cardiol* **33**, 851-872.

Patel SP, Campbell DL & Strauss HC (2002). Elucidating KChIP effects on Kv4.3 inactivation and recovery kinetics with a minimal KChIP2 isoform. *J Physiol* **545**, 5-11.

Patel SP, Campbell DL, Morales MJ & Strauss HC (2002). Heterogeneous expression of KChIP2 isoforms in the ferret heart. *J Physiol* **539**, 649-656.

Rosati B, Grau F, Rodriguez S, Li H, Nerbonne JM & McKinnon D (2003). Concordant expression of KChIP2 mRNA, protein and transient outward current throughout the canine ventricle. *J Physiol* **548**, 815-822.

Rosati B, Pan Z, Lypen S, Wang HS, Cohen I, Dixon JE & McKinnon D (2001). Regulation of KChIP2 potassium channel β subunit gene expression underlies the gradient of transient outward current in canine and human ventricle. *J Physiol* **533**, 119-125.

Rozanski GJ, Xu Z, Zhang K & Patel KP (1998). Altered K^+ current of ventricular myocytes in rats with chronic myocardial infarction. *Am J Physiol Heart Circ Physiol* **274**, H259-H265.

Shibata R, Misonou H, Campomanes CR, Anderson AE, Schrader LA, Doliveira LC, Carroll KI, Sweatt JD, Rhodes KJ & Trimmer JS (2003). A fundamental role for KChIPs in determining the molecular properties and trafficking of Kv4.2 potassium channels. *J Biol Chem.* **278**, 36445-36454.

Wettwer E, Amos GJ, Posival H & Ravens U (1994). Transient outward current in human ventricular myocytes of supepicardial and subendocardial origin. *Circ Res* **75**, 473-482.

Wickenden AD, Jegla TJ, Kaprielian R & Backx PH (1999). Regional contributions of Kv1.4, Kv4.2, and Kv4.3 to transient outward K^+ current in rat ventricle. *Am J Physiol Heart Circ Physiol* **276**, H1599-H1607.

Yan GX & Antzelevitch C (1999). Cellular basis for the Brugada syndrome and other mechanisms of arrhythmogenesis associated with ST-segment elevation. *Circulation* **100**, 1660-1666.

Zicha S, Moss I, Allen B, Varro A, Papp J, Dumaine R, Antzelevich C & Nattel S (2003). Molecular basis of species-specific expression of repolarizing K+ currents in the heart. *Am J Physiol Heart Circ Physiol* **285**, H1641-h1649.

Zicha S, Stafford S, Cha TJ, Han W & Nattel S (2003). Molecular basis for transmural potassium current remodeling in heart failure. *Circulation* (Suppl IV): IV-75 (abstract).

Table 1. Hemodynamic data confirming the presence of CHF

	Body weight (kg)	SBP (mm Hg)	DBP (mm Hg)	Mean BP (mm Hg)	RA BP (mm Hg)	LV Sys (mm Hg)	LVEDP (mm Hg)
Control $n = 5$	25.1 ± 2.4	118.8 ± 6.2	73.6 ± 4.8	85.8 ± 5.5	2.2 ± 0.4	113.2 ± 5.7	2.8 ± 1.1
Heart failure $n = 5$	27.1 ± 1.0	99.8 ± 4.0*	61.0 ± 3.0	73.6 ± 3.3	9.8 ± 3.2	93.4 ± 3.4*	24.9 ± 3.3**

Significantly different from CTL, *$P < 0.05$; ** $P < 0.005$.
SBP = systolic blood pressure; DBP = diastolic blood pressure; Mean BP = mean arterial blood pressure; RA BP = mean right atrial pressure; LV Sys = left ventricular systolic blood pressure; LVEDP = left ventricular end-diastolic pressure.

Table 2. Gene-specific primers for RT-PCR

Clone	Primer pair	Bases spanned, bp	Size, bp	Tm, °C
dKv4.3 Competitive RT-PCR	F: TAGATGAGCAGATGTTTGAGC R: ACTGCCCTGGATGTGGATG	1532-1742	210	54.5
dKv4.3 Real Time RT-PCR	F: CCTGCTGCTCCCGTCGTA R: AGTGGCTGGCAGGTTGGA	1634-1695	61	60
dKChIP2 Competitive RT-PCR	F: GAGGACTTTGTGGCTGG R: CCATCCTTGTTTCTGTCC	358-596	239	52

FIGURES

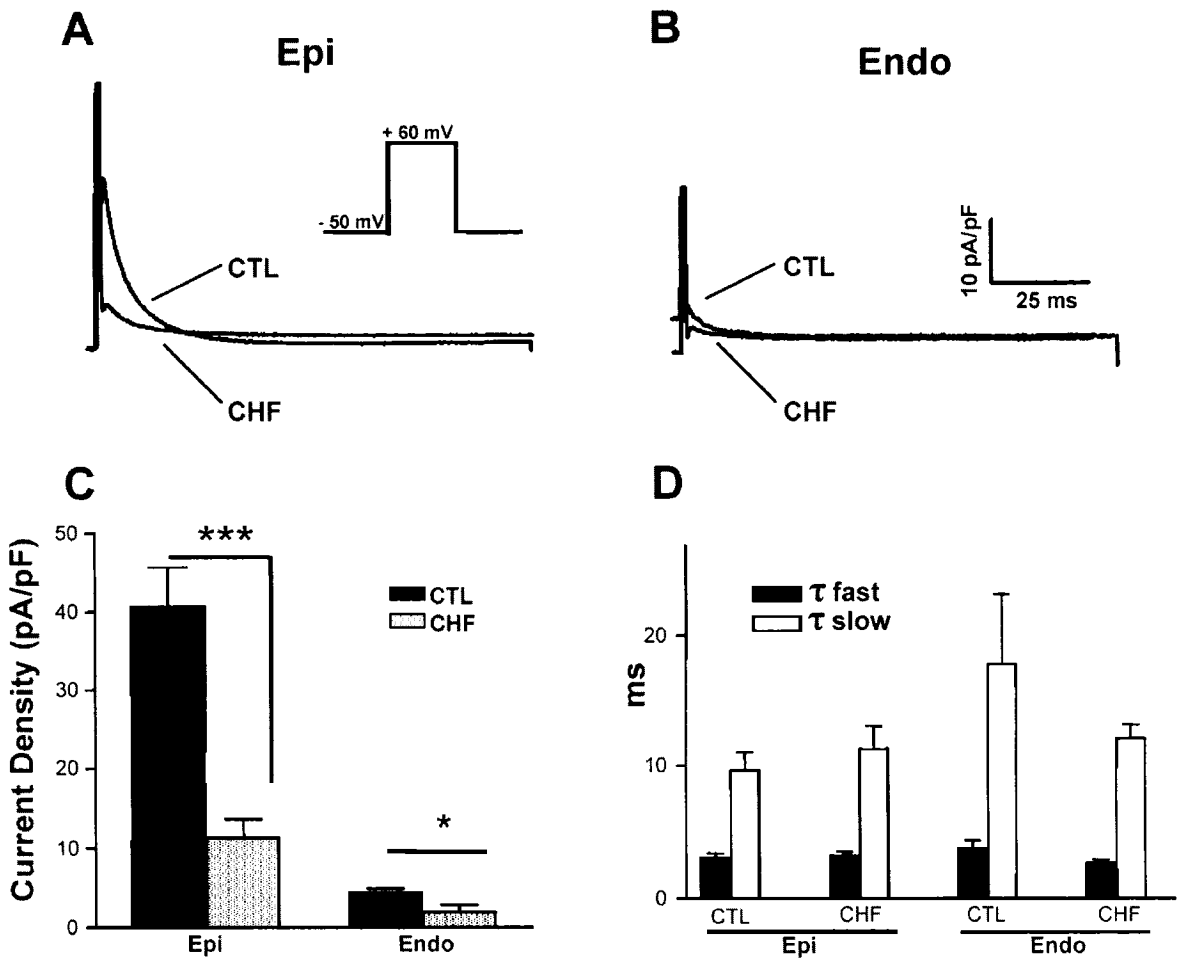

Figure 1 **Properties of I_{to} in control and failing canine ventricles.** Representative I_{to} recordings from control (CTL) and CHF myocytes in epicardium (**A**) and endocardium (**B**). Currents were elicited by a 100-ms test pulse at 0.1 Hz from a holding potential of -50 mV to +60 mV. **C**, Mean current densities for CTL and CHF epicardial (Epi) and endocardial (Endo) I_{to}. A transmural gradient is seen in CTL hearts, and I_{to} is significantly downregulated in CHF (n = 7 cells in EPI CTL, CHF; 8 cells in ENDO CTL, CHF; $^{*}P < 0.05$, $^{***}P < 0.001$ for CTL vs CHF). **D**, Mean ± SEM inactivation kinetics. τ fast, τ slow= fast and slow phase inactivation time constants. There were no statistically significant differences in time constants between Epi and Endo, CHF and CTL.

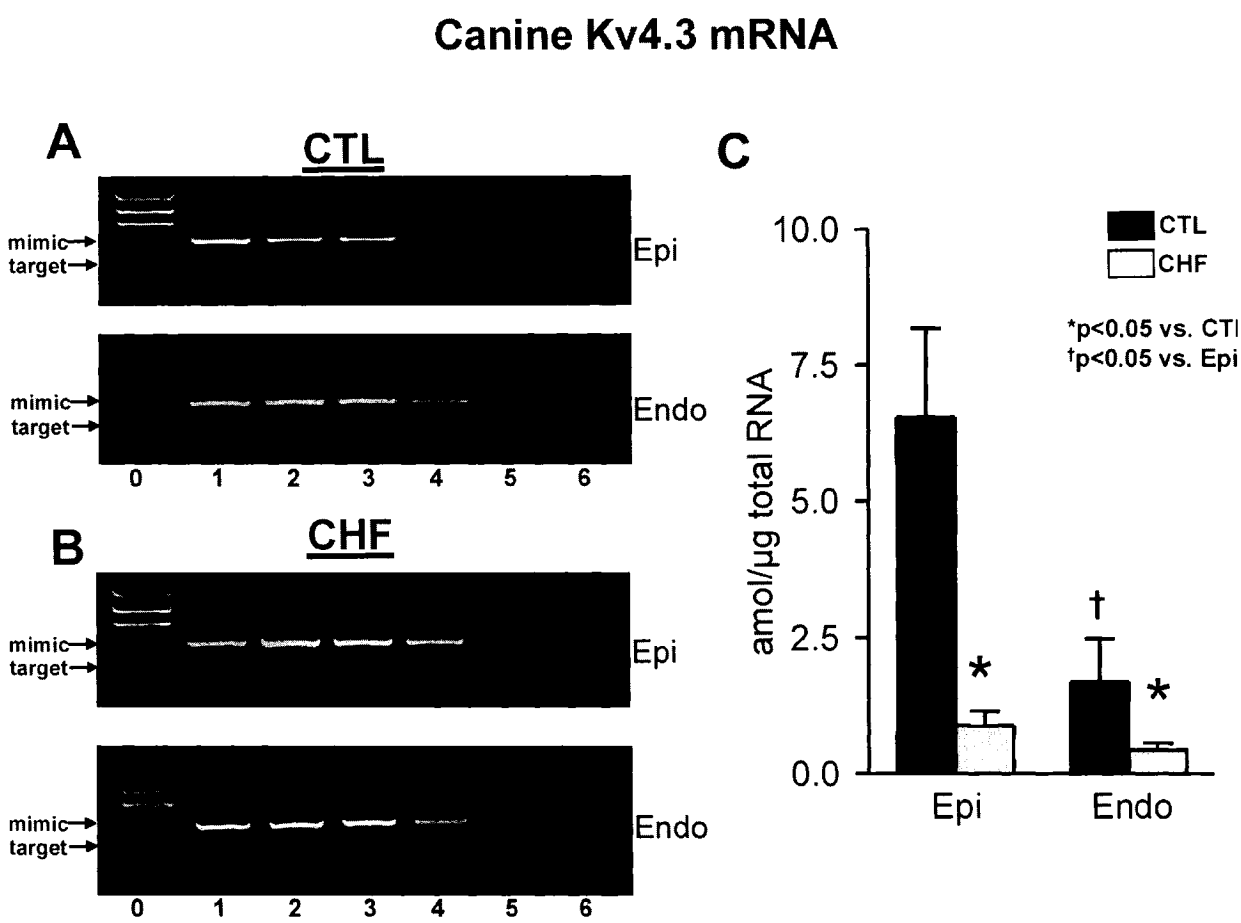

Figure 2 **Kv4.3 competitive RT-PCR.** Representative gels from Epi and Endo samples are shown for CTL in **A**, for CHF in **B**. Mimic concentrations decrease from left to right. The point where mimic and target band intensities are equal indicates equal mRNA concentrations, and was determined for each experiment by linear regression of ln(mimic/target concentration) against ln(mimic concentration). **C**, Absolute molar concentration of Kv4.3 mRNA (Mean ± S.E.M.). $^{*}P < 0.05$ vs CTL, $^{\dagger}P < 0.05$ vs Epi, $n = 5$ hearts/group.

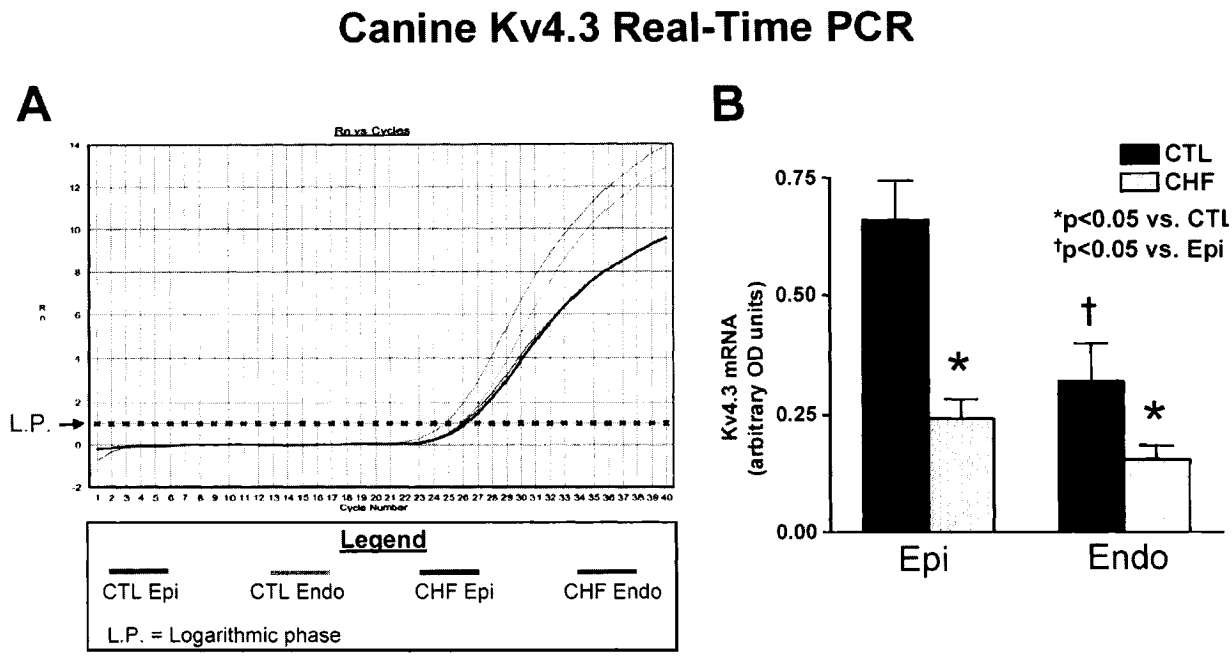

Figure 3 **Kv4.3 Real-time PCR results. A.** A representative amplification plot obtained from Kv4.3 real-time PCR with CTL and CHF, Epi and Endo tissue samples. L.P. = log amplification phase threshold for calculation of mRNA expression. **B.** Mean ± S.E.M. data from Kv4.3 real-time PCR. A transmural gradient is observed for Kv4.3 mRNA, as well as downregulation in CHF. $^{*}P < 0.05$ vs CTL, $^{\dagger}P < 0.05$ vs CTL Epi, $n = 7$ hearts/group.

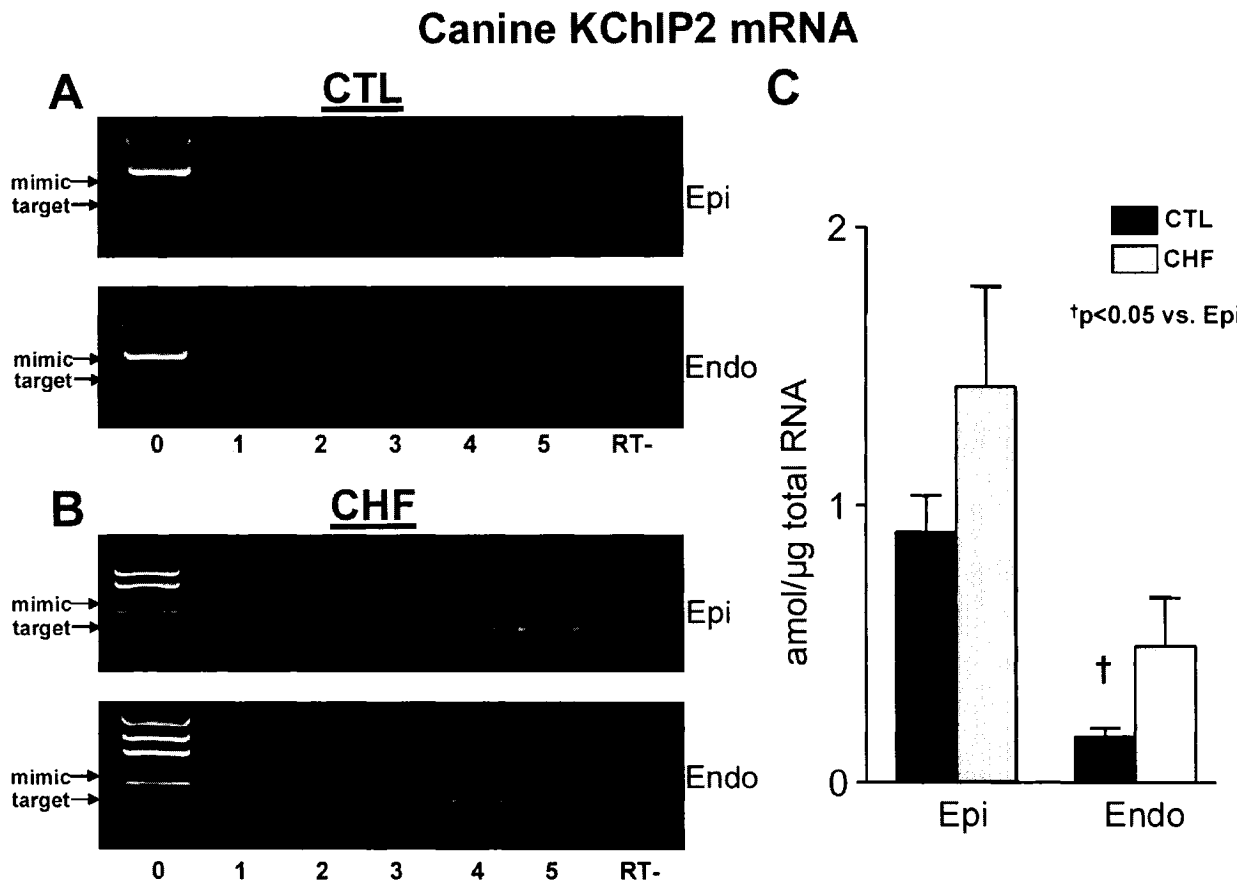

Figure 4 **KChIP2 competitive RT-PCR.** Examples of Epi and Endo KCHIP2 competitive RT-PCR gels from a CTL (**A**) and a CHF (**B**) heart. **C**, Absolute expression levels of KChIP2 mRNA (Mean ± S.E.M.). $^{\dagger}P < 0.05$ CTL Endo vs CTL Epi, $n = 5$ hearts/group.

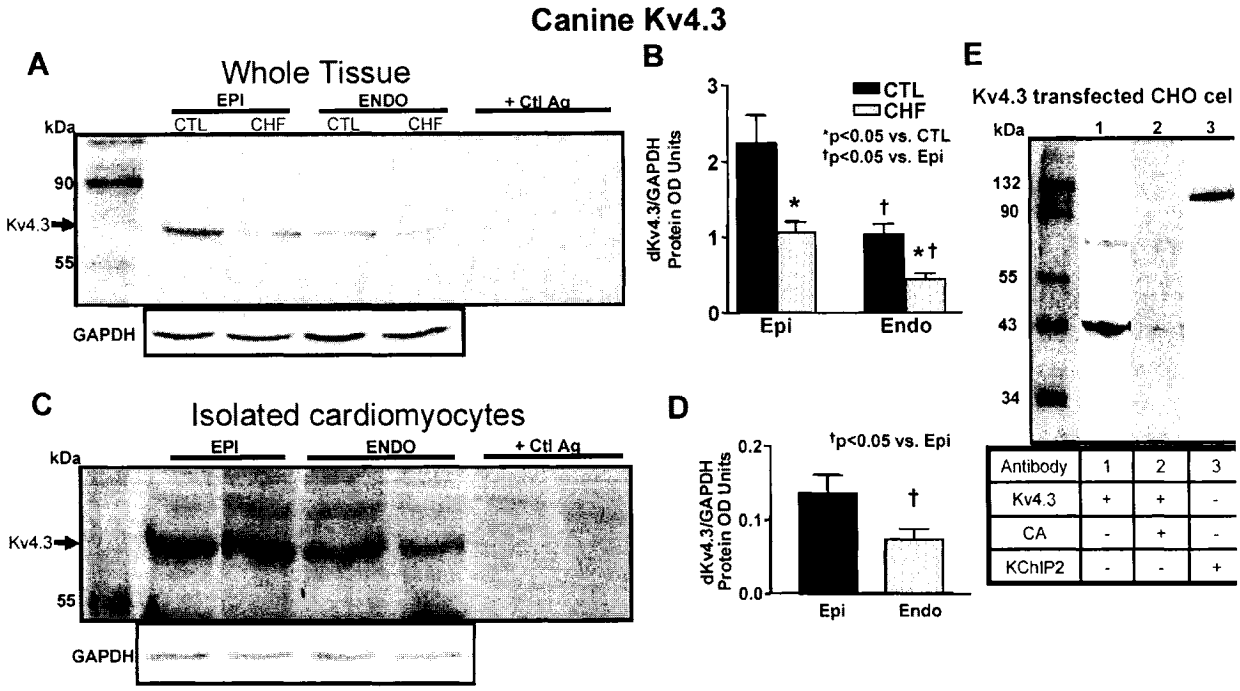

Figure 5 **Canine Kv4.3 Western blot results.** **A**, Western blot membrane with whole-tissue membrane protein probed with anti-Kv4.3 antibody (Alomone). The expected molecular mass for Kv4.3 (~75 kDa) is indicated. Last two lanes show samples for which the primary antibody was pre-incubated with control antigen. Lower panel shows GAPDH bands corresponding to lanes at the top, to which Kv4.3 results were normalized. **B**, Mean ± S.E.M. Kv4.3 protein expression values. $^{*}P < 0.05$ vs Epi, $^{\dagger}P < 0.05$ vs CTL Epi, $n = 5$ hearts/group. **C**, Experiments of the type shown in **A** were performed with membrane proteins from isolated cardiomyocytes, to eliminate contamination from non-myocyte cell species. Last two lanes show samples probed with primary Kv4.3 antibody pre-incubated with control antigen (band at ~75 kDa disappears). **D**, Mean ± S.E.M. Kv4.3 protein expression values in isolated cardiomyocytes ($^{\dagger}P < 0.05$ vs CTL Epi, $n = 5$ hearts/group). **E**, Western blot of proteins isolated from Kv4.3-transfected CHO cells. Lane 1 shows bands at ~75 and 43 kDa. Lane 2 shows result when antibody was pre-incubated along with its control antigen: the ~75 kDa band completely disappeared. Lane 3 shows membrane probed with a monoclonal KChIP2 antibody. A single high-molecular weight band at ~125 kDa was detected, but KChIP2 antibody did not detect a band with the expected molecular mass for Kv4.3. CA = anti-Kv4.3 antibody pre-incubated with control antigen. Results similar to those in E were obtained in 3 experiments.

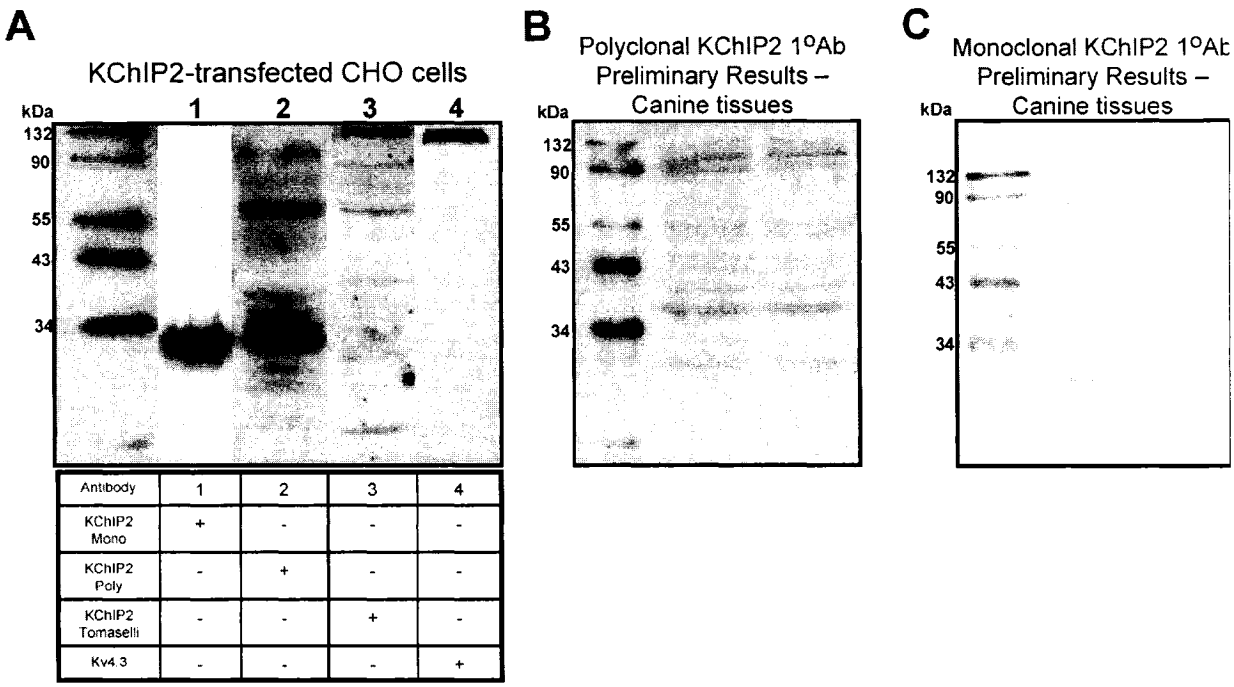

Antibody	1	2	3	4
KChIP2 Mono	+	-	-	-
KChIP2 Poly	-	+	-	-
KChIP2 Tomaselli	-	-	+	-
Kv4.3	-	-	-	+

Figure 6 **Western blots on KChIP2 proteins in transfected CHO cells and canine cardiac tissues. A**, Western blots of membrane protein from KChIP2-transfected CHO cells. Lane 1 shows result of a membrane probed with monoclonal KChIP2 antibody: a single band was detected at ~30 kDa. A commercially available polyclonal KChIP2 antibody was used in Lane 2. Many nonspecific bands were detected. Lane 3 shows KChIP2 protein probed with a polyclonal antibody kindly provided by Dr. Gordon Tomaselli. Again, many bands were detected. Lane 4 shows KChIP2 protein probed with a Kv4.3 antibody. No band is detected at the expected size for KChIP2, confirming the lack of cross-reactivity of the Kv4.3 antibody with KChIP2. **B**, Preliminary Western blots performed on canine cardiac tissue membrane proteins using the commercially available KChIP2 antibody. **C**, Preliminary Western blots on canine cardiac tissues using monoclonal antibody. A single clear band was detected at ~30 kDa, along with a band at a much higher molecular mass. This antibody was used for subsequent studies. Results similar to those in A, B and C were obtained for 3, 5 and 5 samples respectively.

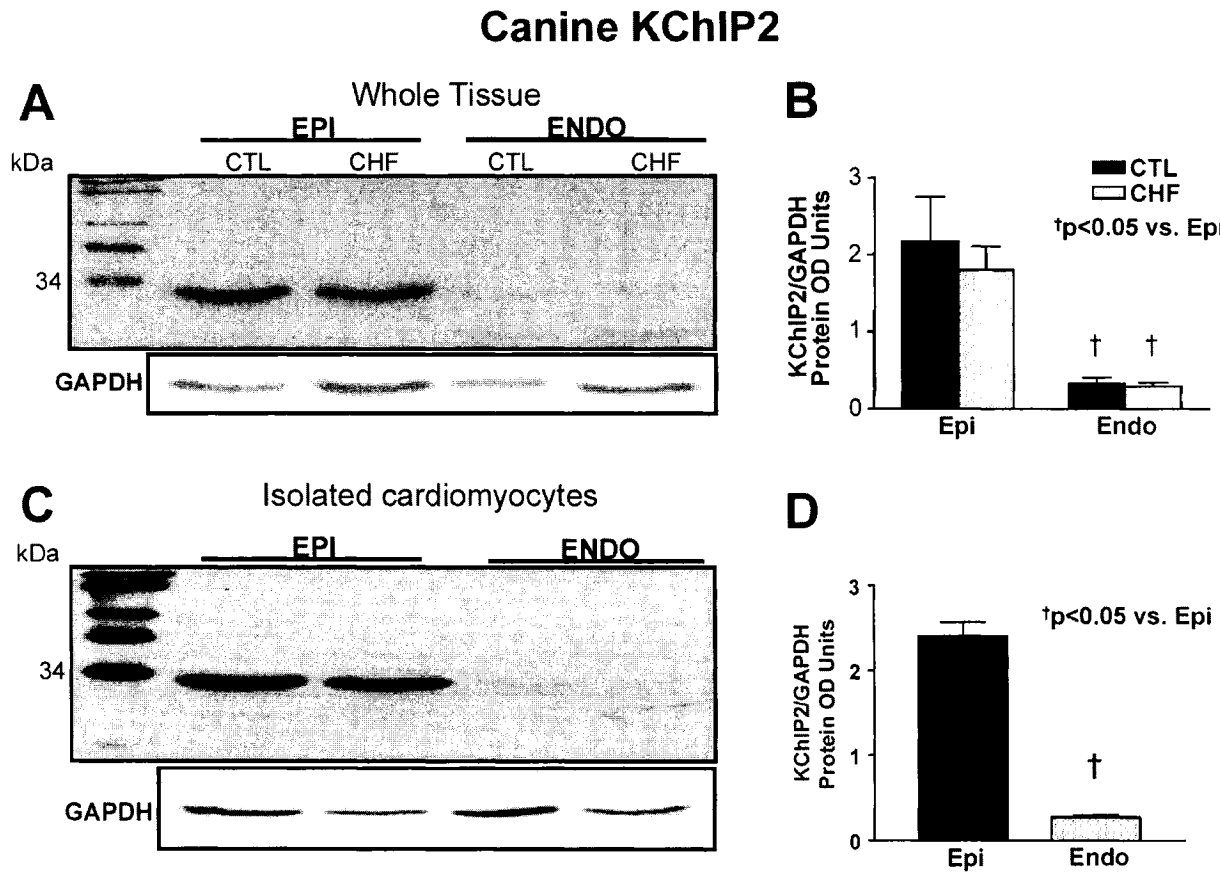

Figure 7 **Canine KChIP2 Western blot results.** **A**, Example of KChIP2 Western blot obtained with monoclonal KChIP2 antibody applied to canine ventricular tissue membrane proteins. A single band at ~32 kDa was detected. **B**, Expression of KChIP2 protein (Mean ± S.E.M.) in whole tissue samples. $^{\dagger}P < 0.05$ vs Epi. **C**, Example of KChIP2 Western blot on samples of isolated cardiomyocyte membrane protein using the monoclonal KChIP2 antibody. Single bands were detected at ~32 kDa. Lower panel shows a representative GAPDH blot performed on the same samples as in the lanes immediately above. **D**, KChIP2 protein expression in isolated cardiomyocytes (Mean ± S.E.M.). $^{\dagger}P < 0.05$, $n = 5$ hearts/group.

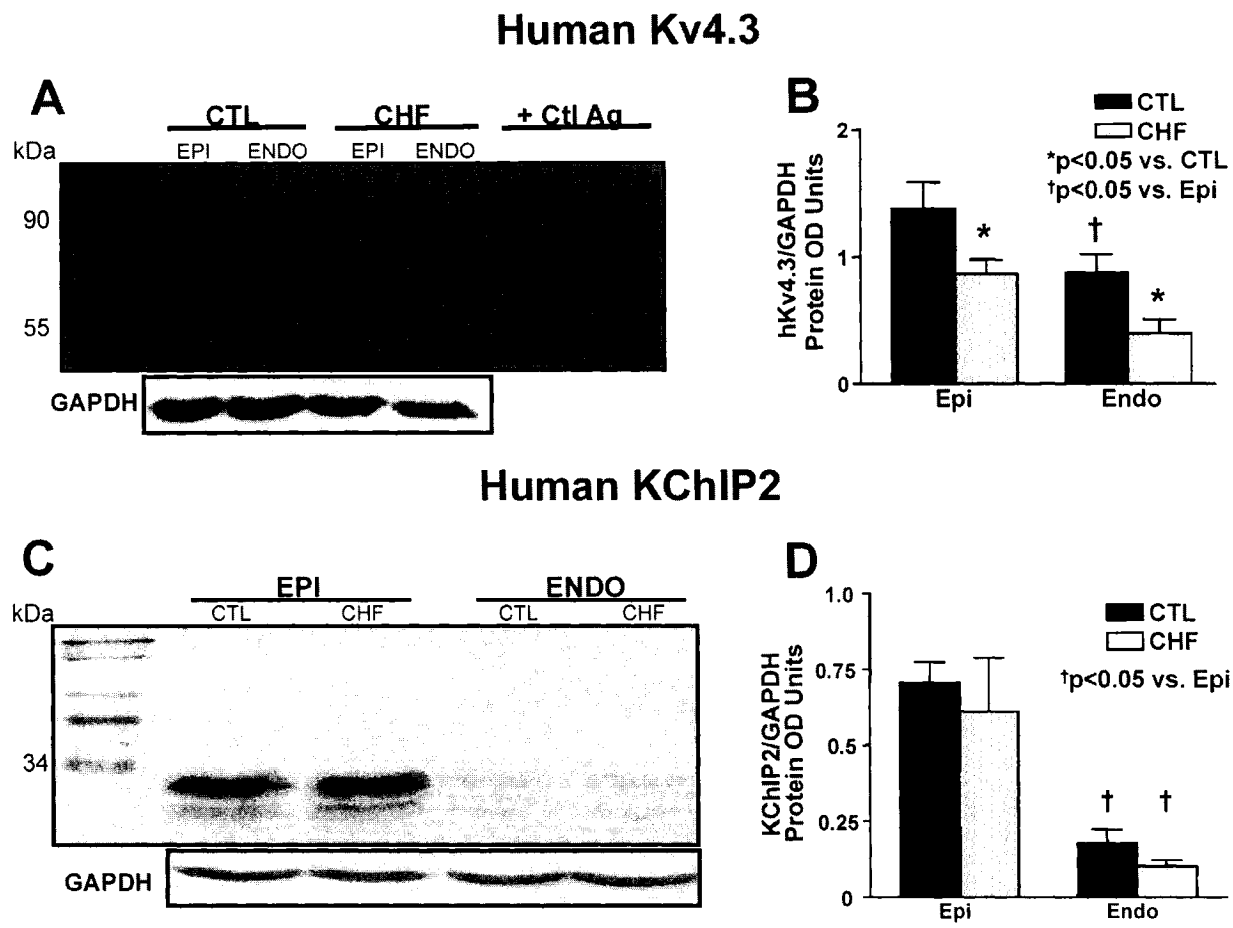

Figure 8 **Human I_{to} subunit Western blot results.** **A**, Western blot of membrane probed with anti-Kv4.3 antibody (Alomone). Last two lanes: samples blotted with primary antibody pre-incubated with antigenic peptide. **B**, Kv4.3 protein expression. $^{*}P < 0.05$ CHF vs CTL, $^{\dagger}P < 0.05$ Endo vs Epi, n = 5/group. **C**, Example of KChIP2 Western blot, band detected at ~32 kDa. Lower panel shows GAPDH Western blot on same samples as lanes above. **D**, KChIP2 protein expression. $^{\dagger}P < 0.05$ Endo vs Epi, n = 5 hearts/group.

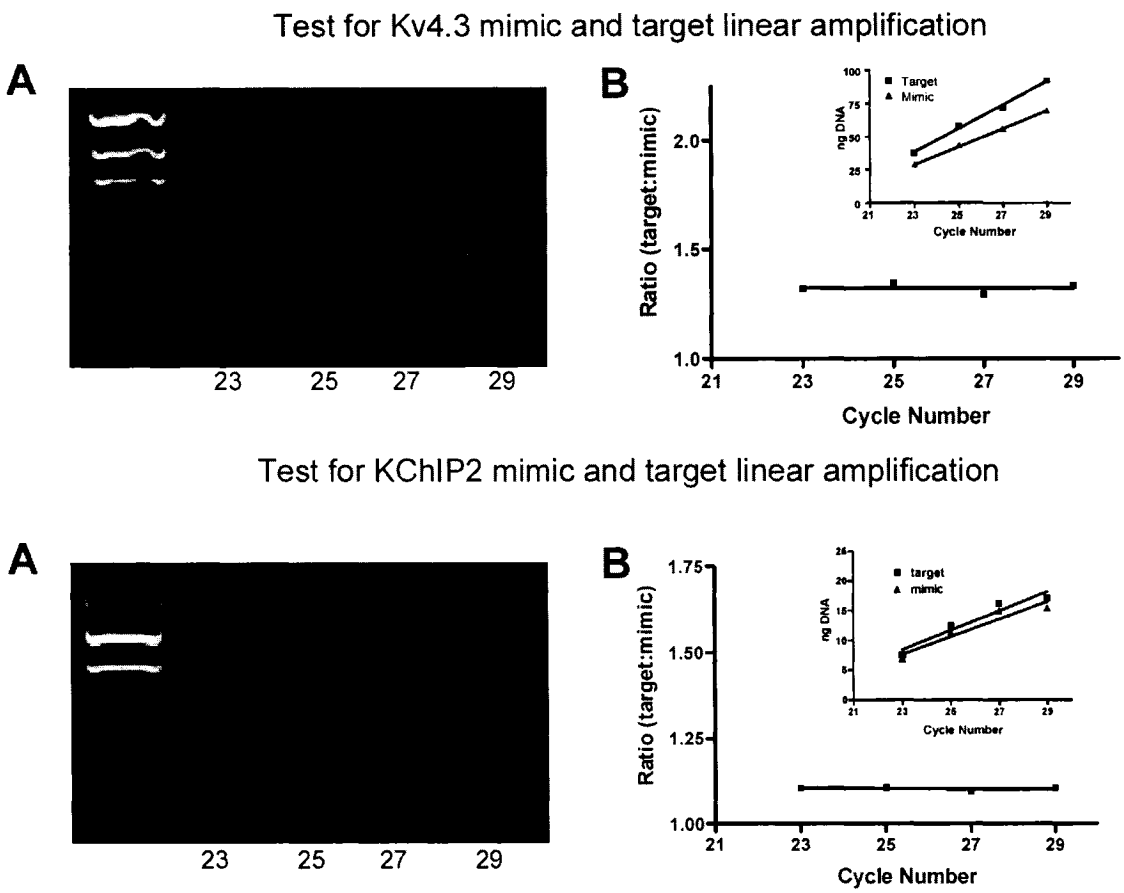

Figure 9 **Linearity of competitive RT-PCR reactions. A.** Example of gel used to verify that the Kv4.3 mimic and target PCR amplicons are amplified at the same rate and that neither reaches a saturation point before the last cycle is completed. The numbers under each lane denote the cycle number from which the sample was taken. **B.** The ratio of target:mimic was plotted vs. the cycle number from which the samples were taken. Slope=0.0005±0.006 and not significantly different from 0, indicating an equal amplification of both mimic and target. Inset shows the individual amplification plots for the target and mimic. **C.** Example of gel used to verify that the KChIP2 mimic and target PCR amplicons are amplified at the same rate. **D.** The ratio of target:mimic was plotted vs. the cycle number. Slope = 0.0005±0.002 which is not significantly different from 0, indicating equal amplification. Inset shows individual regression analysis for target and mimic.

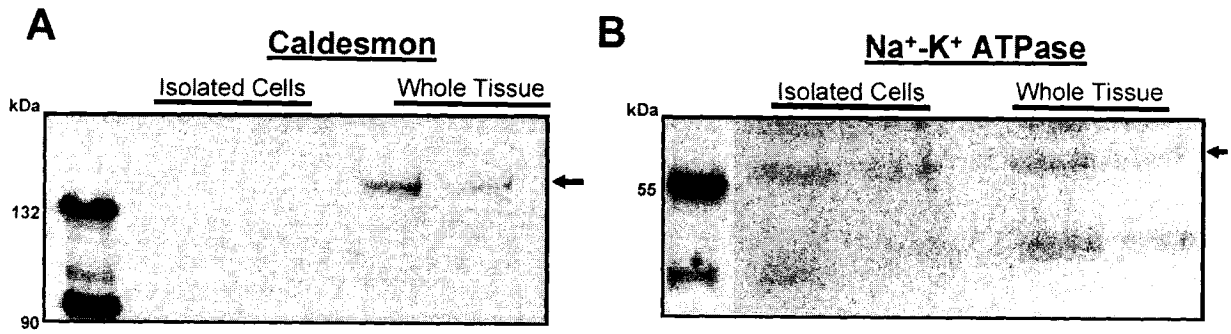

Figure 10 **Western blot used to determine purity of protein samples. A.** Example of an immunoblot probed with an anti-caldesmon antibody. Caldesmon is a smooth muscle cell marker and the lack of this protein in isolated myocyte membrane protein samples confirms that there is little contamination from cell types other than cardiomyocytes. **B.** Example of an immunoblot probed with an anti-Na^+-K^+ ATPase antibody. This was used to verify that the protein samples used were in fact membrane protein fractions.

CHAPTER 5: SINUS NODE DYSFUCTION AND PACEMAKER-CURRENT SUBUNIT REMODELING IN CONGESTIVE HEART FAILURE

The sinoatrial node (SAN) is a specialized highly innervated region in the right atrium responsible for the maintenance of normal cardiac rhythm. Its characteristic slow depolarizations are able to suppress ectopic beat formation in other regions of the heart by overdrive suppression. It is heavily modulated by the sympathetic nervous system whose influences can alter the heart rate. The pacemaker current, or I_f, is highly expressed in the SAN and is responsible for depolarizing cells in this region, allowing Ca^{2+} currents to initiate a new action potential (DiFrancesco, 1993). The exact molecular basis of human and canine I_f has not been elucidated, although it is known that these currents are encoded by the HCN family of channel subunits. In addition, data concerning the basis of the heterogeneous expression of I_f in different areas of the heart such as the SAN and the right atrium are lacking.

CHF is associated with an increased propensity for arrhythmias such as AF, and while mechanistic links to ion channel remodelling have been noted, none have examined the effect of CHF on I_f. In this study, we examine the molecular basis for I_f heterogeneity in the right atrium and the SAN. In addition, the effects of CHF are also studied in order to ascertain what changes may contribute to the increased risk of arrhythmia. I_f is studied in this regard because of its ability to depolarize SAN cells under normal conditions, and an arrhythmogenic setting would indicate that this intrinsic pacemaker activity is removed from this region.

ABSTRACT

Background The pacemaker current, I_f, underlies sinoatrial node pacemaker function and ectopic arrhythmogenesis. Little is known about expression of various pacemaker-channel (HCN) subunits in normal hearts and HCN-remodeling by diseases, like congestive heart failure (CHF), associated with disturbances of cardiac rhythm. ***Methods and Results*** We assessed expression of HCN1, 2 and 4 in normal mongrel dogs and dogs subjected to 2-week ventricular tachypacing-induced CHF. Competitive RT-PCR and Western blot were used to quantify HCN subunit mRNA and protein respectively in the right atrium (RA) and sinoatrial node. CHF approximately doubled sinus-node recovery time, indicating suppressed sinus-node pacemaker function. HCN expression under control conditions was HCN4 > HCN2 >> HCN1. HCN2 and HCN4 expression was greater at both protein and mRNA levels in sinoatrial node than RA. CHF significantly decreased sinus-node HCN expression at both mRNA and protein levels (HCN2 by 78% and 82%; HCN4 by 42% and 77% respectively). RA HCN2 expression was unaltered by CHF, but HCN4 was significantly upregulated (by 209%). ***Conclusions*** HCN4 is the dominant subunit in canine sinoatrial node and RA; strong sinus node HCN expression likely contributes to its pacemaker function; downregulation of HCN4 and HCN2 expression contribute to CHF induced sinus node dysfunction; and upregulation of atrial HCN4 may help to promote atrial arrhythmia formation. These findings provide novel information about the molecular basis of normal and disease-related impairments of cardiac impulse formation.

Key Words: pacemaker current ■ sinoatrial node ■ congestive heart failure

CONDENSED ABSTRACT

Little is known about cardiac pacemaker-channel (HCN) subunit expression and remodeling by congestive heart failure (CHF). We quantified HCN-subunit mRNA and protein in normal and CHF canine right atrium (RA) and sinus-node. HCN expression under control conditions was HCN4>HCN2>>HCN1 and was stronger in sinus-node than RA. CHF significantly decreased sinus-node HCN expression. RA HCN2 expression was unaltered by CHF, but HCN4 was upregulated 2-3 fold. We conclude that HCN4 is the dominant canine pacemaker-subunit, strong sinus-node HCN expression contributes to its pacemaker function, HCN downregulation causes CHF-induced sinus-node dysfunction, and atrial HCN4 upregulation may promote CHF-induced atrial arrhythmia formation.

INTRODUCTION

The sinoatrial node is responsible for controlling normal cardiac rhythm. Phase 4 diastolic depolarization is due to the activity of the funny current (I_f), also known as the pacemaker current, which is particularly prominent in the sinus node.[1] I_f is a voltage-gated current with many unique features, including an ability to carry both K^+ and Na^+ with a reversal potential around -20 mV,[2] and activation by polarization to negative voltages.[3,4] Sympathetic nervous system stimulation accelerates cardiac rate via β-adrenergic increases in intracellular cAMP, which shift the voltage-dependence of I_f activation to more positive potentials.[5,6] Increases in I_f can lead to enhanced automaticity and ectopic rhythm formation.

Despite the importance of I_f in cardiac electrophysiology, its molecular composition was only recently elucidated.[7] The family of voltage-gated HCN subunits, including HCN1-4, encode I_f in many excitable tissues. Only HCN1,[8] HCN2[9] and HCN4[10] are expressed in the heart. Few studies have examined the expression profiles of these subunits in the sinoatrial node and other regions of the heart.[8,10-16] Furthermore, most of these studies were performed in rodents, which may have different ion-channel subunit dependence compared to larger mammals.

Congestive heart failure (CHF) is a common cause of sudden arrhythmic death and is an important risk factor for atrial fibrillation (AF).[17] Abnormalities in sinus node function are common in CHF and may contribute to bradyarrhythmic death.[17] CHF impairs single sinus-node cell automaticity by downregulating I_f.[18] There is no information available about CHF-induced remodeling of the HCN subunits underlying I_f. This study examined the expression profiles of HCN subunits in the sinoatrial node and RA of dogs and their modification by CHF.

MATERIALS AND METHODS

CHF Model

Seven dogs were outfitted with custom modified pacemakers (Medtronic) as previously reported.[19] Briefly, pacemakers were inserted in subcutaneous pockets in the necks and attached to pacing leads inserted into the right ventricular apex under fluoroscopy. After 24 hours for recovery, ventricular tachypacing was initiated at 240 bpm and maintained for 2 weeks. The dogs were then confirmed to have CHF based on clinical signs and hemodynamic findings, sinus-node function was assessed under morphine (2 mg/kg s.c.) and α-chloralose (100 mg/kg IV) anesthesia, and then dogs were euthanized with an α-chloralose overdose. The hearts were removed and the right atrial (RA) free wall and sinoatrial node isolated. The sinoatrial node was identified as a whitish endocardial region near the junction of the RA free wall and the atrial appendage near the crista terminalis, with subsequent histological confirmation. The RA free wall and sinoatrial node were removed (avoiding epicardial arteries), cleaned in Tyrode solution containing (mM): NaCl 136, KCl 5.4, $MgCl_2$ 1, $CaCl_2$ 2, NaH_2PO_4 0.33, HEPES 5 and dextrose 10, pH 7.35 (NaOH), then flash-frozen in liquid-N_2 and stored at -80°C. Seven non-paced dogs served as controls. All animal-handling procedures adhered to the guidelines of the Canadian Council on Animal Care and were approved by the Montreal Heart Institute Animal Research Ethics Committee.

Sinus-Node Recovery Time Changes

Bipolar pacing and recording hook electrodes were inserted into the right atrial appendage. Vagal and β-adrenergic influences were prevented respectively by administering nadolol (0.5 mg/kg IV) and severing the vagus nerves in the neck. The baseline cardiac rate (assumed to represent sinus-node rate when standard ECG criteria for sinus rhythm were met) was measured and then the RA was paced at a cycle length of 250 or 300 ms for 30 seconds. The post-pacing interval until the first sinus escape beat was recorded and subtracted from the pre-pacing spontaneous cycle length to obtain the corrected sinus-node recovery time ($SNRT_C$).

RNA Isolation

RNA was isolated from 0.1-1.0 g samples using Trizol reagent (Invitrogen) followed by chloroform extraction and isopropanol precipitation. Genomic DNA was eliminated by incubating in DNase I (0.1 U/μL, 37°C) for 30 minutes followed by acid phenol-chloroform extraction. RNA was quantified by spectrophotometric absorbency at 260 nm, purity confirmed by A_{260}/A_{280} ratio and integrity evaluated by ethidium bromide staining on a denaturing agarose gel. RNA samples were stored at -80°C in RNAsecure Resuspension Solution (Ambion).

PCR Primers and the Synthesis of the RNA Mimic

Gene-specific primers (GSPs) for competitive RT-PCR were designed based on previously-published cDNA sequences for HCN1, HCN2 and HCN4, with specificity confirmed with BLAST and FASTA (Table 1). Resulting PCR products

were sequenced to ensure subunit-specificity. The canine-specific sequences obtained from cardiac mRNA are registered in GenBank as AY686750 (HCN2) and AY686751 (HCN4). Chimeric primer pairs for RNA mimic synthesis were constructed with rabbit cardiac α-actin sequences flanked by the same GSPs. An 8-nucleotide sequence, GGCCGCGG, corresponding to the 3' end of the T7 promoter, was conjugated to the 5' end of each forward primer. First-strand cDNA (synthesized by reverse transcription with canine ventricular mRNA samples) was used as a template for subsequent PCR amplification steps with chimeric primer pairs. The resulting cDNA-mimic contained a 460-bp α-actin sequence flanked at the 5'-end by the sense GSP sequence and an 8-bp T7 promoter sequence at the 3'-end flanking the antisense GSP sequence. Products were gel-purified with the QIAquick Gel Extraction Kit (Qiagen). The RNA-mimic (internal standard) was created by *in vitro* transcription (mMESSAGE MACHINE, Ambion). The product was incubated with RNase-free DNase I (30 min, 37°C) to eliminate cDNA contamination, followed by phenol/chloroform-extraction and isopropanol-precipitation. Mimic size and concentration were determined by migration on a denaturing RNA gel alongside markers of known molecular weight and pre-determined RNA concentrations to create a standard curve.

Competitive RT-PCR

RNA-mimic samples were added with serial 10-fold dilutions to reaction mixtures containing 1-μg sample RNA. RNA was denatured at 65°C (15 min). RT was conducted in a 20-μL reaction mixture containing reaction buffer (10 mmol/L Tris-HCl, pH 8.3, 50 mmol/L KCl), 2.5 mmol/L $MgCl_2$, 1 mmol/L dNTPs (Roche),

3.2 μg random primers $p(dN)_6$ (Roche), 5 mmol/L DTT, 50 U RNase inhibitor (Promega), and 200 U M-MLV reverse transcriptase (Gibco-BRL). First strand cDNAs were synthesized at 42°C (1 hr) and remaining enzymes heat-deactivated (99°C, 5 min).

First-strand cDNA from the RT step was used as a template in 25-μL reaction mixtures including 10 mmol/L Tris-HCl (pH 8.3), 50 mmol/L KCl, 1.5 mmol/L $MgCl_2$, 1 mmol/L dNTPs, 0.5 μmol/L GSPs, 0.625 mmol/L DMSO and 2.5 U of Taq Polymerase (Gibco-BRL). Reactions were hot-started at 93°C for 3 minutes of denaturing, followed by 30 amplification cycles (93°C, 30 sec [denaturing]; 55°C, 30 sec [annealing]; 72°C, 30 sec [extension]). A final 72°C extension step was performed for 5 minutes. RT-negative controls were obtained for all RT-PCR reactions to exclude genomic contamination.

PCR-products were visualized under UV light with ethidium-bromide staining in 1.5% agarose gels. Images were captured with a Nighthawk camera, and band intensity determined with Quantity One software. A DNA Mass Marker (100 ng) was used to determine the size and quantity of DNA bands, and to create standard curves in each experiment for absolute quantification.

Western Blot Studies

Membrane protein was extracted from tissue samples with 5-mmol/L Tris-HCl (pH 7.4), 2-mmol/L EDTA, 5-μg/mL leupeptin, 10-μg/mL benzamidine, and 5-μg/mL soybean trypsin inhibitor, followed by tissue homogenization. All procedures were performed at 4°C. Membrane proteins were fractionated on 8% SDS-polyacrylamide gels and transferred electrophoretically to Immobilon-P

polyvinylidene fluoride membranes (Millipore) in 25-mmol/L Tris-base, 192-mmol/L glycine and 5% methanol at 0.09 mA for 18 hours. Membranes were blocked in 5% non-fat dry milk (Bio-Rad) in TTBS (Tris-HCl 50-mmol/L, NaCl 500-mmol/L; pH 7.5, 0.05% Tween-20) for 2 hours (room temperature) and then incubated with primary antibody (1:500 dilution) in 5% non-fat dry milk in TTBS for 4 hours at room temperature. All antibodies were purchased from Alomone Labs: HCN2 catalogue #APC-030 and HCN4 catalogue #APC-052. Membranes were washed 3 times in TTBS, reblocked in 5% non-fat dry milk in TTBS (15 min) and then incubated with horseradish peroxidase-conjugated goat anti-rabbit IgG secondary antibody (1:5000) in 5% non-fat dry milk in TTBS (40 min). They were subsequently washed 3 times in TTBS and once in TBS (same as TTBS but without Tween-20). Signals were obtained with Western Lightning Chemiluminescence Reagent Plus (PerkinElmer Life Sciences). Band densities were determined with a laser-scanning densitometer (PDI 420oe) and Quantity One software (PDI). Protein loading was controlled by probing all Western blots with anti-GAPDH antibody (Research Diagnostics Incorporated) and normalizing ion-channel protein-band intensity to that of GAPDH. Blots with antibody pre-incubated with antigenic peptide served as negative controls.

Data Analysis

All data are expressed as mean±SEM. Each biochemical determination was performed on an individual heart: n-values represent the number of hearts studied. Western-blot band intensities are expressed as OD units corresponding to densitometric band-intensity following background subtraction, divided by GAPDH-

signal intensity for the same sample. HCN-subunit mRNA levels are expressed as absolute concentrations (attomol/μg total RNA). Statistical comparisons were performed with ANOVA and Student's *t*-test with Bonferroni's correction. A 2-tailed $P<0.05$ was taken to indicate statistical significance.

RESULTS

Sinus-Node Recovery Time and *in vivo* Measurements

The QTc interval was prolonged in CHF dogs (Table 2), compatible with known effects on repolarizing currents and action potential duration.[17] The heart rate was faster in CHF dogs than controls prior to vagotomy and nadolol; however, after vagotomy and nadolol administration the heart rate was slower in CHF, compatible with reduced intrinsic sinus-node automaticity. Figures 1A and 1B show RA-electrogram recordings during the protocol used to calculate the $SNRT_c$. The left panels show baseline measurements before the start of RA-appendage pacing (PS). The right panel shows the recording just before end-pacing (PE), as well as the delay to the first spontaneous post-pacing beat. The mean data in Figure 1C demonstrate that the SNRTc more than doubled in CHF hearts compared to control hearts (n=7/group, $P<0.05$).

HCN-Subunit mRNA Measurements

While HCN2 and HCN4 mRNA were readily detected by RT-PCR in canine RA and sinus-node tissue, HCN1 was not detected in either region (Figure 2, arrow indicates expected size). In contrast, HCN1 was readily detected in dog brain (Figure 2, lanes 5 and 6). Figure 3A shows representative competitive RT-PCR gels for

HCN2 on control RA and sinus-node samples. For all gels, lane 0 contains the DNA Mass Ladder used to create the standard curve for the absolute quantification of PCR products. Lanes 1 through 5 contain 2 ng, 200 pg, 20 pg, 2 pg, and 0.2 pg of mimic RNA respectively. The competition between mimic and target PCR products can be seen as the intensity of the mimic decreases while that of the target increases from left to right. The point of mimic-target equality reflects the sample mRNA concentration and is quantified based on graphs of ln([target]/[mimic]) versus ln([mimic]) as previously described,[20] with linear regression used to determine the absolute concentration of target mRNA. The approximate point of identity is evident from the gels, and for control sinoatrial node was to the left of RA, indicating larger concentrations. Figure 3B shows representative RT-PCR gels on CHF samples. Compared to panel A, the point of target-mimic identity for RA is unchanged but that for sinus node has moved to the right, indicating down-regulation. Under control conditions, the HCN2 mRNA concentration in the sinoatrial node (7.6±1.8 attomol/μg total RNA) is over 6 times larger than that in the RA (1.2±0.5, n=7/group, $P<0.05$, Figure 3C). CHF does not alter the RA HCN2 mRNA concentration (1.1±0.3 attomol/μg total RNA), but decreases sinus-node HCN2 expression to <1/3 of control values (2.7±1.5, n=6/group, $P<0.05$).

HCN4-subunits were more abundant than HCN2 in all regions, averaging ~14 times greater concentration in control RA and ~4 times greater in control sinoatrial node. Figure 4A shows examples of HCN4 competitive RT-PCR in control samples. The concentrations of mimic used in all HCN4 gels were: (from left to right) 2 ng, 200 pg, 20 pg, 2 pg and 0.2 pg. Representative gels for CHF are shown in Figure 4B. The point of target-mimic identity for sinoatrial node is to the left of that for RA in

control, indicating greater HCN4 expression. In the presence of CHF, the identity point moves to the left for RA but to the right for sinus-node tissue, indicating RA HCN4 up-regulation and sinus-node down-regulation respectively. The mean data in Figure 4C show that mean sinus-node HCN4 concentrations (29.1±5.0 attomol/μg total RNA) were about twice those in RA (16.8±3.0, n=7/group, P<0.05). CHF increased RA HCN4 mRNA expression several-fold to 112.3±35.5 attomol/μg total RNA (n=5, P<0.05) while decreasing expression in the sinoatrial node to 5.1±1.0 attomol/μg total RNA (P<0.05).

HCN-Subunit Protein Expression

Figure 5A shows representative Western blots from a membrane probed with anti-HCN2 antibody. The bands detected at the expected molecular mass (~50 kDa, arrow) disappeared when the primary antibody was pre-incubated with the antigen against which it was raised (+ CA lanes). Corresponding GAPDH bands from the same samples are shown at the bottom. Overall, HCN2 protein was more strongly expressed in sinoatrial node (6.7±1.5 arbitrary OD units, Figure 5B) compared to RA (3.2±0.9, n=6/group, P<0.05). CHF had no effect on RA HCN2 protein expression (2.5±0.8), but significantly reduced sinus node expression by >40%, to 3.9±0.2.

Representative anti-HCN4 blots are shown in Figure 5C. The band detected at the expected molecular mass (~120 kDa, arrow) disappeared when antibody was pre-incubated with antigenic peptide. Overall, there was more than twice as much HCN4 protein in the sinoatrial node (0.29±0.06 arbitrary OD units, Figure 5D) compared to the RA (0.11±0.03, n=6/group, P<0.05). CHF increased RA HCN4 expression ~2

fold (0.23±0.05), but decreased sinus node HCN4 expression by ~75%, to 0.07±0.008 arbitrary OD units.

DISCUSSION

In this study, we evaluated the expression of HCN subunits in the normal and remodeled sinoatrial node and RA. Our results indicate that HCN4 is the primary subunit, that HCN2 likely contributes as well, and that HCN1 is not expressed. Greater HCN subunit expression in the sinoatrial node likely contributes to its specialized pacemaking function. CHF remodels HCN subunit expression non-congruently in sinoatrial node versus RA, with sinus-node HCN down-regulation likely contributing to sinus-node dysfunction and RA up-regulation possibly predisposing to ectopic impulse formation.

Comparison with Previous Studies of HCN Expression

Since the first cloning of the HCN family subunits which underlie I_f,[7,9-11,14] there have been relatively few studies examining their expression profiles. To our knowledge, this is the first study to compare the mRNA and protein expression of HCN subunits in the sinoatrial node and RA under normal and CHF conditions. In agreement with our findings, HCN1 was not detected in whole heart samples from humans.[12] However, HCN1 mRNA has been detected in the sinoatrial node of rabbits and mice.[8,13,16] The activation kinetics of human sinus node I_f[4] more closely resemble those of HCN2 or HCN4 than HCN1.[8,10] The possible participation of heteromeric HCN channels[21,22] complicates analysis of the relationship between native currents

and currents carried by individual subunits. Our findings are consistent with mRNA evidence of HCN4 predominance in mouse[13] and rabbit[16] sinoatrial node. HCN4 mRNA is more strongly expressed in rabbit sinoatrial node than atrium.[10] We are not aware of studies of HCN expression changes in animal models of CHF. Gene microarray analysis points to HCN4 mRNA upregulation in the failing human ventricle.[23]

Possible Functional and Clinical Significance

Intrinsic sinus-node automaticity is impaired in rabbits with CHF,[24] as well as in the dog in the present study. Decreased I_f underlies CHF-induced reductions in sinus-node automaticity.[18] Reduced sinus-node automaticity may have a protective effect in CHF, at least in part by preventing delayed afterdepolarization-related triggered activity.[17,24] On the other hand, bradyarrhythmias contribute to sudden death in CHF,[25] and may favor the induction of early afterdepolarization-related tachyarrhythmias caused by repolarization impairment due to outward-current downregulation.[26,27] In this study, we show the molecular basis of sinus-node I_f impairment to be reduced expression of HCN2 and HCN4 subunits. Biological pacemakers based on regional HCN-overexpression are a promising tool for inadequate cardiac rhythmicity,[28] and may prove useful for CHF patients with clinically-significant sinus-node dysfunction related to HCN-subunit downregulation.

AF is a common and problematic condition, and present therapy is suboptimal.[29] CHF is one of the most common clinical causes of AF.[30] The basic mechanisms underlying AF are under active investigation and there is hope of developing novel

mechanistically-based therapeutic approaches.[29] Although reentrant mechanisms have traditionally been considered to underlie AF, recent evidence points to ectopic impulse formation as playing a potentially-important role.[31] Stambler et al have described ectopic atrial tachyarrhythmias in dogs with CHF[32] and atrial HCN mRNA expression has been reported to correlate with left-atrial pressure, AF occurrence and atrial ectopic beat frequency in man.[33] Our study suggests atrial HCN4-upregulation as a potential molecular mechanism for enhanced atrial ectopic-beat formation in states associated with atrial dilation. It would be interesting to assess the potential value of HCN current inhibitors, such as zatebridine and ivabradine, in clinical and experimental AF.

CONCLUSIONS

Regional HCN-subunit expression parallels and may serve to maintain physiological sinus-node pacemaker dominance in the dog. CHF-induced remodeling of HCN-subunit expression may be an important contributor to the abnormal sinus-node function and atrial dysrhythmias F. Therapies that target HCN expression and/or HCN-based currents may be an interesting approach to treating CHF-related dysrhythmias.

ACKNOWLEDGMENTS

The authors thank Evelyn Landry for technical assistance and Diane Campeau for secretarial help. Funding was provided by the Canadian Institutes of Health Research, the Quebec Heart and Stroke Foundation, and the Mathematics of Information Technology and Complex Systems (MITACS) Network of Centers of Excellence. Stephen Zicha was supported by a "Fonds de la recherche en santé de Québec (FRSQ)" graduate-studentship.

REFERENCES

1. **Brown HF, DiFrancesco D, Noble SJ.** How does adrenaline accelerate the heart? *Nature.* 1979;280:235-236.

2. **Ho WK, Brown HF, Noble D.** High selectivity of the i(f) channel to Na+ and K+ in rabbit isolated sinoatrial node cells. *Pflugers Arch.* 1994;426:68-74.

3. **DiFrancesco D.** Characterization of single pacemaker channels in cardiac sino-atrial node cells. *Nature.* 1986;324:470-473.

4. **DiFrancesco D.** Pacemaker mechanisms in cardiac tissue. *Annu Rev Physiol.* 1993;55:455-472.

5. **Bois P, Renaudon B, Baruscotti M, et al.** Activation of f-channels by cAMP analogues in macropatches from rabbit sino-atrial node myocytes. *J Physiol.* 1997;501:565-571.

6. **DiFrancesco D, Tortora P.** Direct activation of cardiac pacemaker channels by intracellular cyclic AMP. *Nature.* 1991;351:145-147.

7. **Santoro B, Grant SG, Bartsch D, et al.** Interactive cloning with the SH3 domain of N-src identifies a new brain specific ion channel protein, with homology to eag and cyclic nucleotide-gated channels. *Proc Natl Acad Sci U S A.* 1997;94:14815-14820.

8. **Moroni A, Gorza L, Beltrame M, et al.** Hyperpolarization-activated cyclic nucleotide-gated channel 1 is a molecular determinant of the cardiac pacemaker current I(f). *J Biol Chem.* 2001;276:29233-29241.

9. **Vaccari T, Moroni A, Rocchi M, et al.** The human gene coding for HCN2, a pacemaker channel of the heart. *Biochim Biophys Acta.* 1999;1446:419-425.

10. **Ishii TM, Takano M, Xie LH, et al.** Molecular characterization of the hyperpolarization-activated cation channel in rabbit heart sinoatrial node. *J Biol Chem.* 1999;274:12835-12839.

11. **Ludwig A, Zong X, Jeglitsch M, et al.** A family of hyperpolarization-activated mammalian cation channels. *Nature.* 1998;393:587-591.

12. **Ludwig A, Zong X, Stieber J, et al.** Two pacemaker channels from human heart with profoundly different activation kinetics. *EMBO J.* 1999;18:2323-2329.

13. **Moosmang S, Stieber J, Zong X, et al.** Cellular expression and functional characterization of four hyperpolarization-activated pacemaker channels in cardiac and neuronal tissues. *Eur J Biochem.* 2001;268:1646-1652.

14. **Santoro B, Liu DT, Yao H, et al.** Identification of a gene encoding a hyperpolarization-activated pacemaker channel of brain. *Cell.* 1998;93:717-729.

15. **Seifert R, Scholten A, Gauss R, et al.** Molecular characterization of a slowly gating human hyperpolarization-activated channel predominantly expressed in thalamus, heart, and testis. *Proc Natl Acad Sci U S A.* 1999;96:9391-9396.

16. **Shi W, Wymore R, Yu H, et al.** Distribution and prevalence of hyperpolarization-activated cation channel (HCN) mRNA expression in cardiac tissues. *Circ Res.* 1999;85:e1-e6.

17. **Janse MJ.** Electrophysiological changes in heart failure and their relationship to arrhythmogenesis. *Cardiovasc Res.* 2004;61:208-217.

18. **Verkerk AO, Wilders R, Coronel R, et al.** Ionic remodeling of sinoatrial node cells by heart failure. *Circulation.* 2003;108:760-766.

19. **Cha TJ, Ehrlich JR, Zhang L, et al.** Dissociation between ionic remodeling and ability to sustain atrial fibrillation during recovery from experimental congestive heart failure. *Circulation.* 2004;109:412-418.

20. **Zicha S, Moss I, Allen B, et al.** Molecular basis of species-specific expression of repolarizing K+ currents in the heart. *Am J Physiol (Heart Circ Physiol.)* 2003;285:H1641-H1649.

21. **Altomare C, Terragni B, Brioschi C, et al.** Heteromeric HCN1-HCN4 channels: a comparison with native pacemaker channels from the rabbit sinoatrial node. *J Physiol.* 2003;549:347-359.

22. **Ulens C, Tytgat J.** Functional heteromerization of HCN1 and HCN2 pacemaker channels. *J Biol Chem.* 2001;276:6069-6072.

23. **Borlak J, Thum T.** Hallmarks of ion channel gene expression in end-stage heart failure. *FASEB J.* 2003;17:1592-1608.

24. **Opthof T, Coronel R, Rademaker HM, et al.** Changes in sinus node function in a rabbit model of heart failure with ventricular arrhythmias and sudden death. *Circulation.* 2000;101:2975-2980.

25. **Faggiano P, d'Aloia A, Gualeni A, et al.** Mechanisms and immediate outcome of in-hospital cardiac arrest in patients with advanced heart failure secondary to ischemic or idiopathic dilated cardiomyopathy. *Am J Cardiol.* 2001;87:655-665.

26. **Nuss HB, Kaab S, Kass DA, et al.** Cellular basis of ventricular arrhythmias and abnormal automaticity in heart failure. *Am J Physiol.* 1999;277:H80-H91.

27. **Li GR, Lau CP, Ducharme A, et al.** Transmural action potential and ionic current remodeling in ventricles of failing canine hearts. *Am J Physiol. (Heart Circ Physiol.)* 2002;283:H1031-H1041.

28. **Plotnikov AN, Sosunov EA, Qu J, et al.** Biological pacemaker implanted in canine left bundle branch provides ventricular escape rhythms that have physiologically acceptable rates. *Circulation.* 2004;109:506-512.

29. **Nattel S, Khairy P, Roy D, et al.** New approaches to atrial fibrillation management: a critical review of a rapidly evolving field. *Drugs.* 2002;62:2377-2397.

30. **Nattel S.** New ideas about atrial fibrillation 50 years on. *Nature.* 2002;10: 219-226.

31. **Ehrlich JR, Nattel S, Hohnloser SH.** Atrial fibrillation and congestive heart failure: specific considerations at the intersection of two common and important cardiac disease sets. *J Cardiovasc Electrophysiol.* 2002;13:399-405.

32. **Fenelon G, Shepard RK, Stambler BS.** Focal origin of atrial tachycardia in dogs with rapid ventricular pacing-induced heart failure. *J Cardiovasc Electrophysiol.* 2003;14:1093-1102.

33. **Lai LP, Su MJ, Lin JL, et al.** Measurement of funny current (I(f)) channel mRNA in human atrial tissue: correlation with left atrial filling pressure and atrial fibrillation. *J Cardiovasc Electrophysiol.* 1999;10:947-953.

TABLE 1. Primer Sequences Used for Competitive RT-PCR

Gene	Sequence (5'-3')	Position	Product Size (bp)	Annealing Temp (°C)
HCN1	**F:**TGGTGGCTACAATGCCTTTA **R:**TTCCTCCGGGACCTCGTT	1406-1725	320	52.3
HCN2	**F:**CGTTACCAGGGCAAGATGTTT **R:**GTTGTCCACGCTCAGCGAAT	1519-1911	393	58.7
HCN4	**F:**GTACTCCTACGCGCTCTTCA **R:**GCTCTCCTCGTCGAACATCT	1392-1704	313	56

TABLE 2. In vivo Measurements

	Body Weight (kg)	QT interval (msec)	QTc (msec)	Baseline Sinus Cycle Length (msec)	Sinus Cycle Length After Vagotomy/Nadolol (msec)
Control n=7	24.6±1.1	246±11	287±7	775±54	415±19
CHF n=7	26.0±1.7	247±15	317±8*	575±75*	516±19*

*$P<0.05$ vs control.
QTc=Corrected QT interval.

FIGURES

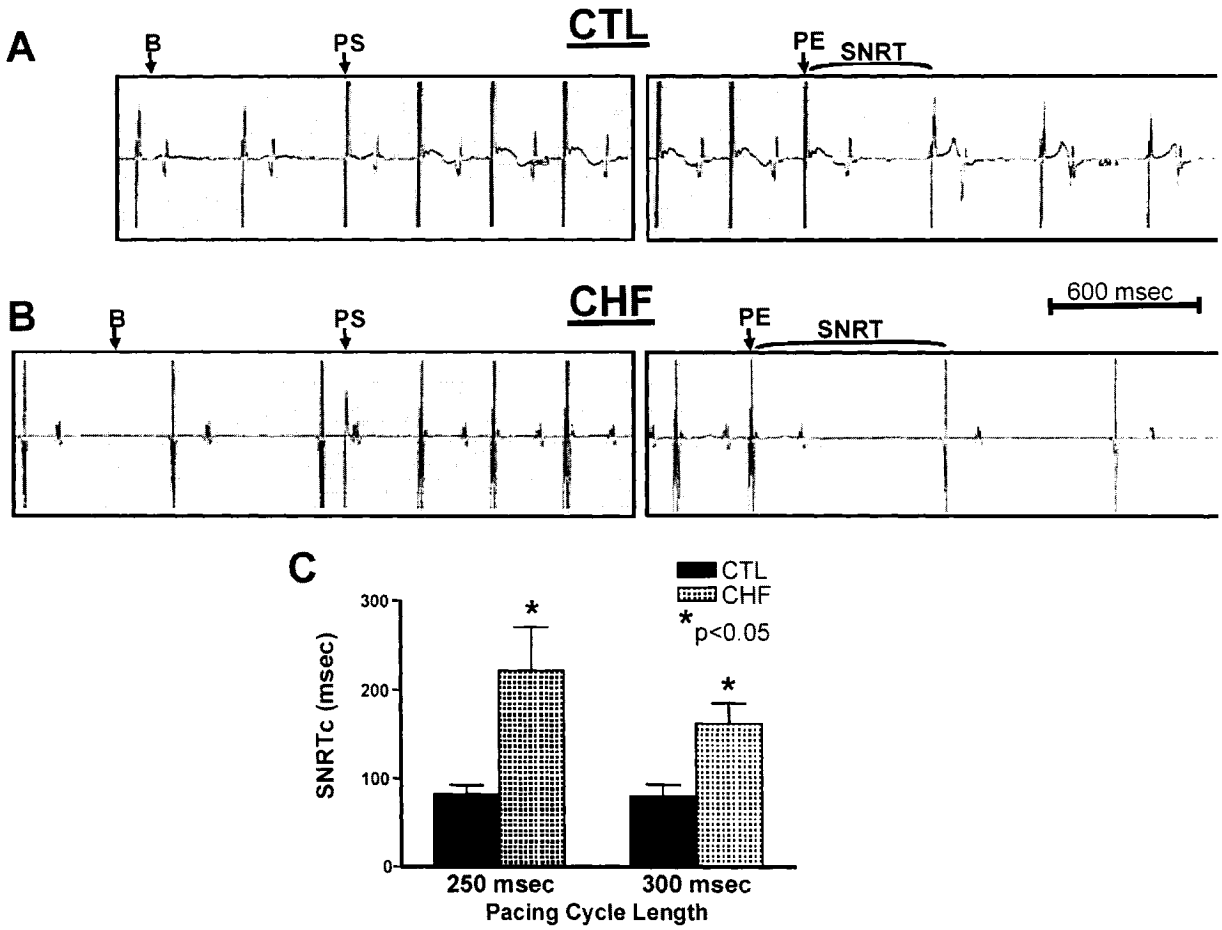

Figure 1 **SNRT measurements in the canine model of CHF. A.** Atrial-electrogram recordings from a non-paced control (CTL) dog. Baseline sinus-node cycle length measurements were taken at "B" before pacing at a cycle-length of 300 msec was initiated at "PS". The right panel shows the last paced cycles before pacing was stopped (PE). The SNRT was defined by the time required for the first post-pacing sinus-node interval. The corrected SNRT ($SNRT_c$) was calculated as the SNRT minus the spontaneous pre-pacing sinus-node cycle length. **B.** Representative atrial-electrogram recordings from a CHF dog. Same format as in **A**. **C.** Mean±SEM $SNRT_c$ at 250 and 300-msec pacing cycle lengths.

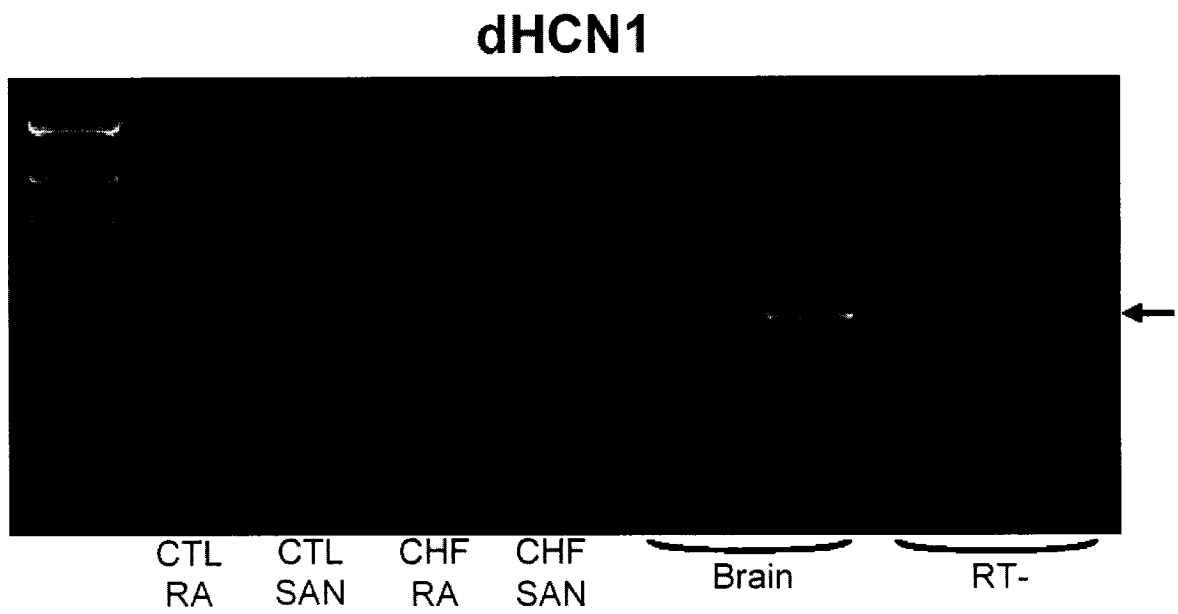

Figure 2 **Standard RT-PCR to identify HCN1 in dog samples.** No HCN1 was detected in control RA, CHF RA, control sinus node or CHF sinus node tissue (first 4 lanes). The primers were tested on canine brain samples as positive controls, and generated products of the expected size. The last 2 lanes are reverse transcriptase-negative controls to ensure that the absence of genomic-DNA contamination.

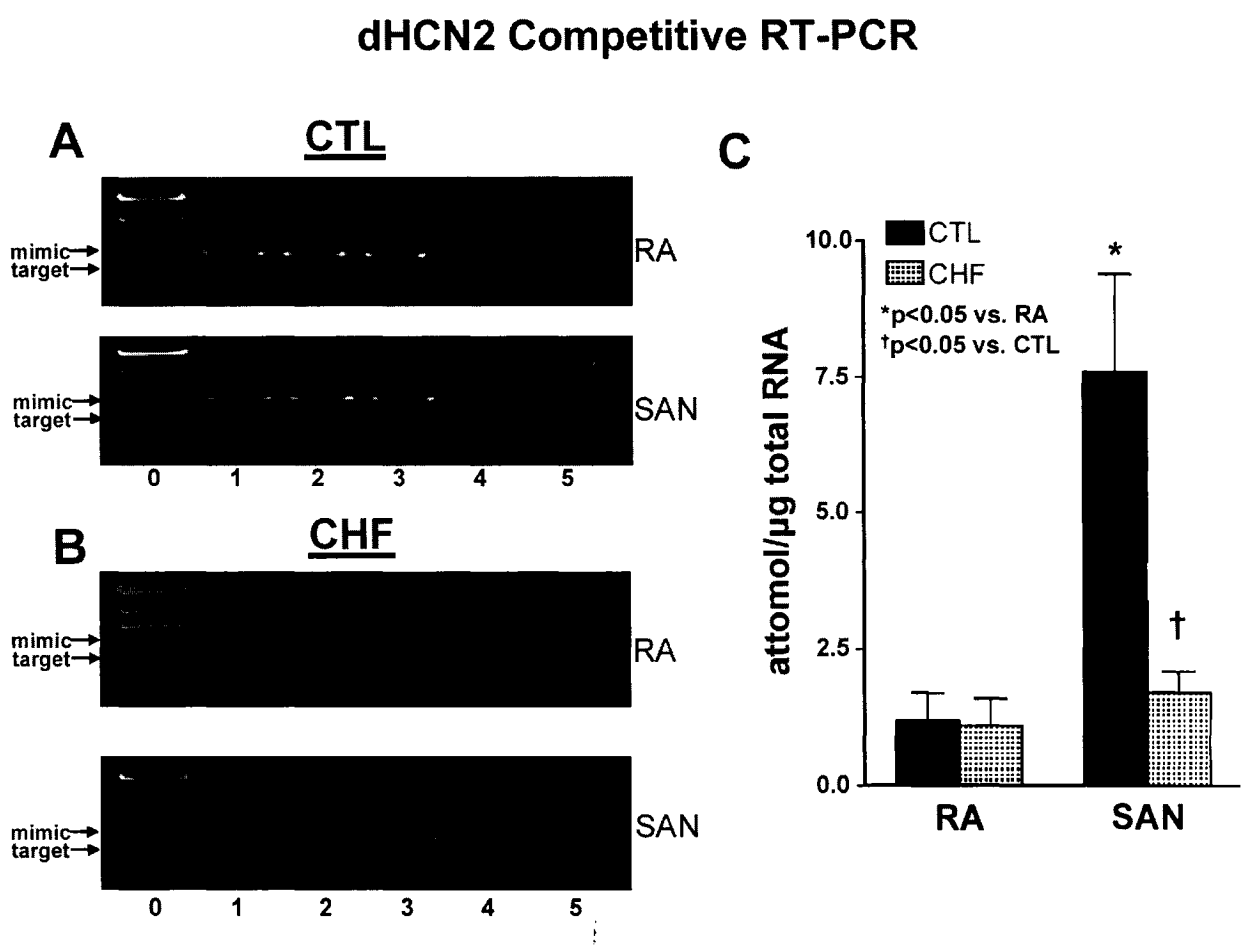

Figure 3 **HCN2 Competitive RT-PCR A.** Results from competitive RT-PCR on control (CTL) RA (upper panel) and sinus-node (lower panel) samples. **B.** Examples of results from competitive RT-PCR experiments using CHF RA (upper panel) and sinus-node (lower panel) tissue samples. **C.** Mean±SEM HCN2 subunit expression. Control sinoatrial node expressed significantly more HCN2 compared to RA. CHF did not affect HCN2 expression in RA, but significantly decreased it in the sinoatrial node.

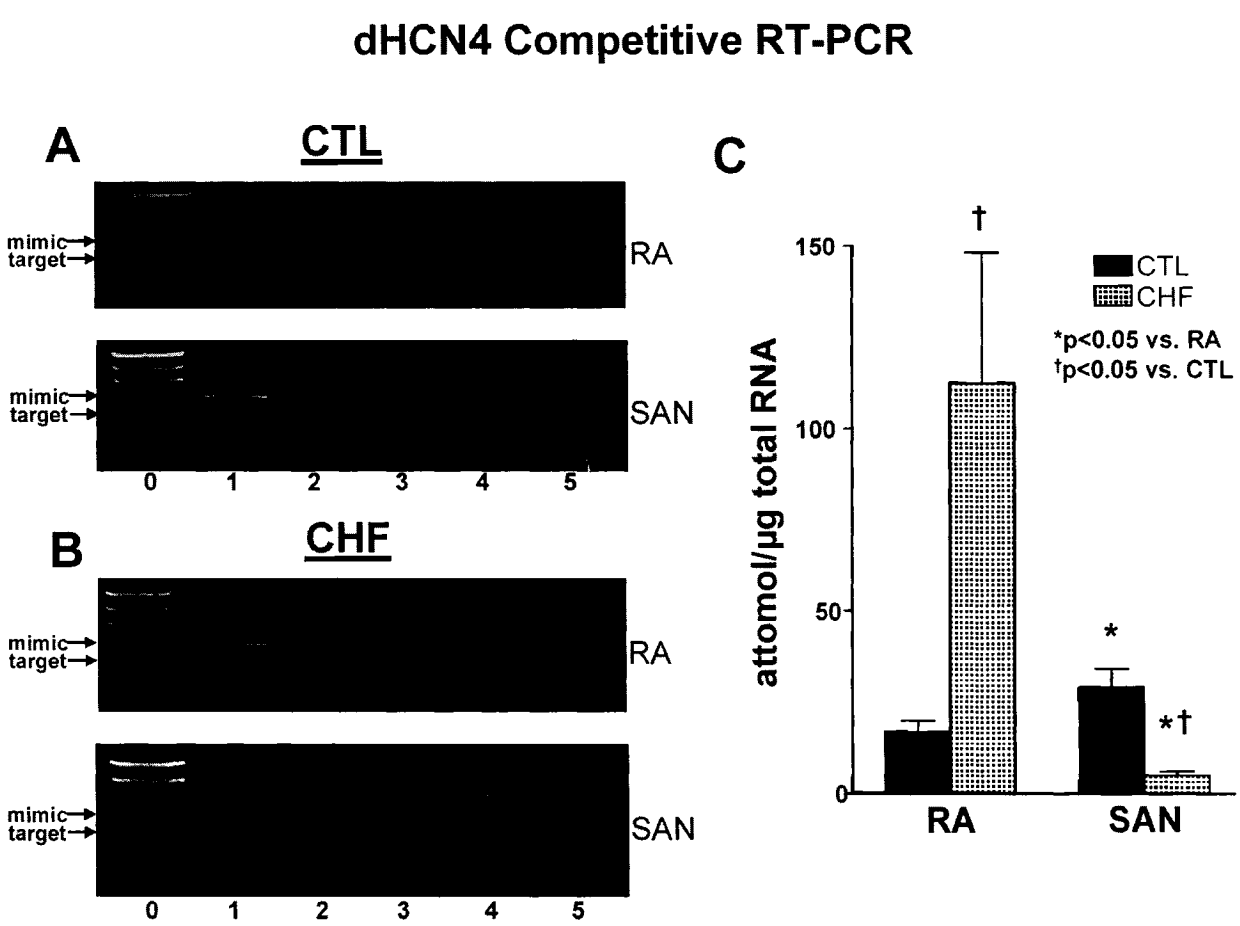

Figure 4 **HCN4 competitive RT-PCR A.** Representive gels from competitive RT-PCR experiments for HCN4 expression in control (CTL) RA (upper panel) and sinus-node (lower panel) tissues. **B.** Examples from HCN4 competitive RT-PCR reactions using CHF RA (upper panel) and sinus-node (lower panel) samples. **C.** Mean±SEM HCN4 expression. HCN4 expression was lower in control RA compared to control sinoatrial node. CHF significantly increased RA HCN4 expression and decreased sinus-node expression.

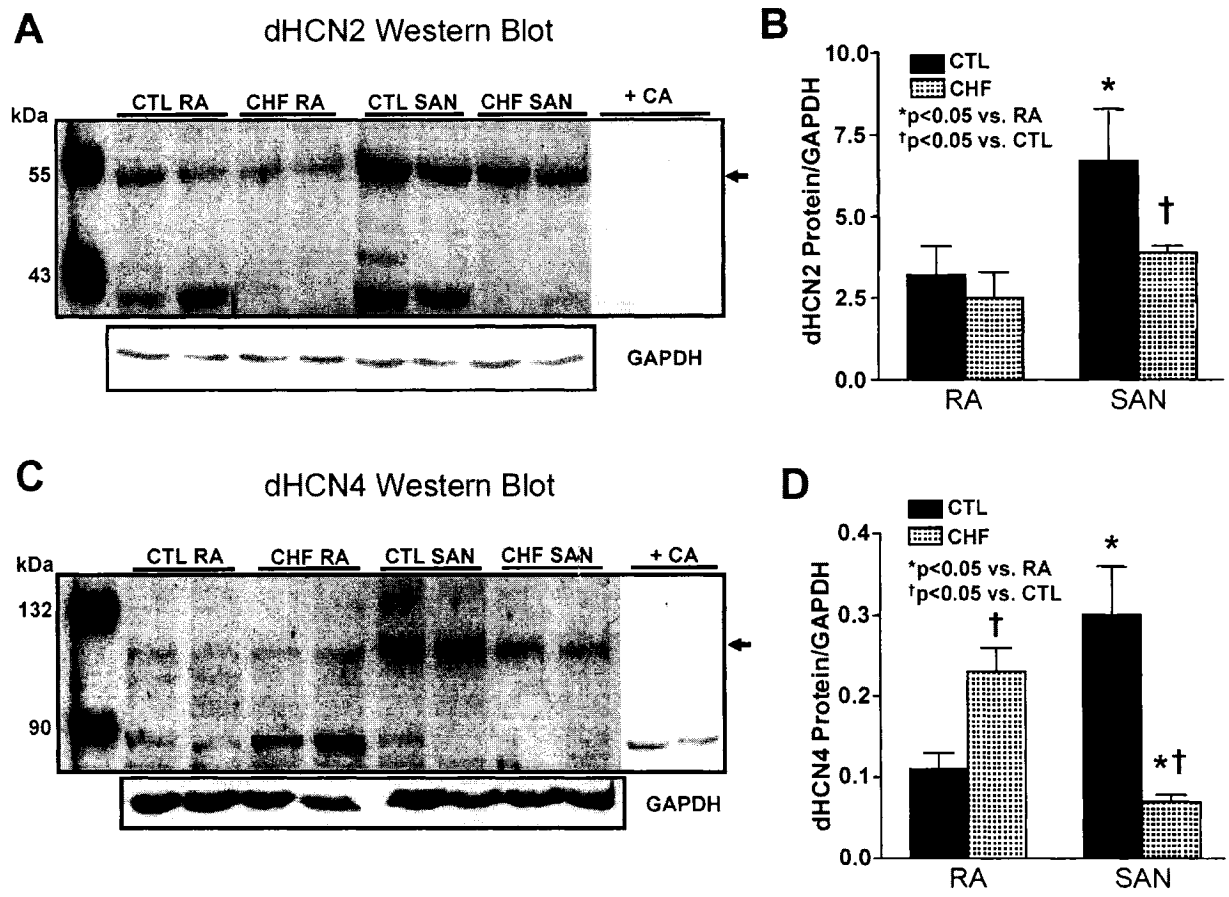

Figure 5 **Western-blot analysis of HCN2 and HCN4 protein expression.** **A.** Representative Blot probed with anti-HCN2 antibody. Last 2 lanes show samples probed with primary antibody that had been pre-incubated with antigenic peptide. A clear band was detected in all samples at the expected molecular mass of ~50 kDa (arrow) and was eliminated with antigen pre-exposure. Bottom bands are GAPDH signals obtained on the same samples. **B.** Mean±SEM HCN2 protein-expression data. **C.** Representative Western blots obtained with anti-HCN4 antibody. Last 2 lanes show samples probed with antibody pre-incubated with antigenic peptide. A band at the expected molecular mass of ~120 kDa was observed (arrow), and eliminated by antigen pre-incubation. A second, lower molecular-weight band was not suppressed by antigen pre-incubation, indicating that it was non-specific. Bottom bands are GAPDH signals on the same samples. **D.** Mean±SEM HCN4 protein expression data. HCN4 expression was significantly greater in control sinoatrial node compared to control RA. CHF caused an up-regulation of HCN4 in RA, but down-regulation in the sinoatrial node.

CHAPTER 6: INHERITED CHANGES TO POTASSIUM CHANNEL FUNCTION AND ITS EFFECT ON THE HEART

Up until now, species-, region- and disease- specific differences which are associated with the heterogeneous expression of voltage-gated ion channel subunits have been studied. In this last study, we sought to determine how heterogeneity within a single channel subunit can affect the expression of the resulting current. There have been many documented cases of how mutations in ion channel subunits can alter their function; the most notable are the Long QT mutations in minK, KvLQT1, HERG, MiRP1 and $Na_v1.5$ channel subunits (Splawski *et al.*, 2000). The one common feature among these mutations is that they all alter the currents they underlie and cause a prolongation of the QT interval on an ECG which increases the propensity to arrhythmia. Similar effects are seen by blocking these currents with pharmacological interventions, especially in the case of I_{Kr}.

As it was mentioned in the introduction, AF is the most common clinically diagnosed arrhythmia in our society today. While most cases have been associated with ion channel remodelling, a genetic predisposition has been noted. A recent clinical study identified a single nucleotide polymorphism in the KCNE1 gene which encodes minK, the β-subunit of I_{Ks} currents (Lai *et al.*, 2002). Therefore, we sought to characterize this polymorphism in order to elucidate how heterogeneities within a channel subunit could affect the expression of the resulting current and possibly lead to an increased risk for AF.

ABSTRACT

Atrial fibrillation (AF) is a very common acquired arrhythmia with multi-factorial pathogenesis. Recently, a single nucleotide polymorphism (SNP, A/G) at position 112 in the KCNE1 gene, resulting in a glycine/serine amino-acid substitution at position 38 of the minK-peptide, was associated with AF occurrence (AF more frequent with minK38G); however, the functional effect of this SNP is unknown. We used patch-clamp recording and confocal microscopy to study the effect of this SNP on delayed-rectifier channel expression. The density of slow delayed-rectifier current (I_{Ks}) resulting from co-expression with KvLQT1 was reduced with minK38G in 2 mammalian expression systems (e.g. at +10 mV: 44±6.3 pA/pF in Chinese hamster ovary (CHO) cells, 44.8±13.7 pA/pF for COS cells) compared to minK38S (114±27.0 pA/pF, 104.2±23.2 pA/pF respectively, $P<0.05$ for each). I_{Ks} kinetics and voltage-dependence were unaffected. KvLQT1 membrane-immunofluorescence was less in CHO cells co-expressing minK38G versus minK38S (KvLQT1/minK membrane-fluorescence ratio 1.2±0.2 with minK38G versus 2.6±0.3 for minK38S, $P<0.05$). Currents resulting from co-expression of human ether-a-go-go related gene (HERG) were not different for minK38G versus minK38S, e.g. tail-current densities upon repolarization to -50 mV: 23.1±4.1 pA/pF (minK38G) versus 22.0±5.3 pA/pF (minK38S, P=ns). We conclude that the AF-linked SNP minK38G is associated with reduced I_{Ks}, likely due to decreased KvLQT1 membrane expression, in contrast to the previously-reported familial KvLQT1 mutation that increases I_{Ks}. This study reveals a novel amino-acid determinant of the minK-KvLQT1 interaction and points to mechanistic heterogeneity in the genetic determinants of AF.

INTRODUCTION

Atrial fibrillation (AF) is a common arrhythmia with a heritable component.[1,2] Autosomal-dominant familial AF has been described but the precise gene defect remains unknown.[3] A variety of genetic abnormalities predispose to AF along with other arrhythmic and/or cardiomyopathic syndromes. These include lamin A/C mutations,[4,5] angiotensin gene polymorphisms,[6] the Brugada syndrome,[7] the short QT syndrome,[8] Long QT Syndrome (LQTS) type 4 with ankyrin mutation,[9,10] and possibly other forms of congenital LQTS.[11] The only known form of monogenic AF occurring in the absence of other recognized cardiac abnormalities is caused by a gain-of-function mutation in *KVLQT1*.[12]

Recently, a single-nucleotide-polymorphism (SNP) in the KCNE1 gene (A→G at position 112), leading to glycine substitution for serine at amino-acid position 38, has been reported to increase AF susceptibility.[13,14] The odds ratio (OR) for AF with one minK38G allele was 2.16 and increased to 3.58 with 2 minK38G alleles (95% confidence-interval 1.38-9.27).[14] The functional consequences of this polymorphism are unclear. The present study examined the hypothesis that a glycine at position 38 of minK alters slow (I_{Ks}) and/or rapid (I_{Kr}) delayed-rectifier current resulting from co-expression with the corresponding α-subunits KvLQT1 and HERG respectively.

MATERIALS AND METHODS

Creation of minK SNP

Our original minK clone (GenBank accession number NM000219) contained glycine at position 38, so minK38S was created by site-directed mutagenesis using overlap-extension PCR, with the primers shown in Online Table 1. The construct

was flanked by HindIII (5') and BamHI (3') restriction sites and subsequently re-ligated into pcDNA3.1. PCR products were verified by cDNA sequencing.

Cell culture

Chinese hamster ovary (CHO) and *Cercopithecus aethiops* kidney (COS 7) cells (ATCC) were cultured at 37°C with 5% CO_2 in F12 or DMEM medium (GIBCO-BRL) supplemented with 10% heat-inactivated fetal bovine serum along with 100-U/mL penicillin and 100-μg/mL streptomycin. Transient transfection was performed with Lipofectamine-plus (Invitrogen) and 0.5-μg minK cDNA subcloned into pcDNA3.1. Co-transfection was performed with KvLQT1 (1 μg cDNA) or HERG (0.5 μg cDNA) in pcDNA3.1. Cells were studied with whole-cell patch-clamp or immunofluorescence confocal-microscopy 36 to 48 hours after transfection. Co-transfected GFP (0.1 μg cDNA) served as a transfection marker.

Confocal Microscopy

For immunofluorescent studies, transiently-transfected CHO cells were plated on sterile glass coverslips for 24 hours. Cells were fixed (20 minutes) with 2% paraformaldehyde (Sigma) and washed 3 times (5 minutes) with PBS. After blocking with 5% normal donkey-serum (Jackson) and 5% bovine serum albumin (BSA, Sigma) cells were permeabilized with 0.2% Triton X-100 (Sigma) for 1 hour. They were then incubated overnight (4°C) with primary antibodies (Santa Cruz goat anti-minK or Chemicon rabbit anti-KvLQT1) at 1:200 dilution, followed by three 5-minute washes with PBS and a 1-hour incubation with secondary antibodies (anti-goat IgG labelled with fluorescent isothiocyanate [FITC] for minK and anti-rabbit IgG with tetra-methyl-rhodamine-isothiocyanate [TRITC] for KvLQT1). Confocal

microscopy was performed with a Zeiss LSM-510 system. TRITC (red) and FITC (green) were excited at 543 and 488 nm with HeNe and Ar Lasers respectively, emitting fluorescence at 566 and 525 nm.

Confocal microscopy experiments were performed on the same day for both groups, with identical parameters used for all manipulations. Control experiments omitting primary antibodies and with non-transfected CHO cells revealed absent or very low-level background staining.

Electrophysiology

Currents were recorded in the whole-cell patch-clamp configuration at 36±0.5°C with an Axopatch 200B amplifier and pClamp software (V6.0, Axon). Borosilicate glass electrodes had 2-3 MΩ tip resistances when filled. Mean compensated cell-capacitances were 15.0±1.1 pF for transfected CHO and 19.6±1.9 for COS-7 cells, with no significant differences between cells transfected with minK38G or 38S. Junction potentials, averaging 7.5±0.5 mV, were not corrected.

The extracellular solution contained (mmol/L) NaCl 136, KCl 5.4, $MgCl_2$ 1, $CaCl_2$ 1, NaH_2PO_4 0.33, HEPES 5 and dextrose 10 (pH 7.35 with NaOH). Internal solution contained (mmol/L) K-aspartate 110, KCl 20, $MgCl_2$ 1, MgATP 5, GTP (lithium salt) 0.1, HEPES 10, Na-phosphocreatine 5 and EGTA 5.0 (pH 7.3 with KOH).

Currents were recorded with 2-second depolarizing pulses from a holding potential (HP) of –80 mV and an inter-pulse interval of 12 seconds, with tail currents observed during 2-second repolarizations to –50 mV for I_{Ks} (4 seconds for I_{HERG}).

Clampfit (Axon Instruments) and GraphPad Prism V3.0 were used for data analysis. Data are presented as mean±SEM. A two-tailed $P<0.05$ (Student's *t*-test) was considered statistically-significant.

RESULTS

KvLQT1 Co-expression

Figures 1A and B show representative currents from CHO cells expressing KvLQT1 with minK38G and minK38S, respectively. I_{Ks} densities were smaller for minK38G-expressing cells (Figure 1C); e.g. at +10 mV, 44±6.3 (minK38G) vs 114±27.0 pA/pF (minK38S; n=11, 14 cells, $P<0.05$). Tail currents were also smaller with minK38G (following pulse to +10 mV, 12.3±1.5 versus 21.8±3.2 pA/pF, $P<0.05$). Half-activation voltages (V_{50}) obtained from Boltzmann fits to normalized tail-currents did not differ: 11.6±3.5 (minK38G) vs 14.5±1.4 mV (minK38S; *P*=ns, Figure 1D). Activation time-constants were similar (Figure 1E); e.g. at +10 mV: 1241±159 ms (minK38G), 1251±195 ms (minK38S, *P*=ns). Mono-exponential deactivation time-constants upon repolarization to -50 mV were slightly but not significantly slower for minK38G (293±52 versus 181±20 ms, Figure 1F).

Similar results were obtained with COS-7 cells (representative recordings in Figures 1G and H). I_{Ks} density upon depolarization to +10 mV averaged 44.8±13.7 (minK38G) vs 104.2±23.2 (minK38S) pA/pF (n=10, 7 cells, respectively, $P<0.05$). Activation kinetics at +10 mV were mono-exponential with time-constants averaging 740±114 (minK38G) vs 688±115 (minK38S) ms (*P*=ns) and tail-current time-constants were also similar: 298±48 (minK38G) vs 293±39 ms (minK38S).

We then evaluated the effect of minK SNP co-expression on KvLQT1 membrane localization. Figure 2 shows confocal microscopic images of double-labelled CHO cells co-transfected with either minK38G (panel A) or 38S (panel B) and KvLQT1 (both panels). Similar results were obtained in seven experiments with each SNP. Cells co-transfected with minK38G showed less intense 566-nm red-fluorescence (corresponding to TRITC-labelled KvLQT1) at the cell membrane. The 525-nm green-fluorescence signal (FITC-labelled minK) was similar between groups. Upon laser line-scanning quantification with identical settings, KvLQT1 membrane-fluorescence was significantly greater in the presence of minK38S compared with minK38G, whereas minK fluorescence intensity did not differ (Figure 2C). The membrane KvLQT1/minK fluorescence ratio was approximately twice as great for minK38S compared to minK38G (Figure 2D), in rough agreement with relative I_{Ks} densities.

HERG Co-expression

Representative currents in COS7 cells co-transfected with HERG+minK38G or minK38S are shown in Figures 3A and B. MinK38G coexpression did not obviously alter I_{HERG} compared to minK38S. Mean±SEM tail-current density was similar for the 2 groups (Figure 3C); e.g. repolarization from a TP of +10 mV evoked I_{HERG} of 23.1±4.0 (minK38G) vs 22.0±5.3 pA/pF (minK38S; n=12, 15 cells respectively). Activation V_{50} was also similar (-9.8±2.7, minK38G versus -10.1±1.9 mV, minK38S). Deactivation kinetics were biexponential and time-constants were similar between groups (e.g. repolarizing from +10 mV: 1596±222 (minK38G), 1345±101 (minK38S) ms, τ_{slow}; 260±37 (minK38G), 278±35 ms, τ_{fast}, Figure 3D).

There was no difference in the relative contribution of the fast component to repolarization: 38±3%, minK38G; 39±3%, minK38S.

DISCUSSION

The minK38G/S polymorphism is a common variant believed to be associated with AF occurrence.[13,14] MinK is known to be crucial for the formation of a normal I_{Ks} phenotype in association with KvLQT1,[15,16] and may also interact with HERG in the formation of I_{Kr}.[17,18] In the present study, we examined the effects of the minK38G/S polymorphism on currents resulting from KvLQT1 and HERG co-expression, finding significant effects on I_{Ks} density and KvLQT1-protein membrane localization but no effects on I_{HERG}.

The first gene-abnormality identified to cause familial AF in the absence of other arrhythmic or structural abnormalities was a missense mutation of *KvLQT1* leading to I_{Ks} gain-of-function.[12] Increased repolarizing K^+-current would tend to shorten action-potential duration (APD), decrease the wavelength and favor the occurrence of multiple-circuit reentrant AF.[19] We found the AF-associated minK38G isoform to have an opposite effect on I_{Ks}, reducing current density. Although this seems counterintuitive, there is evidence that APD-prolongation can promote atrial tachyarrhythmias in both experimental[20,21] and clinical[11] models. AF is known to be associated with both long-QT[9,10] and short-QT[8] syndromes, pointing to potential variability in underlying mechanisms and the possibility that destabilization of repolarization in either direction may be arrhythmogenic.

The mechanisms of minK-KvLQT1 interaction are not completely elucidated. While changes in I_{Ks} gating are clearly of great importance,[22] there is also evidence that alterations in membrane-trafficking may occur.[23] The differences in KvLQT1 immunolocalization associated with co-expression of the minK38S/G isoforms that we studied points to such a mechanism, which warrants further investigation in future work. Finally, the variations in I_{Ks} resulting from minK38S/G polymorphism that we noted may result in differences to susceptibility to acquired LQTS, a possibility that merits evaluation in future pharmacogenomic studies.

ACKNOWLEDGEMENTS

We thank Louis Villeneuve for excellent technical assistance and Monique Brouillard for secretarial help. The study was supported by the Canadian Institutes of Health Research. JRE was a Heart and Stroke Foundation of Canada (HSFC) Fellow. SZ was supported by a Fonds de Recherche en Santé de Québec studentship. TEH is an HSFC McDonald Scholar.

REFERENCES

1. **Darbar D, Herron KJ, Ballew JD, Jahangir A, Gersh BJ, Shen WK, Hammill SC, Packer DL, Olson TM.** Familial atrial fibrillation is a genetically heterogeneous disorder. *J Am Coll Cardiol.* 2003;41:2185-2192.

2. **Ellinor PT, Macrae CA.** The genetics of atrial fibrillation. *J Cardiovasc Electrophysiol.* 2003;9:1007-1009.

3. **Brugada R, Tapscott T, Czernuszewicz GZ, Marian AJ, Iglesias A, Mont L, Brugada J, Girona J, Domingo A, Bachanski LL, Roberts R.** Identification of a genetic locus for familial atrial fibrillation. *N Engl J Med.* 1997;336:905-911.

4. **Garg A, Speckman RA, Bowcock AM.** Multisystem dystrophy syndrome due to novel missense mutations in the amino-terminal head and alpha-helical rod domains of the lamin A/C gene. *Am J Med.* 2002;7:549-555.

5. **Sebillon P, Bouchier C, Bidot LD, Bonne G, Ahamed K, Charron P, Drouin-Garraud V, Millaire A, Desrumeaux G, Benaiche A, Charniot JC, Schwartz K, Villard E, Komajda M.** Expanding the phenotype of LMNA mutations in dilated cardiomyopathy and functional consequences of these mutations. *J Med Genet.* 2003;8:560-567.

6. **Tsai CT, Lai LP, Lin JL, Chiang FT, Hwang JJ, Ritchie MD, Moore JH, Hsu KL, Tseng CD, Liau CS, Tseng YZ.** Renin-angiotensin system gene polymorphisms and atrial fibrillation. *Circulation.* 2004;109:1640-1646.

7. **Morita H, Kusano-Fukushima K, Nagase S, Fujimoto Y, Hisamatsu K, Fujio H, Haraoka K, Kobayashi M, Morita ST, Nakamura K, Emori T, Matsubara H, Hina K, Kita T, Fukatani M, Ohe T.** Atrial fibrillation and atrial vulnerability in patients with Brugada syndrome. *J Am Coll Cardiol.* 2002;40:1437-1444.

8. **Gaita F, Giustetto C, Bianchi F, Wolpert C, Schimpf R, Riccardi R, Grossi S, Richiardi E, Borggrefe M.** Short QT Syndrome: a familial cause of sudden death. *Circulation.* 2003;108:965-970.

9. **Schott JJ, Charpentier F, Peltier S, Foley P, Drouin E, Bouhour JB, Donnelly P, Vergnaud G, Bachner L, Moisan JP, et al.** Mapping of a gene for long QT syndrome to chromosome 4q25-27. *Am J Hum Genet.* 1995;57:1114-1122.

10. **Mohler PJ, Schott JJ, Gramolini AO, Dilly KW, Guatimosim S, duBell WH, Song LS, Haurogne K, Kyndt F, Ali ME, Rogers TB, Lederer WJ, Escande D, Le Marec H, Bennett V.** Ankyrin-B mutation causes type 4 long-QT cardiac arrhythmia and sudden cardiac death. *Nature.* 2003;421:634-639.

11. **Kirchhof P, Eckardt L, Franz MR, Monnig G, Loh P, Wedekind H, Schulze-Bahr E, Breithardt G, Haverkamp W.** Prolonged atrial action potential durations and polymorphic atrial tachyarrhythmias in patients with long QT syndrome. *J Cardiovasc Electrophysiol.* 2003;14:1027-1033.

12. **Chen YH, Xu SJ, Bendahhou S, Wang XL, Wang Y, Xu WY, Jin HW, Sun H, Su XY, Zhuang QN, Yang YQ, Li YB, Liu Y, Xu HJ, Li XF, Ma N, Mou CP, Chen Z, Barhanin J, Huang W.** KCNQ1 gain-of-function mutation in familial atrial fibrillation. *Science.* 2003;299:251-254.

13. **Lai LP, Deng CL, Moss AJ, Kass RS, Liang CS.** Polymorphism of the gene encoding a human minimal potassium ion channel (minK). *Gene.* 1994;151:339-340.

14. **Lai LP, Su MJ, Yeh HM, Lin JL, Chiang FT, Hwang JJ, Hsu KL, Tseng CD, Lien WP, Tseng YZ, Huang SK.** Association of the human minK gene 38G allele with atrial fibrillation: evidence of possible genetic control on the pathogenesis of atrial fibrillation. *Am Heart J.* 2002;144:485-490.

15. **Sanguinetti MC, Curran ME, Zou A, Shen J, Spector PS, Atkinson DL, Keating MT.** Coassembly of K(V)LQT1 and minK (IsK) proteins to form cardiac I(Ks) potassium channel. *Nature.* 1996;384:80-83.

16. **Barhanin J, Lesage F, Guillemare E, Fink M, Lazdunski M, Romey G.** K(V)LQT1 and lsK (minK) proteins associate to form the I(Ks) cardiac potassium current. *Nature.* 1996;384:78-80.

17. **Yang T, Kupershmidt S, Roden DM.** Anti-minK antisense decreases the amplitude of the rapidly activating cardiac delayed rectifier K+ current. *Circ Res.* 1995;77:1246-1253.

18. **Ohyama H, Kajita H, Omori K, Takumi T, Hiramoto N, Iwasaka T, Matsuda H.** Inhibition of cardiac delayed rectifier K+ currents by an antisense oligodeoxynucleotide against IsK (minK) and over-expression of IsK mutant D77N in neonatal mouse hearts. *Pflugers Arch.* 2001;442:329-335.

19. **Nattel S.** New ideas about atrial fibrillation 50 years on. *Nature.* 2002;415:219-226.

20. **Satoh T, Zipes DP.** Cesium-induced atrial tachycardia degenerating into atrial fibrillation in dogs: atrial torsades de pointes? *J Cardiovasc Electrophysiol.* 1998;9:970-975.

21. **Burashnikov A, Antzelevitch C.** Reinduction of atrial fibrillation immediately after termination of the arrhythmia is mediated by late phase 3 early afterdepolarization-induced triggered activity. *Circulation* 2003;107:2355-2360.

22. **Tapper AR, George AL Jr.** MinK subdomains that mediate modulation of and association with KvLQT1. *J Gen Physiol.* 2000;116:379-390.

23. **Krumerman A, Gao X, Bian JS, Melman YF, Kagan A, McDonald TV.** An LQT mutant minK alters KvLQT1 trafficking. *Am J Physiol Cell Physiol.* 2004;286:C1453-C1463

FIGURES

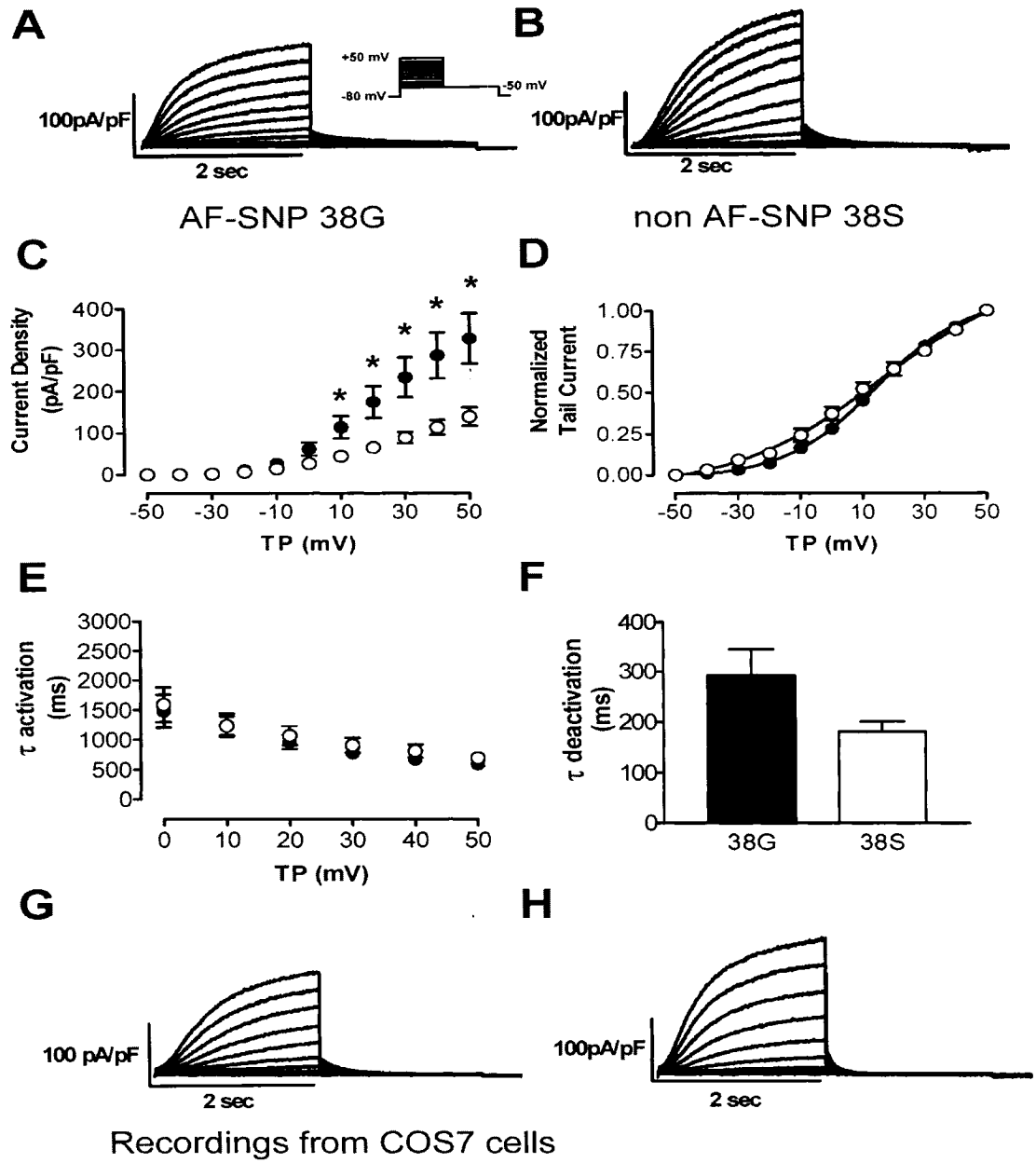

Figure 1 **A, B**: Recordings from transiently-transfected CHO cells expressing KvLQT1 and minK38G (**A**) or minK38S (**B**). **C**: mean±SEM I_{Ks}-voltage relationships from 11 and 14 CHO cells per group, respectively. **D**: mean±SEM tail-current/voltage relation fitted by Boltzmann equation. **E**: mean±SEM activation time-constants. **F**: deactivation time-constants upon repolarization to -50 mV after a 2-second step to +10 mV. **G, H**: representative currents recorded from COS-7 cells co-transfected with KvLQT1 and minK38G (**G**) or minK 38S (**H**). TP=test-potential; **P*<0.05.

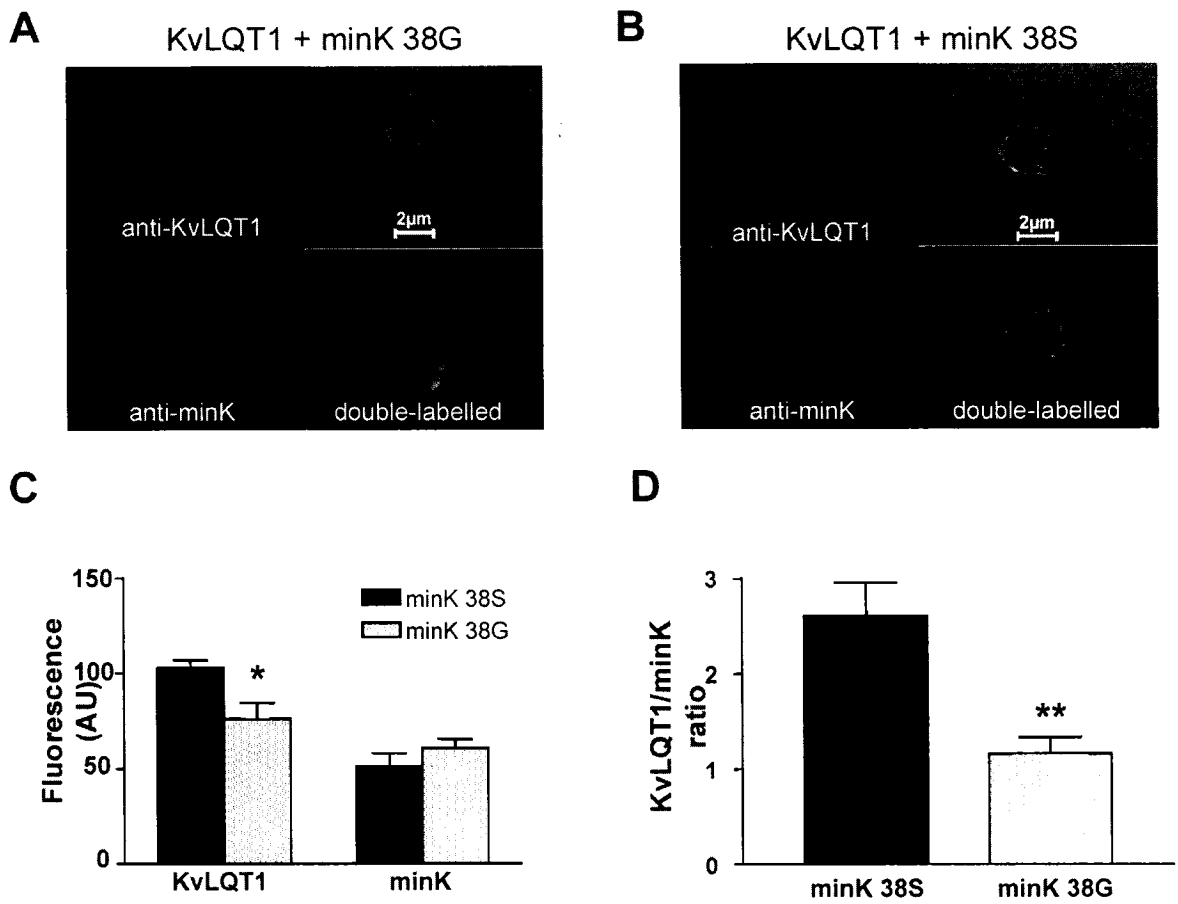

Figure 2 Immunofluorescent images of transiently-transfected CHO cells double-labelled with anti-minK and anti-KvLQT1 antibodies. **A, B**: composite images of CHO cells with identical imaging-settings. Top left: fluorescence at 566-nm (KvLQT1-secondary label); top right: phase-contrast microscopic image; bottom left: fluorescence at 525-nm (minK-secondary label); bottom right: superimposed images. **C**: mean±SEM membrane-fluorescence at 566-nm (KvLQT1) and 525-nm (minK). **D**: KvLQT1/minK intensity-ratio. n=7 per group; $*P<0.05$; $**P<0.005$ vs minK38S.

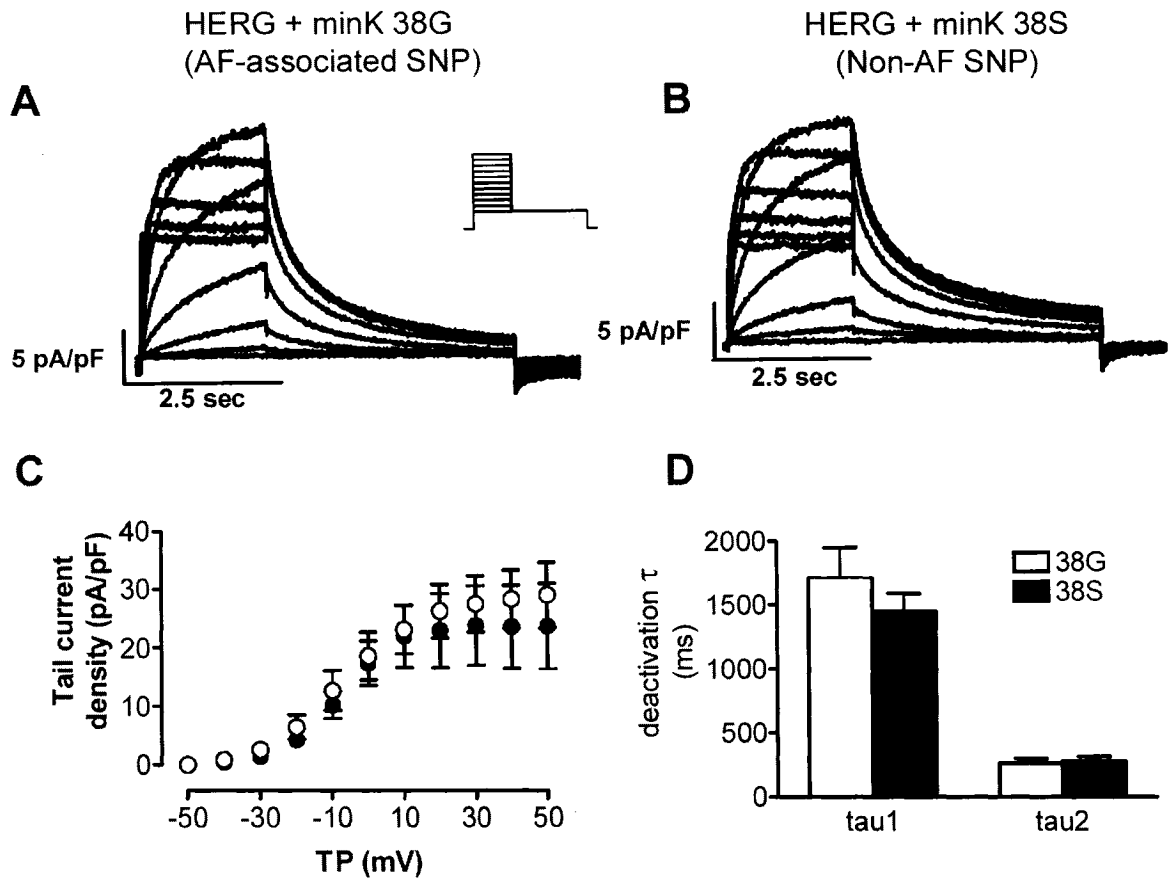

Figure 3 Recordings of I_{HERG} upon co-transfection with minK38G (**A**) or minK38S (**B**) in COS-7 cells. **C**: mean±SEM I_{HERG} tail-currents. **D**: I_{HERG} inactivation kinetics at –50 mV after an activating-pulse to +10 mV. (n=12, 15 cells for HERG+minK38G, HERG+minK38S).

CHAPTER 7: GENERAL DISCUSSION

This final chapter will summarize the novel findings of our studies, as well as highlight the significance of these findings and address the issue of future directions for research.

7.1 Summary of the novel findings in this thesis and significance of this work

Previous work in the area of ion channel heterogeneity across species, across different regions and in the face of cardiac diseases, has focused on electrophysiological differences. The work in this thesis stresses attempts to determine the molecular basis for many of these observations. For the first time, the molecular basis for species-specific differences in repolarizing K^+ currents has been elucidated. In addition, the molecular basis for the observed I_{to} transmural gradient in human and canine ventricle was clarified. The effects of CHF on the expression of I_{Na} in the ventricle, the ventricular I_{to} gradient and on SAN I_f subunit expression were also elucidated. Finally, the effects of a minK single nucleotide polymorphism were characterized. These findings demonstrate that the expression of voltage-gated ion channels is not uniform, but is rather dynamic in that it changes depending on the species, region and /or disease state.

7.2 The heterogeneous expression of voltage-gated K^+ channel subunits amongst species

The results dealing with the mRNA and protein expression of I_{to} and I_K subunits in Chapter 2 help elucidate the molecular basis for previous electrophysiological observations that guinea pigs, rabbits and humans rely on

repolarizing K^+ currents quite differently (Lu *et al.*, 2001). Competitive RT-PCR was used in order to make correct comparisons between species. The use of species-specific primers to amplify a gene in question would eliminate the use of a relative-type of comparison since differences in the affinity of a given primer for the target gene, as well as intrinsic differences in the PCR process and total RNA loading could not be accounted for. Since the epitopes recognized by KvLQT1 and minK antibodies were identical in all three species studied, a relative comparison could be made for these subunits. However, in the case of ERG1, the epitopes varied and therefore no comparison could be made at the protein level.

Although some previous reports have indicated that there might be a small transient outward current in guinea pig myocytes (Li *et al.*, 2000b), the general consensus is that in fact none is present (Lu *et al.*, 2001). Our finding that none of the hypothesized subunits believed to underlie I_{to} in most mammals including Kv1.4, Kv4.2 and Kv4.3, are expressed offers compelling evidence of the molecular basis for the lack of this current in the guinea pig. Rather, guinea pigs have been shown to express large delayed rectifier currents, especially I_{Ks} (Lu *et al.*, 2001). Our finding that guinea pigs express minK at very high levels and that this might underlie the large I_{Ks} currents is a novel finding as well. minK is not only responsible for slowing KvLQT1 kinetics, but also significantly increases current density (Barhanin *et al.*, 1996;Sanguinetti *et al.*, 1996), therefore it would be expected that a greater expression of this β-subunit could increase the density of its underlying current.

Expression of voltage-gated K^+ currents is almost the opposite in rabbits compared to guinea pigs. Rabbits rely heavily on I_{to} for repolarization, and our finding that all three putative α-subunits are expressed in this species provides

molecular evidence for this observation. As opposed to guinea pigs, rabbits have very small delayed rectifier currents, although they are still detectable. While KvLQT1 expression was fairly similar between the two species, rabbit minK expression at both the mRNA and protein levels was quite low. Therefore it is believed that minK may play a large role in determining the species-specific differences of I_{Ks} expression.

As for humans, they lie in between rabbits and guinea pigs in terms of their I_K subunit expression. We did not examine the expression of I_{to} subunits as this has already been the subject of many other publications (Wang *et al.*, 1999). Our results that humans have a high expression of both I_K α-subunits, HERG and KvLQT1, may dispel reports which diminish the importance of these currents for repolarization in this species. Instead, it is more likely that difficulties in recording these delayed rectifier currents, especially I_{Kr}, may be due to the sensitivity of these channels to current isolation techniques (Yue *et al.*, 1996).

These results indicate that the heterogeneous expression of voltage-gated K^+ channel subunits amongst different species can partially determine the currents upon which they rely for repolarization. Furthermore, we gain more insight into possible arrhythmia mechanisms and the importance of these currents for repolarization. Rabbits, which have a low expression of ERG1, KvLQT1 and minK, are susceptible to Torsades de pointes arrhythmias when given I_{Kr}-blockers (Carlsson *et al.*, 1990). Our results indicate that I_{Ks} may be important in determining action potential repolarization when I_{Kr} is blocked, acting as a "buffer". Therefore, using Class III anti-arrhythmic drugs on patients who might have an underlying deficiency in I_{Ks} would not be advisable. In addition, our findings may help in determining what type of species might be used for the assessment of novel drugs during pre-clinical animal

testing. An animal model which is able to recapitulate all the currents seen in humans is most desirable. In light of this, guinea pigs would not be a suitable model based on their lack of I_{to}, while rabbits would be favoured since they appear to have more similar current profiles to humans.

7.3 Regional heterogeneity in K^+ channel subunit expression

Action potential morphologies differ quite significantly between the different regions of the human and canine heart. In Chapters 4 and 5, we sought to elucidate molecular mechanisms for some of these differences, especially across the ventricular wall and between the right atrium and the SAN. By assessing the expression of channel subunits in these regions, we were able to determine which are most likely important in underlying a number of physiological functions of the heart.

In Chapter 4, we found that the expression of both Kv4.3 and KChIP2 contribute to an I_{to} transmural gradient where its current density is greatest in the epicardium and lowest in the endocardium in human and canine ventricles (Antzelevitch & Fish, 2001). Previous reports indicated that Kv1.4 and Kv4.3 expression was constant throughout the ventricular wall (Rosati *et al.*, 2001). After the discovery of KChIP2 and its association with Kv4.3 (An *et al.*, 2000), observations regarding its transmural expression have been conflicting: some report a KChIP2 transmural gradient which may underlie the I_{to} gradient (Rosati *et al.*, 2003) while others see no gradient at the protein level (Deschenes *et al.*, 2002). The purpose of our study was to help elucidate the molecular mechanism for this transmural gradient and clear up some of these conflicting results. Our finding that Kv4.3 expression varies across the ventricular wall is novel, and contradicts some previous

studies concerning Kv4.3 expression (Rosati *et al.*, 2001). However, the expression of Kv α-subunits in other species has been found to determine regional current differences (Dixon & McKinnon, 1994), so it is not entirely surprising that a similar phenomenon is found in humans and dogs. We were also able to detect a KChIP2 mRNA and protein gradient, which is in agreement with some previous studies (Rosati *et al.*, 2003). Therefore, our results indicate that both Kv4.3 and KChIP2 likely contribute to the I_{to} transmural gradient. One of the main arguments against the presence of a KChIP2 expression gradient was that no kinetic differences were seen for I_{to} between the epicardium and endocardium. Since KChIP2 is known to modify Kv4.3 kinetic properties, one wouldn't expect there to be a KChIP2 gradient since no kinetic differences are seen (Deschenes *et al.*, 2002). However, more recent work unrelated to the KChIP2 debate has identified differences in I_{to} kinetics between the two layers (Yu *et al.*, 2000), supporting the idea that both Kv4.3 and KChIP2 likely contribute to the I_{to} gradient.

In Chapter 5, we examined the regional expression heterogeneities in HCN subunit expression in the SAN compared to the right atrium. We found that HCN2 and HCN4 expression is highest in the SAN, consistent with its pacemaker function. HCN1 was not detected in either the right atrium or the SAN. HCN4 expression is the greater than HCN2, making it the predominant I_f α-subunit in the SAN. Very little work has been done in this area, partly because of the difficulties in precisely localizing the SAN. The fact that we used a canine model also helped since the SAN region is much larger than in small rodents such as mice and rabbits where most previous research has been performed. Native I_f inactivates much faster than HCN4 currents seen in heterologously expressed cells (Altomare *et al.*, 2003), therefore it is

not surprising that HCN2 is expressed as well. It is entirely possible that these two subunits may form heteromeric channel complexes as has been previously suggested (Altomare *et al.*, 2003;Chen *et al.*, 2001), allowing the resulting current to have current properties in between the two. The importance of HCN4 for cardiac pacemaking activity has also been demonstrated in other species where it is the predominant pacemaker subunit during embryogenesis and development (Garcia-Frigola *et al.*, 2003;Stieber *et al.*, 2003). Our novel finding of the higher expression of both HCN4 and HCN2 subunits in the SAN help elucidate the molecular basis for the large pacemaker current in this region, and which is necessary for the SAN to initiate impulses which will go on to excite the entire heart.

Taken together, our findings in Chapters 4 and 5 demonstrate how the expression of voltage-gated K^+ channel subunits varies according to the region studied. Furthermore, these heterogeneities can help explain regional action potential morphologies which also reflect some of the specialized functions in the regions studied. In the case of the ventricles, the transmural expression differences of Kv4.3 and KChIP2 subunits underlie an I_{to} transmural gradient which partially contributes to the dispersion of action potential repolarization. As for the SAN, the higher expression of HCN2 and HCN4 subunits, as compared to the rest of the right atrium, underlies the predominant I_f current in the region and contributes to its specialized pacemaker function.

7.4 Voltage-gated ion channel subunit heterogeneity associated with disease

The results in Chapters 3-5 examined the effects of disease on voltage-gated ion channel heterogeneity. CHF is one of the most prevalent cardiovascular diseases in our Western society and is the endpoint for many other diseases. CHF is associated with many other pathophysiological complications, including an increased risk for cardiac arrhythmias. This increased propensity has been attributed to changes in action potential morphology, generally resulting in a prolongation of the action potential duration. Many electrophysiological studies have been performed to ascertain what kinds of changes occur to voltage-gated ion channels which underlie the action potential, however much of the molecular basis for these changes remain unknown. Therefore there is great interest in elucidating these molecular changes in order to help our understanding of the pathogenesis of CHF and how it alters the myocardium to render it more susceptible to arrhythmia. Information regarding molecular changes in CHF can also help in identifying potential novel pharmacological targets for the treatment of the disease, especially in light of the fact that current therapies are suboptimal.

Firstly, we found a reduction in the expression of $Na_v1.5$ may underlie a reduction of I_{Na} density in the midmyocardium associated with CHF (Maltsev *et al.*, 2002). While we were not able to detect a reduction of $Na_v1.5$ mRNA expression, a novel post-transcriptional mechanism is most likely responsible for its protein expression. The activation of cardiac I_{Na} is one of the main determinants of conduction velocity. Conduction slowing has been associated with the pathogenesis of CHF and allows tissue to become non-refractory before the termination of an

initial wave of excitation. We saw no changes in the expression of any of the Na^+ channel β-subunits Naβ1 and Naβ2. This is the first time, to our knowledge, that a relationship between conduction slowing in CHF and a change in I_{Na} can be made. These findings also support the notion of how Class I anti-arrhythmic agents which block I_{Na} can contribute to conduction slowing and become pro-arrhythmogenic.

Continuing with our investigation into changes occurring in the ventricle during CHF, we sought to determine how this disease affected the transmural I_{to} gradient. We found that Kv4.3, and not KChIP2, is downregulated in both the epicardium and endocardium. Previous results have demonstrated that I_{to} is downregulated during CHF (Kaab *et al.*, 1996;Li *et al.*, 2000a), with changes in Kv4.3 expression being responsible (Kaab *et al.*, 1998). Our findings regarding the fact that KChIP2 expression does not change in CHF are novel and strengthen the notion that Kv4.3 expression can play a large role in determining I_{to} expression in the ventricle. In light of this, KChIP2 still plays a role in determining the transmural gradient, but the extent of exactly how much would be hard to characterize. KChIP2 deficient mice were found to completely lack I_{to} currents even when I_{to} α-subunits were present (Kuo *et al.*, 2001). These observations were made in an artificially created KChIP2 knockout, and our results indicate that under more physiological conditions, Kv4.3 appears to be the greater determinant of I_{to} expression, especially in CHF. A reduction of I_{to} in CHF can have two very important effects with regards to increasing the susceptibility to arrhythmia. Firstly, the transmural dispersion of repolarization is important for the proper synchronization of ventricular excitation. By reducing the magnitude of the transmural I_{to} gradient, the myocardium may be more susceptible to the creation of re-entrant arrhythmogenic circuits. Secondly,

although the reduction of I_{to} does not directly affect action potential repolarization as changes in the delayed rectifiers or an increase in I_{Ca} would, it is responsible for setting the "height" (voltage) of the action potential plateau phase where I_{Ca} is activated (Hoppe *et al.*, 2000). Given this information, a downregulation of Kv4.3 would lead to decreased I_{to} currents and therefore set a higher plateau phase resulting in a prolongation of the APD. Such a prolongation could lead to an increased propensity for EAD triggered arrhythmias.

Lastly, we examined the effects of CHF on SAN function. We identified a significant remodelling of HCN subunits where both HCN2 and 4 were downregulated in the SAN, while HCN4 was increased in the right atrium. AF is associated with many cases of CHF (Carson *et al.*, 1993), however the mechanisms leading to this complication are not completely known. Independently, AF and CHF are associated with different remodelling profiles, especially in I_{Ks} which is downregulated in CHF and contributes to the APD lengthening, but unchanged in AF where APD is actually shortened. Some studies have noted that CHF is associated with some SAN dysfunction (Opthof *et al.*, 2000), and I_f has been demonstrated to be downregulated in the SAN (Verkerk AO *et al.*, 2003), however the molecular basis for these changes has never been elucidated. Our findings represent the first time, to our knowledge, that I_f molecular remodelling has been noted in CHF. Through the greater of expression of HCN4 in the right atrium in CHF, it would appear that the normal pacemaking activity of the heart is removed from the SAN, while other regions such as the right atrium have increased expression of I_f subunits. This has important implications in terms of the pathogenesis of CHF because increasing the amount of I_f in a region other than the SAN could lead to the formation of abnormal

ectopic beats in such regions. The occurrence of ectopic beats (abnormal automaticity) can predispose the myocardium to arrhythmias, especially if these depolarizations have a large enough magnitude to reach the activation threshold and initiate an action potential.

7.5 Genetic heterogeneity in voltage-gated channel subunits as a determinant of arrhythmia

The last part of our studies on ion channel heterogeneities also involved cardiovascular disease, this time AF, but that was associated with differences in a single ion channel subunit, rather than expression differences as was seen with CHF. Genetic influences have been noted in familial AF; however the exact molecular determinants have not been characterized. Our findings are actually the second report on a modification of a I_{Ks} subunit which underlies inherited AF, and the first involving minK. A single nucleotide polymorphism in the minK KCNE1 gene, where a glycine at position 38 is substituted for a serine, is associated with many cases of AF. The purpose of our study was to characterize the effects of this polymorphism on KvLQT1 currents in order to elucidate any changes which may predispose to AF. We found the AF-associated minK 38G allele to produce significantly smaller currents when co-expressed with KvLQT1 as compared to the 38S allele. In doing so, one would expect a prolongation of the action potential duration which could predispose the atrial myocardium to EAD triggered arrhythmias as has been suggested previously (Kirchhof *et al.*, 2003). Our findings are actually mechanistically different than a previous report of a gain-of-function KvLQT1 mutation associated with AF (Chen *et al.*, 2003b) where I_{Ks} is increased and shortens the APD, facilitating the

establishment of a re-entrant circuit. Taken together, it appears that there is heterogeneity in the molecular determinants and mechanisms underlying genetically based AF.

7.6 Directions for future research

While the results presented here have helped achieve a better understanding of the molecular heterogeneity which underlies voltage-gated ion channel expression in different species, regions and diseases, there are still many areas and issues which need to be resolved.

7.6.1 Additional *in vivo* characterization of I_f remodelling

We have identified remodeling of I_f subunits in the SAN and right atrium in a canine model of CHF. While dogs are normally an excellent model for humans, our other work on species-specific differences in voltage-gated K^+ channel subunits does indicate that differences between the two species may be present. Therefore extending this research to humans is essential to be able to draw final conclusions concerning the importance of HCN subunit heterogeneity in that species. Further more, characterizing the electrophysiological properties of I_f currents in the atria and SAN, under control conditions and in CHF, will also help confirm our molecular observations.

Although we identified changes in HCN subunit expression associated with CHF, the precise functional significance of these changes still has to be determined, especially in terms of increasing the myocardium's propensity to arrhythmia by increasing automaticity. This may be achieved by increasing β-adrenergic tone to

increase the stimulation of I_f channels, albeit others as well. Isoproterenol may be given as an agonist to elicit β-adrenergic responses, and since there is an increased HCN4 expression in the right atrium under CHF conditions, one would expect there to be increased ectopic beat formation as well. Other recent studies have implicated cellular localization of HCN subunits as a large determinant of I_f current properties. These include interactions with cytoskeletal scaffold proteins and organization in membrane rafts (Barbuti *et al.*, 2004;Gravante *et al.*, 2004;Kimura *et al.*, 2004). It would interesting to see if these interactions are altered in CHF, as well as how they may contribute to the association of I_f channel complexes *in vivo* as a means of elucidating the true composition of these channels. These additional experiments could help solidify the physiological relevance of the changes we have observed.

7.6.2 Genotyping patients for minK polymorphism and cardiomyocyte electrophysiology

Our characterization of a minK single nucleotide polymorphism revealed significant changes in the resulting current from minK-KvLQT1 co-expression. We hypothesized that this was due to an increased KvLQT1 membrane expression. Other, more quantitative experiments could help support this notion; including immunoblotting highly purified outer membrane protein preparations for both KvLQT1 and minK.

In addition, it is widely accepted now that although heterologous expression systems are ideal for examining basic electrophysiological effects, they lack the complexity of a cardiomyocyte environment. The cellular milieu plays a large role in determining I_{Ks} electrophysiological properties as it is modulated by interactions with

cytoskeletal proteins, other ion channel α-subunits, and β-adrenergic signalling (Ehrlich *et al.*, 2004;Furukawa *et al.*, 2001). It would be interesting to be able to genotype dog, or even better human, tissue samples and record I_{Ks} currents. The changes we saw were quite significant, and one would expect a parallel increase in the action potential duration and, by extension, the QT interval as well. These additional *in vivo* experiments would help elucidate the true effects of this polymorphism, including how it increases a patients risk for developing AF.

7.6.3 Pharmacological implications and practical applicability

We have obtained a vast amount of results concerning the expression profiles of voltage-gated ion channel subunits in different species, cardiac regions, and in disease. However, much work still remains in terms of applying these observations so that they may help improve current pharmacological treatment. Most notably, our characterization of voltage-gated ion channel expression profiles in CHF can help gain insight into potential targets for pharmacological intervention for the treatment of the disease. At first glance, one could argue that since our results demonstrate ion channel remodelling in CHF, treatment which restores the normal electrical properties of the heart may possibly a favourable approach. This may include ambitious techniques such as gene therapy to restore the expression of those channels which have been downregulated in CHF. This approach has already been attempted and is promising (Plotnikov AN *et al.*, 2004;Nuss HB *et al.*, 1999), especially in light of the fact that no voltage-gated ion channel agonists exist. Agonists do exist for some ion channels, such as the ATP-sensitive K^+ channels. These are known to be ligand gated channels and are not typical six-transmembrane domain proteins, but rather are part

of a large "pharmaceutical friendly" group of G-protein coupled receptors. The discovery of pharmacophores which are able to act as voltage-gated K^+ channel agonists, may prove to be a beneficial strategy for the treatment of cardiac arrhythmias due to repolarization abnormalities. Even before such projects are considered, the actual effects of reversing some of these CHF induced changes must be examined in terms of its applicability in restoring normal cardiac function. In other words, will reversing the observed changes induced by CHF actually be of any benefit in treating the disease? The downregulation of I_{to} in the ventricle can contribute to APD prolongation as mentioned above, but some animal models of cardiovascular disease which are associated with APD show no change in I_{to} (Wang Z *et al.*, 2001). Therefore, more investigation is still required to determine precisely how the reduction of I_{to} can render the myocardium more susceptible to arrhythmia in CHF. Along the same lines, although we identified an increase in HCN4 expression in the right atrium of dogs with CHF, more electrophysiological characterization remains to be done in order to determine if this increased expression can lead to an increased I_f current and automaticity. Functional evidence, such as being able to block ectopic beat formation in the atrium with HCN antagonists such as zatebradine and capsazepine (Gill CH *et al.*, 2004), would also help support the notion that our findings may provide a suitable pharmacological target for the treatment of arrhythmias associated with CHF.

7.7 General conclusions

Heterogeneous expression of voltage-gated ion channel subunits underlies species-, region-, and disease- specific differences in ion current expression. These

differences play a large role in determining cardiac function under normal and disease conditions. Still, there is much to be explored in terms of the modulation and functions of voltage-gated ion channels. Increased understanding of the molecular determinants of cardiac function and disease may provide new avenues for the development of better pharmacological agents for the prevention and treatment of cardiovascular disease.

CHAPTER 8: REFERENCES

(1989). Preliminary report: effect of encainide and flecainide on mortality in a randomized trial of arrhythmia suppression after myocardial infarction. The Cardiac Arrhythmia Suppression Trial (CAST) Investigators *N.Engl.J.Med.* **321**, 406-412.

Abbott, G. W., Butler, M. H., Bendahhou, S., Dalakas, M. C., Ptacek, L. J., & Goldstein, S. A. (2001). MiRP2 forms potassium channels in skeletal muscle with Kv3.4 and is associated with periodic paralysis. *Cell* **104**, 217-231.

Abbott, G. W., Sesti, F., Splawski, I., Buck, M. E., Lehmann, M. H., Timothy, K. W., Keating, M. T., & Goldstein, S. A. (1999). MiRP1 forms I_{Kr} potassium channels with HERG and is associated with cardiac arrhythmia. *Cell* **97**, 175-187.

Accili, E. A., Robinson, R. B., & DiFrancesco, D. (1997). Properties and modulation of I_f in newborn versus adult cardiac SA node. *Am.J.Physiol* **272**, H1549-H1552.

Agnew, W. S., Moore, A. C., Levinson, S. R., & Raftery, M. A. (1980). Identification of a large molecular weight peptide associated with a tetrodotoxin binding protein from the electroplax of Electrophorus electricus. *Biochem.Biophys.Res.Commun.* **92**, 860-866.

Akopian, A. N., Souslova, V., Sivilotti, L., & Wood, J. N. (1997). Structure and distribution of a broadly expressed atypical sodium channel. *FEBS Lett.* **400**, 183-187.

Allessie, M. A. (1998). Atrial electrophysiologic remodeling: another vicious circle? *J.Cardiovasc.Electrophysiol.* **9**, 1378-1393.

Allessie, M. A., Bonke, F. I., & Schopman, F. J. (1977). Circus movement in rabbit atrial muscle as a mechanism of tachycardia. III. The "leading circle" concept: a new model of circus movement in cardiac tissue without the involvement of an anatomical obstacle. *Circ.Res.* **41**, 9-18.

Altomare, C., Bucchi, A., Camatini, E., Baruscotti, M., Viscomi, C., Moroni, A., & DiFrancesco, D. (2001). Integrated allosteric model of voltage gating of HCN channels. *J.Gen.Physiol* **117**, 519-532.

Altomare, C., Terragni, B., Brioschi, C., Milanesi, R., Pagliuca, C., Viscomi, C., Moroni, A., Baruscotti, M., & DiFrancesco, D. (2003). Heteromeric HCN1-HCN4 channels: a comparison with native pacemaker channels from the rabbit sinoatrial node. *J.Physiol* **549**, 347-359.

Amos, G. J., Wettwer, E., Metzger, F., Li, Q., Himmel, H. M., & Ravens, U. (1996). Differences between outward currents of human atrial and subepicardial ventricular myocytes. *J.Physiol* **491 (Pt 1)**, 31-50.

An, R. H., Wang, X. L., Kerem, B., Benhorin, J., Medina, A., Goldmit, M., & Kass, R. S. (1998). Novel LQT-3 mutation affects Na^+ channel activity through interactions between alpha- and beta1-subunits. *Circ.Res.* **83**, 141-146.

An, W. F., Bowlby, M. R., Betty, M., Cao, J., Ling, H. P., Mendoza, G., Hinson, J. W., Mattsson, K. I., Strassle, B. W., Trimmer, J. S., & Rhodes, K. J. (2000). Modulation of A-type potassium channels by a family of calcium sensors. *Nature* **403**, 553-556.

Antzelevitch, C. (2000). Electrical heterogeneity, cardiac arrhythmias, and the sodium channel. *Circ.Res.* **87**, 964-965.

Antzelevitch, C. & Fish, J. (2001). Electrical heterogeneity within the ventricular wall. *Basic Res.Cardiol.* **96**, 517-527.

Antzelevitch, C., Sicouri, S., Litovsky, S. H., Lukas, A., Krishnan, S. C., Di Diego, J. M., Gintant, G. A., & Liu, D. W. (1991). Heterogeneity within the ventricular wall. Electrophysiology and pharmacology of epicardial, endocardial, and M cells. *Circ.Res.* **69**, 1427-1449.

Anumonwo, J. M., Freeman, L. C., Kwok, W. M., & Kass, R. S. (1992a). Delayed rectification in single cells isolated from guinea pig sinoatrial node. *Am.J.Physiol* **262**, H921-H925.

Anumonwo, J. M., Freeman, L. C., Kwok, W. M., & Kass, R. S. (1992b). Delayed rectification in single cells isolated from guinea pig sinoatrial node. *Am.J.Physiol* **262**, H921-H925.

Apkon, M. & Nerbonne, J. M. (1988). Alpha 1-adrenergic agonists selectively suppress voltage-dependent K^+ current in rat ventricular myocytes. *Proc.Natl.Acad.Sci.U.S.A* **85**, 8756-8760.

Apkon, M. & Nerbonne, J. M. (1991). Characterization of two distinct depolarization-activated K^+ currents in isolated adult rat ventricular myocytes. *J.Gen.Physiol* **97**, 973-1011.

Attali, B., Romey, G., Honore, E., Schmid-Alliana, A., Mattei, M. G., Lesage, F., Ricard, P., Barhanin, J., & Lazdunski, M. (1992). Cloning, functional expression, and regulation of two K^+ channels in human T lymphocytes. *J.Biol.Chem.* **267**, 8650-8657.

Backx, P. H., Yue, D. T., Lawrence, J. H., Marban, E., & Tomaselli, G. F. (1992). Molecular localization of an ion-binding site within the pore of mammalian sodium channels. *Science* **257**, 248-251.

Bailly, P., Benitah, J. P., Mouchoniere, M., Vassort, G., & Lorente, P. (1997). Regional alteration of the transient outward current in human left ventricular septum during compensated hypertrophy. *Circulation* **96**, 1266-1274.

Baker, L. C., London, B., Choi, B. R., Koren, G., & Salama, G. (2000). Enhanced dispersion of repolarization and refractoriness in transgenic mouse hearts promotes reentrant ventricular tachycardia. *Circ.Res.* **86**, 396-407.

Balser, J. R., Bennett, P. B., Hondeghem, L. M., & Roden, D. M. (1991). Suppression of time-dependent outward current in guinea pig ventricular myocytes. Actions of quinidine and amiodarone. *Circ.Res.* **69**, 519-529.

Balser, J. R., Bennett, P. B., & Roden, D. M. (1990). Time-dependent outward current in guinea pig ventricular myocytes. Gating kinetics of the delayed rectifier. *J.Gen.Physiol* **96**, 835-863.

Barajas-Martinez, H., Elizalde, A., & Sanchez-Chapula, J. A. (2000). Developmental differences in delayed rectifying outward current in feline ventricular myocytes.. *Am.J.Physiol Heart Circ.Physiol* **278**, H484-H492.

Barbuti, A., Gravante, B., Riolfo, M., Milanesi, R., Terragni, B., & DiFrancesco, D. (2004). Localization of pacemaker channels in lipid rafts regulates channel kinetics. *Circ.Res.* **94**, 1325-1331.

Barhanin, J., Lesage, F., Guillemare, E., Fink, M., Lazdunski, M., & Romey, G. (1996). K(V)LQT1 and IsK (minK) proteins associate to form the I(Ks) cardiac potassium current. *Nature* **384**, 78-80.

Barry, D. M. & Nerbonne, J. M. (1996). Myocardial potassium channels: electrophysiological and molecular diversity. *Annu.Rev.Physiol* **58**, 363-394.

Barry, D. M., Xu, H., Schuessler, R. B., & Nerbonne, J. M. (1998). Functional knockout of the transient outward current, long-QT syndrome, and cardiac remodeling in mice expressing a dominant-negative Kv4 alpha subunit. *Circ.Res.* **83**, 560-567.

Baruscotti, M., Westenbroek, R., Catterall, W. A., DiFrancesco, D., & Robinson, R. B. (1997). The newborn rabbit sino-atrial node expresses a neuronal type I-like Na^+ channel. *J.Physiol* **498 (Pt 3)**, 641-648.

Beck, E. J., Sorensen, R. G., Slater, S. J., & Covarrubias, M. (1998). Interactions between multiple phosphorylation sites in the inactivation particle of a K^+ channel. Insights into the molecular mechanism of protein kinase C action. *J.Gen.Physiol* **112**, 71-84.

Beeler, G. W. & McGuigan, J. A. (1978). Voltage clamping of multicellular myocardial preparations: capabilities and limitations of existing methods. *Prog.Biophys.Mol.Biol.* **34**, 219-254.

Belcher, S. M. & Howe, J. R. (1996). Cloning of the cDNA encoding the sodium channel beta 1 subunit from rabbit. *Gene* **170**, 285-286.

Belardinelli, L. & Isenberg G. (1983). Actions of adenosine and isoproterenol on isolated mammalian ventricular myocytes. *Circ. Res.* **53**, 587-597.

Benjamin, E. J., Levy, D., Vaziri, S. M., D'Agostino, R. B., Belanger, A. J., & Wolf, P. A. (1994). Independent risk factors for atrial fibrillation in a population-based cohort. The Framingham Heart Study. *JAMA* **271**, 840-844.

Benndorf, K., Boldt, W., & Nilius, B. (1985). Sodium current in single myocardial mouse cells. *Pflugers Arch.* **404**, 190-196.

Bennett, P., McKinney, L., Begenisich, T., & Kass, R. S. (1986). Adrenergic modulation of the delayed rectifier potassium channel in calf cardiac Purkinje fibers. *Biophys.J.* **49**, 839-848.

Bennett, P. B., McKinney, L. C., Kass, R. S., & Begenisich, T. (1985). Delayed rectification in the calf cardiac Purkinje fiber. Evidence for multiple state kinetics. *Biophys.J.* **48**, 553-567.

Benz, I., Herzig, J. W., & Kohlhardt, M. (1992). Opposite effects of angiotensin II and the protein kinase C activator OAG on cardiac Na^+ channels. *J.Membr.Biol.* **130**, 183-190.

Beuckelmann, D. J., Nabauer, M., & Erdmann, E. (1993). Alterations of K^+ currents in isolated human ventricular myocytes from patients with terminal heart failure. *Circ.Res.* **73**, 379-385.

Bezzina, C., Veldkamp, M. W., van Den Berg, M. P., Postma, A. V., Rook, M. B., Viersma, J. W., van Langen, I. M., Tan-Sindhunata, G., Bink-Boelkens, M. T., Der Hout, A. H., Mannens, M. M., & Wilde, A. A. (1999). A single $Na(^+)$ channel mutation causing both long-QT and Brugada syndromes. *Circ.Res.* **85**, 1206-1213.

Bianchi, L., Shen, Z., Dennis, A. T., Priori, S. G., Napolitano, C., Ronchetti, E., Bryskin, R., Schwartz, P. J., & Brown, A. M. (1999). Cellular dysfunction of LQT5-minK mutants: abnormalities of I_{Ks}, I_{Kr} and trafficking in long QT syndrome. *Hum.Mol.Genet.* **8**, 1499-1507.

Bleeker, W. K., Mackaay, A. J., Masson-Pevet, M., Bouman, L. N., & Becker, A. E. (1980). Functional and morphological organization of the rabbit sinus node. *Circ.Res.* **46**, 11-22.

Blumenthal, E. M. & Kaczmarek, L. K. (1994). The minK potassium channel exists in functional and nonfunctional forms when expressed in the plasma membrane of Xenopus oocytes. *J.Neurosci.* **14**, 3097-3105.

Bodewei, R., Hering, S., Lemke, B., Rosenshtraukh, L. V., Undrovinas, A. I., & Wollenberger, A. (1982). Characterization of the fast sodium current in isolated rat myocardial cells: simulation of the clamped membrane potential. *J.Physiol* **325**, 301-315.

Bonhaus, D. W., Herman, R. C., Brown, C. M., Cao, Z., Chang, L. F., Loury, D. N., Sze, P., Zhang, L., & Hunter, J. C. (1996). The beta 1 sodium channel subunit modifies the interactions of neurotoxins and local anesthetics with the rat brain IIA alpha sodium channel in isolated membranes but not in intact cells. *Neuropharmacology* **35**, 605-613.

Borlak, J. & Thum T. (2003). Hallmarks of ion channel gene expression in end-stage heart failure. *FASEB J.* **17**, 1592-1608.

Bosch, R. F., Gaspo, R., Busch, A. E., Lang, H. J., Li, G. R., & Nattel, S. (1998). Effects of the chromanol 293B, a selective blocker of the slow, component of the delayed rectifier K^+ current, on repolarization in human and guinea pig ventricular myocytes. *Cardiovasc.Res.* **38**, 441-450.

Bou-Abboud, E. & Nerbonne, J. M. (1999). Molecular correlates of the calcium-independent, depolarization-activated K^+ currents in rat atrial myocytes. *J.Physiol* **517 (Pt 2)**, 407-420.

Bouman, L. N. & Jongsma, H. J. (1986). Structure and function of the sino-atrial node: a review. *Eur.Heart J.* **7**, 94-104.

Boyett, M. R. (1981a). A study of the effect of the rate of stimulation on the transient outward current in sheep cardiac Purkinje fibres. *J.Physiol* **319**, 1-22.

Boyett, M. R. (1981b). Effect of rate-dependent changes in the transient outward current on the action potential in sheep Purkinje fibres. *J.Physiol* **319**, 23-41.

Boyle, W. A. & Nerbonne, J. M. (1991). A novel type of depolarization-activated K^+ current in isolated adult rat atrial myocytes. *Am.J.Physiol* **260**, H1236-H1247.

Boyle, W. A. & Nerbonne, J. M. (1992). Two functionally distinct 4-aminopyridine-sensitive outward K^+ currents in rat atrial myocytes. *J.Gen.Physiol* **100**, 1041-1067.

Brahmajothi, M. V., Campbell, D. L., Rasmusson, R. L., Morales, M. J., Trimmer, J. S., Nerbonne, J. M., & Strauss, H. C. (1999). Distinct transient outward potassium current (I_{to}) phenotypes and distribution of fast-inactivating potassium channel alpha subunits in ferret left ventricular myocytes. *J.Gen.Physiol* **113**, 581-600.

Brahmajothi, M. V., Morales, M. J., Liu, S., Rasmusson, R. L., Campbell, D. L., & Strauss, H. C. (1996). In situ hybridization reveals extensive diversity of K^+ channel mRNA in isolated ferret cardiac myocytes. *Circ.Res.* **78**, 1083-1089.

Braun, A. P., Fedida, D., Clark, R. B., & Giles, W. R. (1990). Intracellular mechanisms for alpha 1-adrenergic regulation of the transient outward current in rabbit atrial myocytes. *J.Physiol* **431**, 689-712.

Brown, A. M., Lee, K. S., & Powell, T. (1981). Sodium current in single rat heart muscle cells. *J.Physiol* **318**, 479-500.

Brown, H. F., DiFrancesco, D., & Noble, S. J. (1979). How does adrenaline accelerate the heart? *Nature* **280**, 235-236.

Bryant, S. M., Wan, X., Shipsey, S. J., & Hart, G. (1998). Regional differences in the delayed rectifier current (I_{Kr} and I_{Ks}) contribute to the differences in action potential duration in basal left ventricular myocytes in guinea-pig. *Cardiovasc.Res.* **40**, 322-331.

Burgess, M. J. (1979). Relation of ventricular repolarization to electrocardiographic T wave-form and arrhythmia vulnerability. *Am.J.Physiol* **236**, H391-H402.

Busch, A. E., Suessbrich, H., Waldegger, S., Sailer, E., Greger, R., Lang, H., Lang, F., Gibson, K. J., & Maylie, J. G. (1996). Inhibition of I_{Ks} in guinea pig cardiac myocytes and guinea pig IsK channels by the chromanol 293B. *Pflugers Arch.* **432**, 1094-1096.

Bustamante, J. O. & McDonald, T. F. (1983). Sodium currents in segments of human heart cells. *Science* **220**, 320-321.

Butler, A., Wei, A. G., Baker, K., & Salkoff, L. (1989). A family of putative potassium channel genes in Drosophila. *Science* **243**, 943-947.

Campbell, D. L., Qu, Y., Rasmusson, R. L., & Strauss, H. C. (1993a). The calcium-independent transient outward potassium current in isolated ferret right ventricular myocytes. II. Closed state reverse use-dependent block by 4-aminopyridine. *J.Gen.Physiol* **101**, 603-626.

Campbell, D. L., Rasmusson, R. L., Qu, Y., & Strauss, H. C. (1993b). The calcium-independent transient outward potassium current in isolated ferret right ventricular myocytes. I. Basic characterization and kinetic analysis. *J.Gen.Physiol* **101**, 571-601.

Carlsson, L., Almgren, O., & Duker, G. (1990). QTU-prolongation and torsades de pointes induced by putative class III antiarrhythmic agents in the rabbit: etiology and interventions. *J.Cardiovasc.Pharmacol.* **16**, 276-285.

Carson, P. E., Johnson, G. R., Dunkman, W. B., Fletcher, R. D., Farrell, L., & Cohn, J. N. (1993). The influence of atrial fibrillation on prognosis in mild to moderate heart failure. The V-HeFT Studies. The V-HeFT VA Cooperative Studies Group. *Circulation* **87**, VI102-VI110.

Catterall, W. A. (2000). From ionic currents to molecular mechanisms: the structure and function of voltage-gated sodium channels. *Neuron* **26**, 13-25.

Catterall, W. A., Goldin, A. L., & Waxman, S. G. (2003). International Union of Pharmacology. XXXIX. Compendium of voltage-gated ion channels: sodium channels. *Pharmacol.Rev.* **55**, 575-578.

Cerbai, E., Crucitti, A., Sartiani, L., De Paoli, P., Pino, R., Rodriguez, M. L., Gensini, G., & Mugelli, A. (2000). Long-term treatment of spontaneously hypertensive rats with losartan and electrophysiological remodeling of cardiac myocytes. *Cardiovasc.Res.* **45**, 388-396.

Cerbai, E., Pino, R., Sartiani, L., & Mugelli, A. (1999). Influence of postnatal-development on $I_{(f)}$ occurrence and properties in neonatal rat ventricular myocytes. *Cardiovasc.Res.* **42**, 416-423.

Chen, C., Westenbroek, R. E., Xu, X., Edwards, C. A., Sorenson, D. R., Chen, Y., McEwen, D. P., O'Malley, H. A., Bharucha, V., Meadows, L. S., Knudsen, G. A., Vilaythong, A., Noebels, J. L., Saunders, T. L., Scheuer, T., Shrager, P., Catterall, W. A., & Isom, L. L. (2004). Mice lacking sodium channel beta1 subunits display defects in neuronal excitability, sodium channel expression, and nodal architecture. *J.Neurosci.* **24**, 4030-4042.

Chen, H., Kim, L. A., Rajan, S., Xu, S., & Goldstein, S. A. (2003a). Charybdotoxin binding in the $I_{(Ks)}$ pore demonstrates two MinK subunits in each channel complex. *Neuron* **40**, 15-23.

Chen, Q., Kirsch, G. E., Zhang, D., Brugada, R., Brugada, J., Brugada, P., Potenza, D., Moya, A., Borggrefe, M., Breithardt, G., Ortiz-Lopez, R., Wang, Z., Antzelevitch, C., O'Brien, R. E., Schulze-Bahr, E., Keating, M. T., Towbin, J. A., & Wang, Q. (1998). Genetic basis and molecular mechanism for idiopathic ventricular fibrillation. *Nature* **392**, 293-296.

Chen, S., Wang, J., & Siegelbaum, S. A. (2001). Properties of hyperpolarization-activated pacemaker current defined by coassembly of HCN1 and HCN2 subunits and basal modulation by cyclic nucleotide. *J.Gen.Physiol* **117**, 491-504.

Chen, Y. H., Xu, S. J., Bendahhou, S., Wang, X. L., Wang, Y., Xu, W. Y., Jin, H. W., Sun, H., Su, X. Y., Zhuang, Q. N., Yang, Y. Q., Li, Y. B., Liu, Y., Xu, H. J., Li, X. F., Ma, N., Mou, C. P., Chen, Z., Barhanin, J., & Huang, W. (2003b). KCNQ1 gain-of-function mutation in familial atrial fibrillation. *Science* **299**, 251-254.

Chiamvimonvat, N., Perez-Garcia, M. T., Ranjan, R., Marban, E., & Tomaselli, G. F. (1996). Depth asymmetries of the pore-lining segments of the Na^+ channel revealed by cysteine mutagenesis. *Neuron* **16**, 1037-1047.

Clay, J. R., Ogbaghebriel, A., Paquette, T., Sasyniuk, B. I., & Shrier, A. (1995). A quantitative description of the E-4031-sensitive repolarization current in rabbit ventricular myocytes. *Biophys.J.* **69**, 1830-1837.

Cohen, S. A. (1996). Immunocytochemical localization of rH1 sodium channel in adult rat heart atria and ventricle. Presence in terminal intercalated disks. *Circulation* **94**, 3083-3086.

Cohn, J.N., Archibald, D.G., Ziesche, S., Franciosa, J.A., Harston, W.E., Tristani, F.E., Dunkman, W.B., Jacobs, W., Francis, G.S., Flohr, K.H., et al. (1986). Effect of vasodilator therapy on mortality in chronic congestive heart failure. Results of a Veterans Administration Cooperative Study. *N Engl J Med.* **314**, 1547-1552.

Colatsky, J. J. & Tsien, R. W. (1979). Sodium channels in rabbit cardiac Purkinje fibres. *Nature* **278**, 265-268.

Coraboeuf, E. & Carmeliet, E. (1982). Existence of two transient outward currents in sheep cardiac Purkinje fibers. *Pflugers Arch.* **392**, 352-359.

Coraboeuf, E., Deroubaix, E., & Coulombe, A. (1979). Effect of tetrodotoxin on action potentials of the conducting system in the dog heart. *Am.J.Physiol* **236**, H561-H567.

Cranefield, P.F. (1977). Action potentials, afterpotentials, and arrhythmias. *Circ. Res.* **41**, 415-423.

Cui, J., Kagan, A., Qin, D., Mathew, J., Melman, Y. F., & McDonald, T. V. (2001). Analysis of the cyclic nucleotide binding domain of the HERG potassium channel and interactions with KCNE2. *J.Biol.Chem.* **276**, 17244-17251.

Cui, J., Melman, Y., Palma, E., Fishman, G. I., & McDonald, T. V. (2000). Cyclic AMP regulates the HERG $K(^{+})$ channel by dual pathways. *Curr.Biol.* **10**, 671-674.

Curran, M. E., Splawski, I., Timothy, K. W., Vincent, G. M., Green, E. D., & Keating, M. T. (1995). A molecular basis for cardiac arrhythmia: HERG mutations cause long QT syndrome. *Cell* **80**, 795-803.

Davis, L. D. & Temte, J. V. (1969). Electrophysiological actions of lidocaine on canine ventricular muscle and Purkinje fibers. *Circ.Res.* **24**, 639-655.

De Biasi, M., Hartmann, H. A., Drewe, J. A., Taglialatela, M., Brown, A. M., & Kirsch, G. E. (1993). Inactivation determined by a single site in K^{+} pores. *Pflugers Arch.* **422**, 354-363.

Decher, N., Bundis, F., Vajna, R., & Steinmeyer, K. (2003). KCNE2 modulates current amplitudes and activation kinetics of HCN4: influence of KCNE family members on HCN4 currents. *Pflugers Arch.* **446**, 633-640.

Decher, N., Uyguner, O., Scherer, C. R., Karaman, B., Yuksel-Apak, M., Busch, A. E., Steinmeyer, K., & Wollnik, B. (2001). hKChIP2 is a functional modifier of hKv4.3 potassium channels: cloning and expression of a short hKChIP2 splice variant. *Cardiovasc.Res.* **52**, 255-264.

De Ferrari, G.M., Landolina, M., Mantica, M., Manfredini, R., Schwartz, P.J., Lotto, A. (1995). Baroreflex sensitivity, but not heart rate variability, is reduced in patients with life-threatening ventricular arrhythmias long after myocardial infarction. *Am Heart J.* **130**, 473-80.

Demolombe, S., Baro, I., Pereon, Y., Bliek, J., Mohammad-Panah, R., Pollard, H., Morid, S., Mannens, M., Wilde, A., Barhanin, J., Charpentier, F., & Escande, D. (1998). A dominant negative isoform of the long QT syndrome 1 gene product. *J.Biol.Chem.* **273**, 6837-6843.

Derakhchan, K., Li, D., Courtemanche, M., Smith, B., Brouillette, J., Page, P. L., & Nattel, S. (2001). Method for simultaneous epicardial and endocardial mapping of in vivo canine heart: application to atrial conduction properties and arrhythmia mechanisms. *J.Cardiovasc.Electrophysiol.* **12**, 548-555.

Deschenes, I., DiSilvestre, D., Juang, G. J., Wu, R. C., An, W. F., & Tomaselli, G. F. (2002). Regulation of Kv4.3 current by KChIP2 splice variants: a component of native cardiac $I_{(to)}$? *Circulation* **106**, 423-429.

Dhar, M. J., Chen, C., Rivolta, I., Abriel, H., Malhotra, R., Mattei, L. N., Brosius, F. C., Kass, R. S., & Isom, L. L. (2001). Characterization of sodium channel alpha- and beta-subunits in rat and mouse cardiac myocytes. *Circulation* **103**, 1303-1310.

Di Diego, J. M., Sun, Z. Q., & Antzelevitch, C. (1996). $I_{(to)}$ and action potential notch are smaller in left vs. right canine ventricular epicardium. *Am.J.Physiol* **271**, H548-H561.

DiFrancesco, D. (1981). A new interpretation of the pace-maker current in calf Purkinje fibres. *J.Physiol* **314**, 359-376.

DiFrancesco, D. (1993). Pacemaker mechanisms in cardiac tissue. *Annu.Rev.Physiol* **55**, 455-472.

DiFrancesco, D. (1995). The onset and autonomic regulation of cardiac pacemaker activity: relevance of the f current. *Cardiovasc.Res.* **29**, 449-456.

DiFrancesco, D. & Ojeda, C. (1980). Properties of the current I_f in the sino-atrial node of the rabbit compared with those of the current I_K, in Purkinje fibres. *J.Physiol* **308**, 353-367.

Dixon, J. E. & McKinnon, D. (1994). Quantitative analysis of potassium channel mRNA expression in atrial and ventricular muscle of rats. *Circ.Res.* **75**, 252-260.

Dixon, J. E., Shi, W., Wang, H. S., McDonald, C., Yu, H., Wymore, R. S., Cohen, I. S., & McKinnon, D. (1996). Role of the Kv4.3 K^+ channel in ventricular muscle. A molecular correlate for the transient outward current. *Circ.Res.* **79**, 659-668.

Doyle, D. A., Morais, C. J., Pfuetzner, R. A., Kuo, A., Gulbis, J. M., Cohen, S. L., Chait, B. T., & MacKinnon, R. (1998). The structure of the potassium channel: molecular basis of K^+ conduction and selectivity. *Science* **280**, 69-77.

Dudel, J., Peper, K., Rudel, R., & Trautwein, W. (1967). The potassium component of membrane current in Purkinje fibers. *Pflugers Arch.Gesamte Physiol Menschen.Tiere.* **296**, 308-327.

Ehrlich, J. R., Pourrier, M., Weerapura, M., Ethier, N., Marmabachi, A. M., Hebert, T. E., & Nattel, S. (2004). KvLQT1 modulates the distribution and biophysical properties of HERG. A novel alpha-subunit interaction between delayed rectifier currents. *J.Biol.Chem.* **279**, 1233-1241.

England, S. K., Uebele, V. N., Shear, H., Kodali, J., Bennett, P. B., & Tamkun, M. M. (1995). Characterization of a voltage-gated K^+ channel beta subunit expressed in human heart. *Proc.Natl.Acad.Sci.U.S.A* **92**, 6309-6313.

Escande, D., Coulombe, A., Faivre, J. F., Deroubaix, E., & Coraboeuf, E. (1987). Two types of transient outward currents in adult human atrial cells. *Am.J.Physiol* **252**, H142-H148.

Eskinder, H., Supan, F. D., Turner, L. A., Kampine, J. P., & Bosnjak, Z. J. (1993). The effects of halothane and isoflurane on slowly inactivating sodium current in canine cardiac Purkinje cells. *Anesth.Analg.* **77**, 32-37.

Eubanks, J., Srinivasan, J., Dinulos, M. B., Disteche, C. M., & Catterall, W. A. (1997). Structure and chromosomal localization of the beta-2 subunit of the human brain sodium channel. *Neuroreport* **8**, 2775-2779.

Fabiato, A., Fabiato, F. (1975). Contractions induced by a calcium-triggered release of calcium from the sarcoplasmic reticulum of single skinned cardiac cells. *J Physiol.*, **249**, 469-495.

Faggiano P, d'Aloia A, Gualeni A, et al. (2001). Mechanisms and immediate outcome of in-hospital cardiac arrest in patients with advanced heart failure secondary to ischemic or idiopathic dilated cardiomyopathy. *Am J Cardiol.* **87**, 655-665.

Fahmi, A. I., Patel, M., Stevens, E. B., Fowden, A. L., John, J. E., III, Lee, K., Pinnock, R., Morgan, K., Jackson, A. P., & Vandenberg, J. I. (2001). The sodium channel beta-subunit SCN3b modulates the kinetics of SCN5a and is expressed heterogeneously in sheep heart. *J.Physiol* **537**, 693-700.

Fedida, D. & Bouchard, R. A. (1992). Mechanisms for the positive inotropic effect of alpha 1-adrenoceptor stimulation in rat cardiac myocytes. *Circ.Res.* **71**, 673-688.

Fedida, D., Braun, A. P., & Giles, W. R. (1991). Alpha 1-adrenoceptors reduce background K^+ current in rabbit ventricular myocytes. *J.Physiol* **441**, 673-684.

Fedida, D., Shimoni, Y., & Giles, W. R. (1989). A novel effect of norepinephrine on cardiac cells is mediated by alpha 1-adrenoceptors. *Am.J.Physiol* **256**, H1500-H1504.

Fedida, D., Shimoni, Y., & Giles, W. R. (1990). Alpha-adrenergic modulation of the transient outward current in rabbit atrial myocytes. *J.Physiol* **423**, 257-277.

Felipe, A., Knittle, T. J., Doyle, K. L., & Tamkun, M. M. (1994). Primary structure and differential expression during development and pregnancy of a novel voltage-gated sodium channel in the mouse. *J.Biol.Chem.* **269**, 30125-30131.

Feng, J., Yue, L., Wang, Z., & Nattel, S. (1998). Ionic mechanisms of regional action potential heterogeneity in the canine right atrium. *Circ.Res.* **83**, 541-551.

Fermini, B., Wang, Z., Duan, D., & Nattel, S. (1992). Differences in rate dependence of transient outward current in rabbit and human atrium. *Am.J.Physiol* **263**, H1747-H1754.

Fiset, C., Clark, R. B., Shimoni, Y., & Giles, W. R. (1997). Shal-type channels contribute to the Ca^{2+}-independent transient outward K^+ current in rat ventricle. *J.Physiol* **500 (Pt 1)**, 51-64.

Folander, K., Smith, J. S., Antanavage, J., Bennett, C., Stein, R. B., & Swanson, R. (1990). Cloning and expression of the delayed-rectifier IsK channel from neonatal rat heart and diethylstilbestrol-primed rat uterus. *Proc.Natl.Acad.Sci.U.S.A* **87**, 2975-2979.

Follmer, C. H. & Colatsky, T. J. (1990). Block of delayed rectifier potassium current, I_K, by flecainide and E-4031 in cat ventricular myocytes. *Circulation* **82**, 289-293.

Follmer, C. H., ten Eick, R. E., & Yeh, J. Z. (1987). Sodium current kinetics in cat atrial myocytes. *J.Physiol* **384**, 169-197.

Fozzard, H. A. & Beeler, G. W., Jr. (1975). The voltage clamp and cardiac electrophysiology. *Circ.Res.* **37**, 403-413.

Fozzard, H. A. & Hiraoka, M. (1973). The positive dynamic current and its inactivation properties in cardiac Purkinje fibres. *J.Physiol* **234**, 569-586.

Freeman, L. C. & Kass, R. S. (1993a). Delayed rectifier potassium channels in ventricle and sinoatrial node of the guinea pig: molecular and regulatory properties. *Cardiovasc.Drugs Ther.* **7 Suppl 3**, 627-635.

Freeman, L. C. & Kass, R. S. (1993b). Expression of a minimal K^+ channel protein in mammalian cells and immunolocalization in guinea pig heart. *Circ.Res.* **73**, 968-973.

Frelin, C., Cognard, C., Vigne, P., & Lazdunski, M. (1986). Tetrodotoxin-sensitive and tetrodotoxin-resistant Na^+ channels differ in their sensitivity to Cd^{2+} and Zn^{2+}. *Eur.J.Pharmacol.* **122**, 245-250.

Frohnwieser, B., Chen, L. Q., Schreibmayer, W., & Kallen, R. G. (1997). Modulation of the human cardiac sodium channel alpha-subunit by cAMP-dependent protein kinase and the responsible sequence domain. *J.Physiol* **498 (Pt 2)**, 309-318.

Furukawa, T., Kimura, S., Furukawa, N., Bassett, A. L., & Myerburg, R. J. (1992). Potassium rectifier currents differ in myocytes of endocardial and epicardial origin. *Circ.Res.* **70**, 91-103.

Furukawa, T., Myerburg, R. J., Furukawa, N., Bassett, A. L., & Kimura, S. (1990). Differences in transient outward currents of feline endocardial and epicardial myocytes. *Circ.Res.* **67**, 1287-1291.

Furukawa, T., Ono, Y., Tsuchiya, H., Katayama, Y., Bang, M. L., Labeit, D., Labeit, S., Inagaki, N., & Gregorio, C. C. (2001). Specific interaction of the potassium channel beta-subunit minK with the sarcomeric protein T-cap suggests a T-tubule-myofibril linking system. *J.Mol.Biol.* **313**, 775-784.

Garcia-Frigola, C., Shi, Y., & Evans, S. M. (2003). Expression of the hyperpolarization-activated cyclic nucleotide-gated cation channel HCN4 during mouse heart development. *Gene Expr.Patterns.* **3**, 777-783.

Gellens, M. E., George, A. L., Jr., Chen, L. Q., Chahine, M., Horn, R., Barchi, R. L., & Kallen, R. G. (1992). Primary structure and functional expression of the human cardiac tetrodotoxin-insensitive voltage-dependent sodium channel. *Proc.Natl.Acad.Sci.U.S.A* **89**, 554-558.

George, A. L., Jr., Knittle, T. J., & Tamkun, M. M. (1992). Molecular cloning of an atypical voltage-gated sodium channel expressed in human heart and uterus: evidence for a distinct gene family. *Proc.Natl.Acad.Sci.U.S.A* **89**, 4893-4897.

Gershon, E., Weigl, L., Lotan, I., Schreibmayer, W., & Dascal, N. (1992). Protein kinase A reduces voltage-dependent Na^+ current in Xenopus oocytes. *J.Neurosci.* **12**, 3743-3752.

Gidh-Jain, M., Huang, B., Jain, P., & El Sherif, N. (1996). Differential expression of voltage-gated K^+ channel genes in left ventricular remodeled myocardium after experimental myocardial infarction. *Circ.Res.* **79**, 669-675.

Giles, W., Nakajima, T., Ono, K., & Shibata, E. F. (1989). Modulation of the delayed rectifier K^+ current by isoprenaline in bull-frog atrial myocytes. *J.Physiol* **415**, 233-249.

Giles, W. R. & Imaizumi, Y. (1988). Comparison of potassium currents in rabbit atrial and ventricular cells. *J.Physiol* **405**, 123-145.

Gill, C. H., Randall, A., Bates, S. A., Hill, K., Owen, D., Larkman, P.M., Cairns, W., Yusaf, S. P., Murdock, P. R., Strijbos, P. J., Powell, A. J., Benham, C. D., Davies, C. H. (2004) Characterization of the human HCN1 channel and its inhibition by capsazepine.*Br J Pharmacol.* Epub ahead of print.

Gintant, G. A. (1996). Two components of delayed rectifier current in canine atrium and ventricle. Does I_{Ks} play a role in the reverse rate dependence of class III agents? *Circ.Res.* **78**, 26-37.

Gintant, G. A. & Liu, D. W. (1992). Beta-adrenergic modulation of fast inward sodium current in canine myocardium. Syncytial preparations versus isolated myocytes. *Circ.Res.* **70**, 844-850.

Goldstein, S. A. & Miller, C. (1991). Site-specific mutations in a minimal voltage-dependent K^+ channel alter ion selectivity and open-channel block. *Neuron* **7**, 403-408.

Goldstein, S. A. & Miller, C. (1993). Mechanism of charybdotoxin block of a voltage-gated K^+ channel. *Biophys.J.* **65**, 1613-1619.

Gordon, D., Merrick, D., Wollner, D. A., & Catterall, W. A. (1988). Biochemical properties of sodium channels in a wide range of excitable tissues studied with site-directed antibodies. *Biochemistry* **27**, 7032-7038.

Grant, A. O. & Starmer, C. F. (1987). Mechanisms of closure of cardiac sodium channels in rabbit ventricular myocytes: single-channel analysis. *Circ.Res.* **60**, 897-913.

Gravante, B., Barbuti, A., Milanesi, R., Zappi, I., Viscomi, C., & DiFrancesco, D. (2004). Interaction of the pacemaker channel HCN1 with filamin A. *J.Biol.Chem.* **279**, 43847-43853.

Grosson, C. L., Cannon, S. C., Corey, D. P., & Gusella, J. F. (1996). Sequence of the voltage-gated sodium channel beta1-subunit in wild-type and in quivering mice. *Brain Res.Mol.Brain Res.* **42**, 222-226.

Gulch, R. W., Baumann, R., & Jacob, R. (1979). Analysis of myocardial action potential in left ventricular hypertrophy of Goldblatt rats. *Basic Res.Cardiol.* **74**, 69-82.

Guo, J., Mitsuiye, T., & Noma, A. (1997). The sustained inward current in sino-atrial node cells of guinea-pig heart. *Pflugers Arch.* **433**, 390-396.

Guo, W., Kamiya, K., Hojo, M., Kodama, I., & Toyama, J. (1998). Regulation of Kv4.2 and Kv1.4 K^+ channel expression by myocardial hypertrophic factors in cultured newborn rat ventricular cells. *J.Mol.Cell Cardiol.* **30**, 1449-1455.

Guo, W., Li, H., London, B., & Nerbonne, J. M. (2000). Functional consequences of elimination of I(to,f) and I(to,s): early afterdepolarizations, atrioventricular block, and ventricular arrhythmias in mice lacking Kv1.4 and expressing a dominant-negative Kv4 alpha subunit. *Circ.Res.* **87**, 73-79.

Hagiwara, S., Kusano, K., & Saito, N. (1961). Membrane changes of Onchidium nerve cell in potassium-rich media. *J.Physiol* **155**, 470-489.

Haissaguerre, M., Jais, P., Shah, D. C., Takahashi, A., Hocini, M., Quiniou, G., Garrigue, S., Le Mouroux, A., Le Metayer, P., & Clementy, J. (1998). Spontaneous initiation of atrial fibrillation by ectopic beats originating in the pulmonary veins. *N.Engl.J.Med.* **339**, 659-666.

Han, W., Chartier, D., Li, D., & Nattel, S. (2001a). Ionic remodeling of cardiac Purkinje cells by congestive heart failure. *Circulation* **104**, 2095-2100.

Han, W., Wang, Z., & Nattel, S. (2000). A comparison of transient outward currents in canine cardiac Purkinje cells and ventricular myocytes. *Am.J.Physiol Heart Circ.Physiol* **279**, H466-H474.

Han, W., Wang, Z., & Nattel, S. (2001b). Slow delayed rectifier current and repolarization in canine cardiac Purkinje cells. *Am.J.Physiol Heart Circ.Physiol* **280**, H1075-H1080.

Hanck, D. A., Makielski, J. C., & Sheets, M. F. (1994). Kinetic effects of quaternary lidocaine block of cardiac sodium channels: a gating current study. *J.Gen.Physiol* **103**, 19-43.

Hanck, D. A. & Sheets, M. F. (1992). Time-dependent changes in kinetics of Na^+ current in single canine cardiac Purkinje cells. *Am.J.Physiol* **262**, H1197-H1207.

Hancox, J. C., Levi, A. J., & Witchel, H. J. (1998). Time course and voltage dependence of expressed HERG current compared with native "rapid" delayed rectifier K current during the cardiac ventricular action potential. *Pflugers Arch.* **436**, 843-853.

Hartmann, H. A., Kirsch, G. E., Drewe, J. A., Taglialatela, M., Joho, R. H., & Brown, A. M. (1991). Exchange of conduction pathways between two related K^+ channels. *Science* **251**, 942-944.

Hauswirth, O., Noble, D., & Tsien, R. W. (1968). Adrenaline: mechanism of action on the pacemaker potential in cardiac Purkinje fibers. *Science* **162**, 916-917.

Heath, B. M. & Terrar, D. A. (1996). Separation of the components of the delayed rectifier potassium current using selective blockers of I_{Kr} and I_{Ks} in guinea-pig isolated ventricular myocytes. *Exp.Physiol* **81**, 587-603.

Heath, B. M. & Terrar, D. A. (2000). Protein kinase C enhances the rapidly activating delayed rectifier potassium current, I_{Kr}, through a reduction in C-type inactivation in guinea-pig ventricular myocytes. *J.Physiol* **522 Pt 3**, 391-402.

Heginbotham, L., Lu, Z., Abramson, T., & MacKinnon, R. (1994). Mutations in the K^+ channel signature sequence. *Biophys.J.* **66**, 1061-1067.

Heinemann, S. H., Terlau, H., Stuhmer, W., Imoto, K., & Numa, S. (1992). Calcium channel characteristics conferred on the sodium channel by single mutations. *Nature* **356**, 441-443.

Himmel, H. M., Wettwer, E., Li, Q., & Ravens, U. (1999). Four different components contribute to outward current in rat ventricular myocytes. *Am.J.Physiol* **277**, H107-H118.

Ho, W. K., Brown, H. F., & Noble, D. (1994). High selectivity of the I_f channel to Na^+ and K^+ in rabbit isolated sinoatrial node cells. *Pflugers Arch.* **426**, 68-74.

Hodgkin, A. L. & Huxley, A. F. (1952). A quantitative description of membrane current and its application to conduction and excitation in nerve. *J.Physiol* **117**, 500-544.

Holmgren, M., Shin, K. S., & Yellen, G. (1998). The activation gate of a voltage-gated K^+ channel can be trapped in the open state by an intersubunit metal bridge. *Neuron* **21**, 617-621.

Hondeghem, L. M. & Snyders, D. J. (1990). Class III antiarrhythmic agents have a lot of potential but a long way to go. Reduced effectiveness and dangers of reverse use dependence. *Circulation* **81**, 686-690.

Honore, E., Attali, B., Romey, G., Heurteaux, C., Ricard, P., Lesage, F., Lazdunski, M., & Barhanin, J. (1991). Cloning, expression, pharmacology and regulation of a delayed rectifier K^+ channel in mouse heart. *EMBO J.* **10**, 2805-2811.

Hoppe, U. C., Marban, E., & Johns, D. C. (2000). Molecular dissection of cardiac repolarization by in vivo Kv4.3 gene transfer. *J.Clin.Invest* **105**, 1077-1084.

Hoshi, T., Zagotta, W. N., & Aldrich, R. W. (1990). Biophysical and molecular mechanisms of Shaker potassium channel inactivation. *Science* **250**, 533-538.

Howarth, F. C., Levi, A. J., & Hancox, J. C. (1996). Characteristics of the delayed rectifier K current compared in myocytes isolated from the atrioventricular node and ventricle of the rabbit heart. *Pflugers Arch.* **431**, 713-722.

Huang, B., El Sherif, T., Gidh-Jain, M., Qin, D., & El Sherif, N. (2001). Alterations of sodium channel kinetics and gene expression in the postinfarction remodeled myocardium. *J.Cardiovasc.Electrophysiol.* **12**, 218-225.

Inoue, M. & Imanaga, I. (1993). Masking of A-type K^+ channel in guinea pig cardiac cells by extracellular Ca^{2+}. *Am.J.Physiol* **264**, C1434-C1438.

Irisawa, H., Brown, H. F., & Giles, W. (1993). Cardiac pacemaking in the sinoatrial node. *Physiol Rev.* **73**, 197-227.

Isacoff, E. Y., Jan, Y. N., & Jan, L. Y. (1991). Putative receptor for the cytoplasmic inactivation gate in the Shaker K^+ channel. *Nature* **353**, 86-90.

Isenberg, G. (1976). Cardiac Purkinje fibers: cesium as a tool to block inward rectifying potassium currents. *Pflugers Arch.* **365**, 99-106.

Ishii, T. M., Takano, M., Xie, L. H., Noma, A., & Ohmori, H. (1999). Molecular characterization of the hyperpolarization-activated cation channel in rabbit heart sinoatrial node. *J.Biol.Chem.* **274**, 12835-12839.

Isom, L. L. (2001). Sodium channel beta subunits: anything but auxiliary. *Neuroscientist.* **7**, 42-54.

Isom, L. L., De Jongh, K. S., Patton, D. E., Reber, B. F., Offord, J., Charbonneau, H., Walsh, K., Goldin, A. L., & Catterall, W. A. (1992). Primary structure and functional expression of the beta 1 subunit of the rat brain sodium channel. *Science* **256**, 839-842.

Isom, L. L., Ragsdale, D. S., De Jongh, K. S., Westenbroek, R. E., Reber, B. F., Scheuer, T., & Catterall, W. A. (1995). Structure and function of the beta 2 subunit of brain sodium channels, a transmembrane glycoprotein with a CAM motif. *Cell* **83**, 433-442.

January, C. T., Riddle, J. M. (1989). Early afterdepolarizations: mechanism of induction and block. A role for L-type Ca^{2+} current. *Circ Res.* **64**, 977-990.

Jessup, M. & Brozena, S. (2003). Heart failure. *N.Engl.J.Med.* **348**, 2007-2018.

Jiang, M., Tseng-Crank, J., & Tseng, G. N. (1997). Suppression of slow delayed rectifier current by a truncated isoform of KvLQT1 cloned from normal human heart. *J.Biol.Chem.* **272**, 24109-24112.

Jurkiewicz, N. K. & Sanguinetti, M. C. (1993). Rate-dependent prolongation of cardiac action potentials by a methanesulfonanilide class III antiarrhythmic agent. Specific block of rapidly activating delayed rectifier K^+ current by dofetilide. *Circ.Res.* **72**, 75-83.

Jurkiewicz, N. K., Wang, J., Fermini, B., Sanguinetti, M. C., & Salata, J. J. (1996). Mechanism of action potential prolongation by RP 58866 and its active enantiomer, terikalant. Block of the rapidly activating delayed rectifier K^+ current, I_{Kr}. *Circulation* **94**, 2938-2946.

Kaab, S., Dixon, J., Duc, J., Ashen, D., Nabauer, M., Beuckelmann, D. J., Steinbeck, G., McKinnon, D., & Tomaselli, G. F. (1998). Molecular basis of transient outward potassium current downregulation in human heart failure: a decrease in Kv4.3 mRNA correlates with a reduction in current density. *Circulation* **98**, 1383-1393.

Kaab, S., Nuss, H. B., Chiamvimonvat, N., O'Rourke, B., Pak, P. H., Kass, D. A., Marban, E., & Tomaselli, G. F. (1996). Ionic mechanism of action potential prolongation in ventricular myocytes from dogs with pacing-induced heart failure. *Circ.Res.* **78**, 262-273.

Kaprielian, R., Wickenden, A. D., Kassiri, Z., Parker, T. G., Liu, P. P., & Backx, P. H. (1999). Relationship between K^+ channel down-regulation and $[Ca^{2+}]_i$ in rat ventricular myocytes following myocardial infarction. *J.Physiol* **517 (Pt 1)**, 229-245.

Kathofer, S., Rockl, K., Zhang, W., Thomas, D., Katus, H., Kiehn, J., Kreye, V., Schoels, W., & Karle, C. (2003). Human beta(3)-adrenoreceptors couple to KvLQT1/MinK potassium channels in Xenopus oocytes via protein kinase C phosphorylation of the KvLQT1 protein. *Naunyn Schmiedebergs Arch.Pharmacol.* **368**, 119-126.

Kenyon, J. L. & Gibbons, W. R. (1979a). 4-Aminopyridine and the early outward current of sheep cardiac Purkinje fibers. *J.Gen.Physiol* **73**, 139-157.

Kenyon, J. L. & Gibbons, W. R. (1979b). Influence of chloride, potassium, and tetraethylammonium on the early outward current of sheep cardiac Purkinje fibers. *J.Gen.Physiol* **73**, 117-138.

Kerr, C. R., Boone, J., Connolly, S. J., Dorian, P., Green, M., Klein, G., Newman, D., Sheldon, R., & Talajic, M. (1998). The Canadian Registry of Atrial Fibrillation: a noninterventional follow-up of patients after the first diagnosis of atrial fibrillation. *Am.J.Cardiol.* **82**, 82N-85N.

Khairy, P. & Nattel, S. (2002). New insights into the mechanisms and management of atrial fibrillation. *CMAJ.* **167**, 1012-1020.

Kiehn, J., Lacerda, A. E., Wible, B., & Brown, A. M. (1996). Molecular physiology and pharmacology of HERG. Single-channel currents and block by dofetilide. *Circulation* **94**, 2572-2579.

Kimura, K., Kitano, J., Nakajima, Y., & Nakanishi, S. (2004). Hyperpolarization-activated, cyclic nucleotide-gated HCN2 cation channel forms a protein assembly with multiple neuronal scaffold proteins in distinct modes of protein-protein interaction. *Genes Cells* **9**, 631-640.

Kirchhof, P., Eckardt, L., Franz, M. R., Monnig, G., Loh, P., Wedekind, H., Schulze-Bahr, E., Breithardt, G., & Haverkamp, W. (2003). Prolonged atrial action potential durations and polymorphic atrial tachyarrhythmias in patients with long QT syndrome. *J.Cardiovasc.Electrophysiol.* **14**, 1027-1033.

Kiyosue, T. & Arita, M. (1989). Late sodium current and its contribution to action potential configuration in guinea pig ventricular myocytes. *Circ.Res.* **64**, 389-397.

Konarzewska, H., Peeters, G. A., & Sanguinetti, M. C. (1995). Repolarizing K^+ currents in nonfailing human hearts. Similarities between right septal subendocardial and left subepicardial ventricular myocytes. *Circulation* **92**, 1179-1187.

Kontis, K. J. & Goldin, A. L. (1997). Sodium channel inactivation is altered by substitution of voltage sensor positive charges. *J.Gen.Physiol* **110**, 403-413.

Kontis, K. J., Rounaghi, A., & Goldin, A. L. (1997). Sodium channel activation gating is affected by substitutions of voltage sensor positive charges in all four domains. *J.Gen.Physiol* **110**, 391-401.

Kuo, H. C., Cheng, C. F., Clark, R. B., Lin, J. J., Lin, J. L., Hoshijima, M., Nguyen-Tran, V. T., Gu, Y., Ikeda, Y., Chu, P. H., Ross, J., Giles, W. R., & Chien, K. R. (2001). A defect in the Kv channel-interacting protein 2 (KChIP2) gene leads to a complete loss of I_{to} and confers susceptibility to ventricular tachycardia. *Cell* **107**, 801-813.

Kupershmidt, S., Yang, T., Anderson, M. E., Wessels, A., Niswender, K. D., Magnuson, M. A., & Roden, D. M. (1999). Replacement by homologous recombination of the minK gene with lacZ reveals restriction of minK expression to the mouse cardiac conduction system. *Circ.Res.* **84**, 146-152.

Kupershmidt, S., Yang, T., & Roden, D. M. (1998). Modulation of cardiac Na^+ current phenotype by beta1-subunit expression. *Circ.Res.* **83**, 441-447.

Kuryshev, Y. A., Gudz, T. I., Brown, A. M., & Wible, B. A. (2000). KChAP as a chaperone for specific K^+ channels. *Am.J.Physiol Cell Physiol* **278**, C931-C941.

Kus, T. & Sasyniuk, B. I. (1975). Electrophysiological actions of disopyramide phosphate on canine ventricular muscle and purkinje fibers. *Circ.Res.* **37**, 844-854.

Lai, L. P., Su, M. J., Yeh, H. M., Lin, J. L., Chiang, F. T., Hwang, J. J., Hsu, K. L., Tseng, C. D., Lien, W. P., Tseng, Y. Z., & Huang, S. K. (2002). Association of the human minK gene 38G allele with atrial fibrillation: evidence of possible genetic control on the pathogenesis of atrial fibrillation. *Am.Heart J.* **144**, 485-490.

Lee, J. H. & Rosen, M. R. (1994). Alpha 1-adrenergic receptor modulation of repolarization in canine Purkinje fibers. *J.Cardiovasc.Electrophysiol.* **5**, 232-240.

Lee, J. K., Kodama, I., Honjo, H., Anno, T., Kamiya, K., & Toyama, J. (1997). Stage-dependent changes in membrane currents in rats with monocrotaline-induced right ventricular hypertrophy. *Am.J.Physiol* **272**, H2833-H2842.

Lee, K. S., Weeks, T. A., Kao, R. L., Akaike, N., & Brown, A. M. (1979). Sodium current in single heart muscle cells. *Nature* **278**, 269-271.

Lees-Miller, J. P., Duan, Y., Teng, G. Q., & Duff, H. J. (2000). Molecular determinant of high-affinity dofetilide binding to HERG1 expressed in Xenopus oocytes: involvement of S6 sites. *Mol.Pharmacol.* **57**, 367-374.

Lees-Miller, J. P., Kondo, C., Wang, L., & Duff, H. J. (1997). Electrophysiological characterization of an alternatively processed ERG K^+ channel in mouse and human hearts. *Circ.Res.* **81**, 719-726.

Lesage, F., Attali, B., Lazdunski, M., & Barhanin, J. (1992). IsK, a slowly activating voltage-sensitive K^+ channel. Characterization of multiple cDNAs and gene organization in the mouse. *FEBS Lett.* **301**, 168-172.

Li, D., Melnyk, P., Feng, J., Wang, Z., Petrecca, K., Shrier, A., & Nattel, S. (2000a). Effects of experimental heart failure on atrial cellular and ionic electrophysiology. *Circulation* **101**, 2631-2638.

Li, D., Zhang, L., Kneller, J., & Nattel, S. (2001). Potential ionic mechanism for repolarization differences between canine right and left atrium. *Circ.Res.* **88**, 1168-1175.

Li, G. R., Feng, J., Yue, L., & Carrier, M. (1998a). Transmural heterogeneity of action potentials and Itol in myocytes isolated from the human right ventricle. *Am.J.Physiol* **275**, H369-H377.

Li, G. R., Feng, J., Yue, L., Carrier, M., & Nattel, S. (1996). Evidence for two components of delayed rectifier K^+ current in human ventricular myocytes. *Circ.Res.* **78**, 689-696.

Li, G. R., Lau, C. P., Ducharme, A., Tardif, J. C., & Nattel, S. (2002a). Transmural action potential and ionic current remodeling in ventricles of failing canine hearts. *Am.J.Physiol Heart Circ.Physiol* **283**, H1031-H1041.

Li, G. R., Lau, C. P., & Shrier, A. (2002b). Heterogeneity of sodium current in atrial vs epicardial ventricular myocytes of adult guinea pig hearts. *J.Mol.Cell Cardiol.* **34**, 1185-1194.

Li, G. R., Sun, H., & Nattel, S. (1998b). Characterization of a transient outward K^+ current with inward rectification in canine ventricular myocytes. *Am.J.Physiol* **274**, C577-C585.

Li, G. R., Yang, B., Sun, H., & Baumgarten, C. M. (2000b). Existence of a transient outward K^+ current in guinea pig cardiac myocytes. *Am.J.Physiol Heart Circ.Physiol* **279**, H130-H138.

Litovsky, S. H. & Antzelevitch, C. (1988). Transient outward current prominent in canine ventricular epicardium but not endocardium. *Circ.Res.* **62**, 116-126.

Litovsky, S. H. & Antzelevitch, C. (1989). Rate dependence of action potential duration and refractoriness in canine ventricular endocardium differs from that of epicardium: role of the transient outward current. *J.Am.Coll.Cardiol.* **14**, 1053-1066.

Liu, D. W. & Antzelevitch, C. (1995). Characteristics of the delayed rectifier current (I_{Kr} and I_{Ks}) in canine ventricular epicardial, midmyocardial, and endocardial myocytes. A weaker I_{Ks} contributes to the longer action potential of the M cell. *Circ.Res.* **76**, 351-365.

Liu, D. W., Gintant, G. A., & Antzelevitch, C. (1993). Ionic bases for electrophysiological distinctions among epicardial, midmyocardial, and endocardial myocytes from the free wall of the canine left ventricle. *Circ.Res.* **72**, 671-687.

Liu, Y., Jurman, M. E., & Yellen, G. (1996). Dynamic rearrangement of the outer mouth of a K^+ channel during gating. *Neuron* **16**, 859-867.

Liu, Y. M., DeFelice, L. J., & Mazzanti, M. (1992). Na channels that remain open throughout the cardiac action potential plateau. *Biophys.J.* **63**, 654-662.

Lombet, A. & Lazdunski, M. (1984). Characterization, solubilization, affinity labeling and purification of the cardiac Na^+ channel using Tityus toxin gamma. *Eur.J.Biochem.* **141**, 651-660.

London, B., Trudeau, M. C., Newton, K. P., Beyer, A. K., Copeland, N. G., Gilbert, D. J., Jenkins, N. A., Satler, C. A., & Robertson, G. A. (1997). Two isoforms of the mouse ether-a-go-go-related gene coassemble to form channels with properties similar to the rapidly activating component of the cardiac delayed rectifier K^+ current. *Circ.Res.* **81**, 870-878.

London, B., Wang, D. W., Hill, J. A., & Bennett, P. B. (1998). The transient outward current in mice lacking the potassium channel gene Kv1.4. *J.Physiol* **509 (Pt 1)**, 171-182.

Lopez-Barneo, J., Hoshi, T., Heinemann, S. H., & Aldrich, R. W. (1993). Effects of external cations and mutations in the pore region on C-type inactivation of Shaker potassium channels. *Receptors.Channels* **1**, 61-71.

Lu, T., Lee, H. C., Kabat, J. A., & Shibata, E. F. (1999). Modulation of rat cardiac sodium channel by the stimulatory G protein alpha subunit. *J.Physiol* **518 (Pt 2)**, 371-384.

Lu, Z., Kamiya, K., Opthof, T., Yasui, K., & Kodama, I. (2001). Density and kinetics of I_{Kr} and I_{Ks} in guinea pig and rabbit ventricular myocytes explain different efficacy of I_{Ks} blockade at high heart rate in guinea pig and rabbit: implications for arrhythmogenesis in humans. *Circulation* **104**, 951-956.

Ludwig, A., Zong, X., Jeglitsch, M., Hofmann, F., & Biel, M. (1998). A family of hyperpolarization-activated mammalian cation channels. *Nature* **393**, 587-591.

Ludwig, A., Zong, X., Stieber, J., Hullin, R., Hofmann, F., & Biel, M. (1999). Two pacemaker channels from human heart with profoundly different activation kinetics. *EMBO J.* **18**, 2323-2329.

Luo, C. H., Rudy, Y. (1994a). A dynamic model of the cardiac ventricular action potential. I. Simulations of ionic currents and concentration changes. *Circ Res.* **74**, 1071-1096.

Luo, C. H., Rudy, Y. (1994b). A dynamic model of the cardiac ventricular action potential. II. Afterdepolarizations, triggered activity, and potentiation. *Circ Res.***74**, 1097-1113.

Lupoglazoff, J. M., Cheav, T., Baroudi, G., Berthet, M., Denjoy, I., Cauchemez, B., Extramiana, F., Chahine, M., & Guicheney, P. (2001). Homozygous SCN5A mutation in long-QT syndrome with functional two-to-one atrioventricular block. *Circ.Res.* **89**, E16-E21.

MacKinnon, R. (1995). Pore loops: an emerging theme in ion channel structure. *Neuron* **14**, 889-892.

MacKinnon, R. & Doyle, D. A. (1997). Prokaryotes offer hope for potassium channel structural studies. *Nat.Struct.Biol.* **4**, 877-879.

MacKinnon, R., Reinhart, P. H., & White, M. M. (1988). Charybdotoxin block of Shaker K^+ channels suggests that different types of K^+ channels share common structural features. *Neuron* **1**, 997-1001.

MacKinnon, R. & Yellen, G. (1990). Mutations affecting TEA blockade and ion permeation in voltage-activated K^+ channels. *Science* **250**, 276-279.

Maier, S. K., Westenbroek, R. E., McCormick, K. A., Curtis, R., Scheuer, T., & Catterall, W. A. (2004). Distinct subcellular localization of different sodium channel alpha and beta subunits in single ventricular myocytes from mouse heart. *Circulation* **109**, 1421-1427.

Maier, S. K., Westenbroek, R. E., Schenkman, K. A., Feigl, E. O., Scheuer, T., & Catterall, W. A. (2002). An unexpected role for brain-type sodium channels in coupling of cell surface depolarization to contraction in the heart. *Proc.Natl.Acad.Sci.U.S.A.* **99**, 4073-4078.

Majumder, K., De Biasi, M., Wang, Z., & Wible, B. A. (1995). Molecular cloning and functional expression of a novel potassium channel beta-subunit from human atrium. *FEBS Lett.* **361**, 13-16.

Makielski, J. C., Limberis, J. T., Chang, S. Y., Fan, Z., & Kyle, J. W. (1996). Coexpression of beta 1 with cardiac sodium channel alpha subunits in oocytes decreases lidocaine block. *Mol.Pharmacol.* **49**, 30-39.

Makielski, J. C., Sheets, M. F., Hanck, D. A., January, C. T., & Fozzard, H. A. (1987). Sodium current in voltage clamped internally perfused canine cardiac Purkinje cells. *Biophys.J.* **52**, 1-11.

Makita, N., Bennett, P. B., Jr., & George, A. L., Jr. (1994). Voltage-gated Na^+ channel beta 1 subunit mRNA expressed in adult human skeletal muscle, heart, and brain is encoded by a single gene. *J.Biol.Chem.* **269**, 7571-7578.

Malfatto, G., Rosen, T. S., Rosen, M. R. (1988). The response to overdrive pacing of triggered atrial and ventricular arrhythmias in the canine heart. *Circulation.* **77**, 1139-1148.

Malhotra, J. D., Kazen-Gillespie, K., Hortsch, M., & Isom, L. L. (2000). Sodium channel beta subunits mediate homophilic cell adhesion and recruit ankyrin to points of cell-cell contact. *J.Biol.Chem.* **275**, 11383-11388.

Maltsev, V. A., Sabbab, H. N., & Undrovinas, A. I. (2002). Down-regulation of sodium current in chronic heart failure: effect of long-term therapy with carvedilol. *Cell Mol.Life Sci.* **59**, 1561-1568.

Maltsev, V. A., Sabbah, H. N., Higgins, R. S., Silverman, N., Lesch, M., & Undrovinas, A. I. (1998). Novel, ultraslow inactivating sodium current in human ventricular cardiomyocytes. *Circulation* **98**, 2545-2552.

Mandapati, R., Skanes, A., Chen, J., Berenfeld, O., & Jalife, J. (2000). Stable microreentrant sources as a mechanism of atrial fibrillation in the isolated sheep heart. *Circulation* **101**, 194-199.

Marban, E. (1999). Heart failure: the electrophysiologic connection. *J.Cardiovasc.Electrophysiol.* **10**, 1425-1428.

Marx, S. O., Kurokawa, J., Reiken, S., Motoike, H., D'Armiento, J., Marks, A. R., & Kass, R. S. (2002). Requirement of a macromolecular signaling complex for beta adrenergic receptor modulation of the KCNQ1-KCNE1 potassium channel. *Science* **295**, 496-499.

Matsuda, J. J., Lee, H., & Shibata, E. F. (1992). Enhancement of rabbit cardiac sodium channels by beta-adrenergic stimulation. *Circ.Res.* **70**, 199-207.

McClatchey, A. I., Cannon, S. C., Slaugenhaupt, S. A., & Gusella, J. F. (1993). The cloning and expression of a sodium channel beta 1-subunit cDNA from human brain. *Hum.Mol.Genet.* **2**, 745-749.

McDonald, T. V., Yu, Z., Ming, Z., Palma, E., Meyers, M. B., Wang, K. W., Goldstein, S. A., & Fishman, G. I. (1997). A minK-HERG complex regulates the cardiac potassium current I_{Kr}. *Nature* **388**, 289-292.

McKinnon, D. (1999). Molecular identity of I_{to}: Kv1.4 redux. *Circ.Res.* **84**, 620-622.

Mitcheson, J. S. & Hancox, J. C. (1997). Modulation by mexiletine of action potentials, L-type Ca current and delayed rectifier K current recorded from isolated rabbit atrioventricular nodal myocytes. *Pflugers Arch.* **434**, 855-858.

Mitcheson, J. S. & Sanguinetti, M. C. (1999). Biophysical properties and molecular basis of cardiac rapid and slow delayed rectifier potassium channels. *Cell Physiol Biochem.* **9**, 201-216.

Mitrovic, N., George, A. L., Jr., & Horn, R. (1998). Independent versus coupled inactivation in sodium channels. Role of the domain 2 S4 segment. *J.Gen.Physiol* **111**, 451-462.

Mitsuiye, T. & Noma, A. (1992). Exponential activation of the cardiac Na^+ current in single guinea-pig ventricular cells. *J.Physiol* **453**, 261-277.

Moorman, J. R., Kirsch, G. E., Lacerda, A. E., & Brown, A. M. (1989). Angiotensin II modulates cardiac Na^+ channels in neonatal rat. *Circ.Res.* **65**, 1804-1809.

Moosmang, S., Stieber, J., Zong, X., Biel, M., Hofmann, F., & Ludwig, A. (2001). Cellular expression and functional characterization of four hyperpolarization-activated pacemaker channels in cardiac and neuronal tissues. *Eur.J.Biochem.* **268**, 1646-1652.

Morales, M. J., Castellino, R. C., Crews, A. L., Rasmusson, R. L., & Strauss, H. C. (1995). A novel beta subunit increases rate of inactivation of specific voltage-gated potassium channel alpha subunits. *J.Biol.Chem.* **270**, 6272-6277.

Morgan, K., Stevens, E. B., Shah, B., Cox, P. J., Dixon, A. K., Lee, K., Pinnock, R. D., Hughes, J., Richardson, P. J., Mizuguchi, K., & Jackson, A. P. (2000). beta 3: an additional auxiliary subunit of the voltage-sensitive sodium channel that modulates channel gating with distinct kinetics. *Proc.Natl.Acad.Sci.U.S.A* **97**, 2308-2313.

Moroni, A., Barbuti, A., Altomare, C., Viscomi, C., Morgan, J., Baruscotti, M., & DiFrancesco, D. (2000). Kinetic and ionic properties of the human HCN2 pacemaker channel. *Pflugers Arch.* **439**, 618-626.

Moroni, A., Gorza, L., Beltrame, M., Gravante, B., Vaccari, T., Bianchi, M. E., Altomare, C., Longhi, R., Heurteaux, C., Vitadello, M., Malgaroli, A., & DiFrancesco, D. (2001). Hyperpolarization-activated cyclic nucleotide-gated channel 1 is a molecular determinant of the cardiac pacemaker current I_f. *J.Biol.Chem.* **276**, 29233-29241.

Mounsey, J. P. & DiMarco, J. P. (2000). Cardiovascular drugs. Dofetilide. *Circulation* **102**, 2665-2670.

Murphy, B. J., Rogers, J., Perdichizzi, A. P., Colvin, A. A., & Catterall, W. A. (1996). cAMP-dependent phosphorylation of two sites in the alpha subunit of the cardiac sodium channel. *J.Biol.Chem.* **271**, 28837-28843.

Murray, K. T., Fahrig, S. A., Deal, K. K., Po, S. S., Hu, N. N., Snyders, D. J., Tamkun, M. M., & Bennett, P. B. (1994). Modulation of an inactivating human cardiac K^+ channel by protein kinase C. *Circ.Res.* **75**, 999-1005.

Murray, K. T., Hu, N. N., Daw, J. R., Shin, H. G., Watson, M. T., Mashburn, A. B., & George, A. L., Jr. (1997). Functional effects of protein kinase C activation on the human cardiac Na^+ channel. *Circ.Res.* **80**, 370-376.

Nabauer, M., Beuckelmann, D. J., & Erdmann, E. (1993). Characteristics of transient outward current in human ventricular myocytes from patients with terminal heart failure. *Circ.Res.* **73**, 386-394.

Nabauer, M., Beuckelmann, D. J., Uberfuhr, P., & Steinbeck, G. (1996). Regional differences in current density and rate-dependent properties of the transient outward current in subepicardial and subendocardial myocytes of human left ventricle. *Circulation* **93**, 168-177.

Nakamura, T. Y., Coetzee, W. A., Vega-Saenz, D. M., Artman, M., & Rudy, B. (1997). Modulation of Kv4 channels, key components of rat ventricular transient outward K^+ current, by PKC. *Am.J.Physiol* **273**, H1775-H1786.

Nakamura, T. Y., Pountney, D. J., Ozaita, A., Nandi, S., Ueda, S., Rudy, B., & Coetzee, W. A. (2001). A role for frequenin, a Ca^{2+}-binding protein, as a regulator of Kv4 K^+-currents. *Proc.Natl.Acad.Sci.U.S.A* **98**, 12808-12813.

Nakashima, H., Gerlach, U., Schmidt, D., & Nattel, S. (2004). In vivo electrophysiological effects of a selective slow delayed-rectifier potassium channel blocker in anesthetized dogs: potential insights into class III actions. *Cardiovasc.Res.* **61**, 705-714.

Nakayama, T. & Fozzard, H. A. (1988). Adrenergic modulation of the transient outward current in isolated canine Purkinje cells. *Circ.Res.* **62**, 162-172.

Nakayama, T. & Irisawa, H. (1985). Transient outward current carried by potassium and sodium in quiescent atrioventricular node cells of rabbits. *Circ.Res.* **57**, 65-73.

Nakayama, T., Palfrey, C., & Fozzard, H. A. (1989). Modulation of the cardiac transient outward current by catecholamines. *J.Mol.Cell Cardiol.* **21 Suppl 1**, 109-118.

Nattel, S. (2002). New ideas about atrial fibrillation 50 years on. *Nature* **415**, 219-226.

Nattel, S., Quantz, M. A. (1988). Pharmacological response of quinidine induced early afterdepolarisations in canine cardiac Purkinje fibres: insights into underlying ionic mechanisms. *Cardiovasc Res.* **198822**, 808-817.

Neher, E. & Sakmann, B. (1976). Single-channel currents recorded from membrane of denervated frog muscle fibres. *Nature* **260**, 799-802.

Nerbonne, J. M. (2000). Molecular basis of functional voltage-gated K^+ channel diversity in the mammalian myocardium. *J.Physiol* **525 Pt 2**, 285-298.

Nitta, J., Furukawa, T., Marumo, F., Sawanobori, T., & Hiraoka, M. (1994). Subcellular mechanism for Ca^{2+}-dependent enhancement of delayed rectifier K^+ current in isolated membrane patches of guinea pig ventricular myocytes. *Circ.Res.* **74**, 96-104.

Noble, D. & Tsien, R. W. (1968). The kinetics and rectifier properties of the slow potassium current in cardiac Purkinje fibres. *J.Physiol* **195**, 185-214.

Noble, D. & Tsien, R. W. (1969). Outward membrane currents activated in the plateau range of potentials in cardiac Purkinje fibres. *J.Physiol* **200**, 205-231.

Noda, M., Ikeda, T., Kayano, T., Suzuki, H., Takeshima, H., Kurasaki, M., Takahashi, H., & Numa, S. (1986). Existence of distinct sodium channel messenger RNAs in rat brain. *Nature* **320**, 188-192.

Noda, M., Shimizu, S., Tanabe, T., Takai, T., Kayano, T., Ikeda, T., Takahashi, H., Nakayama, H., Kanaoka, Y., Minamino, N., & . (1984). Primary structure of Electrophorus electricus sodium channel deduced from cDNA sequence. *Nature* **312**, 121-127.

Noma, A. & Irisawa, H. (1976a). A time- and voltage-dependent potassium current in the rabbit sinoatrial node cell. *Pflugers Arch.* **366**, 251-258.

Noma, A. & Irisawa, H. (1976b). Membrane currents in the rabbit sinoatrial node cell as studied by the double microelectrode method. *Pflugers Arch.* **364**, 45-52.

Nuss, H. B., Kaab, S., Kass, D. A., et al. (1999). Cellular basis of ventricular arrhythmias and abnormal automaticity in heart failure. *Am J Physiol.* **277**, H80-H91.

Nuss, H. B., Chiamvimonvat, N., Perez-Garcia, M. T., Tomaselli, G. F., & Marban, E. (1995). Functional association of the beta 1 subunit with human cardiac (hH1) and rat skeletal muscle (mu 1) sodium channel alpha subunits expressed in Xenopus oocytes. *J.Gen.Physiol* **106**, 1171-1191.

Ohya, S., Morohashi, Y., Muraki, K., Tomita, T., Watanabe, M., Iwatsubo, T., & Imaizumi, Y. (2001). Molecular cloning and expression of the novel splice variants of K^+ channel-interacting protein 2. *Biochem.Biophys.Res.Commun.* **282**, 96-102.

Ono, K., Fozzard, H. A., & Hanck, D. A. (1993). Mechanism of cAMP-dependent modulation of cardiac sodium channel current kinetics. *Circ.Res.* **72**, 807-815.

Ono, K. & Ito, H. (1995). Role of rapidly activating delayed rectifier K^+ current in sinoatrial node pacemaker activity. *Am.J.Physiol* **269**, H453-H462.

Opthof, T., Coronel, R., Rademaker, H. M., Vermeulen, J. T., Wilms-Schopman, F. J., & Janse, M. J. (2000). Changes in sinus node function in a rabbit model of heart failure with ventricular arrhythmias and sudden death. *Circulation* **101**, 2975-2980.

Oudit, G. Y., Kassiri, Z., Sah, R., Ramirez, R. J., Zobel, C., & Backx, P. H. (2001). The molecular physiology of the cardiac transient outward potassium current (I(to)) in normal and diseased myocardium. *J.Mol.Cell Cardiol.* **33**, 851-872.

Panyi, G., Sheng, Z., & Deutsch, C. (1995). C-type inactivation of a voltage-gated K^+ channel occurs by a cooperative mechanism. *Biophys.J.* **69**, 896-903.

Papazian, D. M., Schwarz, T. L., Tempel, B. L., Jan, Y. N., & Jan, L. Y. (1987). Cloning of genomic and complementary DNA from Shaker, a putative potassium channel gene from Drosophila. *Science* **237**, 749-753.

Parker, C., Li, Q., & Fedida, D. (1999). Non-specific action of methoxamine on I_{to}, and the cloned channels hKv 1.5 and Kv 4.2. *Br.J.Pharmacol.* **126**, 595-606.

Pascual, J. M., Shieh, C. C., Kirsch, G. E., & Brown, A. M. (1995). Multiple residues specify external tetraethylammonium blockade in voltage-gated potassium channels. *Biophys.J.* **69**, 428-434.

Patel, S. P., Campbell, D. L., Morales, M. J., & Strauss, H. C. (2002). Heterogeneous expression of KChIP2 isoforms in the ferret heart. *J.Physiol* **539**, 649-656.

Patlak, J. B. & Ortiz, M. (1985). Slow currents through single sodium channels of the adult rat heart. *J.Gen.Physiol* **86**, 89-104.

Patton, D. E., West, J. W., Catterall, W. A., & Goldin, A. L. (1992). Amino acid residues required for fast Na(+)-channel inactivation: charge neutralizations and deletions in the III-IV linker. *Proc.Natl.Acad.Sci.U.S.A* **89**, 10905-10909.

Peper, K. & Trautwein, W. (1969). A note on the pacemaker current in Purkinje fibers. *Pflugers Arch.* **309**, 356-361.

Pereon, Y., Demolombe, S., Baro, I., Drouin, E., Charpentier, F., & Escande, D. (2000). Differential expression of KvLQT1 isoforms across the human ventricular wall. *Am.J.Physiol Heart Circ.Physiol* **278**, H1908-H1915.

Perez-Garcia, M. T., Chiamvimonvat, N., Marban, E., & Tomaselli, G. F. (1996). Structure of the sodium channel pore revealed by serial cysteine mutagenesis. *Proc.Natl.Acad.Sci.U.S.A* **93**, 300-304.

Perez-Garcia, M. T., Chiamvimonvat, N., Ranjan, R., Balser, J. R., Tomaselli, G. F., & Marban, E. (1997). Mechanisms of sodium/calcium selectivity in sodium channels probed by cysteine mutagenesis and sulfhydryl modification. *Biophys.J.* **72**, 989-996.

Petrecca, K., Amellal, F., Laird, D. W., Cohen, S. A., & Shrier, A. (1997). Sodium channel distribution within the rabbit atrioventricular node as analysed by confocal microscopy. *J.Physiol* **501 (Pt 2)**, 263-274.

Petrecca, K., Miller, D. M., & Shrier, A. (2000). Localization and enhanced current density of the Kv4.2 potassium channel by interaction with the actin-binding protein filamin. *J.Neurosci.* **20**, 8736-8744.

Plotnikov, A. N., Sosunov, E. A., Qu, J., et al. (2004). Biological pacemaker implanted in canine left bundle branch provides ventricular escape rhythms that have physiologically acceptable rates. *Circulation.* **109**, 506-512.

Pogwizd, S. M., Bers, D. M. (2004). Cellular basis of triggered arrhythmias in heart failure. *Trends Cardiovasc Med.* **14**, 61-66.

Pond, A. L., Scheve, B. K., Benedict, A. T., Petrecca, K., Van Wagoner, D. R., Shrier, A., & Nerbonne, J. M. (2000). Expression of distinct ERG proteins in rat, mouse, and human heart. Relation to functional I_{Kr} channels. *J.Biol.Chem.* **275**, 5997-6006.

Powell, T. & Twist, V. W. (1976). A rapid technique for the isolation and purification of adult cardiac muscle cells having respiratory control and a tolerance to calcium. *Biochem.Biophys.Res.Commun.* **72**, 327-333.

Priori, S. G. & Napolitano, C. (2004). Genetics of cardiac arrhythmias and sudden cardiac death. *Ann.N.Y.Acad.Sci.* **1015**, 96-110.

Qin, N., D'Andrea, M. R., Lubin, M. L., Shafaee, N., Codd, E. E., & Correa, A. M. (2003). Molecular cloning and functional expression of the human sodium channel beta1B subunit, a novel splicing variant of the beta1 subunit. *Eur.J.Biochem.* **270**, 4762-4770.

Qu, J., Kryukova, Y., Potapova, I. A., Doronin, S. V., Larsen, M., Krishnamurthy, G., Cohen, I. S., & Robinson, R. B. (2004). MiRP1 modulates HCN2 channel expression and gating in cardiac myocytes. *J.Biol.Chem.* **279**, 43497-43502.

Qu, Y., Isom, L. L., Westenbroek, R. E., Rogers, J. C., Tanada, T. N., McCormick, K. A., Scheuer, T., & Catterall, W. A. (1995). Modulation of cardiac Na^+ channel expression in Xenopus oocytes by beta 1 subunits. *J.Biol.Chem.* **270**, 25696-25701.

Qu, Y., Rogers, J., Tanada, T., Scheuer, T., & Catterall, W. A. (1994). Modulation of cardiac Na^+ channels expressed in a mammalian cell line and in ventricular myocytes by protein kinase C. *Proc.Natl.Acad.Sci.U.S.A* **91**, 3289-3293.

Qu, Y., Rogers, J. C., Tanada, T. N., Catterall, W. A., & Scheuer, T. (1996). Phosphorylation of S1505 in the cardiac Na^+ channel inactivation gate is required for modulation by protein kinase C. *J.Gen.Physiol* **108**, 375-379.

Rettig, J., Heinemann, S. H., Wunder, F., Lorra, C., Parcej, D. N., Dolly, J. O., & Pongs, O. (1994). Inactivation properties of voltage-gated K^+ channels altered by presence of beta-subunit. *Nature* **369**, 289-294.

Robinson, R. B., Liu, Q. Y., & Rosen, M. R. (2000). Ionic basis for action potential prolongation by phenylephrine in canine epicardial myocytes. *J.Cardiovasc.Electrophysiol.* **11**, 70-76.

Roden, D. M., Bennett, P. B., Snyders, D. J., Balser, J. R., & Hondeghem, L. M. (1988). Quinidine delays I_K activation in guinea pig ventricular myocytes. *Circ.Res.* **62**, 1055-1058.

Roden, D. M. & Kupershmidt, S. (1999). From genes to channels: normal mechanisms. *Cardiovasc.Res.* **42**, 318-326.

Roden, D. M., Lazzara, R., Rosen, M., Schwartz, P. J., Towbin, J., & Vincent, G. M. (1996). Multiple mechanisms in the long-QT syndrome. Current knowledge, gaps, and future directions. The SADS Foundation Task Force on LQTS. *Circulation* **94**, 1996-2012.

Rogart, R. (1981). Sodium channels in nerve and muscle membrane. *Annu.Rev.Physiol* **43**, 711-725.

Rogart, R. B. (1986). High-STX-affinity vs. low-STX-affinity Na^+ channel subtypes in nerve, heart, and skeletal muscle. *Ann.N.Y.Acad.Sci.* **479**, 402-430.

Rogart, R. B., Cribbs, L. L., Muglia, L. K., Kephart, D. D., & Kaiser, M. W. (1989). Molecular cloning of a putative tetrodotoxin-resistant rat heart Na^+ channel isoform. *Proc.Natl.Acad.Sci.U.S.A* **86**, 8170-8174.

Rosati, B., Grau, F., Rodriguez, S., Li, H., Nerbonne, J. M., & McKinnon, D. (2003). Concordant expression of KChIP2 mRNA, protein and transient outward current throughout the canine ventricle. *J.Physiol* **548**, 815-822.

Rosati, B., Pan, Z., Lypen, S., Wang, H. S., Cohen, I., Dixon, J. E., & McKinnon, D. (2001). Regulation of KChIP2 potassium channel beta subunit gene expression underlies the gradient of transient outward current in canine and human ventricle. *J.Physiol* **533**, 119-125.

Rozanski, G. J., Xu, Z., Whitney, R. T., Murakami, H., & Zucker, I. H. (1997). Electrophysiology of rabbit ventricular myocytes following sustained rapid ventricular pacing. *J.Mol.Cell Cardiol.* **29**, 721-732.

Rozanski, G. J., Xu, Z., Zhang, K., & Patel, K. P. (1998). Altered K^+ current of ventricular myocytes in rats with chronic myocardial infarction. *Am.J.Physiol* **274**, H259-H265.

Rudy, B. (1978). Slow inactivation of the sodium conductance in squid giant axons. Pronase resistance. *J.Physiol* **283**, 1-21.

Saint, D. A., Ju, Y. K., & Gage, P. W. (1992). A persistent sodium current in rat ventricular myocytes. *J.Physiol* **453**, 219-231.

Sakakibara, Y., Wasserstrom, J. A., Furukawa, T., Jia, H., Arentzen, C. E., Hartz, R. S., & Singer, D. H. (1992). Characterization of the sodium current in single human atrial myocytes. *Circ.Res.* **71**, 535-546.

Sakmann, B. F., Spindler, A. J., Bryant, S. M., Linz, K. W., & Noble, D. (2000). Distribution of a persistent sodium current across the ventricular wall in guinea pigs. *Circ.Res.* **87**, 910-914.

Salata, J. J., Jurkiewicz, N. K., Jow, B., Folander, K., Guinosso, P. J., Jr., Raynor, B., Swanson, R., & Fermini, B. (1996). I_K of rabbit ventricle is composed of two currents: evidence for I_{Ks}. *Am.J.Physiol* **271**, H2477-H2489.

Sanders, P., Morton, J. B., Davidson, N. C., Spence, S. J., Vohra, J. K., Sparks, P. B., & Kalman, J. M. (2003). Electrical remodeling of the atria in congestive heart failure: electrophysiological and electroanatomic mapping in humans. *Circulation* **108**, 1461-1468.

Sanguinetti, M. C. (2002). When the KChIPs are down. *Nat.Med.* **8**, 18-19.

Sanguinetti, M. C., Curran, M. E., Zou, A., Shen, J., Spector, P. S., Atkinson, D. L., & Keating, M. T. (1996). Coassembly of K(V)LQT1 and minK (IsK) proteins to form cardiac I(Ks) potassium channel. *Nature* **384**, 80-83.

Sanguinetti, M. C., Jiang, C., Curran, M. E., & Keating, M. T. (1995). A mechanistic link between an inherited and an acquired cardiac arrhythmia: HERG encodes the I_{Kr} potassium channel. *Cell* **81**, 299-307.

Sanguinetti, M. C. & Jurkiewicz, N. K. (1990). Two components of cardiac delayed rectifier K^+ current. Differential sensitivity to block by class III antiarrhythmic agents. *J.Gen.Physiol* **96**, 195-215.

Sanguinetti, M. C. & Jurkiewicz, N. K. (1991). Delayed rectifier outward K^+ current is composed of two currents in guinea pig atrial cells. *Am.J.Physiol* **260**, H393-H399.

Sanguinetti, M. C. & Jurkiewicz, N. K. (1992). Role of external Ca^{2+} and K^+ in gating of cardiac delayed rectifier K^+ currents. *Pflugers Arch.* **420**, 180-186.

Sanguinetti, M. C. & Xu, Q. P. (1999). Mutations of the S4-S5 linker alter activation properties of HERG potassium channels expressed in Xenopus oocytes. *J.Physiol* **514 (Pt 3)**, 667-675.

Santoro, B., Grant, S. G., Bartsch, D., & Kandel, E. R. (1997). Interactive cloning with the SH3 domain of N-src identifies a new brain specific ion channel protein, with homology to eag and cyclic nucleotide-gated channels. *Proc.Natl.Acad.Sci.U.S.A*,**94**, 14815-14820.

Santoro, B., Liu, D. T., Yao, H., Bartsch, D., Kandel, E. R., Siegelbaum, S. A., & Tibbs, G. R. (1998). Identification of a gene encoding a hyperpolarization-activated pacemaker channel of brain. *Cell* **93**, 717-729.

Satin, J., Kyle, J. W., Chen, M., Bell, P., Cribbs, L. L., Fozzard, H. A., & Rogart, R. B. (1992). A mutant of TTX-resistant cardiac sodium channels with TTX-sensitive properties. *Science* **256**, 1202-1205.

Satoh, H. & Hashimoto, K. (1988). Effect of alpha 1-adrenoceptor stimulation with methoxamine and phenylephrine on spontaneously beating rabbit sino-atrial node cells. *Naunyn Schmiedebergs Arch.Pharmacol.* **337**, 415-422.

Schaller, K. L., Krzemien, D. M., McKenna, N. M., & Caldwell, J. H. (1992). Alternatively spliced sodium channel transcripts in brain and muscle. *J.Neurosci.* **12**, 1370-1381.

Schneider, M., Proebstle, T., Hombach, V., Hannekum, A., & Rudel, R. (1994). Characterization of the sodium currents in isolated human cardiocytes. *Pflugers Arch.* **428**, 84-90.

Schonherr, R. & Heinemann, S. H. (1996). Molecular determinants for activation and inactivation of HERG, a human inward rectifier potassium channel. *J.Physiol* **493 (Pt 3)**, 635-642.

Schreibmayer, W., Frohnwieser, B., Dascal, N., Platzer, D., Spreitzer, B., Zechner, R., Kallen, R. G., & Lester, H. A. (1994). Beta-adrenergic modulation of currents produced by rat cardiac Na^+ channels expressed in Xenopus laevis oocytes. *Receptors.Channels* **2**, 339-350.

Schroeder, B. C., Waldegger, S., Fehr, S., Bleich, M., Warth, R., Greger, R., & Jentsch, T. J. (2000). A constitutively open potassium channel formed by KCNQ1 and KCNE3. *Nature* **403**, 196-199.

Schubert, B., VanDongen, A. M., Kirsch, G. E., & Brown, A. M. (1989). Beta-adrenergic inhibition of cardiac sodium channels by dual G-protein pathways. *Science* **245**, 516-519.

Scott, V. E., Rettig, J., Parcej, D. N., Keen, J. N., Findlay, J. B., Pongs, O., & Dolly, J. O. (1994). Primary structure of a beta subunit of alpha-dendrotoxin-sensitive K^+ channels from bovine brain. *Proc.Natl.Acad.Sci.U.S.A* **91**, 1637-1641.

Seoh, S. A., Sigg, D., Papazian, D. M., & Bezanilla, F. (1996). Voltage-sensing residues in the S2 and S4 segments of the Shaker K^+ channel. *Neuron* **16**, 1159-1167.

Sesti, F., Abbott, G. W., Wei, J., Murray, K. T., Saksena, S., Schwartz, P. J., Priori, S. G., Roden, D. M., George, A. L., Jr., & Goldstein, S. A. (2000). A common polymorphism associated with antibiotic-induced cardiac arrhythmia. *Proc.Natl.Acad.Sci.U.S.A* **97**, 10613-10618.

Shi, W., Wymore, R., Yu, H., Wu, J., Wymore, R. T., Pan, Z., Robinson, R. B., Dixon, J. E., McKinnon, D., & Cohen, I. S. (1999). Distribution and prevalence of hyperpolarization-activated cation channel (HCN) mRNA expression in cardiac tissues. *Circ.Res.* **85**, e1-e6.

Shibasaki, T. (1987). Conductance and kinetics of delayed rectifier potassium channels in nodal cells of the rabbit heart. *J.Physiol* **387**, 227-250.

Shibata, E. F., Drury, T., Refsum, H., Aldrete, V., & Giles, W. (1989). Contributions of a transient outward current to repolarization in human atrium. *Am.J.Physiol* **257**, H1773-H1781.

Shimizu, W., Ohe, T., Kurita, T., Takaki, H., Aihara, N., Kamakura, S., Matsuhisa, M., & Shimomura, K. (1991). Early afterdepolarizations induced by isoproterenol in patients with congenital long QT syndrome. *Circulation* **84**, 1915-1923.

Shimoni, Y., Ewart, H. S., & Severson, D. (1998). Type I and II models of diabetes produce different modifications of K^+ currents in rat heart: role of insulin. *J.Physiol* **507 (Pt 2)**, 485-496.

Shimoni, Y., Fiset, C., Clark, R. B., Dixon, J. E., McKinnon, D., & Giles, W. R. (1997). Thyroid hormone regulates postnatal expression of transient K^+ channel isoforms in rat ventricle. *J.Physiol* **500 (Pt 1)**, 65-73.

Shimoni, Y. & Severson, D. L. (1995). Thyroid status and potassium currents in rat ventricular myocytes. *Am.J.Physiol* **268**, H576-H583.

Sicouri, S. & Antzelevitch, C. (1991). A subpopulation of cells with unique electrophysiological properties in the deep subepicardium of the canine ventricle. The M cell. *Circ.Res.* **68**, 1729-1741.

Sicouri, S. & Antzelevitch, C. (1995). Electrophysiologic characteristics of M cells in the canine left ventricular free wall. *J.Cardiovasc.Electrophysiol.* **6**, 591-603.

Sicouri, S., Fish, J., & Antzelevitch, C. (1994). Distribution of M cells in the canine ventricle. *J.Cardiovasc.Electrophysiol.* **5**, 824-837.

Siegelbaum, S. A. & Tsien, R. W. (1980). Calcium-activated transient outward current in calf cardiac Purkinje fibres. *J.Physiol* **299**, 485-506.

Smith, P. L., Baukrowitz, T., & Yellen, G. (1996). The inward rectification mechanism of the HERG cardiac potassium channel. *Nature* **379**, 833-836.

Snyders, D. J. (1999). Structure and function of cardiac potassium channels. *Cardiovasc.Res.* **42**, 377-390.

Spector, P. S., Curran, M. E., Keating, M. T., & Sanguinetti, M. C. (1996a). Class III antiarrhythmic drugs block HERG, a human cardiac delayed rectifier K^+ channel. Open-channel block by methanesulfonanilides. *Circ.Res.* **78**, 499-503.

Spector, P. S., Curran, M. E., Zou, A., Keating, M. T., & Sanguinetti, M. C. (1996b). Fast inactivation causes rectification of the I_{Kr} channel. *J.Gen.Physiol* **107**, 611-619.

Splawski, I., Shen, J., Timothy, K. W., Lehmann, M. H., Priori, S., Robinson, J. L., Moss, A. J., Schwartz, P. J., Towbin, J. A., Vincent, G. M., & Keating, M. T. (2000). Spectrum of mutations in long-QT syndrome genes. KVLQT1, HERG, SCN5A, KCNE1, and KCNE2. *Circulation* **102**, 1178-1185.

Stevens, E. B., Cox, P. J., Shah, B. S., Dixon, A. K., Richardson, P. J., Pinnock, R. D., & Lee, K. (2001). Tissue distribution and functional expression of the human voltage-gated sodium channel beta3 subunit. *Pflugers Arch.* **441**, 481-488.

Stieber, J., Herrmann, S., Feil, S., Loster, J., Feil, R., Biel, M., Hofmann, F., & Ludwig, A. (2003). The hyperpolarization-activated channel HCN4 is required for the generation of pacemaker action potentials in the embryonic heart. *Proc.Natl.Acad.Sci.U.S.A* **100**, 15235-15240.

Stuhmer, W., Conti, F., Suzuki, H., Wang, X. D., Noda, M., Yahagi, N., Kubo, H., & Numa, S. (1989). Structural parts involved in activation and inactivation of the sodium channel. *Nature* **339**, 597-603.

Takimoto, K., Li, D., Hershman, K. M., Li, P., Jackson, E. K., & Levitan, E. S. (1997). Decreased expression of Kv4.2 and novel Kv4.3 K^+ channel subunit mRNAs in ventricles of renovascular hypertensive rats. *Circ.Res.* **81**, 533-539.

Takumi, T., Ohkubo, H., & Nakanishi, S. (1988). Cloning of a membrane protein that induces a slow voltage-gated potassium current. *Science* **242**, 1042-1045.

Tan, H. L., Bink-Boelkens, M. T., Bezzina, C. R., Viswanathan, P. C., Beaufort-Krol, G. C., van Tintelen, P. J., van Den Berg, M. P., Wilde, A. A., & Balser, J. R. (2001). A sodium-channel mutation causes isolated cardiac conduction disease. *Nature* **409**, 1043-1047.

Tapper, A. R. & George, A. L., Jr. (2001). Location and orientation of minK within the I_{Ks} potassium channel complex. *J.Biol.Chem.* **276**, 38249-38254.

Tessier, S., Karczewski, P., Krause, E. G., Pansard, Y., Acar, C., Lang-Lazdunski, M., Mercadier, J. J., & Hatem, S. N. (1999). Regulation of the transient outward K(+) current by Ca(2+)/calmodulin-dependent protein kinases II in human atrial myocytes. *Circ.Res.* **85**, 810-819.

Thomas, D., Zhang, W., Karle, C. A., Kathofer, S., Schols, W., Kubler, W., & Kiehn, J. (1999). Deletion of protein kinase A phosphorylation sites in the HERG potassium channel inhibits activation shift by protein kinase A. *J.Biol.Chem.* **274**, 27457-27462.

Thomas, G. P., Gerlach, U., & Antzelevitch, C. (2003). HMR 1556, a potent and selective blocker of slowly activating delayed rectifier potassium current. *J.Cardiovasc.Pharmacol.* **41**, 140-147.

Tohse, N., Nakaya, H., Hattori, Y., Endou, M., & Kanno, M. (1990). Inhibitory effect mediated by alpha 1-adrenoceptors on transient outward current in isolated rat ventricular cells. *Pflugers Arch.* **415**, 575-581.

Tomaselli, G. F. & Marban, E. (1999). Electrophysiological remodeling in hypertrophy and heart failure. *Cardiovasc.Res.* **42**, 270-283.

Trudeau, M. C., Warmke, J. W., Ganetzky, B., & Robertson, G. A. (1995). HERG, a human inward rectifier in the voltage-gated potassium channel family. *Science* **269**, 92-95.

Tseng, G. N. (2001). I_{Kr}: the hERG channel. *J.Mol.Cell Cardiol.* **33**, 835-849.

Tseng, G. N. & Hoffman, B. F. (1989). Two components of transient outward current in canine ventricular myocytes. *Circ.Res.* **64**, 633-647.

Tsien, R. W. & Carpenter, D. O. (1978). Ionic mechanisms of pacemaker activity in cardiac Purkinje fibers. *Fed.Proc.* **37**, 2127-2131.

Tsien, R. W., Giles, W., & Greengard, P. (1972). Cyclic AMP mediates the effects of adrenaline on cardiac purkinje fibres. *Nat.New Biol.* **240**, 181-183.

Tsuji, Y., Opthof, T., Kamiya, K., Yasui, K., Liu, W., Lu, Z., & Kodama, I. (2000). Pacing-induced heart failure causes a reduction of delayed rectifier potassium currents along with decreases in calcium and transient outward currents in rabbit ventricle. *Cardiovasc.Res.* **48**, 300-309.

Turgeon, J., Daleau, P., Bennett, P. B., Wiggins, S. S., Selby, L., & Roden, D. M. (1994). Block of I_{Ks}, the slow component of the delayed rectifier K^+ current, by the diuretic agent indapamide in guinea pig myocytes. *Circ.Res.* **75**, 879-886.

Tzounopoulos, T., Guy, H. R., Durell, S., Adelman, J. P., & Maylie, J. (1995). minK channels form by assembly of at least 14 subunits. *Proc.Natl.Acad.Sci.U.S.A* **92**, 9593-9597.

Ufret-Vincenty, C. A., Baro, D. J., Lederer, W. J., Rockman, H. A., Quinones, L. E., & Santana, L. F. (2001). Role of sodium channel deglycosylation in the genesis of cardiac arrhythmias in heart failure. *J.Biol.Chem.* **276**, 28197-28203.

Ulens, C. & Tytgat, J. (2001). Functional heteromerization of HCN1 and HCN2 pacemaker channels. *J.Biol.Chem.* **276**, 6069-6072.

Undrovinas, A. I., Maltsev, V. A., & Sabbah, H. N. (1999). Repolarization abnormalities in cardiomyocytes of dogs with chronic heart failure: role of sustained inward current. *Cell Mol.Life Sci.* **55**, 494-505.

Vaccari, T., Moroni, A., Rocchi, M., Gorza, L., Bianchi, M. E., Beltrame, M., & DiFrancesco, D. (1999). The human gene coding for HCN2, a pacemaker channel of the heart. *Biochim.Biophys.Acta* **1446**, 419-425.

Varnum, M. D., Busch, A. E., Bond, C. T., Maylie, J., & Adelman, J. P. (1993). The min K channel underlies the cardiac potassium current I_{Ks} and mediates species-specific responses to protein kinase C. *Proc.Natl.Acad.Sci.U.S.A* **90**, 11528-11532.

Varro, A., Balati, B., Iost, N., Takacs, J., Virag, L., Lathrop, D. A., Csaba, L., Talosi, L., & Papp, J. G. (2000). The role of the delayed rectifier component I_{Ks} in dog ventricular muscle and Purkinje fibre repolarization. *J.Physiol* **523 Pt 1**, 67-81.

Varro, A., Nanasi, P. P., & Lathrop, D. A. (1993). Potassium currents in isolated human atrial and ventricular cardiocytes. *Acta Physiol Scand.* **149**, 133-142.

Vassalle, M. (1966). Analysis of cardiac pacemaker potential using a "voltage clamp" technique. *Am.J.Physiol* **210**, 1335-1341.

Veldkamp, M. W., van Ginneken, A. C., & Bouman, L. N. (1993). Single delayed rectifier channels in the membrane of rabbit ventricular myocytes. *Circ.Res.* **72**, 865-878.

Veldkamp, M. W., Viswanathan, P. C., Bezzina, C., Baartscheer, A., Wilde, A. A., & Balser, J. R. (2000). Two distinct congenital arrhythmias evoked by a multidysfunctional Na(+) channel. *Circ.Res.* **86**, E91-E97.

Verkerk, A. O., Wilders, R., Coronel, R., et al. (2003). Ionic remodeling of sinoatrial node cells by heart failure. *Circulation.* **108**, 760-766.

Volders, P. G., Sipido, K. R., Carmeliet, E., Spatjens, R. L., Wellens, H. J., & Vos, M. A. (1999a). Repolarizing K^+ currents I_{TO1} and I_{Ks} are larger in right than left canine ventricular midmyocardium. *Circulation* **99**, 206-210.

Volders, P. G., Sipido, K. R., Vos, M. A., Spatjens, R. L., Leunissen, J. D., Carmeliet, E., & Wellens, H. J. (1999b). Downregulation of delayed rectifier K(+) currents in dogs with chronic complete atrioventricular block and acquired torsades de pointes. *Circulation* **100**, 2455-2461.

Wainger, B. J., DeGennaro, M., Santoro, B., Siegelbaum, S. A., & Tibbs, G. R. (2001). Molecular mechanism of cAMP modulation of HCN pacemaker channels. *Nature* **411**, 805-810.

Walsh, K. B., Arena, J. P., Kwok, W. M., Freeman, L., & Kass, R. S. (1991). Delayed-rectifier potassium channel activity in isolated membrane patches of guinea pig ventricular myocytes. *Am.J.Physiol* **260**, H1390-H1393.

Walsh, K. B. & Kass, R. S. (1988). Regulation of a heart potassium channel by protein kinase A and C. *Science* **242**, 67-69.

Wang, D. W., Kiyosue, T., Shigematsu, S., & Arita, M. (1995a). Abnormalities of K^+ and Ca^{2+} currents in ventricular myocytes from rats with chronic diabetes. *Am.J.Physiol* **269**, H1288-H1296.

Wang, H., Yang, B., Zhang, Y., Han, H., Wang, J., Shi, H., & Wang, Z. (2001). Different subtypes of alpha1-adrenoceptor modulate different K^+ currents via different signaling pathways in canine ventricular myocytes. *J.Biol.Chem.* **276**, 40811-40816.

Wang, J., Trudeau, M. C., Zappia, A. M., & Robertson, G. A. (1998a). Regulation of deactivation by an amino terminal domain in human ether-a-go-go-related gene potassium channels. *J.Gen.Physiol* **112**, 637-647.

Wang, Q., Shen, J., Splawski, I., Atkinson, D., Li, Z., Robinson, J. L., Moss, A. J., Towbin, J. A., & Keating, M. T. (1995b). SCN5A mutations associated with an inherited cardiac arrhythmia, long QT syndrome. *Cell* **80**, 805-811.

Wang, S., Morales, M. J., Liu, S., Strauss, H. C., & Rasmusson, R. L. (1996). Time, voltage and ionic concentration dependence of rectification of hERG expressed in Xenopus oocytes. *FEBS Lett.* **389**, 167-173.

Wang, W., Xia, J., & Kass, R. S. (1998b). MinK-KvLQT1 fusion proteins, evidence for multiple stoichiometries of the assembled IsK channel. *J.Biol.Chem.* **273**, 34069-34074.

Wang, Z., Feng, J., Shi, H., Pond, A., Nerbonne, J. M., & Nattel, S. (1999). Potential molecular basis of different physiological properties of the transient outward K^+ current in rabbit and human atrial myocytes. *Circ.Res.* **84**, 551-561.

Wang, Z., Fermini, B., & Nattel, S. (1994). Rapid and slow components of delayed rectifier current in human atrial myocytes. *Cardiovasc.Res.* **28**, 1540-1546.

Wang, Z., Yue, L., White, M., Pelletier, G., & Nattel, S. (1998c). Differential distribution of inward rectifier potassium channel transcripts in human atrium versus ventricle. *Circulation* **98**, 2422-2428.

Wang, Z. G., Pelletier, L. C., Talajic, M., & Nattel, S. (1990). Effects of flecainide and quinidine on human atrial action potentials. Role of rate-dependence and comparison with guinea pig, rabbit, and dog tissues. *Circulation* **82**, 274-283.

Wang, Z., Kutschke, W., Richardson, K. E., Karimi, M., Hill, J. A. (2001) Electrical remodeling in pressure-overload cardiac hypertrophy: role of calcineurin. *Circulation*. **104**, 1657-63.

Warmke, J., Drysdale, R., & Ganetzky, B. (1991). A distinct potassium channel polypeptide encoded by the Drosophila eag locus. *Science* **252**, 1560-1562.

Warmke, J. W. & Ganetzky, B. (1994). A family of potassium channel genes related to eag in Drosophila and mammals. *Proc.Natl.Acad.Sci.U.S.A* **91**, 3438-3442.

Wasserstrom, J. A. & Salata, J. J. (1988). Basis for tetrodotoxin and lidocaine effects on action potentials in dog ventricular myocytes. *Am.J.Physiol* **254**, H1157-H1166.

Watson, C. L. & Gold, M. R. (1997). Modulation of Na^+ current inactivation by stimulation of protein kinase C in cardiac cells. *Circ.Res.* **81**, 380-386.

Weerapura, M., Nattel, S., Chartier, D., Caballero, R., & Hebert, T. E. (2002). A comparison of currents carried by HERG, with and without coexpression of MiRP1, and the native rapid delayed rectifier current. Is MiRP1 the missing link? *J.Physiol* **540**, 15-27.

Weidmann, S. (1951). Effect of current flow on the membrane potential of cardiac muscle. *J.Physiol* **115**, 227-236.

West, J. W., Patton, D. E., Scheuer, T., Wang, Y., Goldin, A. L., & Catterall, W. A. (1992). A cluster of hydrophobic amino acid residues required for fast Na(+)-channel inactivation. *Proc.Natl.Acad.Sci.U.S.A* **89**, 10910-10914.

Wettwer, E., Amos, G., Gath, J., Zerkowski, H. R., Reidemeister, J. C., & Ravens, U. (1993). Transient outward current in human and rat ventricular myocytes. *Cardiovasc.Res.* **27**, 1662-1669.

Wettwer, E., Amos, G. J., Posival, H., & Ravens, U. (1994). Transient outward current in human ventricular myocytes of subepicardial and subendocardial origin. *Circ.Res.* **75**, 473-482.

Wible, B. A., Yang, Q., Kuryshev, Y. A., Accili, E. A., & Brown, A. M. (1998). Cloning and expression of a novel K^+ channel regulatory protein, KChAP. *J.Biol.Chem.* **273**, 11745-11751.

Wickenden, A. D., Jegla, T. J., Kaprielian, R., & Backx, P. H. (1999a). Regional contributions of Kv1.4, Kv4.2, and Kv4.3 to transient outward K^+ current in rat ventricle. *Am.J.Physiol* **276**, H1599-H1607.

Wickenden, A. D., Lee, P., Sah, R., Huang, Q., Fishman, G. I., & Backx, P. H. (1999b). Targeted expression of a dominant-negative K(v)4.2 K(+) channel subunit in the mouse heart. *Circ.Res.* **85**, 1067-1076.

Wickenden, A. D., Tsushima, R. G., Losito, V. A., Kaprielian, R., & Backx, P. H. (1999c). Effect of Cd^{2+} on Kv4.2 and Kv1.4 expressed in Xenopus oocytes and on the transient outward currents in rat and rabbit ventricular myocytes. *Cell Physiol Biochem.* **9**, 11-28.

Wijffels, M. C., Kirchhof, C. J., Dorland, R., & Allessie, M. A. (1995). Atrial fibrillation begets atrial fibrillation. A study in awake chronically instrumented goats. *Circulation* **92**, 1954-1968.

Wit, A. L., Cranefield, P. F. (1976). Triggered activity in cardiac muscle fibers of the simian mitral valve. *Circ Res.* **38**, 85-98.

Wolf, P. A., Abbott, R. D., & Kannel, W. B. (1991). Atrial fibrillation as an independent risk factor for stroke: the Framingham Study. *Stroke* **22**, 983-988.

Wollmuth, L. P. & Hille, B. (1992). Ionic selectivity of I_h channels of rod photoreceptors in tiger salamanders. *J.Gen.Physiol* **100**, 749-765.

Wollner, D. A., Scheinman, R., & Catterall, W. A. (1988). Sodium channel expression and assembly during development of retinal ganglion cells. *Neuron* **1**, 727-737.

Workman, A. J., Kane, K. A., Russell, J. A., Norrie, J., & Rankin, A. C. (2003). Chronic beta-adrenoceptor blockade and human atrial cell electrophysiology: evidence of pharmacological remodelling. *Cardiovasc.Res.* **58**, 518-525.

Wright, S. N., Wang, S. Y., Kallen, R. G., & Wang, G. K. (1997). Differences in steady-state inactivation between Na channel isoforms affect local anesthetic binding affinity. *Biophys.J.* **73**, 779-788.

Xu, H., Guo, W., & Nerbonne, J. M. (1999a). Four kinetically distinct depolarization-activated K^+ currents in adult mouse ventricular myocytes. *J.Gen.Physiol* **113**, 661-678.

Xu, H., Li, H., & Nerbonne, J. M. (1999b). Elimination of the transient outward current and action potential prolongation in mouse atrial myocytes expressing a dominant negative Kv4 alpha subunit. *J.Physiol* **519 Pt 1**, 11-21.

Xu, Z. & Rozanski, G. J. (1998). K^+ current inhibition by amphiphilic fatty acid metabolites in rat ventricular myocytes. *Am.J.Physiol* **275**, C1660-C1667.

Yamashita, T., Nakajima, T., Hazama, H., Hamada, E., Murakawa, Y., Sawada, K., & Omata, M. (1995). Regional differences in transient outward current density and inhomogeneities of repolarization in rabbit right atrium. *Circulation* **92**, 3061-3069.

Yanagihara, K. & Irisawa, H. (1980). Inward current activated during hyperpolarization in the rabbit sinoatrial node cell. *Pflugers Arch.* **385**, 11-19.

Yang, E. K., Alvira, M. R., Levitan, E. S., & Takimoto, K. (2001). Kvbeta subunits increase expression of Kv4.3 channels by interacting with their C termini. *J.Biol.Chem.* **276**, 4839-4844.

Yang, N. & Horn, R. (1995). Evidence for voltage-dependent S4 movement in sodium channels. *Neuron* **15**, 213-218.

Yang, T., Kupershmidt, S., & Roden, D. M. (1995). Anti-minK antisense decreases the amplitude of the rapidly activating cardiac delayed rectifier K^+ current. *Circ.Res.* **77**, 1246-1253.

Yarbrough, T. L., Lu, T., Lee, H. C., & Shibata, E. F. (2002). Localization of cardiac sodium channels in caveolin-rich membrane domains: regulation of sodium current amplitude. *Circ.Res.* **90**, 443-449.

Yellen, G., Jurman, M. E., Abramson, T., & MacKinnon, R. (1991). Mutations affecting internal TEA blockade identify the probable pore-forming region of a K^+ channel. *Science* **251**, 939-942.

Yellen, G., Sodickson, D., Chen, T. Y., & Jurman, M. E. (1994). An engineered cysteine in the external mouth of a K^+ channel allows inactivation to be modulated by metal binding. *Biophys.J.* **66**, 1068-1075.

Yokoshiki, H., Kohya, T., Tomita, F., Tohse, N., Nakaya, H., Kanno, M., & Kitabatake, A. (1997). Restoration of action potential duration and transient outward current by regression of left ventricular hypertrophy. *J.Mol.Cell Cardiol.* **29**, 1331-1339.

Yu, F. H., Westenbroek, R. E., Silos-Santiago, I., McCormick, K. A., Lawson, D., Ge, P., Ferriera, H., Lilly, J., DiStefano, P. S., Catterall, W. A., Scheuer, T., & Curtis, R. (2003). Sodium channel beta4, a new disulfide-linked auxiliary subunit with similarity to beta2. *J.Neurosci.* **23**, 7577-7585.

Yu, H., Gao, J., Wang, H., Wymore, R., Steinberg, S., McKinnon, D., Rosen, M. R., & Cohen, I. S. (2000). Effects of the renin-angiotensin system on the current I(to) in epicardial and endocardial ventricular myocytes from the canine heart. *Circ.Res.* **86**, 1062-1068.

Yu, H., Wu, J., Potapova, I., Wymore, R. T., Holmes, B., Zuckerman, J., Pan, Z., Wang, H., Shi, W., Robinson, R. B., El Maghrabi, M. R., Benjamin, W., Dixon, J., McKinnon, D., Cohen, I. S., & Wymore, R. (2001). MinK-related peptide 1: A beta subunit for the HCN ion channel subunit family enhances expression and speeds activation. *Circ.Res.* **88**, E84-E87.

Yue, L., Feng, J., Gaspo, R., Li, G. R., Wang, Z., & Nattel, S. (1997). Ionic remodeling underlying action potential changes in a canine model of atrial fibrillation. *Circ.Res.* **81**, 512-525.

Yue, L., Feng, J., Li, G. R., & Nattel, S. (1996). Transient outward and delayed rectifier currents in canine atrium: properties and role of isolation methods. *Am.J.Physiol* **270**, H2157-H2168.

Zhang, H., Holden, A. V., Kodama, I., Honjo, H., Lei, M., Varghese, T., & Boyett, M. R. (2000). Mathematical models of action potentials in the periphery and center of the rabbit sinoatrial node. *Am.J.Physiol Heart Circ.Physiol* **279**, H397-H421.

Zhang, M., Jiang, M., & Tseng, G. N. (2001). minK-related peptide 1 associates with Kv4.2 and modulates its gating function: potential role as beta subunit of cardiac transient outward channel? *Circ.Res.* **88**, 1012-1019.

Zhang, Z. J., Jurkiewicz, N. K., Folander, K., Lazarides, E., Salata, J. J., & Swanson, R. (1994). K^+ currents expressed from the guinea pig cardiac IsK protein are enhanced by activators of protein kinase C. *Proc.Natl.Acad.Sci.U.S.A* **91**, 1766-1770.

Zhong, Y. & Wu, C. F. (1991). Alteration of four identified K^+ currents in Drosophila muscle by mutations in eag. *Science* **252**, 1562-1564.

Zhong, Y. & Wu, C. F. (1993). Modulation of different K^+ currents in Drosophila: a hypothetical role for the Eag subunit in multimeric K^+ channels. *J.Neurosci.* **13**, 4669-4679.

Zhou, J., Yi, J., Hu, N., George, A. L., Jr., & Murray, K. T. (2000). Activation of protein kinase A modulates trafficking of the human cardiac sodium channel in Xenopus oocytes. *Circ.Res.* **87**, 33-38.

Zhou, Z., Gong, Q., Ye, B., Fan, Z., Makielski, J. C., Robertson, G. A., & January, C. T. (1998). Properties of HERG channels stably expressed in HEK 293 cells studied at physiological temperature. *Biophys.J.* **74**, 230-241.

Zimmer, T., Biskup, C., Bollensdorff, C., & Benndorf, K. (2002). The beta1 subunit but not the beta2 subunit colocalizes with the human heart Na^+ channel (hH1) already within the endoplasmic reticulum. *J.Membr.Biol.* **186**, 13-21.

Zou, A., Curran, M. E., Keating, M. T., & Sanguinetti, M. C. (1997). Single HERG delayed rectifier K^+ channels expressed in Xenopus oocytes. *Am.J.Physiol* **272**, H1309-H1314.

Zygmunt, A. C., Eddlestone, G. T., Thomas, G. P., Nesterenko, V. V., & Antzelevitch, C. (2001). Larger late sodium conductance in M cells contributes to electrical heterogeneity in canine ventricle. *Am.J.Physiol Heart Circ.Physiol* **281**, H689-H697.

Zygmunt, A. C. & Gibbons, W. R. (1991). Calcium-activated chloride current in rabbit ventricular myocytes. *Circ.Res.* **68**, 424-437.

Zygmunt, A. C. & Gibbons, W. R. (1992). Properties of the calcium-activated chloride current in heart. *J.Gen.Physiol* **99**, 391-414.

APPENDIX